A Soluble TNF Receptor 2 Agonist as a New Therapeutic Approach to Treat Autoimmune and Demyelinating Diseases

Von der Fakultät Energie-, Verfahrens- und Biotechnik der Universität Stuttgart zur Erlangung der Würde eines Doktors der Naturwissenschaften (Dr. rer. nat.) genehmigte Abhandlung

Vorgelegt von
Roman Fischer
aus Nürnberg

Hauptberichter: Prof. Dr. Klaus Pfizenmaier
Mitberichter: Prof. Dr. Peter Scheurich

Tag der mündlichen Prüfung: 29.04.2011

Institut für Zellbiologie und Immunologie
Universität Stuttgart
2011

I hereby assure that I performed the present study independently without further help or other materials than stated.

Roman Fischer
Stuttgart, 14th of February 2011

“ In der Wissenschaft gleichen wir alle nur den Kindern,
die am Rande des Wissens hie und da einen Kiesel aufheben,
während sich der weite Ozean des Unbekannten vor unseren Augen erstreckt. “

Sir Isaac Newton (1643 - 1727)

Table of contents

Abbreviations

2-ME	2-mercaptoethanol
°C	degree celsius
aa	amino acid
ADAM	a disintegrin and metalloproteinase
amp	ampicillin
APC	antigen presenting complex
APS	ammonium persulfate
ATV	adjusted trypsin/versen
Bad	Bcl2-associated death promoter
BBB	blood-brain-barrier
BCA	bicinchoninic acid
Bcl-2	B-cell lymphoma 2
bFGF	basic fibroblast growth factor
bp	base pairs
BSA	bovine serum albumin
caspase	cysteine-aspartic protease
CD95	cluster of differentiation 95
CD95L	cluster of differentiation 95 ligand
cDNA	complementary deoxyribonucleic acid
CHO	chinese hamster ovarian
cIAP	cellular inhibitor of apoptosis
CNS	central nervous system
CNTF	ciliary neurotrophic factor
ConA	concanavalin A
CSF	cerebrospinal fluid
DAPI	4′,6-diamidin-2-phenylindol
db-cAMP	N^6,2′-O-dibutyryladenosine 3′,5′-cyclic monophosphate
DD	death domain
DISC	death-inducing signaling complex
DMEM	Dulbecco's modified Eagle's medium
DMSO	dimethylsulfoxide
DN-TNF	dominant-negative tumor necrosis factor
DNA	deoxyribonucleic acid
dNTP	deoxyribonucleoside triphosphate
EC_{50}	effective concentration 50%
EDTA	ethylene di-amine tetra acedic acid
EEA1	early endosome antigen 1
eGFP	enhanced green fluorescent protein
EGTA	ethylene glycole tetra acedic acid
ELISA	enzyme-linked immunosorbent assay
FADD	Fas-associated protein with death domain
Fas	FS-7 cell-associated surface antigen
FCS	fetal calf serum
FITC	fluorescein isothiocyanate
FoxP3	forkhead box P3
g	gram
g	gravitational acceleration
GDNF	glial cell-derived neurotrophic factor
GFAP	glial fibrillary acidic protein

GGGGS	glycine-glycine-glycine-glycine-serine
glc	glucose
h	hour
H_2O_2	hydrogen peroxide
HEPES	4-(2-hydroxyethyl)-1-piperazineethanesulfonic acid
HPLC	high performance liquid chromatography
HRP	horse radish peroxidase
huTNF	human tumor necrosis factor
huTNFR2	human tumor necrosis factor receptor 2
i.p.	intraperitoneal
i.v.	intravenous
IFN	interferon
Ig	immunoglobulin
IκB	nuclear factor kappa-light-chain-enhancer of activated B cells inhibitor
IκK	IκB kinase
IL-2	interleukin-2
IL-2R	interleukin-2 receptor
IMA	immortalized astrocytes
IMAC	immobilized metal ion affinity chromatography
JNK	c-Jun N-terminal kinase
k	kilo
kDa	kilo Dalton
l	liter
LB	Lysogeny broth
LUBAC	linear ubiquitin chain assembly complex
M	molar
mA	milliampere
MAPK	mitogen-activated protein kinase
MCAO	middle cerebral artery occlusion
MEF	mouse embryonic fibroblast
MEM	Eagle's minimum essential medium
memTNF	membrane-bound tumor necrosis factor
MFI	median fluorescence intensity
mg	milligram (10^{-3} g)
Milli-Q H_2O	ultrapure water, purified with Milli-Q Reference
min	minute
ml	milliliter (10^{-3} l)
mM	millimolar (10^{-3} M)
MMP	matrix metalloproteinase
mRNA	messenger ribonucleic acid
MS	multiple sclerosis
mTNF	mouse tumor necrosis factor
mTNFR	mouse tumor necrosis factor receptor
MTT	3-(4,5-dimethylthiazol-2-yl)-2,5-diphenyltetrazolium bromide
MW	molecular weight
NEMO	NFκB essential modulator
NFκB	nuclear factor 'kappa-light-chain-enhancer' of activated B-cells
ng	nanogram (10^{-9} g)
Ni-NTA	nickel nitrilotriacetic acid
NIK	NFκB-inducing kinase
NP-40	nonyl phenoxypolyethoxylethanol

OD	optical density
Opti-MEM	Opti-MEM I Reduced Serum Media
PBA	PBS with BSA and sodium azide
PBMC	peripheral blood mononuclear cell
PBS	phosphate buffered saline
PBST	phosphate buffered saline with Tween-20
PCR	polymerase chain reaction
PDK-1	3-phosphoinositide dependent protein kinase-1
PDL	poly-D-lysine
PFA	paraformaldehyde
PI3K	phosphatidylinositol 3-kinase
PIP	phosphatidylinositol phosphate
PKB/Akt	protein kinase B
PLAD	pre-ligand assembly domain
PLO	poly-L-ornithine
PMSF	phenylmethanesulfonyl fluoride
PTEN	phosphatase and tensin homolog
Rel	reticuloendotheliosis oncogene
RIP1	receptor interacting protein 1
RNA	ribonucleic acid
ROS	reactive oxygen species
rpm	revolutions per minute
RPMI 1640	Roswell Park Memorial Institute medium 1640
scTNF	single-chain tumor necrosis factor
scTNF$_{R2}$	TNFR2-selective scTNF
SDS-PAGE	sodium dodecyl sulfate polyacrylamide gel electrophoresis
s	second
SEM	standard error of the mean
sTNF	soluble tumor necrosis factor
sTNFR	soluble tumor necrosis factor receptor
TACE	tumor necrosis factor-α converting enzyme
TEMED	N,N,N′,N′-tetramethylethan-1,2-diamin
TNC	tenascin C
TNC-scTNF$_{R2}$	TNFR2-selective scTNF fused to the trimerization domain of tenascin C
TNF	tumor necrosis factor
TNF-A546	tumor necrosis factor-Alexa-Fluor546
TNFR	tumor necrosis factor receptor
TRADD	TNF receptor type 1-associated death domain protein
TRAF	TNF receptor-associated factor
Treg	regulatory T cell
TRIS	tris(hydroxymethyl)aminomethane
TUNEL	TdT-mediated dUTP-FITC nick end labeling
U	units
UV	ultraviolet
V	volt
v/v	volume/volume
w/v	weight/volume
XIAP	X-linked inhibitor of apoptosis protein
µg	microgram (10^{-6} g)
µl	microliter (10^{-6} l)
µM	micromolar (10^{-6} M)

Summary

Tumor necrosis factor (TNF) exerts its biological functions via two distinct receptors. Whereas the TNF receptor (TNFR) 1 mainly mediates inflammatory responses, the TNFR2 is involved in tissue protection and regeneration. Accordingly, TNF variants selectively activating TNFR2 could potentially be useful as therapeutic regimen in a variety of diseases. In this study, there was developed a TNFR2-specific agonist, which may be a promising therapeutic in immune- and neurodegenerative diseases. In addition, the molecular mechanisms of TNFR2 signaling and turnover at the membrane were further unrevealed.

Endocytosis is an important mechanism to regulate TNF signaling. In contrast to TNFR1, the relevance of receptor internalization for signaling as well as the fate and route of internalized TNFR2 is poorly understood. Upon generation of a human TNFR2-expressing mouse embryonic fibroblast cell line in a TNFR1$^{-/-}$/TNFR2$^{-/-}$-background, I could demonstrate that TNFR2 was internalized together with its ligand and cytoplasmic binding partners. The internalization was dependent on a di-leucin motif in the cytoplasmic part of TNFR2 and the colocalization of the receptor-complex with clathrin suggested clathrin-mediated internalization of TNFR2. Internalization-defective TNFR2 mutants were capable to signal, i.e. activate NFκB, demonstrating that the di-leucin motif-dependent internalization is dispensable for this response. Therefore receptor internalization primarily seems to serve as a negative feed-back to limit TNF responses via TNFR2.

Soluble recombinant TNF is a strong mediator of inflammation, predominantly through TNFR1 activation, as soluble TNF is not sufficient to activate TNFR2. In contrast, the membrane-bound form of TNF (memTNF) fully activates both TNFRs. Therefore, TNFR2-specific therapeutics need to comply with two basic requirements: mimicry of memTNF and, in order to avoid dose limiting severe inflammatory responses, receptor selectivity. As a basis for the construction of a memTNF-mimetic, TNFR2-selective TNF variant, a single-chain TNF (scTNF) molecule was used, that consists of three TNF monomers fused by short peptide linkers. Introducing two amino acid exchanges (D143N/A145R) into a scTNF variant resulted in the loss of TNFR1 affinity under retention of TNFR2 binding. To mimic memTNF, such a receptor-selective single-chain TNF (scTNF$_{R2}$) was linked to the tenascin C (TNC) trimerization domain, resulting in stabilized TNC-scTNF$_{R2}$ nonamers with respect to the TNF domains. *In vitro* TNC-scTNF$_{R2}$ demonstrated memTNF-mimetic activity and exclusively activated TNFR2.

TNC-scTNF$_{R2}$-enhanced T cell activation was shown by the increased interleukin 2-dependent interferon gamma production. More revealing, TNC-scTNF$_{R2}$ increased the number of regulatory FoxP3^{+}/CD25^{+} T cells in cultures of human peripheral blood mononuclear cells, suggesting a potential role in downregulation of T cell immune responses.

In cultures of primary astrocytes TNC-scTNF$_{R2}$ induced the upregulation of ciliary neurotrophic factor, a neurotrophic factor, which enhances the formation of myelin. In addition, in *in vitro* cultures, TNC-scTNF$_{R2}$ rescued differentiated neurons from hydrogen peroxide-induced cell death.

First *in vivo* studies on the pharmacokinetic behavior and potential systemic responses in huTNFR2-transgenic mice revealed that compared to TNF, TNC-scTNF$_{R2}$ has a dramatically extended plasma half-life, yet shows no signs of systemic toxicity and thus is well tolerated even at doses several fold above the MTD of wildtype TNF. These results warrant further studies on the therapeutic usefulness of TNC-scTNF$_{R2}$ in appropriate animal models of autoimmune and neurodegenerative diseases.

Zusammenfassung

Der Tumornekrosefaktor (TNF) kann mit zwei unterschiedlichen Rezeptoren interagieren. Dabei vermittelt der TNF Rezeptor (TNFR) 1 vor allem Entzündungsreaktionen, wohingegen der TNFR2 an der Gewebeprotektion und Regeneration beteiligt ist. Demzufolge könnten TNF-Varianten, die selektiv den TNFR2 aktivieren, potentiell als Therapeutika in verschiedenen Krankheiten verwendet werden. In dieser Arbeit wurde ein TNFR2-spezifischer Agonist entwickelt, der einen vielversprechenden Ansatz zur Behandlung von immunologischen und neurodegenerativen Erkrankungen bieten kann. Zusätzlich wurden die molekularen Mechanismen der TNFR2 Signaltransduktion und der Umsatz an der Membran weiter aufgeklärt.

Ein wichtiger Mechanismus zur Regulation der Signaltransduktion von TNF ist die Endozytose des Ligand/Rezeptor-Komplexes. Im Gegensatz zum TNFR1 ist die Bedeutung der Rezeptorinternalisierung für die Signaltransduktion, sowie der Internalisierungsweg und das Schicksal des TNFR2 nur ungenügend verstanden. In einer embryonalen Fibroblasten Zelllinie aus TNFR1$^{-/-}$/TNFR2$^{-/-}$-Mäusen, die den humanen TNFR2 exprimiert, konnte ich zeigen, dass der TNFR2 zusammen mit seinem Liganden und zytoplasmatischen Bindungspartnern internalisiert wird. Die Internalisierung war abhängig von einem Di-Leucin Motiv im zytoplasmatischen Teil des TNFR2. Die Kolokalisation des TNFR2 mit Clathrin legt eine Clathrin-vermittelte Internalisierung des TNFR2 nahe. Internalisierungsdefekte Mutanten des TNFR2 konnten Signale transduzieren, z.B. NFκB aktivieren, was darauf hinweist, dass die Di-Leucin Motiv abhängige Internalisierung für diese zelluläre Antwort nicht benötigt wird. Die Internalisierung des Rezeptors dient deshalb primär als negative Rückkopplung, um TNF-Antworten über den TNFR2 zu limitieren.

Lösliches rekombinantes TNF (sTNF) ist ein starker Mediator von Entzündungsreaktionen. Da sTNF den TNFR2 nicht effizient aktiviert, wird diese biologische Antwort überwiegend durch den TNFR1 vermittelt. Im Gegensatz dazu aktiviert die membrangebundene Form von TNF (memTNF) sowohl den TNFR1 als auch den TNFR2. Demzufolge müssen Therapeutika, die spezifisch den TNFR2 aktivieren, zwei grundlegende Voraussetzungen erfüllen: Sie müssen zum Einen memTNF nachahmen und zum Anderen, um dosislimitierende, schwerwiegende Entzündungsreaktionen zu vermeiden selektiv nur den TNFR2 aktivieren. Als Grundlage zur Konstruktion einer löslichen memTNF-mimetischen und TNFR2-selektiven TNF-Variante wurde ein single-chain TNF (scTNF), welches aus drei TNF Monomeren besteht, die über kurze Peptid-Verknüpfungen verbunden sind, benutzt. Der Austausch von zwei Aminosäuren (D143N/A145R) in einer solchen scTNF-Variante führte zum Verlust der Affinität für den TNFR1, wobei die Binding an den TNFR2 nicht beeinflusst wurde. Um memTNF nachzuahmen, wurde ein TNFR2-selektives scTNF (scTNF$_{R2}$) mit der

Trimerisierungsdomäne des Tenascin C (TNC) verbunden. Dies führte zu einem stabilisierten TNC-scTNF$_{R2}$-Nonamer, bezogen auf die TNF-Domänen. *In vitro* konnte gezeigt werden, dass TNC-scTNF$_{R2}$ memTNF-mimetische Aktivität besitzt und ausschließlich den TNFR2 aktiviert.

Mit der verstärkten Interleukin-2-abhängigen Sekretion des Gamma-Interferons konnte gezeigt werden, dass TNC-scTNF$_{R2}$ zur Aktivierung von T-Zellen beiträgt. Insbesondere, weist die durch TNC-scTNF$_{R2}$ erhöhte Anzahl an regulatorischen FoxP3$^+$/CD25$^+$ T-Zellen in Kulturen von humanen mononukleären Zellen des peripheren Blutes darauf hin, dass der TNFR2 potentiell eine Rolle bei der Suppression von T-Zell-vermittelten Immunantworten spielt. In Kulturen von primären Astrozyten erhöhte TNC-scTNF$_{R2}$ die Expression des „Ciliary Neurotrophic Factor", einem neurotrophen Faktor, welcher die Myelinbildung verstärkt. Zusätzlich konnte gezeigt werden, dass TNC-scTNF$_{R2}$ in *in vitro* Kulturen differenzierte Neuronen vor dem durch Wasserstoffperoxid induzierten Zelltod schützt.

Erste *in vivo* Studien zur Pharmakokinetik und potentiellen systemischen Effekten in huTNFR2-transgenen Mäusen ergaben, dass TNC-scTNF$_{R2}$, verglichen mit TNF, eine drastisch erhöhte Plasma-Halbwertszeit zeigt und dennoch keine Zeichen von akuter systemischer Toxizität aufweist. TNC-scTNF$_{R2}$ wird deshalb auch in Dosen, die deutlich über der maximal tolerierten Dosis des Wildtyp-TNFs liegen toleriert. Diese Resultate bilden die Grundlage, um weiterführende Studien zum therapeutischen Nutzen von TNC-scTNF$_{R2}$ in geeigneten Tiermodellen von Autoimmun- und neurodegenerativen Erkrankungen durchzuführen.

1. Introduction

1.1. The mammalian immune system

Disorders in the immune system can result in diseases, such as autoimmune and inflammatory diseases or even cancer. The healthy immune system protects an organism against diseases by identifying and eliminating pathogens, such as bacteria, viruses or substances that appear foreign and harmful. Therefore the immune system needs to detect a diversity of agents and distinguish them from the organism's own healthy cells and tissues.

The innate immune system serves as the first barrier of defense. It exerts a fast but non-specific immune response, which is usually triggered when common structural motifs of specific pathogens, called pathogen-associated molecular patterns (PAMP) are recognized through pattern-recognition receptors (PRR) (Medzhitov, 2007). The detection of PAMPs triggers the activation of antimicrobial responses, such as activation of tissue-resident macrophages, which coordinate local and systemic inflammatory responses and stimulate adaptive immune responses.

Adaptive immunity is mediated via specific antigen recognition by antigen receptors, which are clonally distributed on B and T lymphocytes. The high diversity of receptors is achieved by somatic recombination. Additional mechanisms, such as somatic hypermutation or gene conversion further increase the diversity (Schatz et al., 1992) leading to random specificities of antigen receptors. Antigens are taken up and presented at the surface by antigen presenting cells (APC) in the peripheral tissue. APCs deliver the antigens to immunological organs, such as the lymph nodes or spleen, where they then are detected by lymphocytes. Upon activation, lymphocytes can differentiate into several types of effector cells, depending on the class of pathogen they recognize, e.g. $CD4^+$ T helper cells (T_H) or $CD8^+$ cytotoxic T cells.

An important component of the non-specific immune response against harmful stimuli, such as pathogens, is inflammation (Ferrero-Miliani et al., 2007), a protective attempt by the organism to remove the injurious stimuli and to initiate the regeneration process (Carson et al., 2006). Inflammation can promote both cell death and cell regeneration. Under normal conditions the inflammatory process is self-limiting, but becomes continuous in some disorders. Chronic inflammatory diseases develop subsequently, such as sarcoidosis**,** psoriasis, inflammatory bowel disease, arteriosclerotic vascular disease or rheumatoid arthritis (Ferrero-Miliani et al., 2007).

1.2. Tregs suppress immune responses

Both protective and harmful immune responses are principally mediated by T and B cells, which possess enormous diversity in antigen recognition, high antigen specificity, potent

effector activity, and a long-lasting immunological memory (Sakaguchi et al., 2008). Since these mechanisms are potentially damaging, misguided or excessive immune responses that are destructive against the host and also against an allogeneic fetus in pregnancy need to be strictly controlled. In principle, self-tolerance is controlled by three mechanisms: clonal deletion, anergy and active suppression. Clonal deletion is the process by which lymphocytes against self-antigens are eliminated before they develop into fully immunocompetent lymphocytes. Anergy is a tolerance mechanism in which lymphocytes are intrinsically functionally inactivated following an antigen encounter, but remain alive for an extended period of time (Schwartz, 2003). Regulatory T cells (Treg), a specialized subpopulation of T cells, modulate the immune system by suppressing immune responses towards self and non-self antigens (Sakaguchi, 2000). Despite these powerful control mechanisms, immune reactions against self-constituents, innocuous environmental substances or commensal microbes occur under certain circumstances, and can lead to autoimmune diseases, allergy and chronic inflammatory diseases (Sakaguchi et al., 2007).

The thymus produces potentially pathogenic self-reactive T cells as well as functionally mature $CD4^+$ Tregs with an autoimmune-suppressive activity. Antigen-specific Tregs migrate to regional lymph nodes, where tissue-specific self-antigens or microbial antigens are presented. Upon antigen exposure, Tregs become activated, proliferate and exert suppression at much lower concentration of antigen than naïve T cells (Sakaguchi et al., 2008). Disruption in the development or function of Tregs is considered to be a primary cause of autoimmune and inflammatory diseases.

FoxP3 (forkhead box P3), a member of the forkhead/winged-helix family of transcription factors is essential for Treg development and function (Fontenot et al., 2003; Hori et al., 2003). A cardinal feature of FoxP3 natural Tregs is that, unlike the majority of thymus-produced naïve T cells, they are already functionally mature and “antigen-primed” in the thymus, before encountering an antigen in the periphery (Itoh et al., 1999; Sakaguchi et al., 1982). Mutations in the human FOXP3 gene cause the genetic disease IPEX (immune dysregulation, polyendocrinopathy, enteropathy, X-linked syndrome), which is characterized by autoimmune disease in multiple endocrine organs, IBD (inflammatory bowel disease) and severe allergy (Bennett et al., 2001). $CD4^+FoxP3^+$ regulatory T cells have been referred to as "naturally-occurring" Tregs. Together with the CD25 molecule (IL-2 receptor α-chain), a component of the high-affinity IL-2 (interleukin-2) receptor (IL-2R), these markers define a subset of suppressive Tregs (Asano et al., 1996; Sakaguchi et al., 1995). Since IL-2 is a key growth and survival factor for natural Tregs, CD25 is an indispensable molecule for their development and maintenance (Sakaguchi et al., 2008). IL-2 was previously considered to be a major cytokine for T cell proliferation and differentiation, since it mediates the differentiation of $CD4^+$ T cells to Th1 and Th2 cells and leads to the expansion of

$CD8^+$ memory T cells and natural killer cells. But interestingly, mice lacking IL-2 do not exhibit serious defects in T cell differentiation and function. Instead, these mice spontaneously develop T cell-mediated fatal lymphoproliferative/inflammatory disease with autoimmune components (such as hemolytic anemia and lymphocytic infiltration into multiple organs) and hyper reactivity to commensal microbes (Malek and Bayer, 2004). Mice deficient in CD25 or CD122 (another component of the IL-2R) also succumb to a similar set of ailments, generally called IL-2 deficiency syndrome (Sakaguchi et al., 2008).

1.3. Is the central nervous system really immune privileged?

The central nervous system (CNS, comprising spinal cord and brain), which coordinates all physiological and cognitive processes, is surrounded by the meninges, a membrane system consisting of three layers (dura mater, arachnoid mater and pia mater). The subarachnoid space between the arachnoid and pia mater contains the cerebrospinal fluid (CSF) that serves as a basic mechanical and immunological protection to the brain.

Electrochemical signals are processed and transmitted by neurons, highly specialized cells that are composed of a cell body (soma), dendrites and an axon. The dendrites receive the signals, which then are conducted along the axon and transmitted via chemical synapses to other neurons. The axons are engulfed by the membranous extensions of oligodendrocytes, which form the myelin sheath. The myelin sheath electrically insulates the axons, exerts an important role in signal transmission and mechanically protects the neurons. In addition to their sustaining and protective role, oligodendrocytes provide trophic support for neuronal somas (McTigue and Tripathi, 2008). Injuries of the myelin sheath therefore lead to serious consequences, such as reduced signal transmission or loss of axons and are associated with several neuroinflammatory or neurodegenerative diseases.

The CNS is an organ that is essential for survival and therefore clearly must be defended from pathogens (Carson, 2002). For a long time, the CNS has been considered to be immunological inert. But this view was recently reconsidered. It has been a subject of debate for several years, which is the role of the immune system in maintaining homeostatic CNS function versus promoting neurodegeneration due to autoimmune reactions against components of the CNS (Carson et al., 2006). For a long time the CNS was believed to be separated from the peripheral immune system (immune privileged), because the blood-brain-barrier (BBB), a tightly regulated barrier formed by tight junctions between the endothelial cells of the brain capillaries, provides a physical separation of the CNS from the systemic blood circulation. The formation and regulation of the BBB requires the interaction of endothelial cells with astrocytes and pericytes, which surround the endothelial cells and provide additional biochemical and mechanical support. The tight junctions between endothelial cells limit the controlled entry of blood-borne metabolites and toxins into the

brain, thereby playing a key role in brain homeostasis and protection against toxic compounds and pathogens (Abbott et al., 2010; Cardoso et al., 2010). Specialized transporters at the luminal side regulate the selective transport of metabolites. The loss of BBB integrity leads to the sudden influx of peripheral leukocytes and blood-borne and toxic substances, thereby directly inducing neuronal stress and activation of CNS innate immune responses (Cardoso et al., 2010).

Over the last years there has been a dramatic revalidation of the type of immune response that can occur within the CNS. Current data indicate that the CNS is immune competent and actively interacts with the peripheral immune system (Cardoso et al., 2010). Inflammation is also recognized as a prominent feature of many neurodegenerative diseases. Similar to inflammation in peripheral organs, neuroinflammation is now realized to have both neuroprotective and neurotoxic aspects (Stoll et al., 2002). Recent data suggest that maintenance of normal CNS function and induction of regeneration may depend on the initiation of specific types of immune response (Polazzi and Contestabile, 2002). According to the current view the immune privilege of the CNS refers only to the specific inhibition of initiating adaptive proinflammatory immune responses. In contrast, innate immune responses, especially the recruitment and activation of peripheral macrophages to the CNS and the activation of microglia, the resident macrophages of the CNS, are readily initiated, e.g. by tissue damage or cytokine overexpression (Carson et al., 2006). Important proinflammatory cytokines, which play major roles in neurodegenerative and autoimmune diseases, include interleukins, interferons, e.g. interferone gamma, and tumor necrosis factor.

1.4. Tumor necrosis factor

Tumor necrosis factor (TNF, formerly also termed TNFα) is a key player in the initiation and orchestration of inflammation and immunity (Aggarwal, 2003), which is produced as a soluble cytokine upon activation of the immune system. TNF is synthesized as a monomeric type II transmembrane protein (memTNF; 26 kDa) that self-assembles into non-covalently linked homotrimers (Kriegler et al., 1988; Locksley et al., 2001). Proteolytic cleavage of the ectodomain by TNFα-converting enzyme (TACE/ADAM17), a member of the ADAM (A Disintegrin And Metalloproteinase protein) family of matrix metalloproteases (MMP), results in the release of soluble circulating TNF-homotrimers (sTNF; 51 kDa) (Black et al., 1997). Trimeric sTNF tends to irreversibly dissociate at subnanomolar concentrations, thereby losing its bioactivity (Smith and Baglioni, 1987).

TNF can bind to two structurally distinct membrane receptors, termed TNF receptor 1 (TNFR1; CD120a) and TNF receptor 2 (TNFR2; CD120b), both belonging to and name-giving for the TNF receptor (TNFR) super family (Locksley et al., 2001). TNFR1 and TNFR2

have marked differences in expression patterns, structure, signaling mechanisms and function. In relation to the cell type, the ratio of the expression levels of TNFR1 or TNFR2 and the signaling-mechanisms, induced by these receptors typically vary. Whereas TNFR1 is expressed constitutively on practically every cell type and tissues, expression of TNFR2 is highly regulated and seems to be restricted to cells of the immune system as well as to neuronal and endothelial cells.

TNFR1 and TNFR2 each contain four cysteine rich repeats (CRR) in their extracellular domains. These CRR interact with the lateral grooves formed by two individual TNF monomers (Banner et al., 1993; Naismith et al., 1996). The preligand binding assembly domain (PLAD) in the membrane distal cysteine rich domain mediates homophilic interaction of receptor molecules in the absence of a ligand. It was proposed that this keeps receptors in a silent, homo-multimerized state and antagonizes spontaneous auto-activation (Chan et al., 2000). Ligand-binding to the preformed TNF receptor complex either induces an activating conformational change or it allows the formation of higher-order receptor complexes to activate downstream signaling (Wajant et al., 2003).

Stoichiometry analysis revealed differences in ligand/receptor interactions between TNFR1 and TNFR2 (Boschert et al., 2010). Covalently stabilized TNF muteins (single-chain TNF, scTNF) with functionally deleted individual receptor binding sites resulted in TNF mutants capable to only bind to one or two receptor molecules, rather than three. For TNFR2, functional abrogation of two receptor-binding sites showed a strong decrease in affinity and bioactivity. In contrast, TNFR1 ligand-binding and receptor activation was only affected after functional deletion of all three receptor-binding sites. Therefore avidity seems to be an important factor for TNF-binding and downstream signaling of TNFR2 (Boschert et al., 2010).

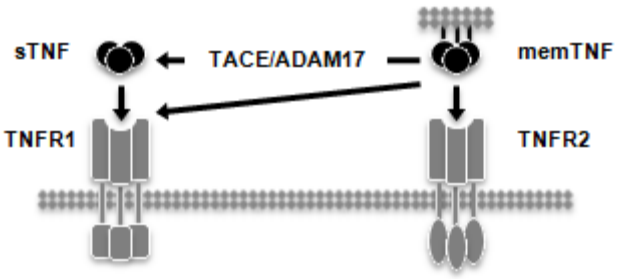

Figure 1: TNF and the TNF receptors. TNF is synthesized as a trimeric transmembrane protein (memTNF). Proteolytic cleavage by TACE/ADAM17 results in the release of soluble TNF (sTNF) trimers. Both TNF forms can activate TNFR1, whereas TNFR2 is only fully activated by memTNF.

Soluble and transmembrane TNF differ in their capability to stimulate signaling via TNFR1 and TNFR2 (Figure 1). Binding of either sTNF or memTNF can activate TNFR1, whereas TNFR2 is only fully activated by memTNF (Grell et al., 1995). The reason for this difference is not fully understood yet, but the different association/dissociation kinetics of the individual

ligand/receptor complexes may contribute to this. Whereas sTNF shows a remarkably high affinity for TNFR1 (K_d = 1.9x10^{-11} M), the affinity for TNFR2 is significantly lower (K_d = 4.2x10^{-10} M) (Grell et al., 1998). It was proposed that the high affinity for TNFR1 is mainly caused by stabilization of the ligand/receptor complexes, while transient binding of sTNF to TNFR2 results in short-lived complexes (Grell et al., 1998) which may be inefficient to induce intracellular signaling (Krippner-Heidenreich et al., 2002).

Both receptors can be regulated by proteolytic cleavage and shedding of the extracellular domain (Reddy et al., 2000; Solomon et al., 1999; Wallach et al., 1991). The intracellular domains of the TNF receptors that do not possess any enzymatic activity define the TNFRs as representatives of the two main subgroups of the TNF receptor family: the DD-containing receptors and the TRAF-interacting receptors, respectively (Wajant et al., 2003).

1.4.1. TNFR1 signaling

TNFR1 initiated signaling is well characterized and includes pathways such as nuclear factor κB (NFκB), c-Jun N-terminal protein kinase (JNK), p38 MAPK (mitogen-activated protein kinase) cascades and apoptosis. The intracellular tail of TNFR1 contains a death domain (DD) (Tartaglia et al., 1993a). Ligand-induced trimerization of the receptor leads to the formation of the TNFR1 signaling complex. The DD is recognized by the adaptor protein TNF receptor associated death domain (TRADD) (Hsu et al., 1995), which acts as an assembly platform for the binding of TNF receptor associated factor (TRAF) 2 via its carboxy-terminal TRAF domain and the DD-containing protein kinase receptor interacting protein 1 (RIP1) via direct interactions between the DDs (Hsu et al., 1996a; Hsu et al., 1996b). RIP1 can interact with TRAF2 via its amino-terminal kinase domain and its central intermediate domain (Hsu et al., 1996a). However both molecules can be independently recruited into the TNFR1/TRADD complex (Devin et al., 2000). In addition cIAP (cellular inhibitor of apoptosis protein) 1 and cIAP2 associate with TRAF2 (Rothe et al., 1995).

Activation of TNFR1 initiates a specific type of ubiquitin signal, consisting of Lys63-linked ubiquitin polymers (Figure 2; Ghosh and Hayden, 2008). The attachment of Lys63-linked ubiquitin chains to receptor substrates such as RIP1 or TRAFs is catalyzed by the Lys63-specific E2 complex Ubc13-Uev1a together with a set of E3 ligases, including TRAFs (Deng et al., 2000) and IAPs (Varfolomeev et al., 2008).

Both TRAF2 and RIP1 are involved in the IκK-dependent activation of the NFκB pathway, which regulates the expression of a high diversity of genes that are involved in immunity, inflammation and inhibition of apoptosis (Ghosh and Hayden, 2008). The IκK (IκBα kinase) complex is composed of two catalytic subunits, IKKα (IκK1) and IKKβ (IκK2) and a regulatory subunit NEMO (NFκB essential modulator, IKKγ) (DiDonato et al., 1997; Mercurio et al., 1997; Rothwarf et al., 1998).

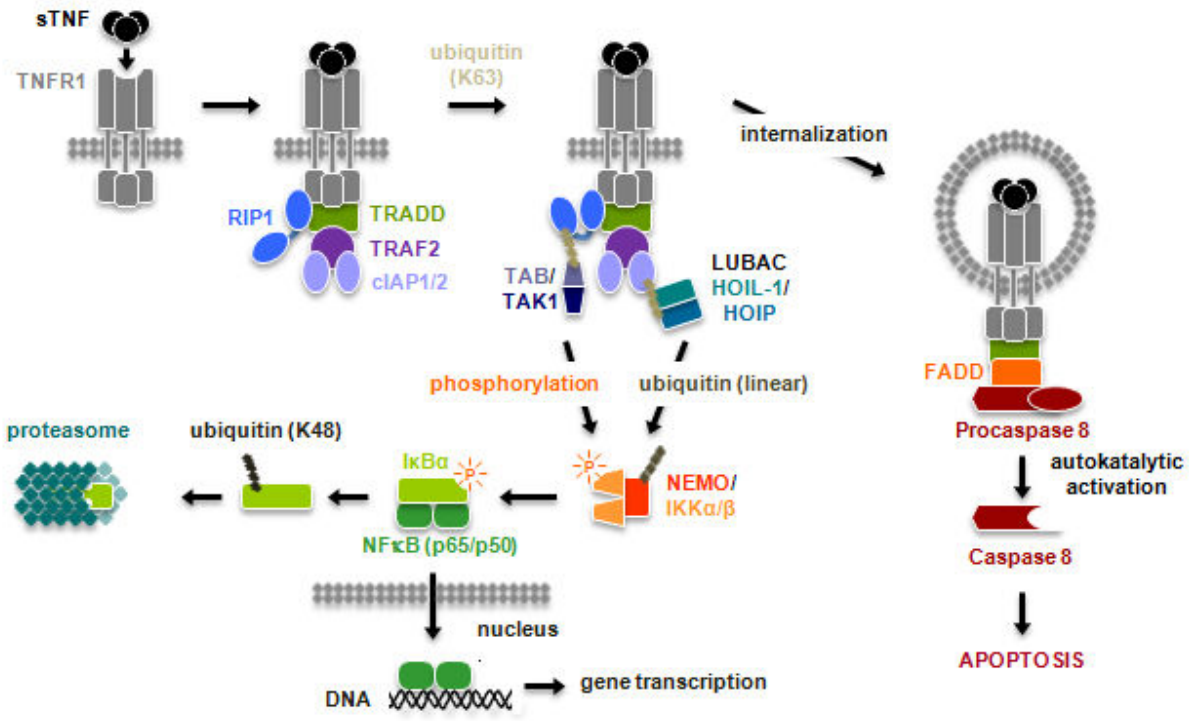

Figure 2: Signaling pathways mediated via TNFR1. Binding of TNF to TNFR1 triggers the formation of the TNFR1 signaling complex, composed of TRADD, RIP1, TRAF2 and cIAP1/2. The TRAF2-associated E3 ligases cIAP1 and cIAP2, and possibly TRAF2, modify RIP1 and themselves with Lys(K)63-linked ubiquitin chains. This modification leads to the recruitment of the TAB/TAK1 complex to RIP1 and LUBAC to cIAP1/2. Both complexes independently activate the IκK complex, resulting in induction of the NFκB pathway. Internalization of TNFR1 leads to the dissociation of RIP1/TRAF2/cIAP1/2 and association of FADD and procaspase 8. Autokatalytic activation of procaspase 8 then triggers the apoptotic signaling pathway.

It is believed that RIP1 is Lys63-ubiquitinated by TRAF2 and cIAPs (Bertrand et al., 2008; Kreuz et al., 2001) thereby providing a platform for the binding of NEMO. The adaptor proteins TAB2/3 (TAK1 binding protein 2/3) bind to Lys63-conjugated substrates, resulting in activation of IKKα/β by its upstream kinase TAK1 (transforming growth factor β-activated kinase 1) and subsequent activation of NFκB (Ghosh and Hayden, 2008; Kanayama et al., 2004). However Ubc13-deficient mice elicit normal NFκB activation (Chiu et al., 2009; Yamamoto et al., 2006), indicating that additional E2 ligases participate in Lys63-chain production.

In addition it has been recently demonstrated that the E3 ligase complex LUBAC (linear ubiquitin chain assembly complex), composed of HOIL-1L (longer isoforms of haem-oxidized iron-regulatory protein ubiquitin ligase 1) and HOIP (HOIL-1L interacting protein) is directly recruited to TNFR1 (Haas et al., 2009) and regulates the canonical NFκB pathway independently of Lys63-chains by generating linear ubiquitin chains (Kirisako et al., 2006; Tokunaga et al., 2009). LUBAC recruitment to TNFR1 is dependent on TRADD, TRAF2 and cIAP1/2, whereas RIP1 and NEMO are not required. Recent studies suggest that LUBAC is

recruited to the TNFR1 signaling complex via cIAP-generated ubiquitin chains. NEMO contains an ubiquitin-binding motif (UBAN), which binds significantly stronger to linear ubiquitin then compared to Lys63-linked chains (Lo et al., 2009). This interaction plays a crucial role in the TNF-induced activation of the IκK complex and NFκB (Rahighi et al., 2009). LUBAC can activate NFκB in Ubc13-deficient MEFs, emphasizing that LUBAC-mediated linear ubiquitination of NEMO has a distinct role from Lys63-chains in TNF-induced NFκB activation (Tokunaga et al., 2009). These data, which indicate a new mechanism for activation of the IκK complex are in line with recent evidence suggesting that RIP1 is not essential for TNFR1-induced activation of NFκB (Wong et al., 2010) and indicate that activation of NFκB is regulated by complex mechanisms.

The NFκB family is composed of five transcription factors (p50, p52, p65/RelA, Rel and RelB) arranged in homo- or heterodimers. All members share the conserved Rel homology domain (RHD), which is responsible for dimerization, nuclear localization, DNA-binding and interaction with members of the inhibitor of κB (IκB) protein family (Wajant et al., 2003). In an uninduced state, IκBα is bound to NFκB dimers to mask their nuclear localization signal (NLS), thereby sequestering the ternary complex of NFκB/IκB in the cytoplasm. Activation of the IκK complex leads to the initiation of the canonical NFκB pathway. The catalytic subunits of the activated IκK complex phosphorylate IκBα on two serine residues (serine 32, serine 36; Regnier et al., 1997; Woronicz et al., 1997) resulting in the dissociation of the NFκB/IκBα complex and subsequently leading to ubiquitination of IκBα with Lys48-linked chains by $SCF^{\beta TrCP}$ (Skp1-cullin-F-box (βTrCP)ubiquitin) thereby targeting it for proteasomal degradation (Ghosh and Hayden, 2008). The released NFκB dimers then can enter the nucleus and induce gene transcription.

The nuclear translocation of NFκB is controlled by two main pathways: the classical, canonical pathway described above and the alternative, non-canonical pathway, through which NFκB dimers containing the p52-precursor p100 are activated. Within the alternative pathway, activation of NFκB-inducing kinase (NIK), a member of the MAP3K family which associates with TRAF2 (Malinin et al., 1997) leads to the phosphorylation and subsequent proteasomal processing of p100 into the mature p52 subunit (Bonizzi et al., 2004). The phosphorylation of p100 leads to limited proteolytic processing in which only the IκB-homologous region within p100 is degraded. The resulting p52 fragment and its dimerization partner, mainly RelB, then can translocate to the nucleus (Ramakrishnan et al., 2004). Regulation of the two pathways, e.g. through prolonged or transient receptor recruitment of the IκK complex seems to be stimulus and cell type dependent (Ramakrishnan et al., 2004).

Interestingly, ligand-induced internalization of TNFR1 leads to the modification and dissociation of the TRADD/RIP1/TRAF2 complex and association of Fas associated DD (FADD) thereby causing a switch from anti-apoptotic to pro-apoptotic signaling (Hsu et al., 1996b; Figure 2). Subsequently procaspase 8 is recruited to the death effector domain (DED) of FADD (Boldin et al., 1996), leading to the assembly of the death inducing signaling complex (DISC) (Micheau and Tschopp, 2003; Schneider-Brachert et al., 2004). The elevated local concentration of procaspase 8 leads to its autoproteolytic activation. Activated initiator caspase 8 then triggers the activation of effector caspase 3. In “type I” cells this signal is sufficient to induce the execution phase of apoptosis via the caspase cascade (Schulze-Osthoff et al., 1998). “Type II” cells are dependent on the processing of the pro-apoptotic Bcl-2 (B-cell lymphoma 2) family member Bid (BH3 interacting domain death antagonist) by Caspase 8 (Gross et al., 1998; Wang et al., 2006a; Zhao et al., 2001). The truncated carboxy-terminal fragment of Bid (tBid) then translocates to the mitochondria where it can interact with other Bcl-2 family members and promotes the oligomerization of Bax (Bcl-2–associated X protein) and Bak (Bcl-2 homologous antagonist/killer), leading to the mitochondrial release of cytochrome c, APAF1 (apoptotic protease activating factor 1) and Smac/Diablo (second mitochondria-derived activator of caspases/direct IAP binding protein with low PI). APAF1 binds to cytochrome c and procaspase 9 to from the apoptosome. Activation of caspase 9 within the apoptosome subsequently leads to activation of effector caspase 3, which then activates caspase 8 outside of the DISC, leading to an amplification of the apoptotic signal (Schütze et al., 2008; Wajant et al., 2003).

In addition to the action of the apoptosome, Smac/Diablo binds and antagonizes the caspase inhibitors XIAP (X-linked inhibitor of apoptosis protein) and cIAP1 and cIAP2. The anti-apoptotic proteins cIAP1 and cIAP2 have diverse functions within TNF signaling. Together with TRAF1 and TRAF2, they promote the NFκB pathway by their ubiquitin ligase activity, are themselves target genes of NFκB transcriptional activity and indirectly regulate TNFR1 mediated apoptosis by blocking activation of caspase 8 (Wang et al., 1998).

1.4.2. TNFR2 signaling

TNFR2 elicits a variety of non-apoptotic cellular responses, such as proliferation of thymocytes (Tartaglia et al., 1993b; Tartaglia et al., 1991) differentiation and survival of T-cells (Kim et al., 2006; Kim and Teh, 2001), proliferation of myofibroblasts (Theiss et al., 2005) and angiogenesis (Pan et al., 2002). In contrast to the wealth of molecular details known about TNFR1-mediated signaling pathways, less is known about the respective mechanisms of TNFR2 signaling (Figure 3). Upon stimulation TRAF2 is directly recruited to TNFR2 (Boucher et al., 1997; Rothe et al., 1994), leading to the activation of cIAPs, induction of the JNK pathway and translocation of the transcription factor NFκB to the nucleus (Jupp et

al., 2001; Rao et al., 1995; Rothe et al., 1995). In addition, the protein kinase PKB/Akt is activated dependent on the phosphatidylinositol 3-kinase (PI3K) (Nicholson and Anderson, 2002) by TNFR2, but the molecular link between TNFR2 and PI3K is unknown yet. PI3K converts the plasma membrane lipid phosphatidylinositol-4,5-bisphosphate (PIP2) to the second messenger phosphatidylinositol 3,4,5-bisphosphate (PIP3) by phosphorylation of the D3 hydroxyl group of the inositol ring (Cantley, 2002). Signaling proteins with pleckstrin-homology (PH) domains, such as PKB/Akt and PDK-1 (3-phosphoinositide dependent protein kinase-1) accumulate at sites of PI3K activation by direct binding to PIP3 (Lawlor and Alessi, 2001). After recruitment to the plasma membrane PKB/Akt is thought to undergo a conformational change. Phosphorylation at residue serine 473 in the hydrophobic motif by the Rictor/mammalian target of rapamycin (mTOR) complex (Sarbassov et al., 2005) and at residue threonine 308 in the activation loop (T loop) of the kinase domain by PDK-1 stimulates the catalytic activity of PKB/Akt (Alessi, 2001).

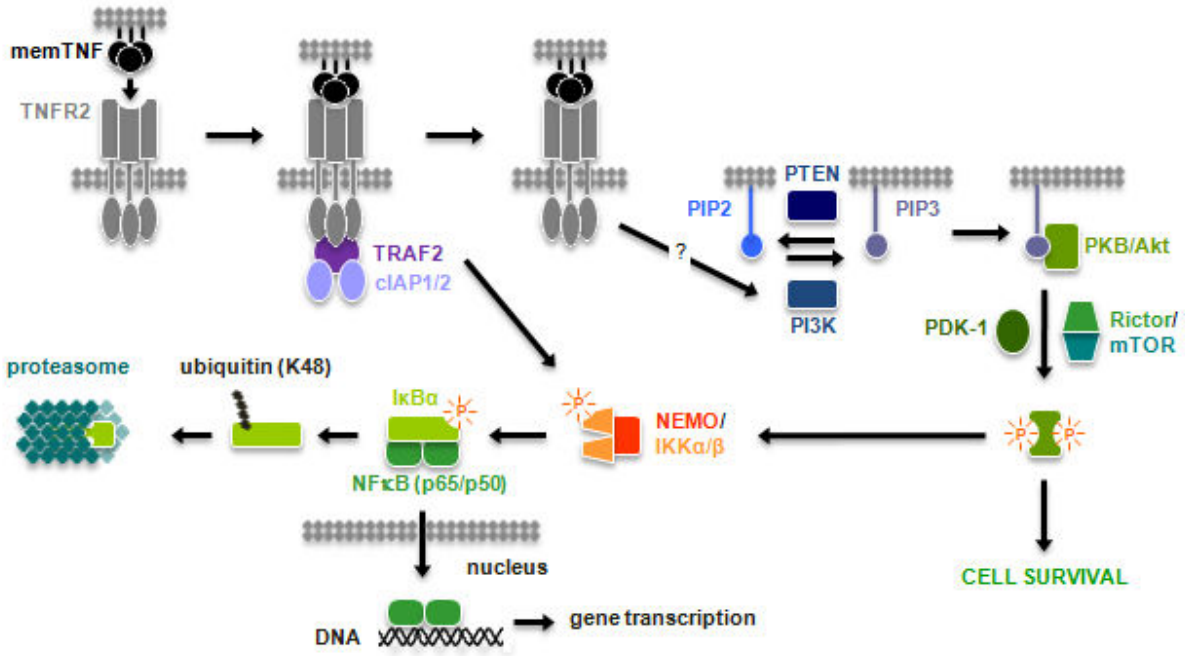

Figure 3: Signaling pathways mediated via TNFR2. Binding of TNF to TNFR2 induces the recruitment of TRAF2 and cIAP1/2. Activation of the IκK complex results in induction of the NFκB pathway. In addition, PI3K is activated via a yet unknown molecular link to TNFR2. Activated PI3K converts PIP2 to the second messenger PIP3, which recruits PKB/Akt to the plasma membrane, where it is activated by phosphorylation. PKB/Akt activates the NFκB pathway and induces multiple cellular survival pathways.

The kinase phosphorylates several proteins that affect cell growth, proliferation, and survival. Most of the known protein targets of PKB/Akt are inhibited by the phosphorylation event (Cantley, 2002). PKB/Akt plays a key role in oncogenesis and was originally identified as the oncogene *v-akt* of the transforming retrovirus from an AKR mouse T-cell lymphoma (Testa

and Tsichlis, 2005). PKB/Akt signaling therefore needs to be tightly controlled. The tumor suppressor phosphatase and tensin homolog (PTEN) is a negative regulator of PKB/Akt activity. PTEN dephosphorylates the D3 hydroxyl group of PIP3 and can therefore regulate the activity of PKB/Akt. Loss of the PTEN protein or function has been found in human cancers, indicating that uncontrolled signaling through PI3K contributes to metastatic cancers (Maehama and Dixon, 1999).

The mechanisms by which PKB/Akt protects cells from cell death are multifactorial. PKB/Akt phosphorylates and inhibits several pro-apoptotic proteins, such as Bad (Bcl-2-associated death promoter) and caspase 9. Bad is associated with the anti-apoptotic protein Bcl-X_L (B-cell lymphoma-extra large) thereby forming non-functional heterodimers. Phosphorylation of Bad prevents this interaction and thereby restores the anti-apoptotic functions of Bcl-X_L (Datta et al., 1997). Additionally PKB/Akt phosphorylates and activates the IκK complex, leading to the activation of the NFκB pathway (Romashkova and Makarov, 1999). This appears of particular relevance in neuroprotection and regeneration. E.g., primary neurons are spared from glutamate-induced excitotoxicity *in vitro* in a PI3K-PKB/Akt-dependent manner (Dolga et al., 2008; Marchetti et al., 2004). In addition, TNFR2 signaling promotes neuronal survival and oligodendrocyte regeneration in *in vivo* models of ischemic and neurotoxic insults (Arnett et al., 2001; Fontaine et al., 2002), respectively.

TNFR2 does not contain a DD and therefore cannot directly induce apoptosis. Nevertheless, TNFR2 has been described to exert pro-apoptotic functions in the context of limiting an immune response after injury or during resolving inflammations (Aggarwal, 2003). TNFR2 can indirectly induce apoptosis by upregulation of memTNF levels leading to elevated sTNF levels through ectodomain shedding, which then secondarily induce TNFR1-dependent apoptosis (Grell et al., 1999; Vercammen et al., 1995). Other experimental models have shown that the pro-apoptotic function of TNFR2 depends on the intracellular crosstalk with TNFR1 (Fotin-Mleczek et al., 2002). TRAF2 mediates the recruitment of cIAP1 and cIAP2 to TNFR2 (Rothe et al., 1995; Shu et al., 1996). Depletion of the TRAF2/cIAP1/cIAP2 complex results in limited cytosolic levels of the proteins. Hence TNFR2-dependent enhancement of TNFR1-induced apoptosis appears to be based on two mechanisms: first, the competitive recruitment of cytosolic TRAF2 and the TRAF2-associated proteins cIAP1 and cIAP2 and second, the cIAP1 and cIAP2 initiated depletion of TRAF2, which in turn enhances competition for the remaining TRAF2, cIAP1 and cIAP2. Therefore cIAPs can switch from an anti-apoptotic function to a pro-apoptotic function associated with TNFR2 (Wajant et al., 2003).

1.5. Signaling modulation by endocytosis

Endocytosis is characterized by the internalization of transmembrane receptors into internal membrane compartments. The endocytic trafficking can be divided into two main pathways: the classic, clathrin-mediated endocytic pathway and the non-classic, clathrin-independent routes (Le Roy and Wrana, 2005). The clathrin-mediated endocytosis is the best-characterized mechanism for the entry of molecules into the cell. Its central feature is the recruitment of soluble clathrin to the plasma membrane. Clathrin has a three-legged structure, called triskelion, formed by three clathrin heavy chains, each with a tightly associated clathrin light chain. The clathrin triskelia assemble into a polygonal lattice at the plasma membrane to form coated pits that bud and pinch off from the membrane (Le Roy and Wrana, 2005). The formation of the clathrin coat and the initiation of the budding process is stimulated by the direct binding of adaptor-protein complexes, such as Adaptor-protein 2 (AP2) and epsin to clathrin, other endocytic regulatory proteins and cargo (Le Roy and Wrana, 2005). The non-classic clathrin-independent endocytic pathways are less well characterized. One important route includes the protein caveolin, which induces the formation of caveolae at the cell surface (Le Roy and Wrana, 2005). Caveolae, a special type of cholesterol-rich microdomains, are sphingolipid- and cholesterol-rich flask-shaped invaginations of the plasma membrane, in which many diverse signaling molecules and membrane transporters are concentrated (Anderson, 1998; Rothberg et al., 1992). Caveolin is a dimeric protein that binds cholesterol, inserts a loop in the inner plasma membrane and self-associates to form a caveolin-coat on the surface of the membrane invaginations (Conner and Schmid, 2003).

Receptor internalization is a widely used mechanism to modulate signaling. Binding of ligands to their cognate receptors typically trigger internalization, leading to transient receptor clearance from the surface, followed by either recycling to the plasma membrane or lasting clearance by degradation in late endosomes/lysosomes (Bonifacino and Traub, 2003).

Endocytosis has long been regarded exclusively as a mechanism to terminate signaling through receptor internalization and subsequent lysosomal degradation. However, emerging data indicate that certain signaling pathways are initiated during receptor internalization. Interestingly, certain members of the TNF receptor superfamily show a dichotomy of pro-apoptotic and anti-apoptotic signaling properties. Dependent on the subcellular localization of the ligand/receptor complex, the cellular response to death-receptor ligands is either initiation of apoptosis or induction of non-apoptotic biological processes, such as differentiation or proliferation. As described above, the type of cellular response induced by TNF is spatially controlled by internalization of the TNF/TNFR1 complex. Binding of TNF to TNFR1 at the plasma membrane results in the recruitment of membrane signal complex I and activation of

the canonical NFκB-pathway, whereas internalization of the TNF/TNFR1 complex causes a switch in the molecular composition of the signaling complex, constituting cytosolic signal complex II to induce the pro-apoptotic pathway (Micheau and Tschopp, 2003; Schütze et al., 2008). CD95 (Fas), another member of the TNF receptor family, is a key mediator of apoptosis. But recent observations suggest that CD95 can also mediate several non-apoptotic signals (Peter et al., 2007). Directly upon ligand binding FADD and procaspase-8 are recruited to CD95. After several minutes the complex is internalized in endosomal vesicles where procaspase-8 is processed and activated (Eramo et al., 2004). Blocking CD95-internalization resulted in the inhibition of DISC recruitment and apoptosis, suggesting that effective DISC assembly is dependent on CD95-internalization and the entry into an early endosomal compartment (Schütze et al., 2008). In contrast, CD95 ligand stimulation of cells unable to internalize CD95 resulted in activation of proliferative ERK and NFκB signaling pathways (Lee et al., 2006). Therefore, the subcellular localization and internalization pathways of TNFR1 and CD95 play important roles in controlling the activation of distinct signaling cascades to determine divergent cellular fates. Although it has been described that TNFR2 can be internalized after ligand binding (Pennica et al., 1992), the relevance of internalization for signal transduction and the fate of the internalized receptor are largely unknown.

1.6. The role of TNF in autoimmune and CNS diseases

1.6.1. Design of anti-TNF therapies in autoimmune diseases

Autoimmune diseases result from a failure to properly distinguish between self and non-self antigens leading to a hyperactive immune system, which is directing immune responses against normal tissue. The proinflammatory activities of TNF, which are mediated mainly through TNFR1, contribute to chronic inflammation and tissue damage. Therefore it is assumed that TNFR1 is a major mediator of TNFs pathological phenotypes (Aggarwal, 2003).

An important role of the TNF/TNFR system in inflammatory/autoimmune diseases has been early on suggested due to an apparent association of abnormalities in TNFR2, such as polymorphisms in the TNFR2 gene, upregulated expression of TNFR2 and enhanced TNFR2 shedding in several autoimmune diseases. In particular, patients with familial rheumatoid arthritis (Cope et al., 1992) or systemic lupus erythematodes (Gabay et al., 1997) who have polymorphisms in TNFR2 exhibit higher levels of soluble TNFR (sTNFR) 2, but not sTNFR1, in serum or other bodily fluids, presumably through enhanced receptor ectodomain shedding into extracellular space.

In cancer patients intravenous infusions of recombinant TNF led to higher systemic levels of sTNFR (Lantz et al., 1990) and the degree of increase correlated with the level of TNF stimulation (Jansen et al., 1995). Therefore, the production and release of sTNFRs may modulate the host response and determine the course and outcome of disease by competing with cell surface receptors and antagonizing TNF action (Diez-Ruiz et al., 1995).

The concept of increasing sTNFR levels to reduce TNF-mediated inflammation was the basis of the first anti-TNF medication for autoimmune disorders (Seckinger et al., 1988; 1989). Several TNF inhibitors, such as monoclonal antibodies or inhibitory molecules that block TNF activity, are clinically approved therapeutics and a number of new, second generation therapeutics targeting the TNF/TNFR system is currently under development for the treatment of peripheral autoimmune disorders including rheumatoid and juvenile rheumatoid arthritis, ankylosing spondylitis and Crohn's disease (McCoy and Tansey, 2008; Pfizenmaier and Szymkowski, 2011). However, even though anti-TNF therapies can reduce the disease-associated inflammation, the treatment sometimes leads to adverse effects. These can include the development of additional autoimmune diseases such as lupus erythematodes, type I diabetes, uveitis, multiple sclerosis, psoriasis as well as lymphomas (Faustman and Davis, 2010).

Since TNF has pleiotropic functions, including proinflammatory but also immune regulatory and anti-apoptotic roles, blocking all effects of TNF can be contraproductive. Because most of the proinflammatory effects of TNF are mediated by TNFR1, a more effective therapeutic approach seems to be the selective blocking of sTNF/TNFR1 signaling. Several approaches, such as the construction of TNFR1-targeting antagonists, have been developed to reach this goal. R1antTNF, a mutant TNF selectively binding to TNFR1, leads to inhibition of TNFR1 signaling (Shibata et al., 2008b) and showed therapeutic efficacy in a murine hepatitis model (Shibata et al., 2008a). ATROSAB, a humanized version of the antagonistic mouse monoclonal antibody H398 directed against human TNFR1, inhibits binding of TNF to TNFR1 and TNFR1-mediated responses at nanomolar concentrations (Kontermann et al., 2008). Another approach to neutralize sTNF signaling is the use of anti-TNF therapeutics with a dominant-negative (DN) mechanism of action (DN-TNF). These DN-TNF monomers are able to interact with native sTNF monomers to form heterotrimers with drastically reduced affinity to TNF receptors. DN-TNF therefore selectively inhibits sTNF signaling and does not interfere with memTNF signaling (Steed et al., 2003; Zalevsky et al., 2007).

The release and signaling capacity of sTNF can also be reduced by inhibition of TACE/ADAM17. Since more that 80% of the unprocessed memTNF was shown to be degraded intracellularly (Newton et al., 2001), the overall systemic sTNF levels should be decreased dramatically, thereby limiting the detrimental effects mediated by TNFR1 signaling. TACE inhibitors are in various stages of clinical development, but there are

limitations including non-specific inhibition of other MMPs and inhibition of other TACE substrates such as the TNF receptors, which may lead to undesired side effects (Moss et al., 2008). Especially the accumulation of memTNF and the inhibition of TNFR1 and TNFR2 shedding increase the risk of hepatotoxicity (Moss et al., 2008). Therefore the safety profile of TACE inhibitors needs to be further evaluated.

1.6.2. TNFR2 promotes death of autoreactive T cells

T cells proliferate and mature in the thymus. Most of these immature cells die by apoptosis during T cell education, a process essential to remove defective progenitor cells. Failures in T cell education can generate naïve autoreactive T cells, which escape from apoptosis and can enter the circulation, where they differentiate on encountering specific self-antigens (Faustman and Davis, 2009). Failed T cell education respectively clonal deletion can lead to various autoimmune diseases, including Crohn's disease, multiple sclerosis and type I diabetes.

Type I diabetes is a form of diabetes mellitus that results from autoimmune destruction of the insulin producing pancreatic islet beta cells. The absence of insulin leads to hyperglycemia. The clinical manifestations of long-lasting hyperglycemia lead to vascular damage, subsequently associated with kidney failure, heart disease, retinopathy and neuropathy (Castro et al., 2010). Although insulin replacement alleviates the symptoms and ameliorates life-threatening complications of diabetes its use cannot prevent disease-related complications in most patients (Castro et al., 2010). Type I diabetes can be caused by protein processing defects that result in a failure to kill autoreactive $CD8^+$ T cells during the process of normal development (Faustman et al., 1991; Hayashi and Faustman, 1999). These autoreactive T cells can enter the circulation and, when reaching the pancreas, they destruct the insulin-producing beta cells. Exposure to exogenous low-dose TNF specifically induces apoptosis in the pathogenic $CD8^+$ T cells but not in normal T cells. This vulnerability is due to several defects in the activation of NFκB: anti-apoptotic effects are no longer mediated and apoptosis of the cells is favored instead (Kodama et al., 2005).

In animal models administration of exogenous TNF effectively killed autoreactive T cells leading to the inhibition or reversal of type I diabetes (Kodama et al., 2003; Satoh et al., 1989). Since administration of recombinant TNF is systemically toxic (Hieber and Heim, 1994; Sidhu and Bollon, 1993) these observations cannot be translated into therapeutic approaches. It is therefore of interest that the insulin-specific autoreactive $CD8^+$ T cells can be selectively destroyed by activation of TNFR2 (Ban et al., 2008). TNFR2 stimulation has been shown to result in the generation and expansion of a subpopulation of protective Tregs (Askenasy et al., 2008; Chen et al., 2008; Nagar et al., 2010; Ryu et al., 2001) that may control the destruction of excessive $CD8^+$ T cells at sites of inflammation by inhibition of

proinflammatory cytokines and the release of immunomodulatory cytokines leading to the regeneration of the inflammatory site (Askenasy et al., 2008). Since TNFR2 has a more restricted expression profile, agonists specifically activating the TNFR2 pathway hold promise as a safer and efficient treatment for autoimmune diseases associated with autoreactive $CD8^+$ T cells.

1.6.3. Blocking of TNF signaling exacerbates MS symptoms

Multiple sclerosis (MS) is another disease, which is associated with autoreactive $CD8^+$ T cells. MS is an inflammatory, demyelinating disease of the CNS with still an unclear and controversially discussed etiology. The location of the lesions within the CNS is variable and a crucial determinant of the clinical outcome. An inflammatory reaction of autoimmune nature is believed to be the driving force of the demyelinating lesions. Autoreactive $CD8^+$ T cells dominate the lesions (Booss et al., 1983) and are a major component of the inflammatory response in MS lesions (Bien et al., 2002). In active lesions this inflammatory process is accompanied by a disturbance of the BBB (Kirk et al., 2003) and the local expression of proinflammatory cytokines and chemokines as well as their cognate receptors (Huang et al., 2000).

Complete demyelination is accompanied by acute axonal injury and loss of axons (Ferguson et al., 1997). Therefore MS patients can develop almost any neurological symptom or sign, including muscle spasms, ataxia, motor deficits and visual problems. But the adult nervous system retains the capacity to regenerate demyelinating lesions through recruitment and differentiation of oligodendrocyte progenitor cells into mature myelinating oligodendrocytes (Nait-Oumesmar et al., 1999). Remyelination is frequently encountered during early stages of MS (Prineas et al., 1989). In most of the MS patients, the disease begins with a relapsing course (relapsing/remitting MS) followed after several years by a progressive phase (secondary progressive MS). Some patients miss the relapsing/remitting phase and show a progressive form (primary progressive) from the onset (Lassmann, 2007b). Several observations suggest that inflammation is the driving force during early stages of the relapsing/remitting MS, whereas the progressive MS may be based on neurodegenerative processes (Lassmann, 2007a).

Due to the inflammatory nature of MS, targeting of the immune response is the most widely used therapeutic approach. The primary aim of the therapeutic approaches is to reduce the frequency of clinical relapses thereby reducing the probability of permanent disabilities. Corticosteroids are used to treat acute attacks, but they have no significant effect on long-term recovery. Two classes of immunomodulatory agents, interferon beta (IFN-β) and glatiramer acetate (GA) are approved for treatment of MS. They shift immune responses from proinflammatory autoimmune conditions towards more beneficial anti-inflammatory

circumstances (Neuhaus et al., 2003). However, IFN-β and GA have limited efficiency and only part of the patients benefit from the therapy. The recently approved therapeutic Natalizumab (Tysabri), a humanized monoclonal antibody against the cellular adhesion molecule α4-integrin, restricts migration of immune cells across the BBB thereby reducing relapse rates and disease progression (Polman et al., 2006). But the safety profile of the drug has to be further evaluated after the occurrence of progressive multifocal leukoencephalopathy (Adelman et al., 2005). Mitoxantrone, an immunosuppressive agent, is used to treat progressive forms of MS and has been shown to delay disability progression (Hartung et al., 2002). But Mitoxantrone treatment leads to severe side-effects, including cardiomyopathy and therefore the medication period is limited to a total life-time dose rate (Fox, 2006). It is obvious that due to their wide spectrum of activity, limited efficiency and responsiveness or serious side-effects of all presently approved MS drugs, the therapeutic approaches need to be improved.

Patients with MS show elevated TNF levels at the site of active lesions (Hofman et al., 1989) and TNF levels correlate with the severity of the lesion (Sharief and Hentges, 1991). CNS-specific overexpression of TNF in transgenic mice showed infiltration of $CD4^+$ and $CD8^+$ T cells, astrocytosis, microgliosis and chronic inflammatory demyelination (Probert et al., 1995). Therefore TNF signaling has been implicated as an important factor for the onset of demyelinating diseases and anti-TNF therapies were evaluated in mouse models of MS. Neutralizing anti-TNF antibodies or receptor fusion proteins were protective in experimental autoimmune encephalomyelitis (EAE) mouse models of autoimmune demyelination (Selmaj et al., 1995; Selmaj et al., 1991a; Selmaj and Raine, 1995). Based on the promising results in the animal models, Lenercept, a recombinant TNFR1 immunoglobulin fusion protein (sTNFR1-IgG), was evaluated in MS patients. But a phase II randomized, multi-center, placebo-controlled study had to be stopped since there were no significant differences on magnet resonance imaging measurement between treatment groups and exacerbations were significantly increased compared with patients receiving placebo. Neurologic deficits tended to be more severe in the lenercept treatment groups (The Lenercept Study Group, 1999). Additionally, subsequent to anti-TNF therapies of juvenile rheumatoid arthritis, some patients developed MS-like exacerbations and demyelinating lesions were observed (Sicotte and Voskuhl, 2001). With the failed Lenercept trial, it became apparent that the mechanistic understanding of the cytokine-driven pathogenesis in MS is limited and the specific role and mechanisms of TNF action in this disease needed further investigations to derive new therapeutic concepts.

1.6.4. TNFR2 can promote neuronal regeneration

Ischemia results from a restriction of the blood supply to an organ. An ischemic insult leads to hypoxic or anoxic tissue causing tissue damage or dysfunction. Especially the tissues with a high oxygen demand, heart and brain, are dependent on permanent supply and therefore ischemia can lead to myocardiac infarction and stroke, respectively.

Unexpectedly, several ischemic animal models revealed a protective or regenerative role of TNFR2 signaling. Thus, whereas TNFR1 apparently promoted tissue destruction in a murine model of retinal ischemia, TNFR2 was protective via activation of the PKB/Akt pathway (Fontaine et al., 2002). Inhibition of sTNF signaling through intraventricular infusion of an anti-TNF therapeutic (sTNFR1 linked to polyethylene glycol) or through systemic administration of a TACE inhibitor resulted in reduced focal cerebral ischemia (Nawashiro et al., 1997a; Wang et al., 2004). In contrast, another study demonstrated that inhibition of TNF signaling with a neutralizing TNF antibody impaired hippocampal neurogenesis after ischemic injury. Together, these data suggest that TNF signaling, probably acting via TNFR2, is necessary for neuronal regeneration after an ischemic insult (Heldmann et al., 2005). Additional studies showed that TNF inhibits seizures via TNFR2 (Balosso et al., 2005), further indicating the important role of TNFR2 in neuronal repair and neurogenesis.

Similar results were observed in demyelinating diseases. In the cuprizone-induced mouse model of demyelination and remyelination, the genomic ablation of TNF resulted in a delayed remyelination and a reduction in the pool of proliferating oligodendrocyte progenitors followed by a reduced number of mature oligodendrocytes. Analysis of mice lacking TNFR1 or TNFR2 indicated that TNFR2 is critical for oligodendrocyte regeneration (Arnett et al., 2001), suggesting that TNFR1 signaling mediates nerve demyelination, whereas signaling via TNFR2 appears to be responsible for remyelination. This dual role of TNF signaling gave an explanation for the failure of Lenercept, indicating that the inhibition of memTNF/TNFR2 signaling was the molecular basis for the aggravated symptoms in the MS patients of this trial. Accordingly, EAE disease onset and progression was suppressed in transgenic animals exclusively expressing physiologically regulated levels of memTNF, whereas the autoimmune suppressive properties of wildtype TNF were retained (Alexopoulou et al., 2006).

The ability of memTNF to preserve a subset of beneficial activities, such as immune functions like self-tolerance and resistance to infection while lacking detrimental effects shows that selective targeting of sTNF as a therapeutic strategy may offer several advantages over complete blocking of TNF in the treatment of chronic inflammatory and autoimmune diseases. Selective inhibition of sTNF/TNFR1 signaling, e.g. via DN-TNF or TNFR1 antagonizing antibodies should lead to the absence of proinflammatory and

neurodegenerative effects, but would spare TNFR2 signaling via memTNF, remaining its homeostatic functions in the brain and immune system. Activation of TNFR2 signaling via TNFR2-selective agonists could further promote neuroprotective and neuroregenerative effects. Since the regenerative potential of TNFR2 signaling has been shown for different organs, such as pancreas, heart and brain (Faustman and Davis, 2010), therapeutics that specifically activate TNFR2 may be protective in a variety of disorders and could be evaluated in autoimmune, heart, demyelinating and neurodegenerative diseases.

1.7. Aim of the work

The aim of the present study was twofold, first, to gain basic insights into the dynamics of TNFR2 signaling and turnover at the plasma membrane and second, the construction of a safe and efficient soluble TNFR2 agonist for the potential use as a therapeutic in autoimmune and neurodegenerative diseases.

As a model system to study TNFR2 signaling and dynamics, a stable huTNFR2-expressing cell line should be generated on a mouse TNFR negative background. For this, mouse embryonic fibroblasts from TNFR1$^{-/-}$/TNFR2$^{-/-}$-mice and huTNFR2 expression constructs were available. A stable cell line was established, characterized and used to define the so far unknown basal mechanisms of TNFR2 dynamic behavior, such as constitutive and ligand-induced turnover as well as the fate and role of internalized receptors for signaling.

Since soluble recombinant TNF is a strong mediator of inflammation, predominantly through TNFR1 activation, and TNFR2 is only fully activated by the membrane-bound form of TNF, TNFR2-specific therapeutics need to comply with two basic requirements in order to avoid dose limiting severe inflammatory responses, namely mimicry of memTNF and receptor selectivity. Therefore, a soluble TNFR2-selective agonist should be generated, which meets these criteria. This was approached by the generation of a fusion protein comprised of a TNFR2-specific single-chain TNF, composed of three covalently fused TNF monomers and the human tenascin C trimerization domain, thereby creating, with respect to TNF, a soluble nonameric ligand with the potential of efficient TNFR2 activation. The functional activity of the resulting construct was analyzed on various cell lines using different *in vitro* assays.

Concerning the potential future use as a therapeutic first assessment of the *in vivo* properties of this new TNF variant was undertaken and the systemic tolerance, as well as the pharmacokinetic behavior was investigated.

2. Materials and Methods

2.1. Materials

2.1.1. Instruments

Balances	Scale Kern EW2200-NM (Kern & Sohn, Balingen-Frommern, Germany)
	Finescale ALC110.4 (Acculab Sartorius Group, Göttingen, Germany)
Centrifuges	Heraeus Fresco 17 (Thermo, Schwerte, Germany)
	Eppendorf 5415D (Eppendorf, Hamburg, Germany)
	Eppendorf 5804R (Eppendorf, Hamburg, Germany)
Cryomicrotome	CM-3050S (Leica, Wetzlar, Germany)
Electroblotting System	Semi Dry Blotter PEGASUS (Phase, Lübeck, Germany)
Electrophoresis System	MIDI PLUS Electrophoresis Chamber (Roth, Karlsruhe, Germany)
	Mini-PROTEAN 3 Electrophoresis Cell System (BioRad, Munich, Germany)
Film Developing Machine	Agfa Curic 60 (Agfa, Düsseldorf, Germany)
Flow Cytometer	Cytomics FC500 (Beckman Coulter, Krefeld, Germany)
	FACSVantage SE + FACSDiVa Option (BD Biosciences, Heidelberg, Germany)
Gel Documentation	Camera Felix 2000, Dark hood DH-50, transilluminator UST-20M-8R (Biostep, Jahnsdorf, Germany)
Heat Block	Dry-Block DB-2D (Techne, Jahnsdorf, Germany)
HPLC System	Waters HPLC-System (Millipore, Billerica, USA),
Laboratory Incubator	Cell culture: Autoflow 4850 (NuAire, Plymouth, MN, USA)
	Bacteria: Function Line B6 73 (Thermo, Schwerte, Germany)
Magnetic Stirrer	7-2020 (neoLab, Heidelberg, Germany)
Microscope	Leica DMIL LED (Leica, Wetzlar, Germany)
	CellObserver (Carl Zeiss MicroImaging GmbH, Jena, Germany)
	LSM710 (Carl Zeiss MicroImaging GmbH, Jena, Germany)
PCR Cycler	Gradient TC-512 (Techne, Jahnsdorf, Germany)
pH meter	FiveEasy (Mettler Toledo, Giessen, Germany)
Photometer	NanoDrop ND-1000 (Peqlab, Erlangen, Germany)
	BioPhotometer plus (Eppendorf, Hamburg, Germany)
Plate Reader	Multiscan FC (Thermo, Schwerte, Germany)
	TECAN infinite M200 (Tecan Austria, Grödig, Austria)
Power Supply	EPS-300 (Amersham Pharmica Biotech, Freiburg, Germany)
Thermomixer	Thermomixer compact (Eppendorf, Hamburg, Germany)
Vortexer	444-1372 (VWR International, Bruchsal, Germany)
Water Bath	WNB 10 (Memmert, Schwabach, Germany)

Water Purification	Milli-Q Reference (Millipore, Schwalbach, Germany)
Workbench	Flow V (Varolab, Giessen, Germany)

2.1.2. Special implements and consumables

Blotting Membrane	Pure nitrocellulose blotting membrane (Pall Filtersystems, Crailsheim, Germany)
Blotting Paper	Whatman Filter Paper 703 (VWR International, Bruchsal, Germany
Cell Culture Flasks and Plates	CELLSTAR (Greiner, Frickenhausen, Germany)
	Nunclon Δ (Thermo, Schwerte, Germany)
Counting Chamber	Neubauer counting chamber (Superior Marienfeld, Thüringen, Germany)
Cover Slip	24x60mm; 15x15mm (Menzel-Gläser, Braunschweig, Germany)
Dialysis Membrane	Zellutrans E658.1 MWCO 4-6 kDa (Roth, Karlsruhe Germany)
Dialysis Tubes	D-tube Dialyzer Maxi MWCO 6-8 kDa (Merck, Darmstadt, Germany)
FACS Tubes	Polystyrene Tubes, round bottom (Greiner, Frickenhausen, Germany)
Filter	Zap Cap-S (Whatman, Dassel, Germany)
HPLC Column	BioSep-SEC-S2000 (Phenomenex, Aschaffenburg, Germany)
Microscopy Slides	Lab-Tek 8-well chamber slide (glass) (Thermo, Langenselbold, Germany)
	25-well plate (Sterilin Limited, London, UK)
Syringe filter	FP30/0,2 CA-S (Whatman, Dassel, Germany)
X-Ray film	CEA medical X-Ray screen film (Röntgenbedarf Linhardt, Munich, Germany)

2.1.3. Chemicals and reagents

APS (ammonium persulfate)	Sigma-Aldrich, Steinheim, Germany
BSA (bovine serum albumin)	PAA, Cölbe, Germany
Complete Protease Inhibitor Cocktail	Böhringer, Mannheim, Germany
Coomassie brilliant blue R250	Merck, Darmstadt, Germany
DAPI (4',6-diamidino-2-phenylindole)	Sigma, Steinheim, Germany
Ethidium bromide (EtBr) solution	Sigma, Steinheim, Germany
Ficoll	Sigma-Aldrich, Steinheim, Germany
Fluoromount G	Southern Biotech, Birmingham, USA
GM6001	Merck, Darmstadt, Germany
Hydrogen peroxide solution (contains inhibitor, 30 wt. % in H_2O, ACS reagent)	Sigma, Steinheim, Germany
Lipofectamine 2000	Invitrogen, Karlsruhe, Germany
LY294002	NEB, Frankfurt (Main), Germany
MTT (3-[4,5-dimethyl-thiazol-2-yl]-2,5-diphenyl tetrazolium bromide)	Sigma, Steinheim, Germany

Ni-NTA agarose	Qiagen, Hilden, Germany
Protein G agarose	Pierce, Rockford IL, USA
Skim milk powder	Merck, Darmstadt, Germany
Sodium azide	Merck, Darmstadt, Germany
TEMED (N,N,N',N'-Tetramethyl-ethylene-diamine)	Sigma-Aldrich, Steinheim, Germany
Tergitol-type NP-40	Sigma-Aldrich, Steinheim, Germany
TRIzol Reagent	Invitrogen, Karlsruhe, Germany
Ultrapure agarose	Invitrogen, Karlsruhe, Germany

All other chemicals, which are not listed above, were purchased from Carl Roth Chemicals, Karlsruhe, Germany.

2.1.4. Buffers and solutions

Acid isopropanol	Isopropanol, 2.4% [HCl (37%)]
Ampicillin	100mg/ml in Milli-Q H_2O (Roth, Karlsruhe, Germany)
Blotting buffer, 10x	1.92M glycine, 0.25M TRIS, 20% methanol pH 8.3
BSA, 4% (bovine serum albumin)	4% dissolved in PBS
Coomassie destain solution	40% methanol, 10% acetic acid
Coomassie staining solution	40% methanol, 10% acetic acid, 0.1% coomassie brilliant blue
Crystal Violet Solution	0.5% crystal violet, 20% methanol
DAPI (1mg/ml)	dissolved in PBS
DNA-loading buffer, 6x	0.46mM xylene cyanol, 50mM EDTA, 80% (v/v) glycerol
glucose solution, 25x	25% glucose, in Milli-Q H_2O, filter sterilized
IMAC column wash buffer	Sodium phosphate buffer (50mM) + 250mM imidazole
IMAC elution buffer	Sodium phosphate buffer (50mM) + 100mM imidazole
IMAC wash buffer 1	Sodium phosphate buffer (50mM) + 10mM imidazole
IMAC wash buffer 2	Sodium phosphate buffer (50mM) + 30mM imidazole
IP lysis buffer	10mM TRIS pH 7.4, 100mM KCl, 1mM EDTA, 1mM EGTA, 0.5% Triton X-100, 0.5% NP-40, 100µM Na_3VO_4, 0.2mM PMSF, 20mM ß-glycero-phosphate, Roche complete protease inhibitor cocktail
IP washing buffer	10mM TRIS pH 7.4, 100mM KCl, 1mM EDTA, 1mM EGTA
Laemmli-buffer, 3x	50mM TRIS pH 6.8, 4M urea, 1% SDS, 15% glycerol, 0.01% bromophenol blue, 5% (v/v) 2-mercaptoethanol
MTT solution	1.25mg/ml dissolved in PBS
Na_4VO_3 (1M)	dissolved in PBS
PBA	PBS, 0.05% BSA, 0.02% sodium azide
PBS (phosphate buffered saline)	137mM NaCl, 2.68mM KCl, 10mM Na_2HPO_4, 1.76mM KH_2PO_4 pH 7.4
PBST	PBS, 0.1% Tween-20
Permeabilization buffer	PBS, 0.1% Triton-X100

PFA, 4% (paraformaldehyde)	4% dissolved in PBS
PMSF (100mM)	dissolved in DMSO
Protein lysis buffer	10mM HEPES, 1.5mM $MgCl_2$, 1.5mM KCl, 1mM EDTA, 1% NP-40, 0.2mM PMSF, 20mM ß-glycero-phosphate, 100µM Na_3VO_4
SDS-PAGE running buffer, 10x	1.92M glycine, 0.25M TRIS, 1% SDS, pH 8.3
SDS, 10%	dissolved in Milli-Q H_2O
Sodium phosphate buffer, 5x	250mM sodium phosphate (29.82g $Na_2HPO_4 \cdot 2H_2O$, 6.24g $NaH_2PO_4 \cdot 2H_2O$ per liter), 1.25M NaCl pH 7.5
TAE buffer, 50x	2M TRIS acetate, 0.95M acetic acid, 50mM EDTA pH 8.3
Tail lysis buffer	10mM TRIS pH 8.3, 5mM EDTA, 300mM sodium acetate, 1% Triton-X100
β-glycerophosphate (1M)	dissolved in Milli-Q H_2O

2.1.5. Bacterial strains

Subcloning Efficiency DH5α Competent Cells (Invitrogen, Karlsruhe, Germany)

Genotype: F^- Φ80*lac*ZΔM15 Δ(*lac*ZYA-*arg*F)U169 *rec*A1 *end*A1 *hsd*R17(r_k^-, m_k^+) *pho*A *sup*E44 *thi*-1 *gyr*A96 *rel*A1 λ^-

2.1.6. Cell lines

Cell line	Culture medium	Description
CHO-$TNF_{[\Delta 1\text{-}12]}$	RPMI 1640 (5% FCS; P/S)	Chinese hamster ovarian cell line, stably expressing cleavage defective $TNF_{[\Delta 1\text{-}12]}$ (Grell et al., 1995)
HEK293	RPMI 1640 (10% FCS; P/S)	Human embryonic kidney cell line
IMA1335	DMEM (10% FCS; P/S)	Astrocyte cell line from TgE1335 Balb/c mice expressing huTNFR2 (Roman Fischer, IZI)
Kym-I	RPMI 1640 (10% FCS; P/S)	Human rhabdomyosarcoma cell line (Sekiguchi et al., 1985)
LUHMES	see section 2.1.7.2	Human mesencephalic neuron-derived cell line (Lotharius et al., 2005)
MEF TNFR1-Fas	RPMI 1640 (5% FCS; P/S)	Mouse embryonic fibroblasts from $TNFR1^{-/-}$ /$TNFR2^{-/-}$-mice stably expressing huTNFR1-Fas (Krippner-Heidenreich et al., 2002)
MEF TNFR2-Fas	RPMI 1640 (5% FCS; P/S)	Mouse embryonic fibroblasts from $TNFR1^{-/-}$ /$TNFR2^{-/-}$-mice stably expressing huTNFR2-Fas (Krippner-Heidenreich et al., 2002)
R2 MEF	RPMI 1640 (5% FCS; P/S)	Mouse embryonic fibroblasts from $TNFR1^{-/-}$ /$TNFR2^{-/-}$-mice stably expressing huTNFR2 (Fischer et al., 2011)
BV-2	RPMI 1640 (5% FCS; P/S)	Immortalized mouse microglia cell line (Blasi et al., 1990)

2.1.7. Media and supplements

2.1.7.1. Cell culture supplements

Fungizone antimycotic	Gibco/Invitrogen, Carlsbad, USA
ATV-trypsin	138mM NaCl, 5.4mM KCl, 6.9mM $NaHCO_3$, 5.6mM D-glucose, 0.54mM EDTA, 0.05% trypsin from bovine pancreas Type-II-S (Sigma) [one hour at 37°C; sterile filtered (0.22µM)]
BSA (bovine serum albumin)	Sigma, Steinheim, Germany
$CaCl_2$ (1.2% w/v)	Sigma, Steinheim, Germany
db-cAMP (N6,2′-O-Dibutyryladenosine 3′,5′-cyclic monophosphate)	Sigma-Aldrich, Steinheim, Germany
DMSO (dimethyl sulfoxide)	Roth, Karlsruhe, Germany
DNAse I (deoxyribonuclease I) from bovine pancreas (10µg/ml)	Sigma, Steinheim, Germany
FCS (fetal calf serum)	FCS Standard Quality, EU approved (heat inactivated at 56°C for 60 minutes); PAN Biotech, Aidenbach, Germany
Fibronectin	Sigma, Steinheim, Germany
Geneticin (G418)	100mg/ml in PBS (Gibco/Invitrogen, Carlsbad, USA)
$MgSO_4$ (3.82% w/v)	Sigma, Steinheim, Germany
N2 supplement	Gibco/Invitrogen, Carlsbad, USA
Penicillin-Streptomycin (P/S), 100x	10^4U/ml / 10^4µg/ml (Gibco/Invitrogen, Carlsbad, USA)
Poly-D-lysine hydrobromide (PDL; average MW 30000-70000)	Sigma-Aldrich, Steinheim, Germany
Poly-L-ornithine hydrobromide (PLO)	Sigma-Aldrich, Steinheim, Germany
Puromycin	PAA, Cölbe, Germany
Tetracycline hydrochloride	Sigma, Steinheim, Germany
Trypsin/EDTA, 10x	0.5% trypsin, 5.3mM EDTA, diluted to 1x in PBS (Gibco/Invitrogen, Carlsbad, USA)
L-glutamine	Invitrogen, Karlsruhe, Germany
Concanavalin A (ConA)	1mg/ml in PBS (Invitrogen, Karlsruhe, Germany)

2.1.7.2. Cell culture media

Freezing medium	90% (v/v) FCS, 10% (v/v) DMSO
KRB medium	1.4M NaCl, 4.83mM KCl, 1.22mM KH_2PO_4, 0.25M $NAHCO_3$, 2.57% (w/v) glucose, 0.015% phenol red
LUHMES proliferation medium	Advanced DMEM/F12, 1% N2-supplement, 2mM L-glutamine and 40ng/ml bFGF
LUHMES differentiation medium	Advanced DMEM/F12, 1% N2-supplement, 2mM L-glutamine, 1mM db-cAMP, 1µg/ml tetracycline and 2ng/ml GDNF
RPMI 1640, DMEM, Opti-MEM, Advanced DMEM/F12	Invitrogen, Karlsruhe, Germany

2.1.7.3. Bacterial media

LB medium	1% peptone, 0.5% yeast extract, 1% NaCl
LB_{amp} medium	LB medium (100µg/ml ampicillin)
$LB_{amp,glc}$ agar plates	LB-Medium with 1.3% agar, autoclave (100µg/ml ampicillin, 1% glucose after cooling-down)

2.1.8. Cytokines and growth factors

bFGF (fibroblast growth factor basic)	Immunotools, Friesoythe, Germany
$CysHisTNF_{R2}$ (CysHisTNF143N/145R)	Bryde et al., 2005
GDNF (glial cell-derived neurotrophic factor)	R&D Systems, Wiesbaden-Nordenstadt, Germany
human TNF (huTNF)	Immunotools, Friesoythe, Germany
IL-2 (interleukin 2)	Immunotools, Friesoythe, Germany
mouse TNF (mTNF)	Immunotools, Friesoythe, Germany
$scTNF_{R2}$	Roman Fischer, IZI
TNC-$scTNF_{R2}$	Roman Fischer, IZI

2.1.9. Kits

BCA Protein Assay Kit	Pierce, Rockford IL, USA
DyLight 549 Microscale Antibody Labeling Kit	Pierce, Rockford IL, USA
First Strand cDNA Synthesis Kit	Fermentas, St. Leon-Rot, Germany
IFN gamma ELISA	Hbt, Uden, The Netherlands
In Situ Cell Death Detection Kit, Fluorescein (TUNEL assay)	Roche Applied Science, Mannheim, Germany
Nucleo Spin Extract II	Macherey-Nagel, Düren, Germany
Nucleo Spin Plasmid	Macherey-Nagel, Düren, Germany
sTNFR2 ELISA	Hbt, Uden, The Netherlands
SuperSignal West Dura Extended Duration Substrate	Pierce, Rockford IL, USA

2.1.10. DNA and protein markers

Page Ruler prestained protein ladder	Fermentas, St. Leon-Rot, Germany
100 *bp* DNA ladder	NEB, Frankfurt (Main), Germany

2.1.11. Enzymes

5 Prime *Taq* DNA Polymerase	VWR International, Bruchsal, Germany
alkaline phosphatase	NEB, Frankfurt (Main), Germany
Proteinase K (10mg/ml)	Peqlab, Erlangen, Germany
T4 DNA Ligase	Fermentas, St. Leon-Rot, Germany

2.1.12. Restriction enzymes

AgeI	NEB, Frankfurt (Main), Germany
EcoRI	Fermentas, St. Leon-Rot, Germany
PmeI	NEB, Frankfurt (Main), Germany

2.1.13. Antibodies

2.1.13.1. Unconjugated antibodies

Antibody	Name	Species	Distributor
anti-α-tubulin	2144	rabbit	Cell Signaling Technology, Boston MA
anti-6-his	3998-100	rabbit	Biovision, San Francisco, USA
anti-Akt	9272	rabbit	Cell Signaling Technology, Boston MA
anti-CD11b	MAB1387Z	rat	Upstate, Millipore, Eschborn, Germany
anti-clathrin heavy chain	2410	rabbit	Cell Signaling Technology, Boston MA
anti-EEA1	2411	rabbit	Cell Signaling Technology, Boston MA
anti-huTNF	5N	mouse	Hbt, Uden, The Netherlands
anti-huTNF	AF-210-NA	goat	R&D Systems, Wiesbaden, Germany
anti-huTNFR1	H398	mouse	Hbt, Uden, The Netherlands
anti-huTNFR2	80M2	mouse	Institute of Cell Biology and Immunology, Stuttgart, Germany
anti-huTNFR2	HP9003	rabbit	Hbt, Uden, The Netherlands
anti-huTNFR2	MR2-1	mouse	Hbt, Uden, The Netherlands
anti-IκBα	9242	rabbit	Cell Signaling Technology, Boston MA
anti-mTNFR1	HP8002	rabbit	Hbt, Uden, The Netherlands
anti-mTNFR2	HP8003	rabbit	Hbt, Uden, The Netherlands
anti-neurofilament-L	04-1112	rabbit	Upstate, Millipore, Eschborn, Germany
anti-NFκB p65	4764	rabbit	Cell Signaling Technology, Boston MA
anti-phospho-Akt (Ser473)	9271	rabbit	Cell Signaling Technology, Boston MA
anti-Rab7	2094	rabbit	Cell Signaling Technology, Boston MA
anti-TRAF2	AP1040	rabbit	Cell Signaling Technology, Boston MA
anti-β-actin	4967	rabbit	Cell Signaling Technology, Boston MA
anti-β-III-tubulin	BM170S	mouse	Acris Antibodies, Hiddenhausen, Germany

2.1.13.2. Conjugated antibodies

Antibody	Conjugate	Distributor
anti-CD25	phycoerythrin (PE)	Miltenyi Biotech, Bergisch Gladbach, Germany
anti-FoxP3	allophycocyanin (APC)	Miltenyi Biotech, Bergisch Gladbach, Germany

anti-GFAP	Alexa-Fluor488 (A488)	Acris Antibodies, Hiddenhausen, Germany
anti-goat	Alexa-Fluor546 (A546)	Invitrogen, Karlsruhe, Germany
anti-huTNFR2	fluorescein isothiocyanate (FITC)	Hbt, Uden, The Netherlands
anti-mouse	Alexa-Fluor546 (A546)	Invitrogen, Karlsruhe, Germany
anti-mouse IgM + IgG (H+L)	fluorescein isothiocyanate (FITC)	Hbt, Uden, The Netherlands
anti-mouse IgG (H+L)	horseradish peroxidase (HRP)	Jackson Immuno Research, Suffolk, UK
anti-rabbit	Alexa-Fluor546 (A546)	Invitrogen, Karlsruhe, Germany
anti-rabbit	Alexa-Fluor488 (A488)	Invitrogen, Karlsruhe, Germany
anti-rabbit IgM + IgG (H+L)	fluorescein isothiocyanate (FITC)	Hbt, Uden, The Netherlands
anti-rabbit IgG (H+L)	horseradish peroxidase (HRP)	Jackson Immuno Research, Suffolk, UK

2.1.14. Oligonucleotides

Oligonucleotides (primer) were purchased by Thermo Hybaid, Schwerte, Germany.

huTNFR2ex6n2 fwd	5'-ctcctcctccagctgtaacg-3'
huTNFR2ex6n2 rev	5'-cgtgggctctcagtaaaacc-3'
CNTF cDNA fwd	5'-aggcagaaacttggagcgta-3'
CNTF cDNA rev	5'-gcaatcacctctgacccttc-3'
mGFAP cDNA fwd	5'-gtaggtggcgatctcgatgt-3'
mGFAP cDNA rev	5'-aagccaagcacgaagctaac-3'
huTNFR2 cDNA fwd	5'-ggaaactcaagcctgcactc-3'
huTNFR2 cDNA rev	5'-tccaactggaagagcgaagt-3'
mTNFR1 cDNA fwd	5'-acccccaggactcaggtact-3'
mTNFR1 cDNA rev	5'-ccatccaccacagcatacag-3'
mTNFR2 cDNA fwd	5'-ctgcatctgtgcttgcattt-3'
mTNFR2 cDNA rev	5'-acagcagaaccgagtgtgtg-3'
β-actin cDNA fwd	5'-gctgtggtggtgaagctgta-3'
β-actin cDNA rev	5'-tgttaccaactgggacgaca-3'

2.1.15. Vectors

pEFpuroTNFR2	Vector containing the gene sequence of wildtype TNFR2
pEFpuroTNFR2[L319A/L320A]	Vector containing the gene sequence of a mutated TNFR2
pMA	GENEART standard vector
pMA[scTNF$_{R2}$]	GENEART standard vector with scTNF$_{R2}$ gene sequence
pMA[TNC]	GENEART standard vector with human TNC gene sequence

pSecTag	Standard vector for eukaryotic protein expression (Invitrogen, Karlsruhe, Germany)
pSecTag[scTNF$_{R2}$]	Vector for eukaryotic production of scTNF$_{R2}$
pSecTag[TNC-scTNF$_{R2}$]	Vector for eukaryotic production of TNC-scTNF$_{R2}$
pSV3neo	Vector containing the gene sequence of the large T antigen from SV40 virus; used for immortalization of primary astrocytes
pTRAF2-eGFP	Vector containing the gene sequence of TRAF2 linked to eGFP

2.1.16. Software and database

argusX1	Biostep, Jahnsdorf, Germany
AxioVision V4.6	Carl Zeiss MicroImaging GmbH, Jena, Germany
Clarity Lite v.2.4.1.65	Millipore, Billerica, USA
Clone Manager 7.04	Scientific & Educational Software, Cary, NC
ExPASy Proteomics Server	Swiss Institute of Bioinformatics, Lausanne, Switzerland
GraphPad Prism 4.03	GraphPad, La Jolla, CA, USA
pDRAW32	AcaClone Software
Primer3	Primer Design (Rozen and Skaletsky, 2000)
UCSC genome browser	Genome Browser (Kent et al., 2002)
ZEN (LSM software)	Carl Zeiss MicroImaging GmbH, Jena, Germany

2.1.17. Animal experiments

Animal care and all experiments performed were in accordance with federal guidelines and have been approved by university and state authorities (file number 35-9185.81/0285). The animals were purchased by the company “Centre d’Elevage Roger Janvier” or were derived from the breeding of the animal facility from the Institute of Cell Biology and Immunology; University of Stuttgart. The animals were kept in a 14 hour light and 10 hour dark cycle and were given food and water ad libitum.

C57BL/6	Inbred strain; used for pharmacokinetic and as control animals in systemic tolerance experiments
TgE1335 C57BL/6	huTNFR2 transgene strain; used for systemic tolerance experiments

2.2. Methods

2.2.1. Molecular biology

2.2.1.1. Cloning strategies for scTNF$_{R2}$ and TNC-scTNF$_{R2}$

The TNFR2-selective scTNF$_{R2}$ (D143N/A145R) and the human tenascin C (TNC) domain (aa 110-139) were synthesized with optimized eukaryotic codon usage and delivered in the vector pMA (ampR), with *AgeI* (5'-end) and *PmeI* (3'-end; scTNF$_{R2}$) or *EcoRI* (3'-end; TNC domain) restrictions sites by Geneart. The scTNF$_{R2}$ construct, which is composed of three TNF monomers (aa 80-231) connected by GGGGS-linkers was provided with a N-terminal his-tag for purification. The sequence of the scTNF$_{R2}$ construct was cloned into the expression vector pSecTag A (Invitrogen) using the restriction enzymes *AgeI* and *PmeI* (pSecTag[scTNF$_{R2}$]). The sequence of the TNC domain was further cloned into the vector pSecTag[scTNF$_{R2}$] using the enzymes *AgeI* and *EcoRI* (pSecTag[TNC-scTNF$_{R2}$]), yielding in the TNC-scTNF$_{R2}$ construct. All vectors sequences were verified by sequencing.

2.2.1.2. Polymerase chain reaction

Specific DNA fragments were exponential amplified using the polymerase chain reaction (PCR) (Saiki et al. 1988). The PCR was performed using the PCR mixture listed in Table 1. The reaction was performed in a PCR cycler using the PCR program RF3T60 (Table 2).

Reagent	Volume
DNA template (10ng/µl)	2µl
10x buffer	2µl
dNTPs [2mM]	2µl
forward primer (10pmol/µl)	1µl
reverse primer (10pmol/µl)	1µl
Taq DNA-Polymerase (1U/µl)	0.5µl
Milli-Q H_2O	add to 20µl

Table 1: Reaction mixture for PCR amplification.

Step	Temperature	Time	Cycles
Initial denaturation	95°C	3min	
Denaturation	95°C	45s	36 cycles
Annealing	60°C	45s	
Elongation	72°C	60s	
Final elongation	72°C	10min	

Table 2: Standard PCR program.

2.2.1.3. Agarose gel electrophoresis and DNA gel extraction

Nucleic acids (vectors, PCR products or isolated RNA) were analyzed and purified by horizontal agarose gel electrophoresis. For this purpose, DNA samples were mixed with a 6x DNA loading buffer and separated by an agarose gel (0.8 to 1.5%) containing 1µg/ml ethidium bromide in TAE buffer. Samples were run at 130V for 45 minutes. DNA bands of relevant size were excised under UV light and extracted with the NucleoSpin Extract II kit according to the manufacturer's protocol. DNA was eluted in 30µl Milli-Q H_2O.

2.2.1.4. Restriction digestion and ligation

2µg DNA vector or extracted and purified PCR products were incubated with restriction enzymes (30U) in the corresponding buffer for two hours at 37°C. The enzymes were inactivated according to the manufacturer's protocol. For buffer exchange the NucleoSpin Extract II kit (Macherey-Nagel) was used. Vector religation was avoided by dephosphorylation of the insert vector after digestion. For this purpose, an alkaline phosphatase buffer and 1U alkaline phosphatase was added to the digestion mixture and incubated for one hour at 37°C. The digested DNA was isolated by agarose gel electrophoresis and the linearized and dephosphorylated vector was ligated with the insert at a molar ratio of 1:2 to 1:5 using T4 DNA ligase (5U) according to the manufacturer's protocol. The ligation was performed over night at 15°C and inactivated for five minutes at 70°C.

2.2.1.5. Transformation and plasmid isolation from *E.coli*

50µl of chemically competent cells (Subcloning efficiency DH5α Competent cells, Invitrogen) were thawed on ice and incubated for 20 minutes with 10µl of the ligated DNA. The cells were heat shocked for one minute at 42°C and cooled down on ice for two minutes. 1ml of prewarmed LB medium was added and the cells were incubated for one hour at 37°C to express the selection marker. The cells were harvested by centrifugation (30 seconds; 5000*g*), plated on $LB_{amp,glc}$ agar plates (100µg/ml ampicillin; 2% glucose) and incubated over night at 37°C.

Clones from the $LB_{amp,glc}$ plates were inoculated to an over-night culture of 4ml LB_{amp} medium (100µg/ml ampicillin) at 37°C and 180rpm. On the next day, the cells were harvested by centrifugation (30 seconds; 10000*g*) and the plasmid DNA was isolated using the NucleoSpin Plasmid kit (Macherey-Nagel) according to the manufacturer's instruction. The DNA was collected in 50µl Milli-Q H_2O and stored at -20°C. The purity and concentration of the plasmids were determined photometrically by UV-absorption. The identity of the resulting DNA was confirmed by control digestion or PCR amplification with appropriate restriction enzymes or primers, respectively. The correct sequence of inserts was determined by sequencing (GATC Biotech, Konstanz, Germany).

2.2.2. Cell culture

2.2.2.1. Fibroblasts, IMA and CHO

Mammalian cell lines were cultivated in a CO_2 incubator at 37°C, 5% CO_2 and 96% humidity on CELLSTAR (Greiner) culture flasks. For harvesting of MEF, IMA and CHO cells, the culture medium was washed away with sterile PBS and the cells were incubated with trypsin/EDTA for 20 seconds. Then the trypsin/EDTA was removed and the cells were incubated for approximately one to two minutes at room temperature, until the cells began to detach. Kym-I cells were incubated for five to 10 minutes with trypsin/EDTA. The cells were collected with culture medium, centrifuged (260*g*; five minutes) and the cell pellet was resuspended in medium or the appropriate buffer. The cell number was determined by counting with a Neubauer counting chamber.

2.2.2.2. LUHMES

The human neuronal-like cell line LUHMES, a clone of MESC2.10, has been described and further characterized earlier (Lotharius et al., 2002; Lotharius et al., 2005; Schildknecht et al., 2009). For the cultivation of LUHMES cells, Nunclon Δ culture flasks (Nunc) were coated with poly-L-ornithin (PLO; 50µg/ml) and fibronectin (1µg/ml) diluted in sterile Milli-Q H_2O. After three hours incubation at 37°C, the flasks were washed with sterile Milli-Q H_2O before seeding of the cells.

For harvesting of LUHMES cells, the culture medium was washed away with sterile PBS and the cells were incubated with ATV-trypsin diluted 1:2 in sterile PBS for 30 seconds. The ATV-trypsin was removed and the cells were incubated for two minutes at 37°C. Then the cells were collected in Advanced DMEM/F12 medium, centrifuged (260*g*; five minutes) and the cell pellet was resuspended in proliferation medium.

For differentiation, $5x10^6$ cells were plated in PLO and fibronectin-coated T175 flasks and incubated for 24 hours at 37°C with proliferation medium. Then, the medium was exchanged to differentiation medium and the cells were incubated for further 48 hours at 37°C to initiate the differentiation process. The cells were harvested with ATV-trypsin as described above and plated in Nunclon Δ culture plates (Sterilin plate with cover slips 15x15mm: $4x10^5$ cells/well; 96-well: $8x10^4$ cells/well; 6-well: $1.25x10^6$ cells/well). Then the cells were differentiated for further 72 hours.

2.2.2.3. Isolation of primary astrocytes

Primary glial cells were prepared from postnatal mice day one to two of age. The mouse brains were chopped into small pieces after removal of olfactory bulbs, cerebellum and meninges and collected in 10ml “solution 1” (1x KRB-medium; 0.3% BSA; 0.03% $MgSO_4$). The tissue was centrifuged at 120*g* for 10 minutes at room temperature and the pellet was

resuspended in 2ml trypsin/EDTA containing 100µl DNAse I (0.5µg/ml). This suspension was incubated for 15 minutes at 37°C for the enzymatic dissociation of the tissue. Then, 1ml FCS was added to stop the digestion and the suspension was centrifuged at 120*g* for 10 minutes at room temperature. The supernatant was removed carefully and the pellet was resuspended in 2ml of "solution 1". The tissue was triturated using a 1ml pipette with a blue tip (25 passes) and incubated for 10 minutes at room temperature. The supernatant containing the dissociated cells was added to 3ml of "solution 2" (1x KRB-medium; 0.3% BSA; 0.06% $MgSO_4$; 0.00144% $CaCl_2$). The part of the tissue, which was not dissociated staying on the bottom of the tube, was dissociated again in 2ml "solution 1" and then transferred to the dissociated cells. The cells were centrifuged at 120*g* for 10 minutes at room temperature and the cell pellet was resuspended in 3 ml of DMEM (10% FCS; L-glutamin; P/S). Living cells were counted with trypan blue and $3x10^6$ cells were plated in a PDL-coated (10µg/ml; 60 minutes at room temperature) T75 culture flask in 10ml DMEM (10% FCS; L-glutamin; 1% P/S; 1% fungizone). The medium was exchanged after one day and then every third day.

After eight to 10 days in culture an astrocytes layer had formed, on top of which numerous microglial cells, oligodendrocyte precursors and oligodendrocytes grow. The medium was exchanged and the culture flask was shaken vigorously for several seconds, so that microglia, oligodendrocyte precursors and oligodendrocytes were released into the medium. The medium was removed and the astrocyte layer was washed with sterile PBS. Astrocytes were incubated with trypsin/EDTA for 60 seconds, then the trypsin/EDTA was removed and the cells were incubated at 37°C for approximately five minutes until they detach from the flask. Then, the cells were collected with DMEM (10% FCS), transferred to a non-coated T175 culture flask and incubated for 20 minutes at room temperature, to remove residual microglial cells, which adhere more rapidly to the plastic. The flask was shaken carefully to recover the supernatant, containing the astrocytes, which were then transferred into a new PDL-coated (10µg/ml; 60 minutes at room temperature) T175 culture flask for expansion or directly used for experiments.

2.2.2.4. Isolation of human PBMC

Blood from human donors (DRK-Blutspendedienst Baden-Württemberg-Hessen; 20ml) was used to isolate PBMCs (peripheral blood mononuclear cells; performed by Dr. Dafne Müller). Therefore, the blood was diluted 1:12 in RPMI 1640 and 30ml of the dilution were slowly layered above a Ficoll-Paque (10ml). After centrifugation (720*g*; 20 minutes) the PBMCs, which remain in the interphase (buffy coat) were collected in 40ml RPMI 1640. The cells were washed with RPMI 1640 by sequential centrifugation (580*g*; 15 minutes followed by 180*g*; 10 minutes) and the cell pellet was collected in freezing medium and stored at -80°C.

2.2.3. Stable transfection and establishment of stable cell lines

2.2.3.1. Establishment of R2 MEF AND LL/AA MEF

pEFpuroTNFR2[L319A/L320A] expression constructs coding for the LL/AA TNFR2 mutant were generated by site-directed mutagenesis of pEFpuroTNFR2 plasmid containing wildtype TNFR2 (Fischer et al., 2011; performed by Matthias Naumer). To generate cell lines expressing the human TNFR2 muteins, Simian Virus 40 large T antigen immortalized mouse embryonic fibroblasts from TNFR1$^{-/-}$/TNFR2$^{-/-}$-mice (DKO MEF), generously provided by Daniela Männel (University of Regensburg, Regensburg, Germany), were transfected with the plasmids pEFpuroTNFR2 (Bryde et al., 2005) (R2 MEF) or pEFpuroTNFR2[L319A/L320A] (LL/AA MEF) using lipofectamine 2000 (Invitrogen). To this end DKO MEF (5x10^5 cells/well) were grown over night in 6-well plates (RPMI1640, 5% FCS, 1% P/S).

The following day the culture medium was exchanged to 2ml Opti-MEM and the cells were incubated at 37°C. Lipofectamine 2000 was diluted 1:50 in Opti-MEM and incubated for five minutes at room temperature. Plasmids (500ng) were diluted in Opti-MEM and mixed in a ratio of 1:1 with lipofectamine dilution. The resulting transfection complexes were incubated at room temperature for additional 20 minutes. The transfection mixture (500µl/well) was added carefully and cells were incubated at 37°C for six hours. Then the transfection mixture was replaced by standard cell culture medium and incubated for further 24 hours. Stably transfected cells were selected with 5µg/ml puromycin. After two weeks the huTNFR2-positive cells were sorted by flow cytometry. To achieve stably expressing cells, the sorting step was performed two times.

2.2.3.2. Immortalization of primary astrocytes

IMA1335 cells were established from freshly isolated primary astrocytes from TgE1335 Balb/c mice (Douni and Kollias, 1998). Primary astrocytes (5x10^5 cells/well) were grown to confluence in 6-well plates (DMEM, 10% FCS, 1% P/S). On the day of transfection the medium was exchanged to Opti-MEM and the cells were transfected with large T antigen from SV40 (psV3neo) using lipofectamine as described above (section 2.2.3.1). Stable cells were selected with 800µg/ml G418 on the next day.

2.2.3.3. Establishment of TNF-producing cells

HEK293 (5x10^5 cells/well) cells were seeded over night in 6-well plates (RPMI 1640, 5% FCS, 1% P/S). On the next day the cells were transfected with scTNF$_{R2}$ and TNC-scTNF$_{R2}$ expression constructs, respectively, following the described lipofectamine method above (section 2.2.3.1). Stable cells were selected with 500µg/ml Zeocin 24 hours after transfection. After two weeks, the Zeocin concentration was reduced to 50µg/ml.

2.2.4. Production and purification of TNF variants

Due to the N-terminal Igκ leader sequence the transfected HEK293 cells secrete the TNF variants into the culture medium. For production, the cells were expanded in T175 culture flasks to 80% confluence (RPMI 1640, 10% FCS, 1% P/S). Then the medium was exchanged to Opti-MEM without FCS. The medium was exchanged and collected every second day.

To eliminate residual cells, the supernatant was centrifuged (720*g*; five minutes) and stored at 4°C until purification. The TNF variants were purified by immobilized metal ion affinity chromatography (IMAC). Therefore a column containing 1ml Ni-NTA agarose was equilibrated with 20ml "IMAC wash buffer 1" followed by 10ml "IMAC wash buffer 2". The supernatant containing the TNF variant was loaded onto the column and unbound proteins were washed away using "IMAC wash buffer 1" and 2 as described above. Bound proteins were eluted with 8ml IMAC elution buffer in fractions of 1ml. The Ni-NTA column was recycled with 10ml IMAC column wash buffer, followed by 50ml Milli-Q H_2O. The purity of the protein in the eluted fractions was analyzed by SDS-PAGE and pure fractions were pooled and dialyzed (Zellutrans E658.1 MWCO 4-6kDa, Roth) against 5l PBS over night at 4°C. Protein concentration (c) was determined by measuring the absorbance at 280nm (OD_{280}). Concentrations were calculated using the following equations:

$$c\ [mg/ml] = MW\ [g/mol] \times (OD_{280} / \varepsilon)$$

$$\varepsilon = (n(Trp) \times 5540) \times (n(Tyr) \times 1480)$$

2.2.5. Transient transfection

Lab-Tek 8-well chamber glass slides (Nunc) were coated with 10µg/ml poly-D-lysine for one hour at 37°C. R2 MEF were seeded ($3x10^4$ cells/well) and grown overnight. The following day the culture medium was exchanged to 200µl Opti-MEM and the cells were incubated at 37°C during the preparation of transfection complexes. Lipofectamine was diluted 1:50 in Opti-MEM and incubated for five minutes at room temperature. The plasmid pTRAF2-eGFP (500ng) was diluted in Opti-MEM and mixed 1:1 with the lipofectamine dilution.

The resulting transfection complexes were incubated at room temperature. After 20 minutes 100µl/chamber of the transfection mixture was added to the cells. The cells were incubated for six hours at 37°C, then the medium was exchanged to standard culture medium and the cells were incubated over night at 37°C. After 16 hours the transfected cells were stimulated with TNF as indicated and stained for fluorescence analysis.

2.2.6. RNA isolation and cDNA synthesis

RNA from animal cells was isolated using *TRIzol* reagent. For this purpose approximately $1x10^6$ cells were collected in 500µl *TRIzol* reagent and incubated for five minutes at room temperature. Then 100µl chloroform was added and the suspension was mixed vigorously for 15 seconds and incubated for further three minutes. The suspension was centrifuged (12000*g*; 15 minutes; 4°C) and the RNA, which resided in the upper aqueous phase was collected. For the precipitation of RNA, the aqueous phase was incubated with 250µl isopropanol for 10 minutes. The precipitated RNA was centrifuged (12000*g*; 10 minutes; 4°C) and washed with 75% ethanol (7500*g*; 5 minutes; 4°C). The eluted RNA was air-dried and resolved in 30µl RNAse-free water.

Purity and concentration of RNA was determined by UV-absorption measured photometrically. 2µg of RNA were directly converted into cDNA with the First Strand cDNA Synthesis Kit (Fermentas) and the remaining RNA was stored at -80°C. For cDNA synthesis, the RNA was mixed with oligo(dT) primers (0.5µg/ml), incubated at 70°C for five minutes and regenerated on ice for five minutes. Then 5x reaction buffer, RiboLock Ribonuclease inhibitor (20U/µl) and dNTP-mix (10mM) were added and the mixture was incubated at 37°C. After five minutes M-MuLV Reverse Transcriptase (20U/µl) was added and conversion was performed for 60 minutes at 37°C. The enzyme was inhibited at 70°C for 10 minutes. The synthesized cDNA was diluted 1:10 in Milli-Q H_2O and used as a template for PCR amplification (2µl per reaction).

2.2.7. Cytotoxicity assays

2.2.7.1. Crystal violet staining

MEFs or Kym-I cells ($1x10^4$ cells/well) were grown in 96-well flat bottom cell culture plates over night. If indicated in a figure's legend, the cells were stimulated with 80M2 (1µg/ml) for 30 minutes. Then the cells were incubated with different concentrations of TNF variants for 24 hours at 37°C. The cells were washed with PBS and incubated with crystal violet (20% methanol; 0.5% crystal violet) for 20 minutes to stain viable cells. The dye was washed away under rinsing water and the cells were air-dried. Crystal violet was resolved with methanol and the optical density at 550nm was determined. Each sample was analyzed in triplicates and data were analyzed using the software Microsoft Excel and GraphPad Prism 4.

2.2.7.2. MTT assay

Differentiated (two days) LUHMES cells were seeded in PLO/fibronectin-coated 96-well plates ($8x10^4$ cells/well) and differentiated for additional 72 hours. Then, LUHMES cells were stimulated with hydrogen peroxide, washed after one hour with medium and regenerated for additional 24 hours in medium with or without TNC-scTNF$_{R2}$ (100ng/ml). Then, the medium

was removed carefully and 60µl MTT solution diluted 1:6 in DMEM (1% FCS) was added. Cells were incubated for 90 minutes at 37°C. Then 150µl acid isopropanol was added and the cells were dissolved. Absorbance was measured at 550nm. Each sample was analyzed in triplicates and the cell viability was calculated using the software Microsoft Excel and GraphPad Prism 4.

2.2.7.3. TUNEL assay

Differentiated (two days) LUHMES cells ($4x10^5$ cells/well) were seeded on PLO/fibronectin-coated glass coverslips (15x15mm) and differentiated for additional 72 hours. Then, LUHMES cells were stimulated with hydrogen peroxide, washed after one hour with medium and regenerated for the indicated times in medium with or without TNC-scTNF$_{R2}$ (100ng/ml). At point in time zero, the cells were washed with PBS, fixed with PBS/4%PFA for 20 minutes at 37°C and permeabilized with PBS/0.1% TritonX-100 for five minutes at room temperature. Labeling with the TUNEL reaction mix was performed due to the recommendations of the manufacturer (Roche Applied Science). The coverslips were mounted with Fluoromount G. The fluorescence was analyzed by wide-field fluorescence microscopy (CellObserver, Carl Zeiss). A minimum of 2500 cells per sample was analyzed to calculate the amount of TUNEL-positive cells.

2.2.7.4. *In vitro* stability of TNC-scTNF$_{R2}$

A 10µg/ml solution of TNC-scTNF$_{R2}$ was prepared in FCS and incubated for different time periods at 37°C. At day zero titrations of TNC-scTNF$_{R2}$ were prepared in culture medium. As a control, scTNF$_{R2}$ and TNC-scTNF$_{R2}$ were freshly titrated at day zero. The titrations of the TNF muteins were incubated on Kym-I cells for 20 hours and the cell viability was determined by crystal violet staining as described above (section 2.2.7.1). Each sample was analyzed in triplicates.

2.2.8. Proliferation assay

IMA1335 cells (7500 cells/well) were seeded in 96-well plates and grown over night in 10% FCS. The following day, the cells were incubated with LY294002 (25µM) for one hour, followed by addition of mTNF (100ng/ml) or TNC-scTNF$_{R2}$ (100ng/ml). The cells were incubated for additional 48 hours and the number of cells was determined using the crystal violet staining method as described above (section 2.2.7.1). Each sample was analyzed in triplicates.

2.2.9. Immunoblot/Western blot analysis

2.2.9.1. Coomassie staining and immunoblot analysis of TNF muteins

2µg (SDS-PAGE) or 1µg (immunoblot) of scTNF$_{R2}$ or TNC-scTNF$_{R2}$ were supplemented with Laemmli buffer with 2-mercaptoethanol (2-ME; reduced) or without 2-ME (non-reduced) and boiled for five minutes at 95°C. The proteins were resolved by 8% SDS-PAGE (100V; 200mA; 90 minutes). For coomassie staining of proteins the SDS-PAGE was washed with Milli-Q H_2O and incubated in coomassie staining solution for 60 minutes at room temperature. The SDS-PAGE was destained using coomassie destain solution.

For immunoblot analysis the proteins were transferred onto nitrocellulose membranes (semi-dry blot; 1.5mA/cm^2 gel for 90 minutes). Non-specific protein binding was blocked with 5% skimmed milk powder solution in PBS/0.1% Tween20 for 30 minutes at room temperature and the membrane was incubated overnight at 4°C using antibodies specific for the his-tag. After incubation with anti-rabbit HRP-conjugated secondary antibodies for 90 minutes at room temperature the signals were detected by enhanced chemiluminescence (Super Signal, Pierce).

2.2.9.2. Immunoblot analysis of cell lysates

IMA and MEF (500000 cells/well) were seeded in 6-well plates and grown over night. LUHMES cells (1.25x10^6 cells/well) were differentiated in PLO/fibronectin-coated 6-well plates. If indicated in a figure's legend, the cells were stimulated with inhibitors and/or TNF. The cells were lysed in 100µl lysis buffer at 4°C for 30 minutes. The lysates then were centrifuged (2 minutes at 9600*g*) and the protein concentration of the supernatants was determined using the BCA method. 20µg total protein were denatured in Laemmli buffer and resolved by SDS-PAGE. The immunoblot analysis was performed as described above (section 2.2.9.1).

For quantification of protein amounts detected by immunoblot analysis, films were scanned and integrated optical densities were calculated using ImageJ. Integrated optical densities were corrected for background intensities.

2.2.10. Immunoprecipitation

Approximately 5x10^6 R2 MEF were seeded in T75 cell culture flask (Greiner) and cultivated overnight. Cells were stimulated as indicated and homogenized with 200µl IP lysis buffer for 30 minutes on ice. The lysate was centrifuged (2 minutes; 9600*g*; 4°C) and the supernatant was incubated with 5µg TNFR2-specific antibodies MR2-1 (Hbt) for 2 hours at 4°C. The immunocomplexes were precipitated with Protein G agarose (75µl; Pierce) for two hours at 4°C. The precipitates were washed four times with IP washing buffer and dissolved in 100µl

PBS, supplemented with Laemmli buffer. To elute bound proteins, the precipitates were boiled for five minutes at 95°C. 30 µl of the eluted proteins were separated by SDS-PAGE and analyzed by immunoblot analysis (section 2.2.9.2).

2.2.11. Flow cytometry

2.2.11.1. Flow cytometry analysis of living cell

$5x10^5$ cells/well were seeded in 6-well plates (Greiner), cultivated overnight and harvested with trypsin/EDTA. The cells were incubated with specific antibodies for mouse TNFR1 (HP8002; 0.5µg/ml), mouse TNFR2 (HP8003; 0.5µg/ml) or human TNFR2 (HP9003; 2µg/ml) in PBS containing 0.05% BSA and 0.02% sodium azide (PBA) for one hour at 4°C. The cells were washed three times with PBA and incubated for 45 minutes with appropriate FITC-labeled secondary antibodies. Before analysis by flow cytometry (Cytomics FC500, Beckmann-Coulter), the cells were washed three times with PBA. 20000 cells were analyzed per sample and the data were evaluated with the program CXP analysis (Beckmann-Coulter).

For the establishment of the huTNFR2-expressing cell lines, 20000 cells were sorted with the FACSDiVa and collected in culture medium. The huTNFR2-expressing cells were seeded in RPMI with 5% FCS containing the selection medium for expansion of the selected cells.

2.2.11.2. Flow cytometry analysis of fixed cells

To analyze the amount of cell surface-expressed TNFR2 in TNF-stimulated cells, R2 MEF were seeded in 6-well plates ($5x10^5$ cells/well), cultivated overnight and stimulated with TNF as indicated. After harvesting with trypsin/EDTA, the cells were fixed with PBS/1% PFA for 10 minutes at 4°C. After three washing steps with PBS, the cells were incubated with FITC-labeled MR2-1 antibodies (2µg/ml) for 45 minutes. Then, after three additional washing steps with PBS, the fluorescence intensities were determined using flow cytometry. 20000 cells were analyzed per sample. Median fluorescence intensities were calculated using WinMDI 2.9 and corrected for background intensities obtained by measuring the auto fluorescence of the cells.

2.2.11.3. Flow cytometry analysis of human PBMCs

Human PBMCs ($2x10^5$ cells/well) were seeded in 96-well plates (Greiner) and stimulated with ConA, IL-2 and TNC-scTNF$_{R2}$. After 48 hours cells were centrifuged (300*g*; 10 minutes) and stained with anti-CD25-APC and anti-FoxP3-PE antibodies according to the manufacturer's recommendations. 10000 cells were analyzed per sample. Data were evaluated with the program CXP analysis (Beckmann-Coulter).

2.2.12. High Performance Liquid Chromatography

The oligomerization-state of the TNF variants under native conditions was analyzed by high performance liquid chromatography (performed by Dr. Martin Siegemund). 50µl sample (0.1 to 0.5mg/ml) was applied to a HPLC column (BioSep-SEC-S2000). For determining the size of recombinant proteins, standard proteins of size between 29kDa and 669kDa (669kDa thyroglobulin, 443kDa apoferritin, 200kDa β-amylase, 67kDa, bovine serum albumin 29 kDa were run under the same conditions.

2.2.13. ELISA

2.2.13.1. sTNFR2 ELISA

R2 MEF ($1x10^4$ cells/well) were seeded in 96-well plates (Greiner) and cultivated overnight. The cells were stimulated as indicated and supernatants were collected at the indicated time intervals and analyzed by an ELISA specific for soluble huTNFR2, according to the instructions of the manufacturer (Hbt). The absorbance at 450nm was determined with an absorbance reader (Multiskan FC, Thermo). The amount of released TNFR2 was determined with the provided soluble TNFR2 standard and calculated using the software GraphPad Prism 4.

2.2.13.2. IFN gamma ELISA

Human PBMCs ($2x10^5$ cells/well) were seeded in 96-plates (Greiner) and stimulated with ConA, IL-2 and TNC-scTNF$_{R2}$ at the indicated concentrations. After 48 hours supernatants were collected and analyzed by an ELISA specific for human interferon gamma (IFN-γ), according to the instructions of the manufacturer (Hbt). The absorbance at 450nm was determined with an absorbance reader (Multiskan FC, Thermo). The amount of released IFN-γ was determined with the provided standard and calculated using the software GraphPad Prism 4.

2.2.14. Immunofluorescence microscopy

2.2.14.1. Cytoplasmic staining

For immunofluorescence analysis of MEF, astrocytes or Kym-I cells, Lab-Tek 8-well chamber glass slides (Nunc) were coated with 10µg/ml poly-D-lysine for one hour at 37°C. The cells were seeded ($3x10^4$ cells/well) and grown overnight. If indicated in a figure's legend, the cells were stimulated with different TNF muteins followed by fixation with PBS/4% PFA for 30 minutes on ice. If cells were not stimulated with TNF, fixation was performed for 30 minutes at room temperature.

LUHMES cells (400000 cells/cover slip) were differentiated on PLO-fibronectin-coated cover slips (15x15mm), stimulated as indicated and fixed with PBS/4% PFA for 20 minutes at 37°C. All cells were permeabilized with PBS/0.1% Triton X-100 for 10 minutes at room temperature and unspecific binding sites were blocked with PBS/4% BSA for 30 minutes. Subsequently, cells were incubated with primary antibodies in PBS/2% BSA for 60 minutes followed by three washing steps with PBS and the incubation with appropriate fluorescence-labeled secondary antibodies for 45 minutes in PBS/2% BSA. After staining the nuclei with DAPI (10µg/ml) for 10 minutes at room temperature the cells were washed three times with PBS and mounted with Fluoromount G.

Fluorescence was analyzed using wide-field fluorescence microscopy (CellObserver with Colibri LED modules, Carl Zeiss) or confocal laser scanning microscopy (LSM710, Carl Zeiss). Projections of optical sections taken with the CellObserver were prepared using the "*extended focus image"*. For confocal laser scanning microscopy, the fluorophores were excited according to their excitation wavelength with an Ar laser (488nm), a He/Ne laser (543nm) and a diode laser (405nm).

The analysis of the obtained data and imaging was performed with the AxioVision Rel 4.7 (Carl Zeiss; CellObserver) or ZenLightEdition (Carl Zeiss; LSM710) software. Isotype or secondary antibodies control stainings were used to determine background fluorescence and to adjust the intensity of specific stainings. For quantification of the nuclear translocation of NFκB in immunofluorescence experiments, the number of cells with NFκB-positive nuclei of at least 100 cells per experiment and condition was determined.

2.2.14.2. Surface staining

Cells were seeded and cultivated as described above (section 2.2.14.1). The whole staining was performed on ice. Unspecific binding sites were blocked with PBS/4% BSA for 30 minutes. Then, the cells were incubated with primary antibodies in PBS/2% BSA for 60 minutes followed by three washing steps with PBS and the incubation with appropriate fluorescence-labeled secondary antibodies in PBS/2% BSA for 45 minutes. After staining the nuclei with DAPI (10µg/ml) for 10 minutes, the cells were washed three times with PBS and fixed with PBS/4% PFA for 30 minutes on ice.

If necessary, cytoplasmic proteins were stained using the method described above (section 2.2.14.1). After three washing steps with PBS, the cells were mounted with Fluoromount G and fluorescence was analyzed using fluorescence microscopy (CellObserver, Carl Zeiss) or confocal laser scanning microscopy (LSM710, Carl Zeiss).

2.2.14.3. Internalization of TNFR2

Lab-Tek 8-well chamber glass slides (Nunc) were coated with 10µg/ml poly-D-lysine for one hour at 37°C, then R2 MEF were seeded ($3x10^4$ cells/well) and grown overnight. To analyze the internalization of huTNFR2, R2 MEF were incubated with 1µg/ml 80M2 for 30 minutes before adding 100ng/ml CysHisTNF_{R2}, labeled with Alexa-Fluor546 (TNF-A546) according to the manufacturer's protocol (Pierce). After five minutes TNF-A546 was removed, the cells were washed with cell culture medium and incubated for the indicated time periods at 37°C. At point in time zero cells were washed two times with PBS and fixed with PBS/4% PFA at 4°C for 30 minutes. For further characterization different proteins were counterstained and the cells were analyzed as described above (section 2.2.14.1).

2.2.14.4. Complexation of TNFR2

Lab-Tek 8-well chamber glass slides (Nunc) were coated with 10µg/ml poly-D-lysine for one hour at 37°C, then Kym-I cells were seeded ($3x10^4$ cells/well) and grown overnight. If indicated the cells were incubated for 30 minutes with 80M2 (1µg/ml) before addition of TNF. The cells were further incubated with TNF muteins (10ng/ml) for five or 10 minutes at 37°C. At point in time zero, the cells were washed two times with PBS and fixed with PBS/4% PFA at 4°C for 30 minutes. Unspecific binding sites were blocked with PBS/4% BSA for 30 minutes. The cells were subsequently incubated with goat anti-TNF and rabbit anti-TNFR2 antibodies for 60 minutes followed by three washing steps with PBS and incubation with appropriate fluorescence-labeled secondary antibodies for 45 minutes in PBS/2% BSA. After staining the nuclei with DAPI (10µg/ml) for 10 minutes at room temperature the cells were mounted with Fluoromount G. Fluorescence was analyzed using confocal laser scanning microscopy (LSM710, Carl Zeiss).

2.2.14.5. Staining of tissue slices

Spleens were cut into serial cross sections at a thickness of 10µm on a cryomicrotome. The cryosections were dried and fixed for 15 minutes in PBS/4%PFA. Then, the sections were washed with PBS and permeabilized with PBS/0.1% Triton-X100 for 10 minutes. Unspecific binding sites were blocked with PBS/4% BSA for one hour. Subsequently, the sections were incubated with primary antibodies diluted in PBS/4% BSA for two hours followed by three washing steps with PBS and incubation with appropriate fluorescence-labeled secondary antibodies for one hour in PBS/4% BSA. After staining the cell nuclei with DAPI (10µg/ml) for 10 minutes the sections were washed three times with PBS, mounted with Fluoromount G and analyzed by fluorescence microscopy (CellObserver, Carl Zeiss).

To quantify the number of nuclei or CD11b-positive cells at least 500 cells from two different experiments were counted.

2.2.15. Genotyping

Tail biopsies (2 to 3mm) from transgenic animals were digested in tail lysis buffer for 20 hours at 54°C and 800rpm. The digested tissue was diluted 1:20 in 10mM TRIS pH 8.5 and incubated for five minutes at 95°C to inactivate proteinase K. Specific DNA fragments were amplified by PCR (2µl lysate as template) using the primers huTNFR2e6n2_fwd and huTNFR2e6n2_rev and analyzed with agarose gel electrophoresis as described above (section 2.2.1.3).

2.2.16. Pharmacokinetics of TNC-scTNF$_{R2}$

Female C57BL/6 mice (8 to 10 weeks old; 21 to 23g; n = 3) were injected intraperitoneal (i.p.) with 50µg scTNF$_{R2}$ or TNC-scTNF$_{R2}$, diluted in 500µl PBS. Blood samples (50µl) from the tail vain were taken in time intervals of 1, 2, 4, 8, 24, 72 and 168 hours, diluted 1:9 in sodium citrate (3.8%) to avoid blood clotting and incubated on ice. Blood plasma was generated by centrifugation for 15 minutes at 2000*g* at 4°C and samples were stored at -20°C.

TNF concentration in the blood samples was determined by an sTNF-specific ELISA (Hbt) (as described in section 2.2.13.1), interpolating the corresponding calibration curves. For comparison, the first value (after one hour) was set to 100%. The pharmacokinetic parameters AUC, $t_{1/2}\alpha$ and $t_{1/2}\beta$ were calculated with Excel (PK Functions; Joel I. Usansky) using the first four points in time to calculate $t_{1/2}\alpha$ and the last three points in time to calculate $t_{1/2}\beta$.

2.2.17. Systemic tolerance of TNC-scTNF$_{R2}$

Female TgE1335 C57BL/6 mice (8 to 10 weeks old; 25 to 30g; n = 3) were injected intraperitoneal (i.p.) with PBS, TNC-scTNF$_{R2}$ (100µg) or mTNF (20µg), diluted in 500µl PBS. The mice were monitored over 24 hours and the body temperature was measured in time intervals up to 24 hours. After eight and 24 hours, the mice were killed and their organs were removed. The spleens were cut into serial cross sections at a thickness of 10µm on a cryomicrotome and the number of CD11b-positive cells were determined by indirect immunofluorescence analysis as described above (section 2.2.14.5).

2.2.18. Additional statistical analysis

2.2.18.1. Quantification of NFκB translocation

Cell nuclei were segmented by thresholding of the DAPI fluorescence image. Segmented objects that had contact to the border of the image or did not have a reasonable nucleus size were removed and the border of the nuclei was smoothened. Touching nuclei were

separated based on a watershed segmentation. The cell morphology was segmented by thresholding of the NFκB fluorescence image. Segments containing more than one nucleus were divided into one cell per nucleus. The borders between touching cells were identified by a Voronoi-based segmentation (Jones, 2005). Since the contrast in the NFκB fluorescence image at the edges of Kym-I cells was too low for the segmentation of the entire cell, the area with a maximal distance of 16µm to the edge of a nucleus was taken as a cell segment. Pixels were always assigned to the nearest nucleus.

Mean nuclear and cytosolic fluorescence intensities were determined within a cell. Ratios of nuclear to cytosolic fluorescence intensities were calculated from at least 75 cells for every condition.

2.2.18.2. General statistics

Results shown are represented as mean ± SEM. The statistical analysis was performed by the Student–Neumann test with a 95% confidence interval, i.e. p values less than 0.05 were considered to be significant.

3. Results

3.1. Dynamics of TNFR2 signaling and turnover

3.1.1. Characterization of mouse fibroblasts expressing huTNFR2

In contrast to the wealth of molecular details known about TNFR1 signal pathways, little is known about the respective mechanisms of TNFR2 signaling. To study TNFR2 signaling and turnover at the membrane, I constructed a cell line selectively expressing human TNFR2 (huTNFR2). Immortalized MEFs from TNFR1$^{-/-}$/TNFR2$^{-/-}$ mice (DKO MEF) were stably transfected with huTNFR2 expression constructs and sorted by flow cytometry for high expression of the receptor (R2 MEF).

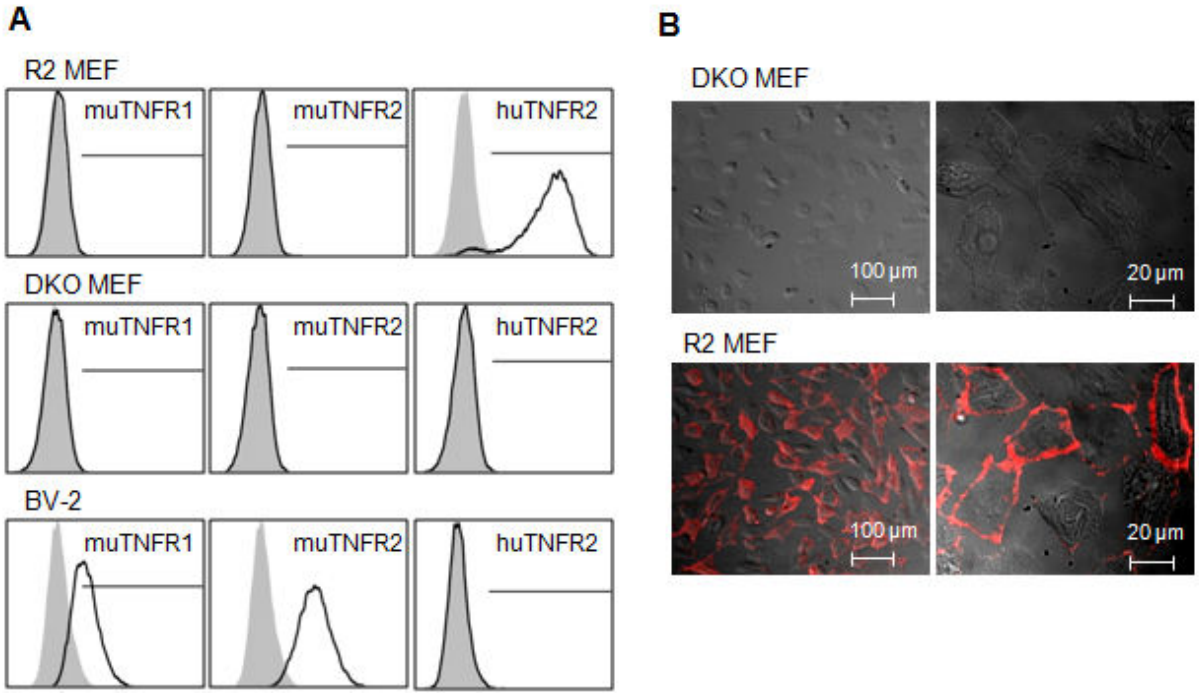

Figure 4: R2 MEF express human TNF receptor 2. Immortalized fibroblasts from TNFR1$^{-/-}$/TNFR2$^{-/-}$-mice (DKO MEF) were transfected with human TNFR2 (huTNFR2) expression constructs. Transfected cells were sorted twice for high expression of huTNFR2 (R2 MEF). (A) Surface expression of mouse TNFR1 (muTNFR1) and mouse TNFR2 (muTNR2) as well as huTNFR2 were analyzed using flow cytometry (black histogram). BV-2 cells were used as a positive control for the expression of mouse TNF receptors. Control histograms with secondary antibodies are also shown (gray histogram) (B) Homogeneity of surface expression of huTNFR2 was demonstrated via immunofluorescence microscopy. R2 MEF were fixed with 4% PFA and huTNFR2 was detected with specific antibodies and Alexa-Fluor546-labeled secondary antibodies. Cell morphology was visualized by bright field images.

The absence of the endogenous mouse TNF receptors was demonstrated by flow cytometry. The mouse cell line BV-2 was used as a positive control for the expression of mouse TNF receptors. huTNFR2 was highly expressed in R2 MEF (more than 95% positive cells, MFI = 126.92 ± 9.71) whereas the cell lines DKO MEF and BV-2 served as negative controls

(Figure 4A). Homogeneous distribution of TNFR2 expression at the cell surface of single cells was demonstrated by immune fluorescence microscopy (Figure 4B).

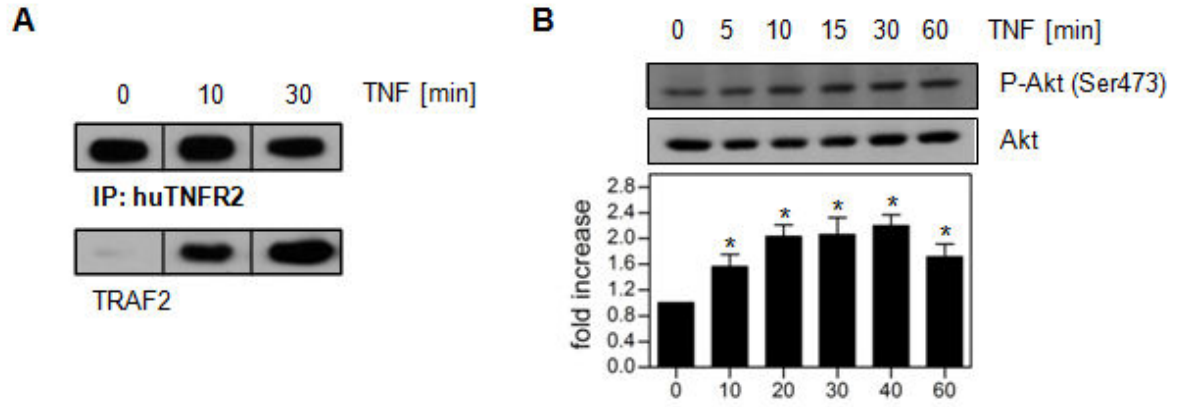

Figure 5: R2 MEF express a functional huTNFR2. For analysis of functionality of huTNFR2, R2 MEF were stimulated for 30 minutes with 80M2 (1µg/ml), followed by CysHisTNF$_{R2}$ (100ng/ml) for the indicated time intervals. (A) huTNFR2 was immunoprecipitated using MR2-1 antibodies and protein G agarose. The precipitates were analyzed by immunoblot using anti-huTNFR2 (HP9003) and anti-TRAF2 antibodies. (B) Total cell lysates were analyzed by immunoblot for expression of phospho-Akt (Ser473). Akt was used as a loading control. Representative blot and bar graph showing the quantification of the phosphorylation level of Akt. *p values less than 0.05 versus untreated cells were considered to be significant (n = 3).

To analyze the TNFR2 pathway cells were always incubated for 30 min with the monoclonal mouse antibody 80M2 (1µg/ml) to preactivate the TNFR2 on the cell surface, thereby mimicking receptor activation by the membrane form of TNF, if soluble recombinant TNF is added. Stimulation with 80M2 did not activate TNFR2 signaling pathways, e.g. no NFκB translocation or PKB/Akt phosphorylation was observed (data not shown).

Since TRAF2 directly interacts with TNFR2 (Rothe et al., 1994), it was next investigated, whether the endogenous mouse TRAF2 interacts with the ectopically expressed human TNFR2. Association of TRAF2 with TNFR2 was examined by immunoprecipitation of TNFR2 from unstimulated and TNF-stimulated cells. Indeed, TNF stimulation induced recruitment of TRAF2 to TNFR2 (Figure 5A), indicating that an active TNFR2 signaling complex is assembled.

In addition to TRAF2-mediated downstream signaling, activation of the protein kinase PKB/Akt is known to be involved in TNF-induced anti-apoptotic pathways (Ozes et al., 1999). Further investigations had demonstrated that PKB/Akt phosphorylation can be induced by TNFR2 and is involved in neuroprotection against cytotoxic insults *in vivo* and *in vitro* (Dolga et al., 2008; Fontaine et al., 2002; Marchetti et al., 2004). To analyze whether TNFR2 stimulation activates the PKB/Akt pathway in R2 MEF, phosphorylation levels of PKB/Akt at position serine 473 were investigated using immunoblot analysis. The phosphorylated form of PKB/Akt was detected in unstimulated cells, indicating that PKB/Akt is constitutively active

in R2 MEF. Stimulation with TNF resulted in a 1.6-fold increased phosphorylation level after 10 minutes, with a maximum 2.0-fold increase after 20 to 40 minutes (Figure 5B).

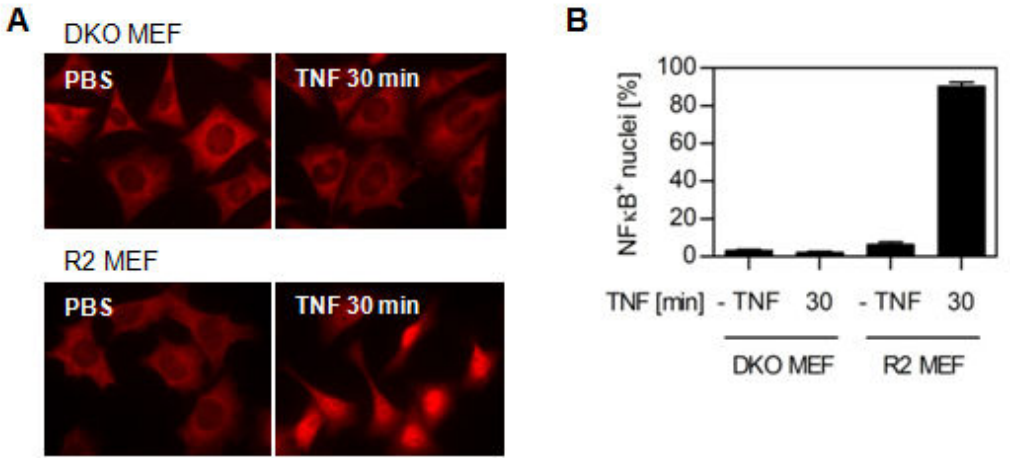

Figure 6: R2 MEF induce NFκB p65 translocation via TNFR2. R2 MEF were stimulated for 30 minutes with 80M2 (1µg/ml), followed by CysHisTNF$_{R2}$ (100ng/ml) for 30 minutes. Cells were fixed with 4% PFA, permeabilized with 0.1% Triton-X100 and localization of NFκB p65 was detected with specific antibodies and Alexa-Fluor546-labeled secondary antibodies (B) Quantification of cells showing NFκB translocation (more than 100 cells per sample; n = 4).

Since the neuroprotective effects mediated by PKB/Akt were reported to be dependent on the NFκB pathway (Marchetti et al., 2004), activation of NFκB was analyzed using nuclear translocation of the p65-subunit as a read-out system (Figure 6A and Figure 6B). Nuclei were visualized by co-staining with DAPI (data not shown). NFκB was predominantly localized in the cytoplasm of unstimulated DKO MEF and R2 MEF; in particular, 2% and 6%, respectively, of the cell nuclei were positive for the NFκB subunit p65. As expected, DKO MEF were unresponsive to TNF treatment and no changes in the localization of NFκB p65 were observed. Stimulation of R2 MEF with TNF for 30 minutes resulted in the nuclear translocation of NFκB p65 in approximately 90% of the cells (Figure 6A and Figure 6B), indicated by a reduced cytoplasm staining and an increased nuclear staining of NFκB p65.

3.1.2. Nuclear translocation of NFκB is controlled by PKB/Akt

The activation of PKB/Akt was dependent on PI3K. Inhibition of PI3K by the specific inhibitor LY294002 resulted in a complete abrogation of the endogenous, as well as the TNF-induced phospho-PKB/Akt (Ser473) level (Figure 7), demonstrating that PKB/Akt activation was dependent on PI3K, as described in the literature (Nicholson and Anderson, 2002).

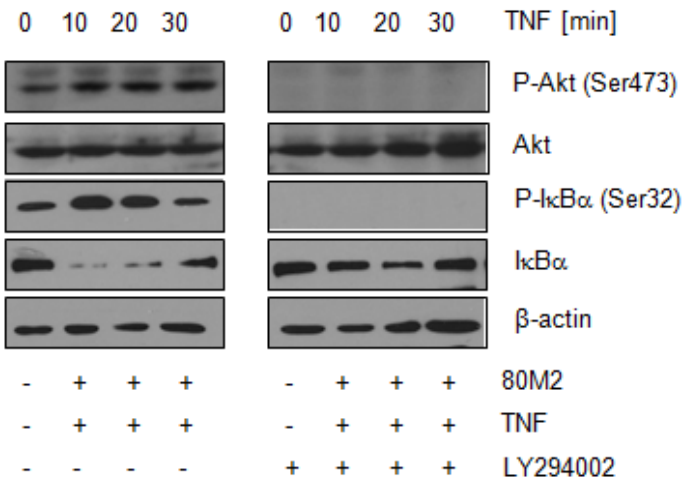

Figure 7: PKB/Akt phosphorylation is mediated via PI3K. R2 MEF were incubated with LY294002 (25µM). After 30 minutes 80M2 (1µg/ml) was added, cells were incubated for additional 30 minutes and subsequently stimulated with CysHisTNF$_{R2}$ (100ng/ml) for the indicated time intervals. Total cell lysates were analyzed by immunoblot for expression of different TNFR2 signaling components. β-actin was used as a loading control.

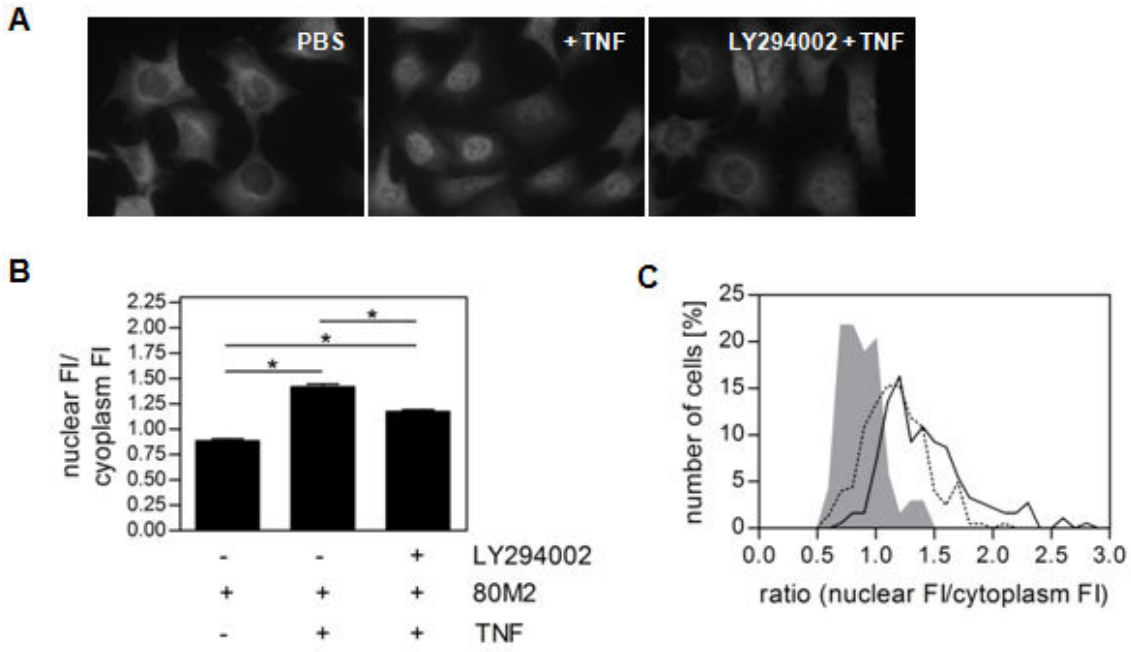

Figure 8: The nuclear translocation of NFκB is modulated by the PI3K-PKB/Akt pathway. R2 MEF were stimulated with LY294002 (25µM). After 30 minutes 80M2 (1µg/ml) was added. Cells were incubated for additional 30 minutes and afterwards stimulated with CysHisTNF$_{R2}$ (100ng/ml) for the indicated time intervals. Cells were fixed with 4% PFA, permeabilized with 0.1% Triton-X100 and localization of NFκB p65 was detected with specific antibodies and Alexa-Fluor546-labeled secondary antibodies. Shown are representative images (A), the ratio of nuclear to cytosolic fluorescence intensity (FI; B) and the ratio of nuclear to cytosolic FI in relation to the number of cells (C). At least 50 cells were analyzed per condition. *p values less than 0.05 were considered to be significant (n = 2).

Since PKB/Akt is involved in controlling the translocation as well as the activation of NFκB (Madrid et al., 2000; Ozes et al., 1999), the impact of the PI3K-PKB/Akt on NFκB signaling

was further analyzed. Inhibition of the PI3K-PKB/Akt pathway by LY294002 decreased the endogenous as well as induced phosphorylation levels of IκBα at residue serine 32 and inhibited the subsequent degradation of IκBα (Figure 7).

As expected, the reduced degradation of IκBα affected the nuclear translocation of NFκB subunit p65 (Figure 8). The quantification of the NFκB concentration relative to its subcellular localization revealed that less NFκB was translocated to the nucleus after pretreatment with LY294002, indicating that PKB/Akt plays a role in controlling TNFR2-induced NFκB activation.

3.1.3. Shedding and internalization of huTNFR2

Subsequent to ligand binding and activation of TNFR2, the extracellular part of the receptor can be either shed by TACE/ADAM17 (Porteu and Nathan, 1990; Solomon et al., 1999) or the complete receptor molecule can be internalized (Fotin-Mleczek et al., 2005). To determine the extent of spontaneous and ligand-induced ectodomain shedding, a soluble TNFR2-specific ELISA was performed with supernatants from unstimulated and TNF-stimulated cells.

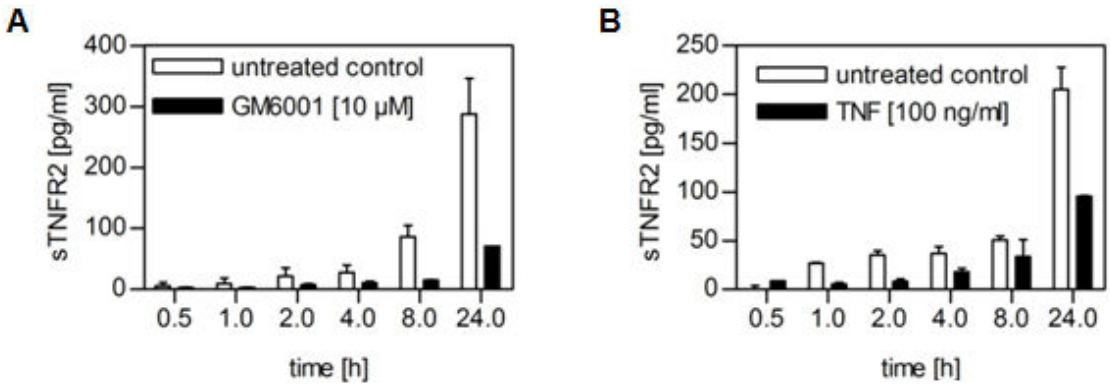

Figure 9: Shedding of huTNFR2 is mediated by matrix metalloproteinases (MMP) and is reduced after TNF stimulation. (A) R2 MEF were incubated for one hour in presence or absence of 10µM MMP inhibitor GM6001. Culture medium was replaced with new medium with or without 10µM GM6001 and medium samples were collected for up to 24 hours (n = 3). (B) R2 MEF were stimulated with 80M2 (1µg/ml; 30 minutes) followed by $CysHisTNF_{R2}$ (100ng/ml) for 24 hours and culture medium samples were collected at the indicated times. The concentrations of the shed TNFR2 ectodomain (sTNFR2) in the supernatants were determined by ELISA (n = 3).

A substantial constitutive shedding of TNFR2 was noted, indicating a high turnover rate of membrane-expressed TNFR2. Prestimulation of the R2 MEF with the MMP inhibitor GM6001 significantly decreased the release of the TNFR2 ectodomain demonstrating that shedding of TNFR2 is dependent on MMP activity (Figure 9A). The amount of released receptor ectodomain was decreased after TNF treatment suggesting that either TNFR2 was

internalized upon TNF binding or TNF/TNFR2 complexes were stabilized in the membrane and thereby prevent rather than promote shedding (Figure 9B).

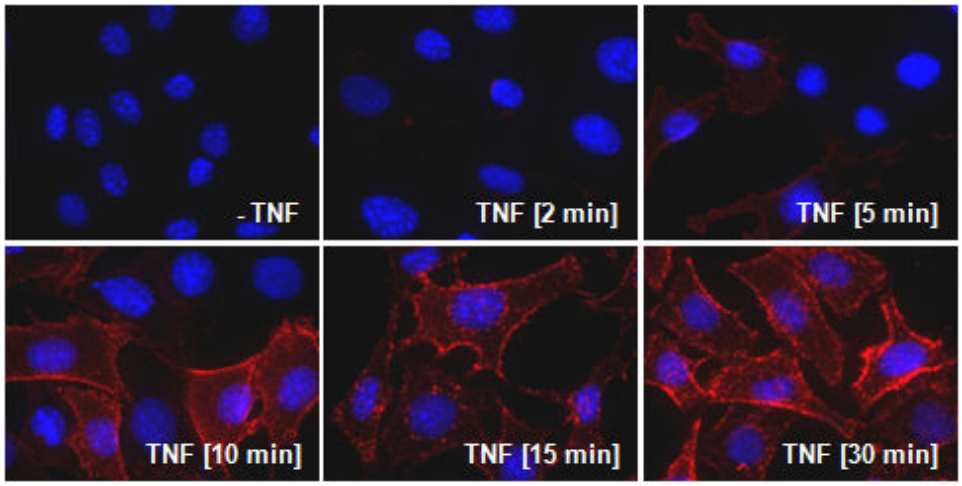

Figure 10: TNFR2 can be visualized using a fluorescence-labeled TNF. R2 MEF were stimulated for 30 minutes with 80M2 (1µg/ml), then Alexa-Fluor546-labeled CysHisTNF$_{R2}$ (TNF-A546; 100ng/ml) was added for the indicated times. Cells were washed with PBS to remove unbound TNF-A546 and fixed with 4% PFA. Cell nuclei were visualized using DAPI. Localization of TNF-A546 was analyzed using wide-field fluorescence microscopy. Pictures are projections of eight optical sections (0.4µm each).

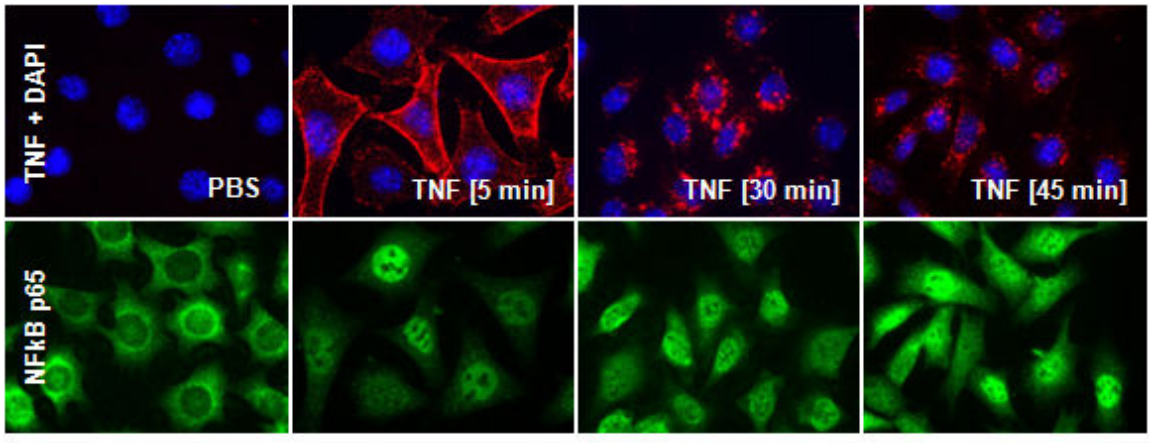

Figure 11: TNF/TNFR complex is internalized after stimulation. R2 MEF were stimulated for 30 minutes with 80M2 (1µg/ml), then TNF-A546 (100ng/ml) was added for five minutes, the cells were washed and further incubated for the indicated times. Cells were washed with PBS to remove unbound TNF-A546 and fixed with 4% PFA. Then, cells were permeabilized using 0.1% Triton X-100 and NFκB p65 was detected with specific antibodies and Alexa-Fluor488-labeled secondary antibodies. Cell nuclei were visualized using DAPI. Fluorescence was analyzed by wide-field fluorescence microscopy using Zeiss Cell Observer. Pictures are projections of eight optical sections (0.4µm each).

The internalization of TNFR2 was confirmed with an Alexa-Fluor546-labeled CysHisTNF$_{R2}$ (TNF-A546). After incubation for five minutes at 37°C sufficient TNF-A546 had bound to the

cell surface to be visualized via fluorescence microscopy (Figure 10). For this purpose, in the following experiments, non-bound TNF-A546 was always washed away after five minutes incubation and the cells were further incubated for various times at 37°C. After 10 minutes most of TNF-A546 was detectable as a homogeneous red staining at the cell surface. In addition, at that point in time, an intracellular staining could be discerned, suggesting beginning internalization of TNF-A546. Internalization became increasingly apparent with incubation time. After 30 minutes surface staining was no longer detectable, suggesting complete internalization (Figure 11). To verify that Alexa-Fluor546-labeled TNF retained its bioactivity, NFκB activation was assessed by costaining of TNF-A546-treated cells with NFκB subunit p65-specific antibodies and nuclear translocation was monitored. After 10 minutes of TNF treatment, the transcription factor was translocated into the nucleus (Figure 11).

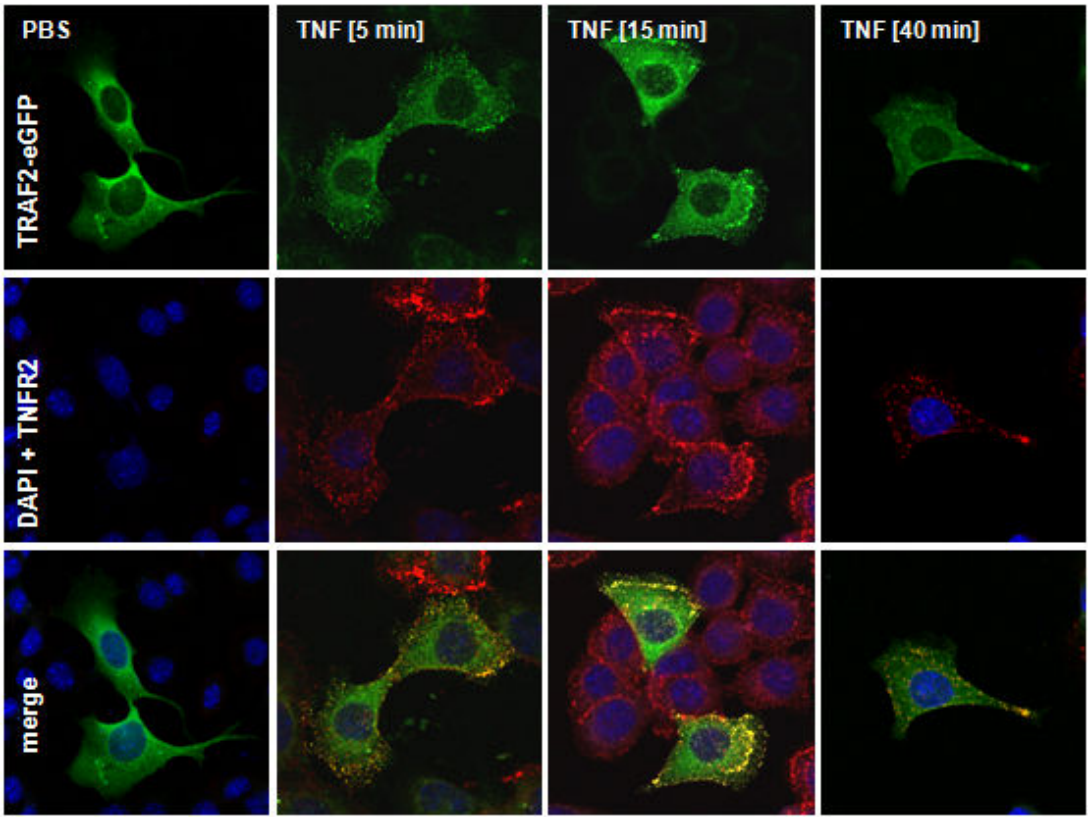

Figure 12: TNFR2 signaling complex is internalized upon TNF stimulation. R2 MEF were transfected with pTRAF2-eGFP. After 16 hours the cells were stimulated with 80M2 (1µg/ml; 30 minutes) followed by TNF-A546 (five minutes; 100ng/ml) and fixed with 4% PFA after 5, 15 and 40 minutes, respectively. Pictures are optical sections obtained by confocal fluorescence microscopy.

It was then asked whether the internalized TNF-A546 is still associated in a TNFR2 signaling complex comprising TRAF2. Therefore, after stimulation with TNF-A546, transiently expressed human TRAF2-eGFP was monitored by confocal laser scanning microscopy. As

expected, unstimulated R2 MEF expressing TRAF2-eGFP showed a homogenous cytosolic distribution of the transgene (Figure 12). Five minutes after addition of TNF, TNF-A546 colocalized with TRAF2-eGFP. Colocalization was still prominent after 15 and 40 minutes. These results demonstrate that by stimulating R2 MEF with TNF-A546 the spatial distribution of TNFR2 signaling complexes can be readily monitored by confocal cell imaging microscopy.

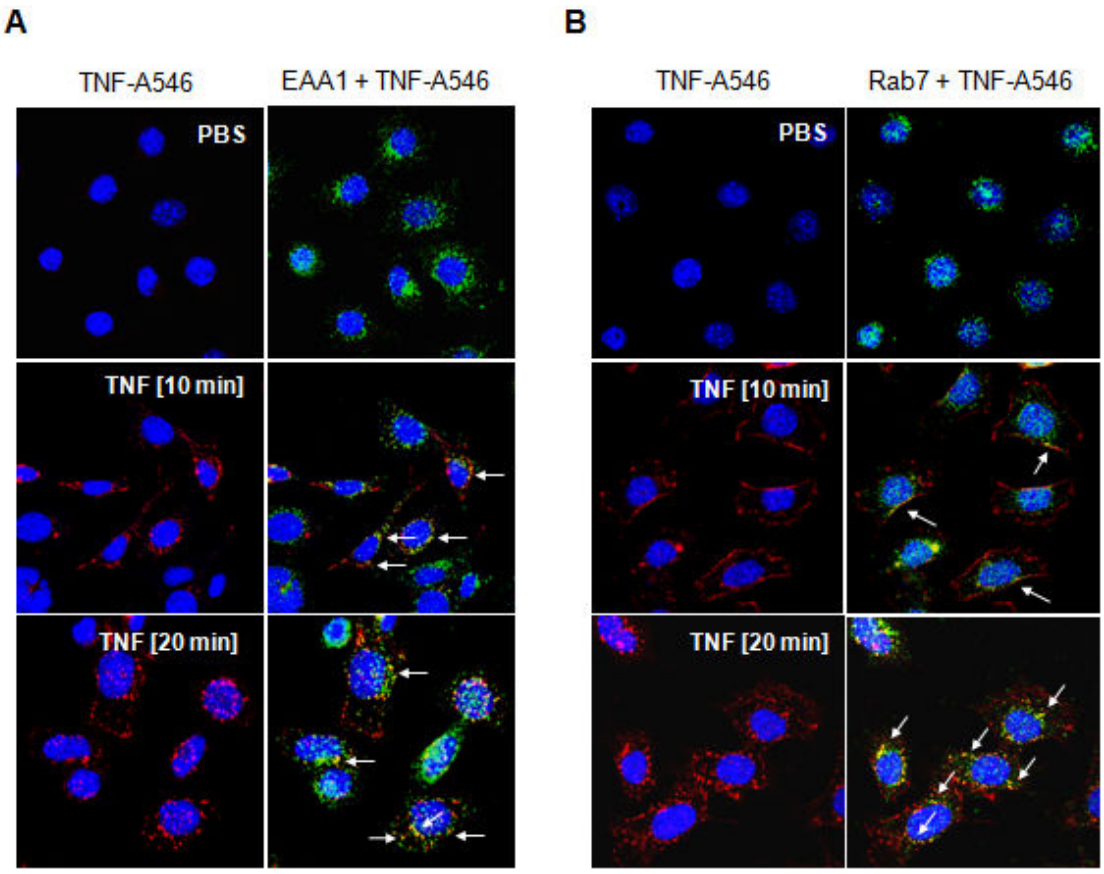

Figure 13: TNFR2 signaling complex colocalizes with endosomal markers. R2 MEF were stimulated with 80M2 (1µg/ml; 30 minutes) followed by TNF-A546 (five minutes; 100ng/ml) for the indicated times. The cells were fixed with 4% PFA and permeabilized using 0.1% Triton X-100. Early endosome marker EEA1 (A) and late endosome/lysosome marker Rab7 (B) were detected with specific antibodies and Alexa-Fluor488-labeled secondary antibodies. Cell nuclei were visualized using DAPI. Pictures are optical sections obtained by confocal fluorescence microscopy. White arrows indicate areas of colocalization.

3.1.4. TNFR2 is internalized into endosomes and afterwards degraded

Having shown that binding of TNF to TNFR2 induced internalization, the fate of the internalized ligand-receptor complexes was further investigated. To analyze the trafficking pathway of internalized TNFR2, colocalization studies with the early endosomal marker early endosome antigen 1 (EEA1) and the late endosomal marker Rab7 were performed.

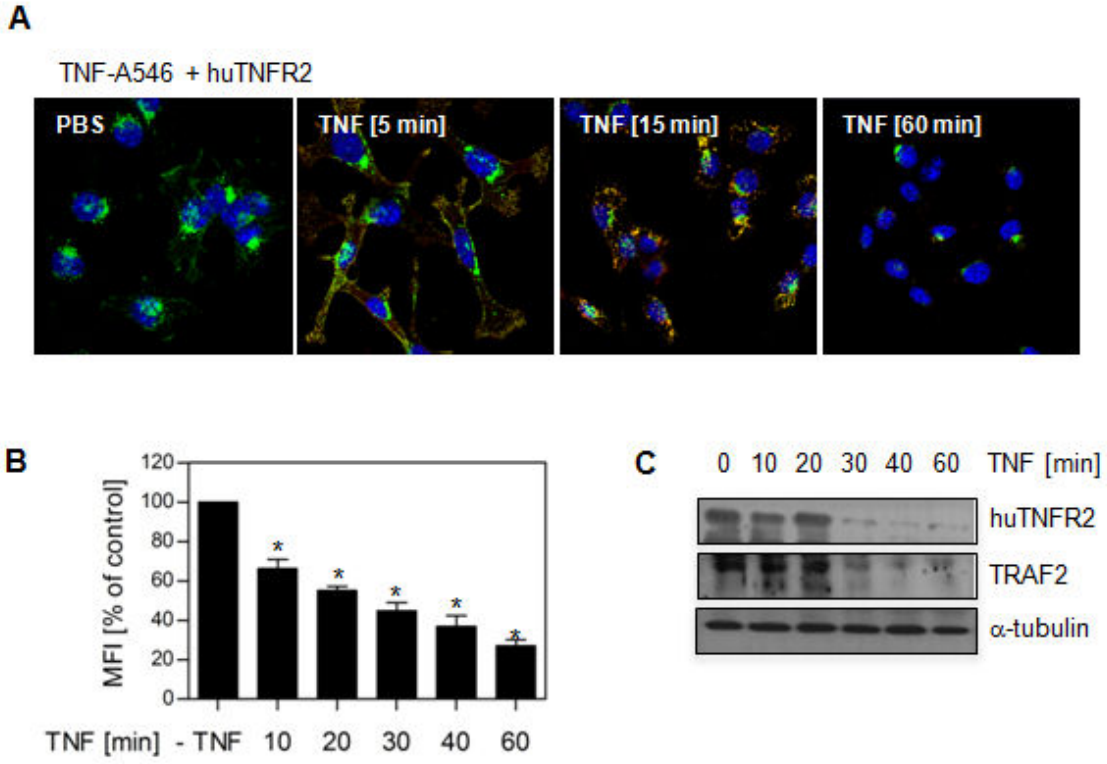

Figure 14: TNFR2 is cleared from the cell surface and degraded upon TNF-stimulation. (A) R2 MEF were stimulated with 80M2 (1µg/ml; 30 minutes) followed by TNF-A546 (five minutes; 100ng/ml) for the indicated times and fixed with 4% PFA. Cells were permeabilized using 0.1% Triton X-100 and stained with anti-huTNFR2 and anti-rabbit Alexa-Fluor488 antibodies. Cell nuclei were visualized using DAPI. Pictures are optical sections obtained by confocal fluorescence microscopy. (B) R2 MEF were stimulated with 80M2 (1µg/ml; 30 minutes), followed by CysHisTNF$_{R2}$ (100ng/ml) for the indicated times and fixed with 1% PFA. Surface expression of huTNFR2 was measured via flow cytometry. The median Fluorescence Intensity (MFI) was calculated relative to the unstimulated control *p values less than 0.05 versus untreated cells were considered to be significant (n = 3). (C) R2 MEF were stimulated with 80M2 (1µg/ml; 30 minutes) followed by CysHisTNF$_{R2}$ (100ng/ml) for the indicated times. Total cell lysates were analyzed by immunoblot for expression of huTNFR2 and TRAF2. α-tubulin was used as a loading control.

After 10 minutes of TNF-A546 stimulation TNF colocalized with EEA1 (Figure 13A) and Rab7 (Figure 13B). Colocalization with Rab7 became more obvious after 20 minutes. Since Rab7 is a key marker for lysosomal degradation (Bucci et al., 2000), it was then analyzed, whether TNFR2 is degraded upon internalization. Therefore TNF-A546-stimulated cells were counterstained with TNFR2-specific antibodies. After 10 minutes incubation, TNF-A546 and TNFR2 formed complexes at the plasma membrane and predominantly colocalized at the cell surface (Figure 14A). After 15 minutes, internalization of the TNF/TNFR2 complex was observed. 30 minutes after onset of treatment, neither TNF nor TNFR2 were visible in the cells, with exception of freshly synthesized TNFR2 in the endoplasmic reticulum and/or Golgi apparatus.

The amount of surface-expressed TNFR2 after TNF stimulation was quantified by flow cytometry, to confirm the TNF-induced clearance of TNFR2 from the cell surface (Figure

14B). After 30 minutes approximately 50% of TNFR2 was cleared from the surface. The clearance of TNFR2 increased to 70% after incubation for 60 minutes. Immunoblot analysis of cell lysates confirmed that the clearance of the TNFR2 receptor complex from the plasma membrane is followed by the degradation of TNFR2 (Figure 14C). Since TNFR2 stimulation induces TRAF2 depletion, thereby accelerating the TNFR1-dependent activation of caspase-8 (Fotin-Mleczek et al., 2002), the protein level of TRAF2 after TNF stimulation was analyzed. Similar to TNFR2, TRAF2 was degraded after 20 to 30 minutes (Figure 14C). This indicates that at least the receptor-proximal components of the TNFR2 signaling complex, including bound TNF and TRAF2, are degraded along with the receptor upon TNF stimulation.

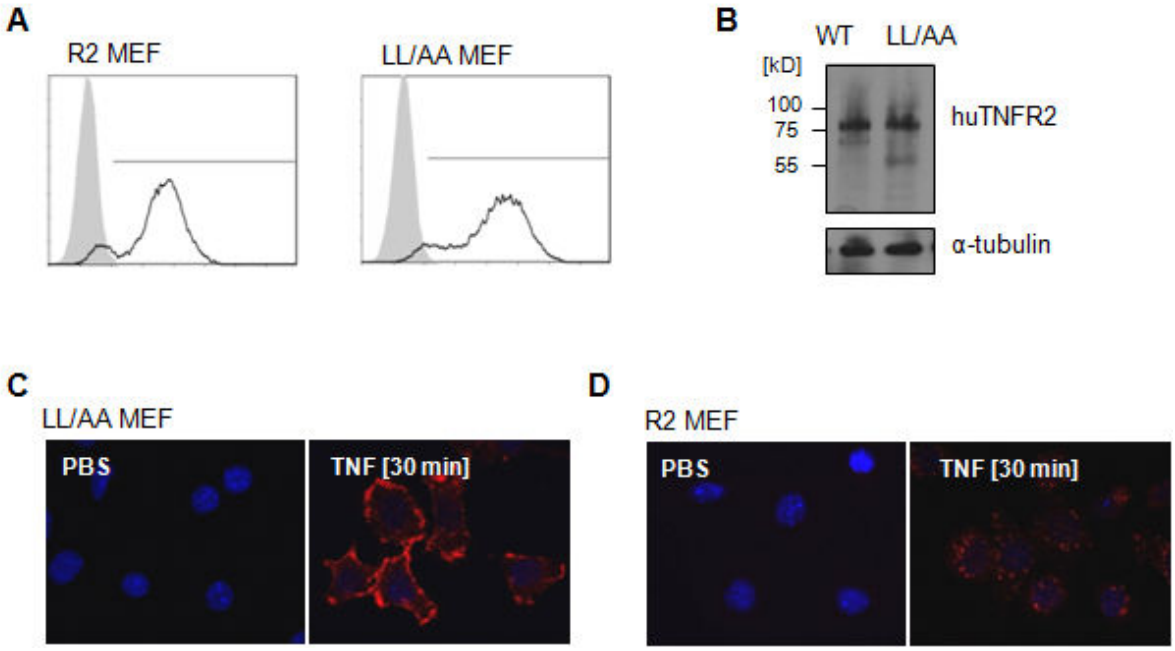

Figure 15: Internalization of TNFR2 is mediated via a di-leucin motif. DKO MEF were transfected with TNFR2 mutant LL/AA and sorted for high expression of TNFR2 LL/AA. R2 MEF (wildtype TNFR2) and LL/AA MEF (LL/AA TNFR2) show comparable receptor surface expression as demonstrated by flow cytometry (A) and immunoblot analysis (B). (C) LL/AA MEF or (D) R2 MEF were stimulated with 80M2 (1µg/ml; 30 minutes) followed by TNF-A546 (five minutes; 100ng/ml) for 30 minutes. Cells were fixed with 4% PFA and permeabilized with 0.1% Triton-X100. Localization of TNF/TNFR2 complexes was analyzed by immunofluorescence microscopy. Cell nuclei were visualized using DAPI. Pictures are projections of eight optical sections (0.4µm).

3.1.5. TNFR2 internalization depends on a di-leucin motif

The TNFR2 sequence contains the conserved di-leucine motif EQQHLL in its cytoplasmic domain (amino acids 315 to 320), an amino acid sequence that has been previously identified as an internalization motif in other membrane proteins (Bonifacino and Traub, 2003). Mutations of this sequence can lead to a complete loss of receptor internalization (Bonifacino and Traub, 2003).

Therefore, the two leucines in TNFR2 were mutated to alanine and a cell line stably expressing the mutated TNFR2 in DKO MEF was generated (LL/AA MEF). Flow cytometry showed that LL/AA MEF express similar levels of TNFR2 on their cell surface as R2 MEF (Figure 15A). Both TNFR2 variants had a molecular weight of approximately 80kDa (Figure 15B), indicating that posttranslational modifications are similar. Overall, the two cell lines showed similar properties and were therefore suitable for comparing the internalization of wildtype TNFR2 and TNFR2 LL/AA.

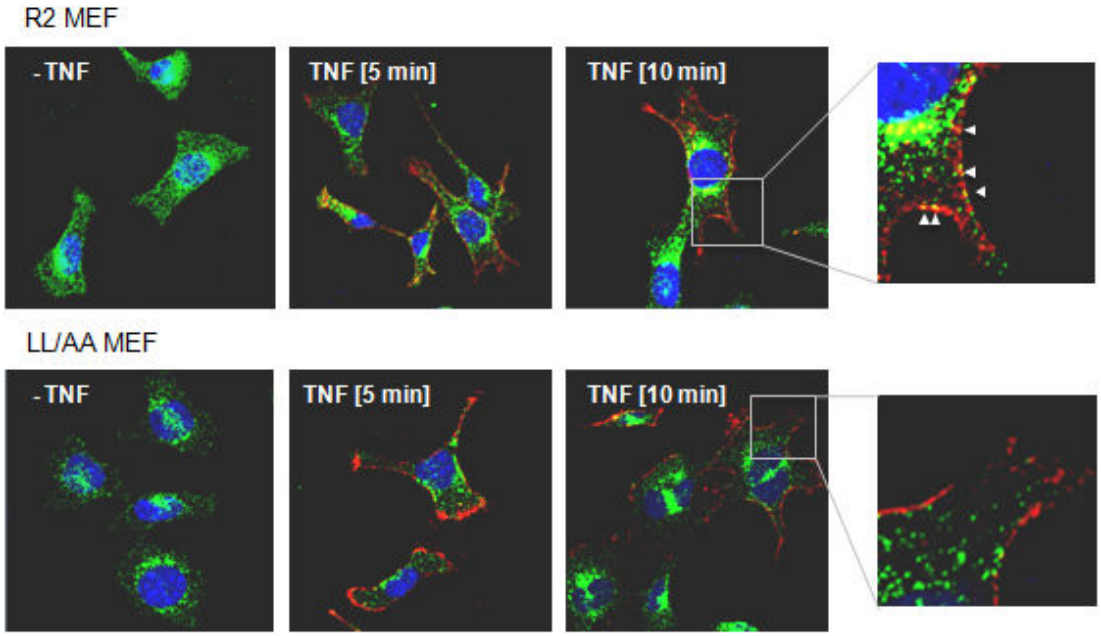

Figure 16: Only wildtype TNFR2 colocalizes with clathrin upon internalization. Cells were stimulated with 80M2 (1µg/ml; 30 minutes) followed by TNF-A546 (five minutes; 100ng/ml) for the indicated times and fixed with 4% PFA. Then, cells were permeabilized using 0.1% Triton X-100 and stained with anti-clathrin and anti-rabbit Alexa-Fluor488 antibodies. Pictures are optical sections obtained by confocal fluorescence microscopy. White arrowheads indicate regions of colocalization of TNF-A546 with clathrin at the cell surface.

LL/AA MEF showed no signs of receptor internalization upon stimulation with TNF (Figure 15C). After 30 minutes wildtype TNFR2 was completely taken up by the cell, whereas the mutated TNFR2 LL/AA still showed a homogenous distribution at the plasma membrane (Figure 15C and Figure 15D). These data clearly indicate that the EQQHLL motif is essential for ligand-induced internalization of TNFR2.

The identification of EQQHLL as the sequence motif responsible for endocytosis of TNFR2 strongly suggests a clathrin-mediated uptake of TNFR2 (Bonifacino and Traub, 2003). For verification, colocalization studies of TNF-A546 with clathrin were performed. In R2 MEF TNF-A546 partially colocalized with clathrin, visible as yellow dots at the plasma membrane

after 10 minutes of incubation (Figure 16). In contrast, upon TNF stimulation LL/AA MEF did not show any signs of colocalization with clathrin.

3.1.6. Ligand-dependent internalization is dispensable for NFκB signaling

Internalization of the TNF/TNFR1 complex has been described to trigger a switch of TNFR1 signaling towards the proapoptotic pathway (Schneider-Brachert et al., 2004) and therefore plays an important role in determining the cell fate in response to TNF. To determine whether inhibition of TNFR2 internalization affects the signaling of the receptor, the activation of NFκB was investigated by analyzing the degradation of its inhibitor IκBα. 10 to 20 minutes after TNF stimulation R2 MEF and LL/AA MEF showed decreased levels of IκBα. Both cell lines showed similar levels of IκBα degradation after 30 minutes, a point in time where internalization of wildtype TNFR2 was complete, but none of the mutated LL/AA TNFR2 was internalized. Resynthesis of IκBα could be observed after 40 minutes of TNF stimulation (Figure 17).

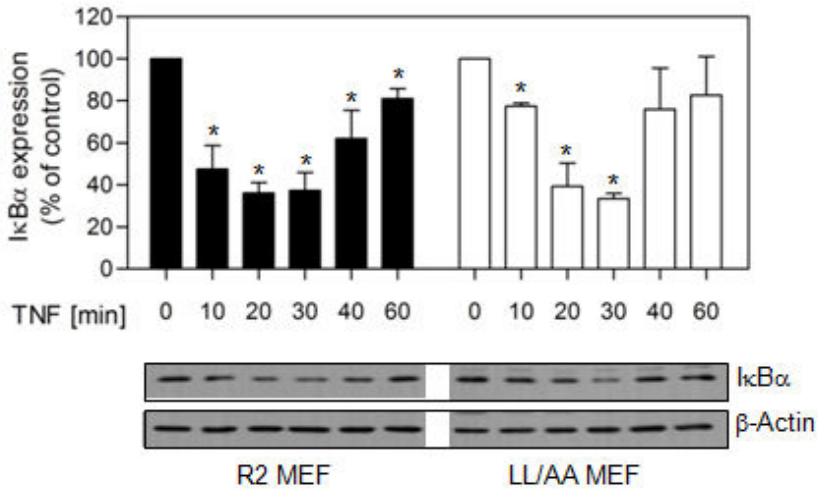

Figure 17: Ligand-dependent internalization is dispensable for TNFR2 signaling. R2 MEF (black bars) and LL/AA MEF (open bars) were stimulated with 80M2 (1µg/ml; 30 minutes) followed by CysHisTNF$_{R2}$ (100ng/ml) for the indicated times. Total cell lysates were analyzed by immunoblot for expression of IκBα. β-actin was used as a loading control. Representative blot and bar graph show the quantification of the IκBα band. *p values less than 0.05 versus untreated cells were considered to be significant (n = 3).

Under physiological conditions TNFR2 is only efficiently activated by memTNF (Grell et al., 1995). Internalization of TNF therefore requires some form of processing of memTNF, such as cleavage of the memTNF ectodomain by TACE/ADAM17. The sequence encoding the first 12 amino acids of sTNF is essential for cleavage of memTNF. A TNF mutant lacking these 12 amino acids (TNF$_{\Delta[1-12]}$) can no longer be processed, but is still highly bioactive (Kriegler et al., 1988; Perez et al., 1990).

CHO cells, stably transfected with this TNF mutant (CHO-TNF$_{\Delta[1-12]}$) (Grell et al., 1995) were used to stimulate R2 MEF with a cleavage-defective memTNF. These cells expressed high amounts of memTNF at the surface, as demonstrated by flow cytometry (Figure 18A).

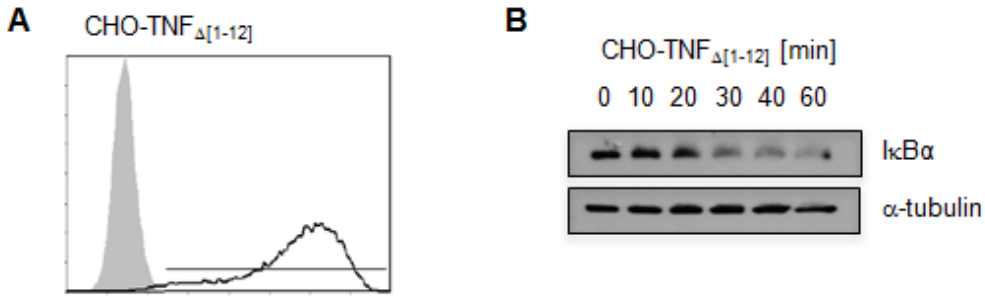

Figure 18: Characterization of CHO cells expressing a cleavage-defective mutant of memTNF. (A) CHO cells stably transfected with a shedding-defective TNF variant (CHO-TNF$_{[\Delta 1-12]}$; Grell et al., 1995) show high surface expression of TNF as demonstrated by flow cytometry. (B) R2 MEF ($5x10^5$ cells/well) were stimulated with CHO-TNF$_{[\Delta 1-12]}$ ($2x10^5$ cells/ml) for the indicated times. Total cell lysates were analyzed by immunoblot for expression of IκBα. α-tubulin was used as a loading control.

Coculture of R2 MEF with CHO-TNF$_{\Delta[1-12]}$ resulted in the degradation of IκBα after 20 minutes (Figure 18B), indicating that induction of the NFκB pathway is independent of receptor internalization. Since it could not be excluded that IκBα was also degraded in the memTNF-expressing CHO cells, which were included in the protein lysate, single cell analysis using fluorescence microscopy were performed. 10 minutes after addition of CHO-TNF$_{\Delta[1-12]}$ to R2 MEF cultures, some of the CHO-TNF$_{\Delta[1-12]}$ cells, which were in close proximity to TNFR2-expressing R2 MEF, had bound to R2 MEF via interaction between TNF and TNFR2, as evident by colocalization of TNF and TNFR2 (Figure 19A).

However, the colocalization was only observed when CHO cells were fully spread. Nevertheless, no signs of internalized receptor complexes could be observed. Surprisingly CHO-TNF$_{\Delta[1-12]}$ expressed high amounts of NFκB, as evident by the strong green staining observed in immunofluorescence experiments (Figure 19B). R2 MEF cells, which were closely associated to CHO-TNF$_{\Delta[1-12]}$ showed translocation of NFκB to the nucleus after 30 minutes (Figure 19B), indicating that binding of CHO-TNF$_{\Delta[1-12]}$ activated TNFR2 signaling in these cells. Since both the internalization-defective TNFR2 mutant and a cleavage-defective transmembrane TNF (TNF$_{\Delta[1-12]}$) are able to induce NFκB nuclear translocation, I propose that TNFR2 internalization is dispensable for the activation of the NFκB pathway.

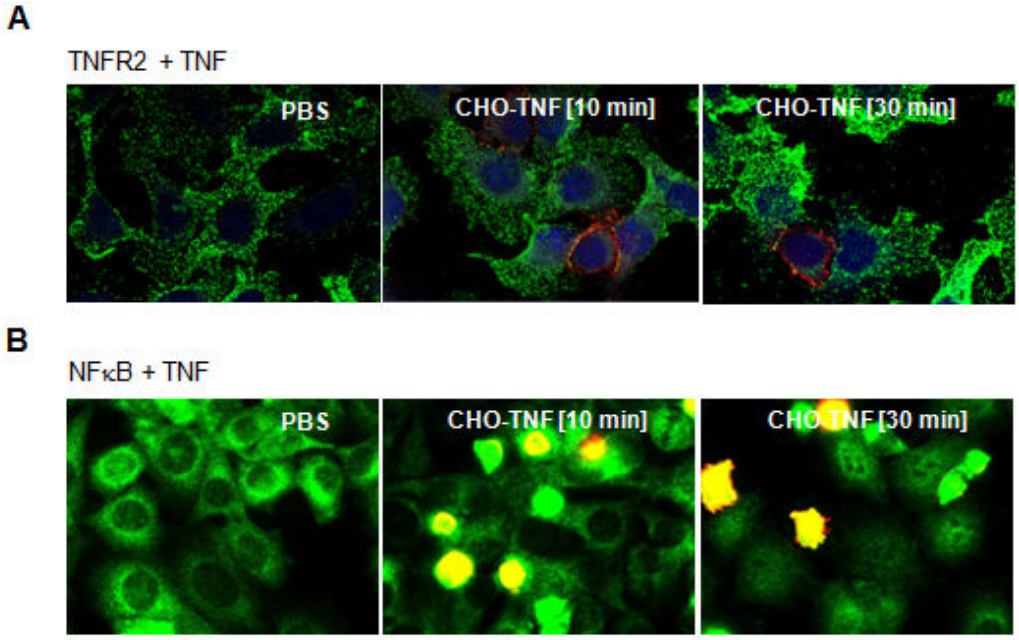

Figure 19: Ligand-dependent internalization is dispensable for TNFR2 signaling. R2 MEF ($3x10^4$ cells/well) were stimulated with CHO-$TNF_{[\Delta 1\text{-}12]}$ ($2x10^5$ cells/ml) for the indicated times. Cells were fixed with 4% PFA. TNF together with TNFR2 (A) or NFκB p65 (B) were detected with specific antibodies and fluorescence-labeled secondary antibodies. TNF was stained with Alexa-Fluor546, TNFR2 and NFκB with Alexa-Fluor488. Cell nuclei were visualized using DAPI. (A) Pictures are optical sections obtained by confocal fluorescence microscopy (B) Pictures are projections of 10 optical sections (0.32µm) obtained by wide-field fluorescence microscopy.

3.2. TNFR2-selective TNF with membrane TNF mimetic activity

TNFR2 signaling is associated with tissue regeneration in several organs. In particular, in the brain TNFR2 signaling stimulates remyelination and neuronal survival after cytotoxic insults. TNFR2-selective agonists therefore may exert protective effects in a variety of disorders, such as autoimmune, demyelinating and neurodegenerative diseases (Faustman and Davis, 2010). Since TNFR2 is only fully activated by memTNF it is essential that a TNFR2-specific therapeutic, while soluble for easy application, mimics the membrane-bound status of TNF.

3.2.1. Genetic engineering of TNC-scTNF$_{R2}$

Soluble TNF tends to dissociate at concentrations below the nanomolar range, thereby losing its bioactivity (Smith and Baglioni, 1987). Previous studies in the institute revealed that a single-chain TNF (scTNF), composed of three covalently fused TNF monomers possessed, compared to soluble recombinant TNF, increased stability *in vitro* and *in vivo* (Krippner-Heidenreich et al., 2008). By exchanging two amino acids in the TNF sequence, mutants can be generated that show high selectivity for TNFR1 (TNF R32W/ S86T) or TNFR2 (TNF D143N/A145R) (Loetscher et al., 1993).

But a TNFR2-specific scTNF was not able to activate TNFR2 without exogenous cross-linking of TNF/TNFR2 complexes via 80M2 (Krippner-Heidenreich et al., 2008), indicating that a covalently linked TNF trimer is not sufficient to mimic transmembrane TNF, the physiologic activating ligand of TNFR2. An additional strategy to stabilize trimeric ligands such as members of the TNF family is the introduction of the tenascin C (TNC) trimerization domain, yielding in stabilized TNC-ligands, which were biologically active without secondary cross-linking (Wyzgol et al., 2009). As a basis for the construction of a memTNF-like, TNFR2-selective TNF mutein, the concept of trimer stabilization was combined with the scTNF-format, resulting in Flag-TNC-TNF variants, with a nonameric oligomerization state (Rauert et al., 2010).

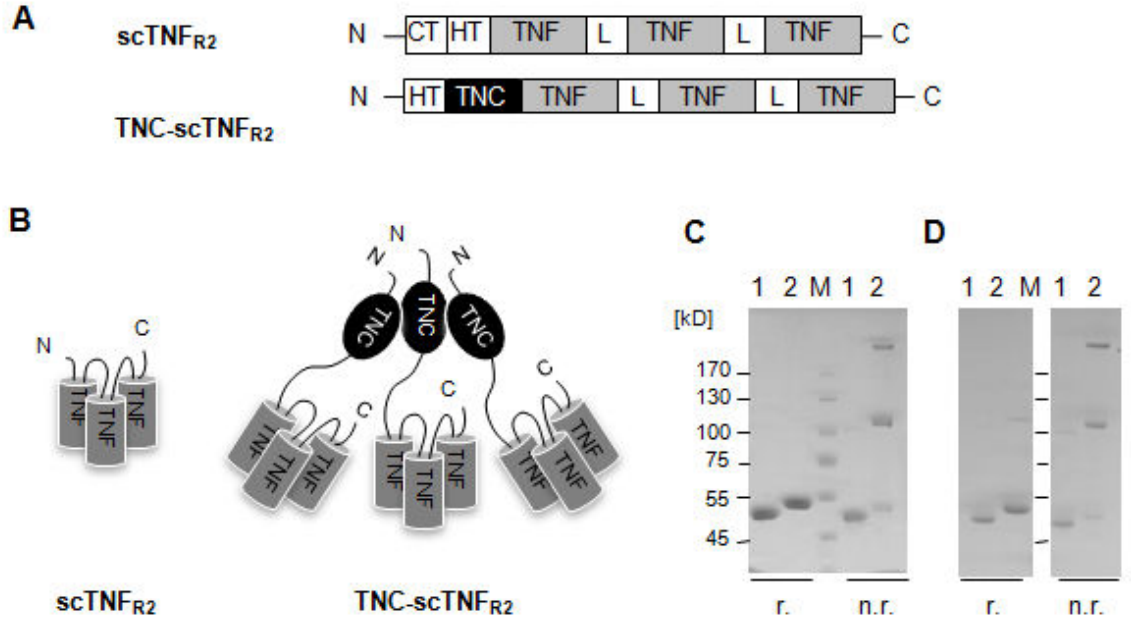

Figure 20: Genetic engineering of TNC-scTNF$_{R2}$. (A) and (B) Schematic representation of the TNF variants used in this study. CT: cys-tag, HT: his-tag; TNF: human TNFR2-specific (D143N/A145R) TNF module (aa 80-231); L: GGGGS-linker; TNC: trimerization domain of human tenascin C (aa 110-139) (C) SDS-PAGE and (D) immunoblot analysis of scTNF$_{R2}$ (1) and TNC-scTNF$_{R2}$ (2). Purified TNF variants were analyzed by 8% SDS-PAGE under reducing (r.) or non-reducing (n.r.) conditions and either stained with Coomassie or immunoblotted with anti-his-tag antibodies.

This TNC-TNF construction principle was used to generate an optimized tool for the potential use as a therapeutic in human diseases. Therefore, first a scTNF, selectively activating human TNFR2 (scTNF$_{R2}$) containing the amino acid exchanges D143N/A145R (Figure 20A) was cloned. Since protein therapeutics are usually produced in eukaryotic cells, the nucleic acid sequence was optimized with respect to eukaryotic codon usage. According to recent scTNF formats (Boschert et al., 2010), the three TNF monomers were fused via short GGGGS-linkers and a N-terminal hexahistidyl-tag for purification was included. An optimized, TNFR2-selective TNC-scTNF variant was cloned by fusion of the human TNC domain to the

N-terminal end of the scTNF$_{R2}$ construct (TNC-scTNF$_{R2}$; Figure 20A). The TNC-domain caused the assembly of three scTNF$_{R2}$ molecules resulting in the formation of a nonameric TNF variant (Figure 20B).

To generate alternative constructs to TNC-scTNF$_{R2}$, such as fusion proteins based on scTNF$_{R2,}$ a variable linker at the N-terminal region, containing an *EcoRI* restriction site was included. In addition, a free cysteine at the N-terminal end allows the coupling of scTNF$_{R2}$ to the surface of nanoparticles or liposomes. Such TNF-functionalized surfaces are a promising strategy to generate nanostructures with memTNF-mimetic activity (Bryde et al., 2005; Messerschmidt et al., 2008; Messerschmidt et al., 2009).

Both scTNF$_{R2}$ and TNC-scTNF$_{R2}$ were expressed in stably transfected HEK293 cells and purified by IMAC. Protein yields varied between 0.2 to 0.5mg per liter culture supernatant. Purity was confirmed by SDS-PAGE and immunoblot analysis. Under reducing conditions the TNF muteins exhibited an apparent molecular mass of approximately 51kDa and 54kDa matching the calculated molecular mass of 53.5kDa and 56.8kDa for scTNF$_{R2}$ and TNC-scTNF$_{R2}$, respectively (Figure 20C and Figure 20D). Under non-reducing conditions additional bands of 110 and above 170 kDa were observed for TNC-scTNF$_{R2}$, indicating that higher molecular structures were assembled. The oligomerization state of TNC-scTNF$_{R2}$ was further characterized by size exclusion chromatography. Both scTNF$_{R2}$ and TNC-scTNF$_{R2}$ eluted as a single major peak (Figure 21A and Figure 21B). scTNF$_{R2}$ eluted with an apparent molecular mass below 29kDa and TNC-scTNF$_{R2}$ between 67 and 200kDa indicating that, as expected, the TNC domain causes the stable trimerization of scTNF$_{R2}$ molecules.

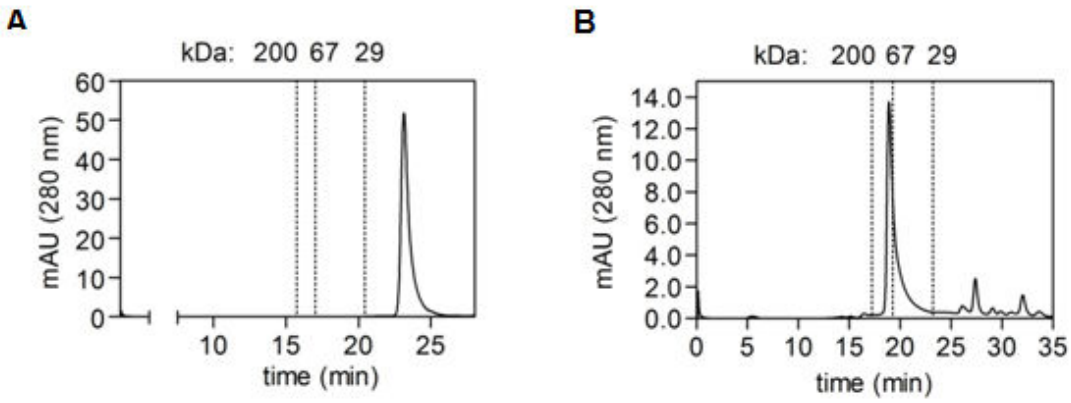

Figure 21: Characterization of TNC-scTNF$_{R2}$. (A) scTNF$_{R2}$ and (B) TNC- scTNF$_{R2}$ were analyzed by HPLC size exclusion chromatography using a BioSep-Sec-2000 column. Peak positions of relevant standard proteins are indicated.

3.2.2. Receptor selectivity and bioactivity of TNC-scTNF$_{R2}$

TNFR1$^{-/-}$/TNFR2$^{-/-}$-mouse embryonic fibroblasts stably expressing TNFR$_{ex}$-Fas$_{cyt}$ chimeric receptors that bind TNF and display Fas-specific signaling were used to address the receptor selectivity of scTNF$_{R2}$ and TNC-scTNF$_{R2}$ (Krippner-Heidenreich et al., 2002). In contrast to human soluble recombinant TNF (huTNF) both TNF muteins, in accordance with the expected selectivity for TNFR2, showed no cytotoxicity on MEF TNFR1-Fas (Figure 22A), thereby verifying that both variants had lost affinity for TNFR1 due to the mutations D143N/A145R.

A strong apoptotic response could be induced in TNFR2-Fas MEF by TNC-scTNF$_{R2}$, whereas treatment with scTNF$_{R2}$ showed only cytotoxicity at high concentrations. In contrast, the presence of the TNFR2-specific antibody 80M2, which is known to additionally cross-link ligand/receptor complexes, thus mimicking the action of memTNF (Grell et al., 1995) resulted in a strong cytotoxic activity of the trimeric scTNF$_{R2}$, too (Figure 22A).

Similar results were obtained using the human rhabdomyosarcoma cell line Kym-I (Figure 22B). Kym-I cells endogenously express both TNF receptors and are highly sensitive to TNF-induced cytotoxicity (Grell et al., 1993). In this cell line, selective stimulation of TNFR2 results in the induction of apoptosis, too, by endogenous production of TNF and autotropic or paratropic activation of TNFR1 (Grell et al., 1999).

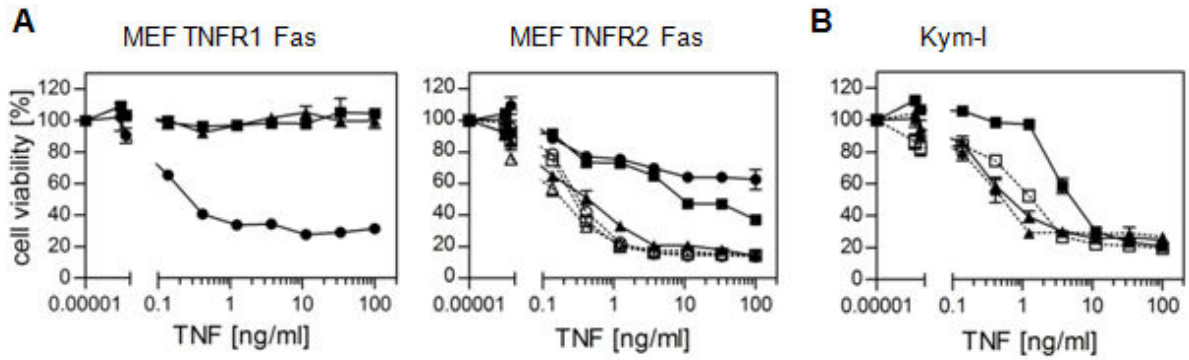

Figure 22: Bioactivity and receptor selectivity of TNC-scTNF$_{R2}$. Mouse embryonic fibroblasts (MEF) from TNFR1$^{-/-}$/TNFR2$^{-/-}$-mice stably transfected with the chimeric receptors TNFR1-Fas or TNFR2-Fas (A) or Kym-I cells (B) were stimulated with wildtype human TNF (huTNF; ●), scTNF$_{R2}$ (■) or TNC-scTNF$_{R2}$ (▲). Where indicated, MEF TNFR2-Fas were pretreated with the ligand/receptor stabilizing monoclonal antibody 80M2 (open symbols; 1µg/ml) before TNF treatment. Cell viability was determined by crystal violet staining after 24 hours (n = 3).

Since TNC-scTNF$_{R2}$ was able to mimic memTNF without cross-linking of ligand/receptor complexes, the bioactivity of TNC-scTNF$_{R2}$ was further addressed, using the previously described cell line R2 MEF (section 3.1). Performing immunoprecipitation analysis it could be demonstrated that TRAF2 is recruited to TNFR2 upon stimulation with TNC-scTNF$_{R2}$ (Figure

23A). Nuclear translocation of the transcription factor NFκB was detected 30 minutes after TNF stimulation (Figure 23B; 90% NFκB-positive nuclei) and increased PKB/Akt phosphorylation levels could be discerned after 10 minutes (Figure 23C). These observations are in full accordance with previous results obtained by stimulating R2 MEF with soluble TNF in combination with 80M2 (Figure 5 and Figure 6), demonstrating that TNC-scTNF$_{R2}$ fully activates TNFR2 without additional cross-linking of ligand/receptor complexes.

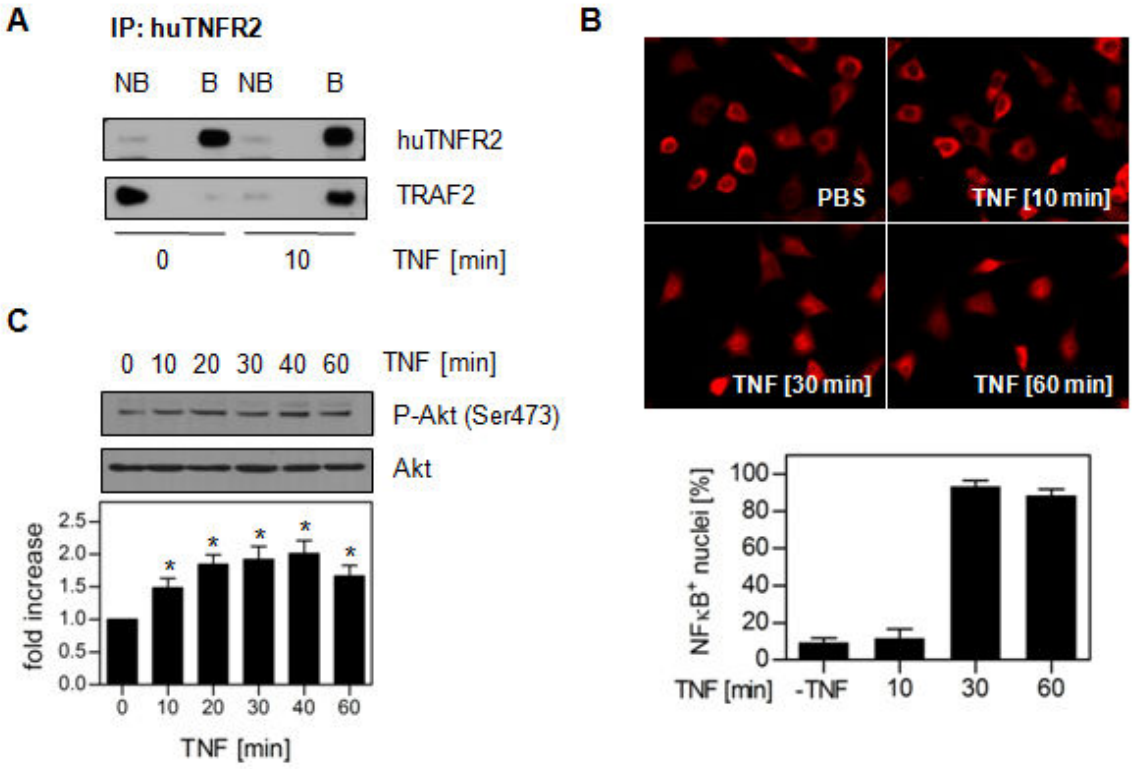

Figure 23: TNC-scTNF$_{R2}$ induces TNFR2 signaling in R2 MEF. R2 MEF were stimulated with TNC-scTNF$_{R2}$ (20ng/ml) for the indicated times. (A) TNFR2 was immunoprecipitated using MR2-1 antibodies and protein G agarose. The precipitates were analyzed by immunoblot analysis using anti-huTNFR2 (HP9003) and anti-TRAF2 antibodies. (B) Localization of NFκB p65 was visualized via immunofluorescence microscopy and the number of cells showing NFκB translocation was counted. At least 200 cells per experiment were analyzed (n = 3). (C) Phospho-Akt (Ser473) levels in cell lysates were analyzed using immunoblot analysis. Akt was used as a loading control. Representative blot and bar graph show the quantification of the phospho-Akt (Ser473) band. *p values less than 0.05 versus untreated cells were considered to be significant (n = 3).

3.2.3. TNC-scTNF$_{R2}$ induces clustering of TNFR2

The bioactivity study using the Kym-I cells showed that 10ng/ml is the lowest concentration, where both TNF variants showed maximal bioactivity after 24 hours (Figure 22A). This concentration was used to determine the ligand-dependent short-time effects on clustering of TNFR2 at the membrane and induction of signaling pathways.

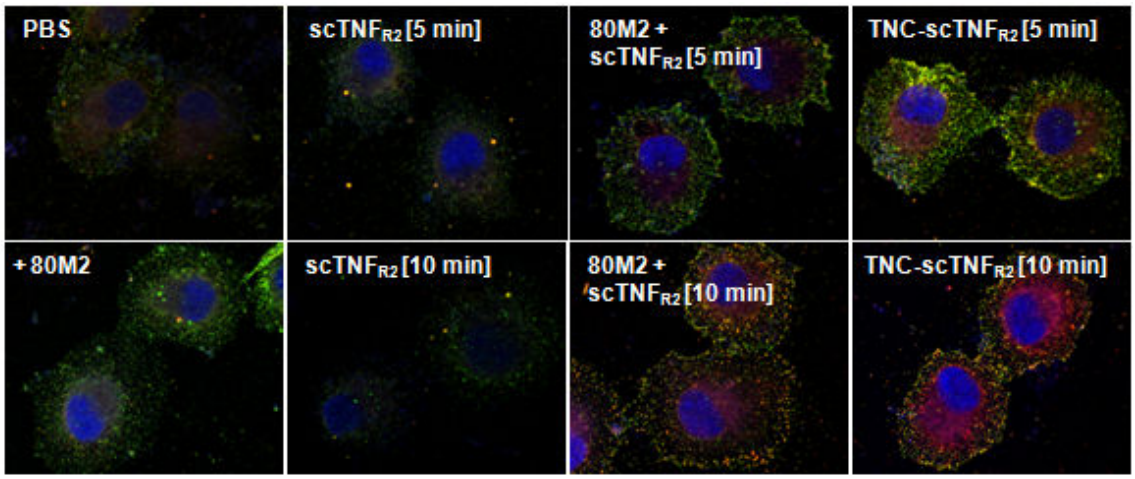

Figure 24: Binding of TNC-scTNF$_{R2}$ leads to clustering of TNFR2. Kym-I cells were left untreated or preincubated with 80M2 (1µg/ml) for 30 minutes. Then scTNF$_{R2}$ or TNC-scTNF$_{R2}$ (10ng/ml) were added for the indicated times and cells were fixed with 4% PFA. Cells were stained with goat anti-TNF and rabbit anti-huTNFR2 antibodies followed by anti-rabbit Alexa-Fluor488 and anti-goat Alexa-Fluor546 antibodies. Cell nuclei were visualized using DAPI. Pictures are optical sections obtained by confocal fluorescence microscopy.

To investigate the ligand-induced cluster formation of TNFR2, Kym-I cells were incubated with the TNF variants for five or 10 minutes, fixed with PFA, and the localization of the TNF/TNFR2 complexes was analyzed by immunofluorescence microscopy (Figure 24). As expected, TNFR2 clusters were observed after addition of 80M2. After five minutes a limited number of TNF/TNFR2 complexes were observed in the TNC-scTNF$_{R2}$ treated sample. The amount of visible TNF/TNFR2 complexes increased dramatically after 10 minutes, when nearly all receptors were observed in clusters colocalized with TNF. Stimulation with scTNF$_{R2}$ did not lead to clustering of TNFR2 within 10 minutes. Only after preincubation with the receptor-cross-linking antibody 80M2 cluster formation was observed, indicating that, in contrast to TNC-scTNF$_{R2}$, the scTNF$_{R2}$ variant alone is not able to form TNF/TNFR2 clusters that can be visualized by immunofluorescence.

The superior bioactivity of TNC-scTNF$_{R2}$ was further analyzed using NFκB p65 nuclear translocation in Kym-I cells as a read-out system (Figure 25). The scTNF$_{R2}$-treated Kym-I cells showed only a limited translocation after 60 minutes, whereas TNC-scTNF$_{R2}$ stimulation resulted in a strong, transient NFκB translocation with an apparent peak at 30 minutes. After 60 minutes, the amount of translocated NFκB was reduced again. Thus, in contrast to scTNF$_{R2}$, TNC- scTNF$_{R2}$ was able to induce receptor clustering at the cell membrane and nuclear translocation of NFκB, demonstrating that TNC- scTNF$_{R2}$ is a TNF derivative with memTNF-mimetic activity that selectively activates TNFR2.

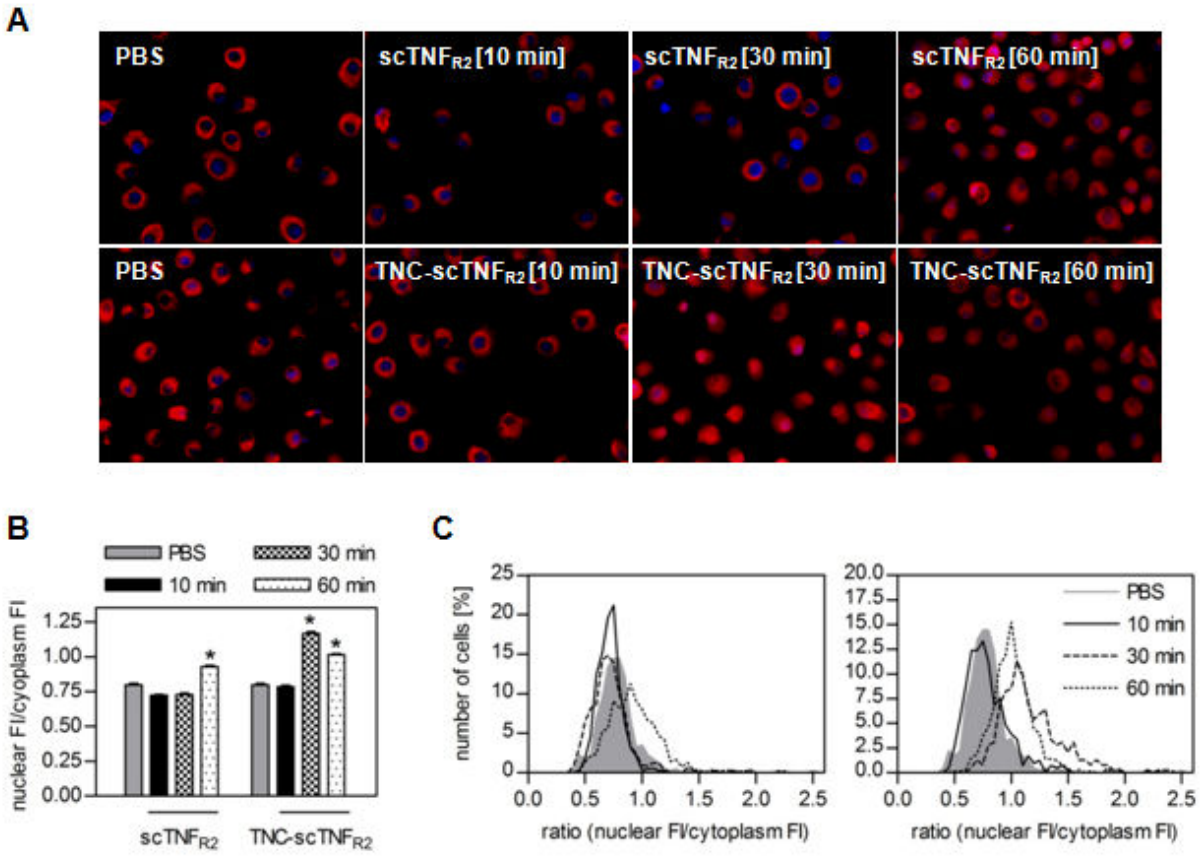

Figure 25: Comparison of the NFκB translocation after stimulation with scTNF$_{R2}$ or TNC-scTNF$_{R2}$. Kym-I cells were stimulated with scTNF$_{R2}$ or TNC-scTNF$_{R2}$ (10ng/ml) for 10, 30 or 60 minutes. Cells were fixed with 4% PFA, permeabilized with 0.1% Triton-X100 and stained with anti-NFκB p65 antibodies and Alexa-Fluor546-labeled secondary antibodies. Cell nuclei were visualized using DAPI. Shown are representative images (A), the ratio of nuclear to cytoplasm fluorescence intensity (FI; B) and the ratio of nuclear to cytoplasm FI in relation to the number of cells (C). At least 100 cells were analyzed per condition. *p values less than 0.05 versus untreated controls were considered to be significant (n = 2).

3.3. Functional activity of TNC-scTNF$_{R2}$

3.3.1. TNFR2 signaling enhances IL-2-dependent T cell activation

TNF impacts nearly all aspects of T cell biology such as development of thymocytes, peripheral T cell homeostasis, primary antigenic responses, apoptosis, effector functions, memory cell formation as well as tolerance induction and maintenance (Chatzidakis and Mamalaki, 2010).

To investigate the effect of the TNFR2-specific TNF on lymphocyte populations human PBMCs were cultivated together with TNC-scTNF$_{R2}$ in combination with suboptimal doses of ConA (0.5µg/ml) and IL-2 (20U/ml). IL-2 was sufficient to increase IFN gamma (IFN-γ) secretion about 3.5-fold, compared to lymphocytes treated only with ConA. Whereas TNC-scTNF$_{R2}$ alone did not induce secretion of IFN-γ, the secretion was enhanced about 6.5-fold

when TNC-scTNF$_{R2}$ was added in combination with IL-2 (Figure 26A), suggesting a synergistic effect of TNF and IL-2 in secretion of the cytokine.

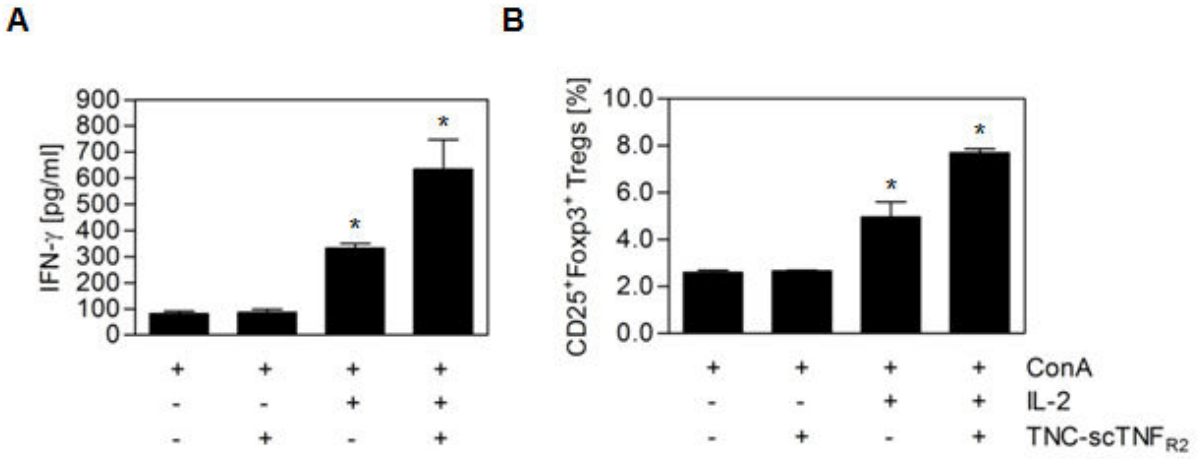

Figure 26: TNC-scTNF$_{R2}$ enhances IL-2-dependent T cell activation. Human PBMCs were activated with ConA (0.5µg/ml) and stimulated with IL-2 (20U/ml) and/or TNC-scTNF$_{R2}$ (100ng/ml) for 48 hours. (A) Culture medium samples were collected and concentrations of the secreted interferon gamma (IFN-γ) in the supernatants were determined by ELISA. *p values less than 0.05 were considered to be significant (n = 3) (B) Surface of PBMCs was stained with APC-conjugated antibodies, specific for CD25. Then cells were fixed, permeabilized and stained with PE-conjugated antibodies, specific for FoxP3. Fluorescence was analyzed by flow cytometry. *p values less than 0.05 were considered to be significant (n = 3).

Since TNF is known to activate and expand Tregs in combination with IL-2 (Chen et al., 2007), the amount of CD25$^+$FoxP3$^+$ T cells after stimulation with TNC-scTNF$_{R2}$ together with IL-2 was determined. In contrast to TNC-scTNF$_{R2}$, treatment with IL-2 was sufficient to induce Treg differentiation, as shown by a 2.0-fold increase in the amount of Tregs (Figure 26B). Stimulation of T cells with TNC-scTNF$_{R2}$ together with IL-2 enhanced the number of Tregs among the activated T cells about 3.5-fold over control cultures, supporting the previous evidence that TNFR2 is involved in the expansion of regulatory T cells.

3.3.2. TNFR2 signaling induces transcription of CNTF in astrocytes

Astrocytes outnumber any other cell type in the CNS. Therefore, the effects of TNC-scTNF$_{R2}$ on astrocytes are of particular importance for the potential use as a therapeutic in the treatment of CNS diseases. Primary astrocyte cultures are usually prepared from brains of postnatal mice (day two to three), as an alternative for these animal-consuming experiments, an immortalized astrocyte cell line was developed by stable transfection of primary astrocytes from huTNFR2-transgenic TgE1335 Balb/c mice (Douni and Kollias, 1998) with SV40 virus large T antigen expression constructs (IMA1335). The immortal mouse cell line IMA1335, displaying ectopic huTNFR2 expression, could be cultivated for up to four weeks

without any changes in marker expression and was used to investigate the expression and regulation of TNFR2.

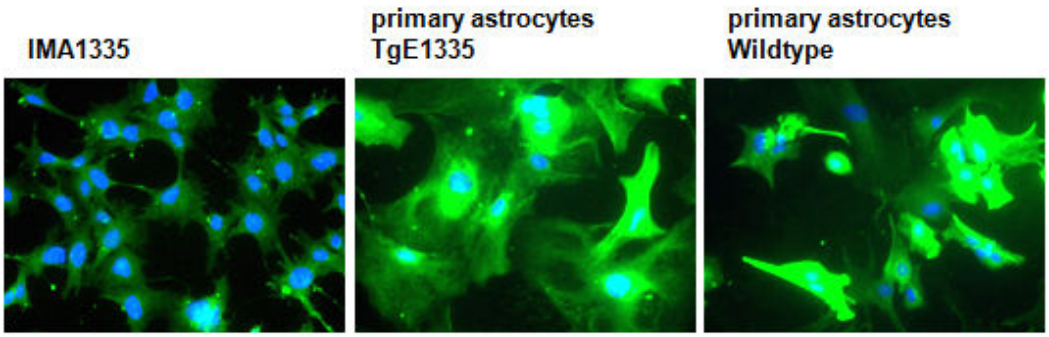

Figure 27: Expression of glial fibrillary acidic protein in the immortalized astrocyte cell line IMA1335. Primary astrocytes from the TNFR2-transgenic mouse line TgE1335 Balb/c were immortalized with large T antigen from SV40 virus, resulting in the cell line IMA1335. (A) Cells were fixed with 4% PFA and permeabilized using 0.1% Triton X-100. The astrocyte marker glial fibrillary acidic protein (GFAP) was detected with specific Alexa-Fluor488-labeled antibodies. Cell nuclei were visualized using DAPI. Fluorescence was analyzed using wide-field fluorescence microscopy. Pictures are projections of eight optical sections (0.4µm).

The expression of glial fibrillary acid protein (GFAP) an intermediate filament protein, which is characteristic for CNS astrocytes, was addressed to analyze the astrocyte-like character of IMA1335. GFAP was homogenously distributed in the cells, but overall GFAP protein levels were significantly lower than in primary astrocytes (Figure 27). Then, the expression and bioactivity of the TNF receptors was analyzed. The endogenous mouse TNFR1 and TNFR2, as well as the transgenic huTNFR2 were constitutively expressed by IMA1335 cells, as demonstrated by RNA and immunofluorescence analysis (Figure 28A and Figure 28B). Whereas huTNFR2 was localized at high levels at the cell surface, mouse TNFR (mTNFR) 1 and especially mTNFR2 were detected at much lower protein levels.

DMEM containing 5% FCS was used as standard cultivation medium. Interestingly, the increase of the serum concentration to 10% or an increase of the cell density elevated the surface expression level of huTNFR2 (Figure 28C), indicating that huTNFR2 expression is regulated at several levels. Using medium containing 10% FCS, it could be demonstrated that both, stimulation of the endogenous mouse receptors and the ectopically expressed huTNFR2 resulted in the degradation of IκBα (Figure 28D and Figure 28E), indicating that both mTNFRs and the human TNFR2 are functional. Whereas mouse TNF (mTNF) showed a strong degradation of IκBα between 10 and 20 minutes, likely through predominant mTNFR1 activation, the effect was more ambiguous in the human TNC-scTNF$_{R2}$-treated cells, targeting the transgenic huTNFR2, where only a minor degradation was observed after 30 minutes.

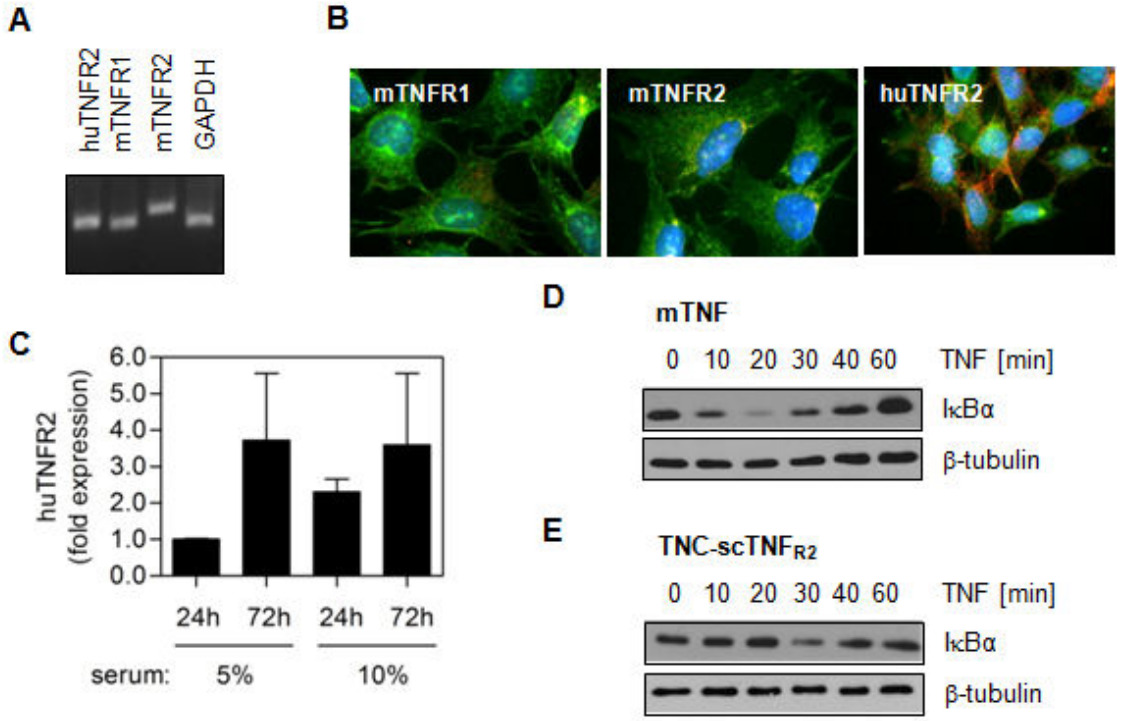

Figure 28: Expression and functionality of the transgenic human TNFR2 in IMA1335 cells. (A) RNA was extracted from IMA1335 cells, transcribed into cDNA and transcript expression of mouse TNFR1 (mTNFR1) and TNFR2 (mTNFR2) and human TNFR2 (huTNFR2) was analyzed using PCR. (B) IMA1335 were fixed with 4%PFA and stained for surface expression of mTNFR1, mTNFR2 and huTNFR2 with specific antibodies and Alexa-Fluor546-labeled secondary antibodies, followed by cytoplasmic staining of GFAP with Alexa-Fluor488-labeled specific antibodies. Cell nuclei were visualized using DAPI. Fluorescence was analyzed using wide-field fluorescence microscopy. Pictures are projections of eight optical sections (0.4µm). (C) IMA1335 (30000 cells/cm^2) were cultivated in DMEM medium containing 5% or 10% FCS. After 24 or 72 hours, cells were harvested and surface expression of huTNFR2 was analyzed using flow cytometry. Mean fluorescence intensity was calculated and presented relative to the sample cultivated in 5% FCS for 24 hours (n = 2; performed by Sandra Böker). (D-E) IMA1335 were grown in medium containing 5% FCS for 24 hours. Then medium was exchanged to 10% and cells were grown for further 48 hours. Cells were stimulated with (D) mouse TNF (mTNF; 10ng/ml; indicated times) or (E) TNC-scTNF$_{R2}$ (10ng/ml; indicated times). IκBα levels were analyzed by immunoblot analysis. β-Tubulin was used as a loading control.

The role of TNF on proliferation of astrocytes is controversially discussed and only seen under specific culture conditions (Barna et al., 1990; Moretto et al., 1993; Selmaj et al., 1991c; Tejada-Berges and Yong, 1994). To investigate the influence of TNF on the proliferation rate of IMA1335, the cells were cultivated in medium containing 10% serum together with mTNF or TNC-scTNF$_{R2}$ for 72 hours and the cell number was determined using the crystal violet assay. Whereas mTNF did not alter the proliferation, TNC-scTNF$_{R2}$ slightly increased the cell numbers about 1.3-fold in a PI3K-PKB/Akt-dependent manner (Figure 29A).

Since proliferation of astrocytes is characteristic for reactive astrogliosis, TNC-scTNF$_{R2}$ was further compared to dibutyryl-cAMP (db-cAMP), which can be used as an *in vitro* model of reactive astrocytosis (Daginakatte et al., 2008). Several neurotrophic and astrocyte-specific

factors, including glial fibrillary acidic protein (GFAP) or ciliary neurotrophic factor (CNTF) were not expressed at a detectable level in IMA1335 (Figure 29B and data not shown), indicating that the immortalization affected the metabolic activity of IMA1335.

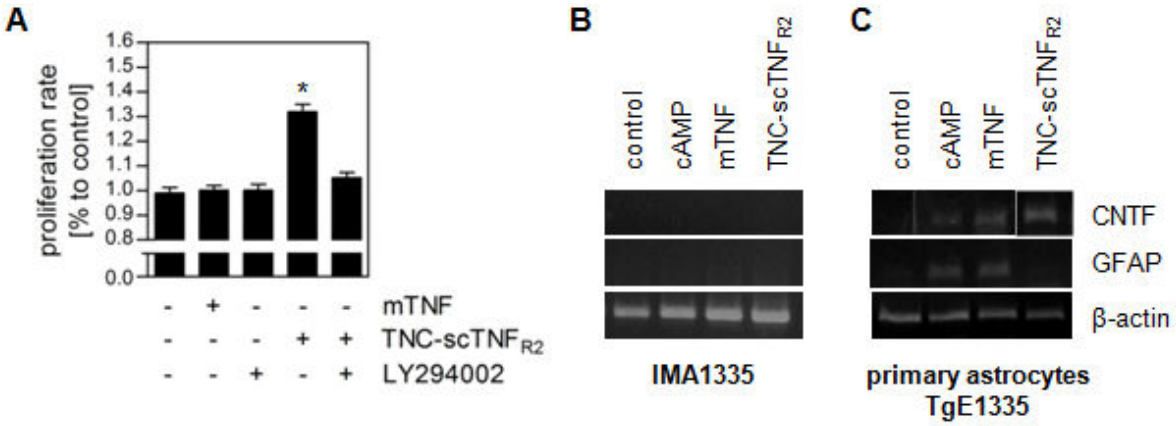

Figure 29: TNF increases the proliferation rate and induces transcription of CNTF via TNFR2 in astrocytes. (A) IMA1335 were grown in medium containing 10% FCS. Cells were left untreated or were prestimulated with LY294002 (25µM; one hour) before addition of mTNF (100ng/ml) or TNC-scTNF$_{R2}$ (100ng/ml). After incubation for 72h, the number of cells was determined by crystal violet staining and proliferation rate was calculated relative to the value obtained for the unstimulated control. *p values less than 0.05 versus untreated cells were considered to be significant (n = 3). (B) IMA1335 or (C) primary astrocytes from TgE1335 Balb/c mice were incubated with db-cAMP (1mM), mTNF (10ng/ml) or TNC-scTNF$_{R2}$ (10ng/ml). After six hours RNA was isolated and transcribed into cDNA. cDNA samples were analyzed for CNTF and GFAP levels using PCR amplification. β-actin was used as a loading control.

Therefore primary astrocyte cultures from TgE1335 Balb/c mice were used to further investigate the effects of TNC-scTNF$_{R2}$ on astrocyte activation (Figure 29C). TNC-scTNF$_{R2}$, in contrast to mTNF and db-cAMP, did not increase the transcription level of GFAP. However, TNC-scTNF$_{R2}$ induced the transcription of the neurotrophic factor CNTF. Interestingly, since CNTF has been implicated in neuronal regeneration and remyelination (Müller et al., 2009; Stankoff et al., 2002), astrocytes may contribute to the regenerative effects of TNFR2 in the CNS.

3.3.3. TNC-scTNF$_{R2}$ preserves neurons from hydrogen peroxide-induced apoptosis

The loss of neurons is the main cause of neurodegenerative diseases and TNFR2 signaling has been associated with protection of neurons after cytotoxic insults (Fontaine et al., 2002; Marchetti et al., 2004). Therefore, the neuroprotective properties of TNC-scTNF$_{R2}$ were investigated using LUHMES, a non-transformed mesencephalic-derived cell line with neuronal-like character (Lotharius et al., 2002; Lotharius et al., 2005; Schildknecht et al., 2009).

Neuron progenitor cells have been conditionally immortalized through the v-myc oncogene under control of a tet-transactivator and are therefore maintained in a progenitor-like proliferative condition. When the v-myc transgene is switched off by tetracycline, the cells differentiate into post-mitotic neurons (Lotharius et al., 2002; Lotharius et al., 2005).

Neurons, differentiated under these conditions developed long dendrites, formed a neural-like network (Figure 30A and Figure 30B) and expressed typical neuronal markers such as the neuronal form of β-III-tubulin, α-synapsin, microtubule-associated protein 2 (MAP2) and neurofilament (Lotharius et al., 2005; Schildknecht et al., 2009; Figure 30B and data not shown).

To determine the effects of TNFR-signaling in these cells, the cell surface localization of both TNF receptors was analyzed. TNFR1 as well as TNFR2 clustered on the soma, as well as on dendrites, as demonstrated by immunofluorescence microscopy (Figure 30C).

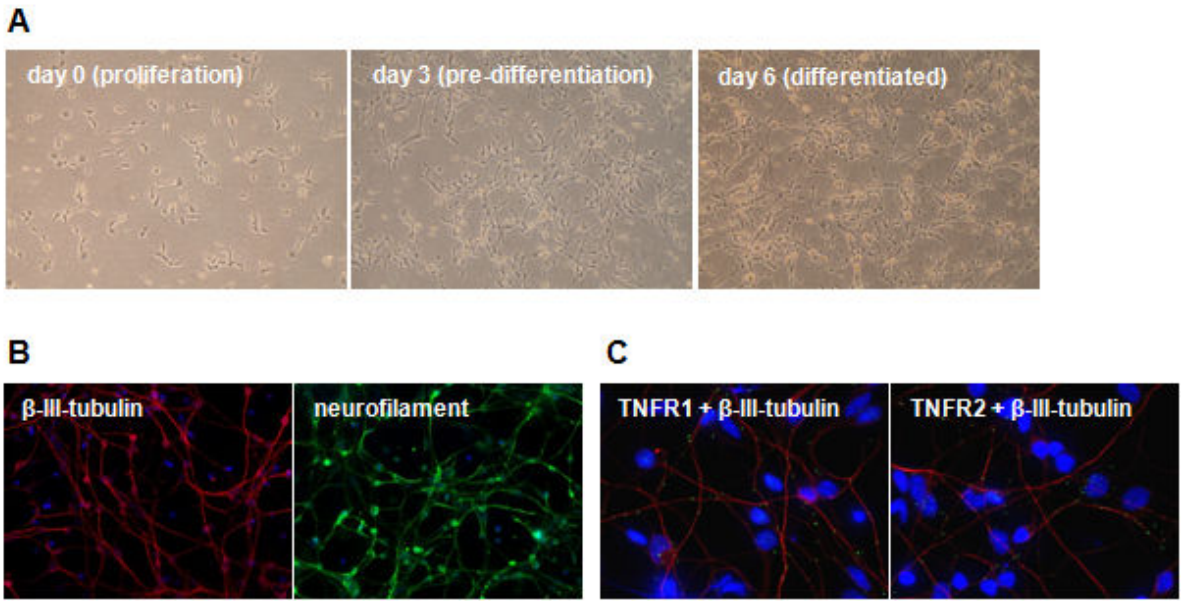

Figure 30: LUHMES is a human immortalized mesencephalic-derived cell line with neuron-like characteristics. LUHMES cells proliferate as progenitor cells. After addition of tetracycline, glial cell line-derived neurotrophic factor (GDNF) and db-cAMP cells differentiate within six days into mature differentiated neurons. (A) Brightfield images from progenitor and differentiated cells. (B) Expression of the neuronal markers β-III-tubulin and neurofilament was analyzed by indirect immunofluorescence. Cells were fixed with 4% PFA, permeabilized with 0.1% Triton-X100 and stained with specific antibodies and Alexa-Fluor546 (β-III-tubulin) or Alexa-Fluor488 (neurofilament) labeled secondary antibodies. Cell nuclei were visualized using DAPI. Pictures are projections of eight optical sections (0.4µm). (C) LUHMES cells were fixed with 4% PFA and stained for surface expression of TNFR1 and TNFR2 with specific antibodies and Alexa-Fluor488-labeled secondary antibodies. Then cells were fixed again with 4% PFA, permeabilized with 0.1% Triton-X100 and the neuronal marker β-III-tubulin was stained with specific antibodies and Alexa-Fluor546-labeled secondary antibodies. Cell nuclei were visualized using DAPI. Pictures are projections of eight optical sections (0.4µm).

Since TNFR2 is involved in neuroprotection in *in vitro* and *in vivo* models (Fontaine et al., 2002; Marchetti et al., 2004), the potential of TNC-scTNF$_{R2}$ to protect LUHMES cells after neurotoxic insults induced by oxidative stress was investigated.

Oxidative stress, a process, which contributes to the damage in neurodegenerative diseases can be mimicked by addition of hydrogen peroxide *in vitro* (Whittemore et al., 1995). To investigate the sensitivity of LUHMES cells to hydrogen peroxide-induced cell death, the cells were incubated for one hour with the toxic chemical, then the medium was changed to remove hydrogen peroxide and the cells were cultivated for additional 24 hours. LUHMES cells died at hydrogen peroxide concentrations higher than 20µM, with a half maximal effective concentration (EC_{50}) of 75µM (Figure 31A). By adding TNC-scTNF$_{R2}$ in a therapeutic setting after the induction of cell death, it was then investigated whether TNC-scTNF$_{R2}$ influences hydrogen peroxide-induced cell death (Figure 31B). TNC-scTNF$_{R2}$ treatment was protective and nearly 80% of the cells survived the treatment, compared to 30% survival without TNC-scTNF$_{R2}$.

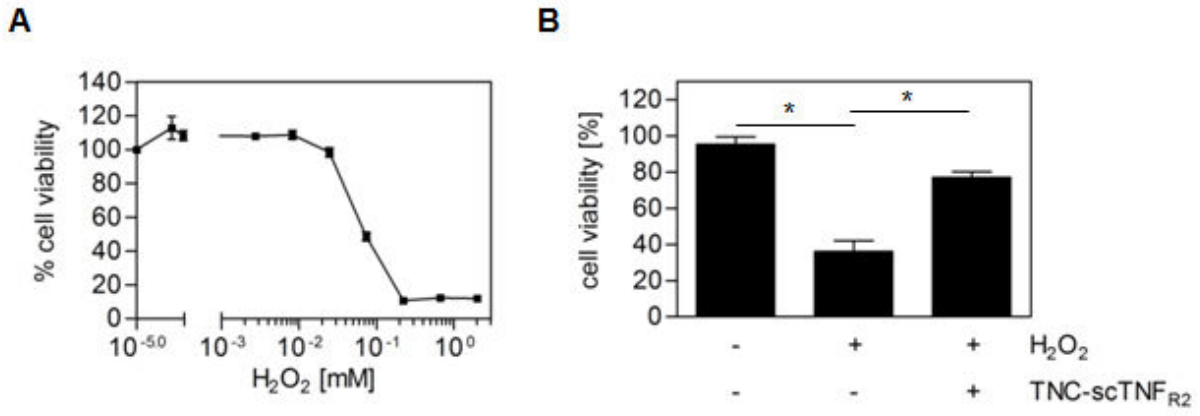

Figure 31: TNC-scTNF$_{R2}$ induces neuroregeneration after oxidative stress. (A) LUHMES cells were incubated with different concentrations of hydrogen peroxide (H_2O_2) for one hour. Then cells were washed with medium und cultivated for additional 24 hours. Cell viability was measured using the MTT assay. The graph shown is a representative (triplicates) from two independent experiments. (B) LUHMES cells were stimulated with hydrogen peroxide (100µM) for one hour, then cells were washed with medium und regenerated for 24 hours in medium with or without TNC-scTNF$_{R2}$ (100ng/ml). Cell viability was measured using the MTT assay. *p values less than 0.05 were considered to be significant (n = 3).

To investigate the neuroprotective effect of TNC-scTNF$_{R2}$ in detail, LUHMES cells were fixed two or four hours after starting the hydrogen peroxide treatment and the β-III-tubulin content (Figure 32A) and the number of cells (Figure 32B) were determined by immunofluorescence analysis. After two hours, a significant decrease in the number of cells was noted in the hydrogen peroxide-treated samples, which was further enhanced after four hours. In contrast no significant changes were observed in the samples cultured with TNC-scTNF$_{R2}$. In addition

this observation was supported by the reduced amount of TUNEL-positive cells after regeneration in presence of TNC-scTNF$_{R2}$ (Figure 32C). Since TNC-scTNF$_{R2}$ affected the hydrogen peroxide-induced cell death already one hour after addition, I propose that TNFR2 signaling directly interferes with the progression of apoptosis, presumably through inactivating components of the apoptosis cascade.

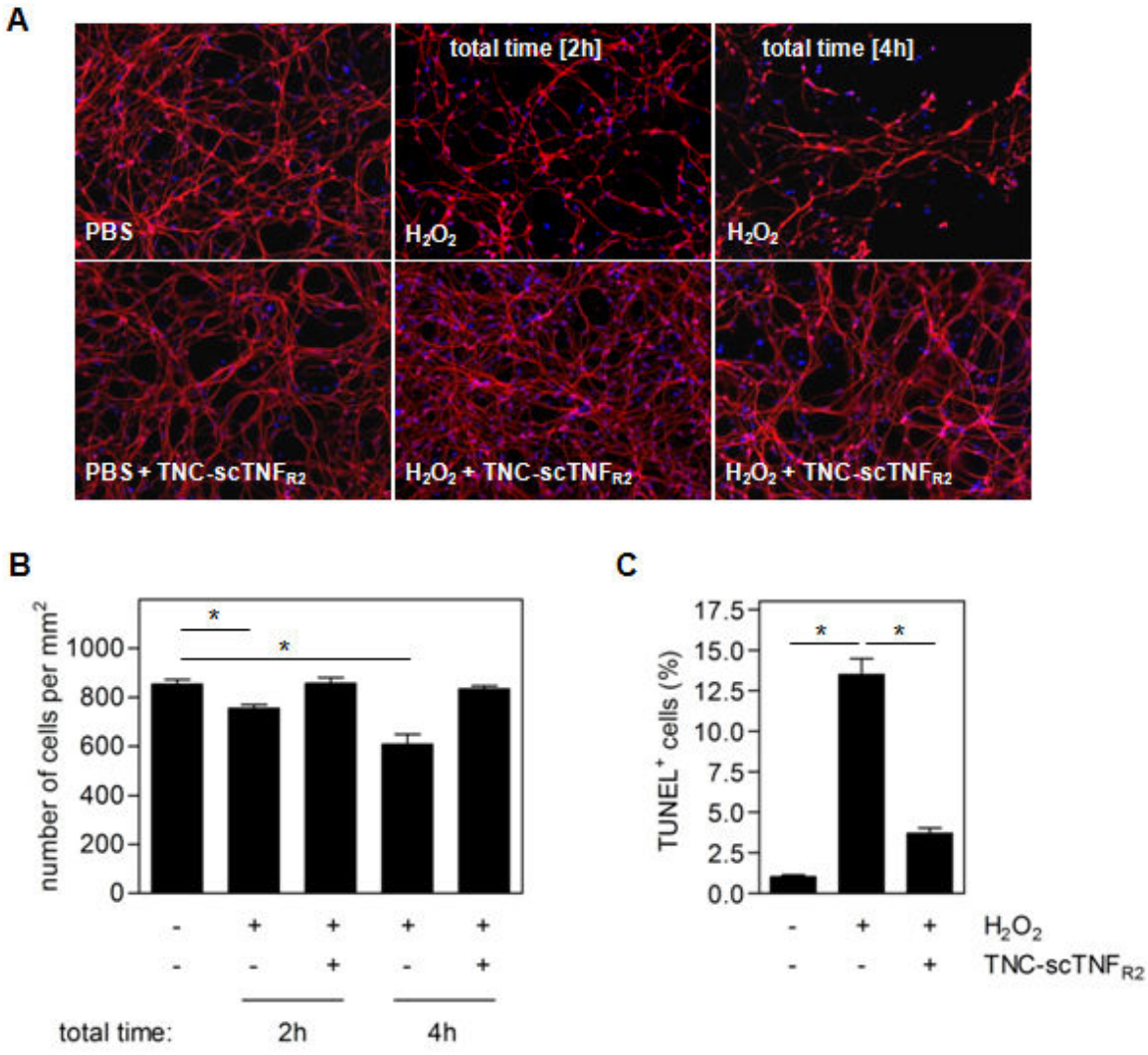

Figure 32: TNC-scTNF$_{R2}$ induces neuroregeneration after oxidative stress. LUHMES cells were stimulated with hydrogen peroxide (H_2O_2; 100µM). After one hour the cells were washed with medium und regenerated for the indicated time intervals in medium with or without TNC-scTNF$_{R2}$ (100ng/ml). (A) Cells were regenerated for one or three hours, fixed with 4%PFA, permeabilized with 0.1% Triton-X100 and β-III-tubulin was detected with specific antibodies. Cell nuclei were visualized using DAPI. Pictures are projections of eight optical sections (0.4µm). (B) The number of cells was determined by counting the nuclei (DAPI staining). (C) Cells were regenerated for one hour and apoptotic cells were identified by terminal deoxynucleotidyl transferase (TdT)-mediated dUTP-FITC nick end labeling (TUNEL). (B and C) At least 10 different image sections containing a minimum of 500 cells were used to determine the number of total and TUNEL-positive cells. *p values less than 0.05 were considered to be significant (n = 2).

3.4. *In vivo* properties of TNC-scTNF$_{R2}$

3.4.1. TNC-scTNF$_{R2}$ is highly stable and shows improved *in vivo* properties

Soluble trimeric TNF is unstable at picomolar levels and slowly converts into inactive monomers (Alzani et al., 1995; Corti et al., 1992). The trimeric scTNF format showed superior *in vitro* stability and was stable in cell culture medium for up to 70 days (Krippner-Heidenreich et al., 2008). The stability in serum is an important parameter for *in vivo* application.

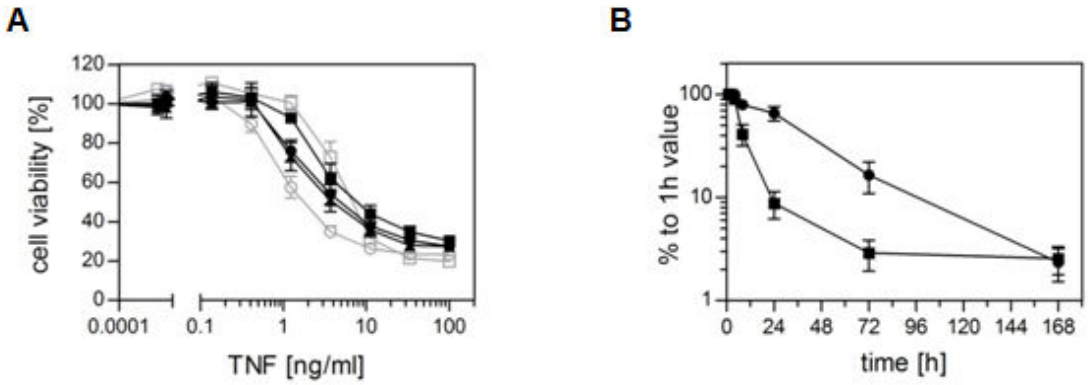

Figure 33: *In vitro* and *in vivo* stability of TNC-scTNF$_{R2}$. (A) TNC-scTNF$_{R2}$ was incubated at 37°C for one (●), three (▲) or seven (■) days in FCS. The bioactivity of the incubated TNF muteins was compared to stocks of scTNF$_{R2}$ (□) and TNC-scTNF$_{R2}$ (○) stored at 4°C in PBS. Kym-I cells were stimulated with the TNF variants and cell viability was determined by crystal violet staining. (B) Pharmacokinetics of TNC-scTNF$_{R2}$ (50µg/mouse; ●) compared to scTNF$_{R2}$ (50µg/mouse; ■) after i.p. injection in huTNFR2-transgenic TgE1335 C57BL/6 mice (n = 3 each). The concentration of TNF in the plasma was quantified by ELISA.

Construct	MW (kD)	$T_{1/2}\alpha$ (h)	$T_{1/2}\beta$ (h)	$AUC_{0\text{-}7d}$ (%·h)
scTNF$_{R2}$	53.5	6.17 ± 0.76	58.44 ± 12.97	1398 ± 258
TNC-scTNF$_{R2}$	170.4	21.59 ± 0.82	27.72 ± 9.04	4593 ± 761

Table 3: Pharmacokinetic properties of the TNF variants.

Construct	time after i.p. injection (hours)				
	1	2	8	24	72
scTNF$_{R2}$	108.06 ± 4.07	108.30 ± 3.14	45.38 ± 11.26	9.62 ± 2.96	2.01 ± 1.27
TNC-scTNF$_{R2}$	132.84 ± 5.29	134.62 ± 6.31	113.83 ± 6.40	84.67 ± 10.84	20.58 ± 6.27

Table 4: Blood concentrations of the TNF variants (ng/ml).

To investigate the serum stability of the TNC-scTNF$_{R2}$ nonamers, the protein was incubated in FCS for various time periods. Even after three days of FCS treatment, TNC-scTNF$_{R2}$

showed an increased bioactivity compared to scTNF$_{R2}$ not treated with FCS. After seven days, the bioactivity of TNC-scTNF$_{R2}$ was similar to scTNF$_{R2}$, indicating that the TNC trimers had dissociated into monomers (Figure 33A).

Another important parameter for *in vivo* application is the circulation time of the molecule in the blood stream. Krippner-Heidenreich et al. showed that, compared to soluble TNF, scTNF was more efficiently retained in the blood stream, indicating that dissociation of TNF into monomers favors the removal of TNF *in vivo* (2008).

The pharmacokinetic properties of TNC-scTNF$_{R2}$ were analyzed after a single dose (50µg/mouse) i.p. injection into C57BL/6 mice and compared to the pharmacokinetic properties of scTNF$_{R2}$ (50µg/mouse). A human TNF-specific ELISA was used to determine the concentration of the TNF variants in the blood plasma. Compared with scTNF$_{R2}$, TNC-scTNF$_{R2}$ showed a strongly prolonged circulation in the blood (Figure 33B), with an initial half-life ($T_{1/2}\alpha$) of 21.59 ± 0.82 hours and a terminal half-life ($T_{1/2}\beta$) of 27.72 ± 9.04 hours. The area under the curve (AUC_{d0-7}) was increased 3.3-fold (Table 3). Two hours after the injection, a maximal concentration of 108.30 ± 3.14ng/ml scTNF$_{R2}$ and 134.62 ± 6.31ng/ml TNC-scTNF$_{R2}$ was measured. After eight hours the scTNF$_{R2}$-concentration was decreased to less than 50%, whereas nearly 85% of TNC-scTNF$_{R2}$ was retained in the circulation (Table 4). All together these results demonstrate that TNC-scTNF$_{R2}$ is retained in the circulation for at least 24 to 72 hours, a time window where the TNF variant was stable in serum and showed increased bioactivity compared to scTNF$_{R2}$.

3.4.2. Systemic tolerance of TNC-scTNF$_{R2}$

TNF is a cytokine with a multitude of effects, including cytotoxic, cytostatic and immunomodulatory roles. Administration of high doses of soluble TNF is associated with septic shock and systemic toxicity due to effects on blood pressure followed by multi-organ failure (Hieber and Heim, 1994; Sidhu and Bollon, 1993).

To investigate the systemic tolerance of the TNFR2-specific TNF variant, I injected (i.p.) a single-dose TNC-scTNF$_{R2}$ (100µg/mouse) into huTNFR2-transgenic TgE1335 C57BL/6 mice (Douni and Kollias, 1998) and compared systemic effects to injection (i.p.) of a single-dose of mouse TNF (20µg/mouse) into C57BL/6 mice. Over a time period of 24 hours no significant changes of the body temperature were observed in the PBS or TNC-scTNF$_{R2}$-treated mice, whereas the mTNF-treated mice showed a drastic temperature reduction of up to 4°C eight hours after the injection (Figure 34A) and severe signs of systemic toxicity, such as piloerection, shivering and reduced activity. In contrast no signs of systemic toxicity were observed in PBS or TNC-scTNF$_{R2}$-treated animals. To further investigate the systemic tolerance of TNC-scTNF$_{R2}$, the amount of activated immune cells was analyzed by staining spleen sections with CD11b, a marker for activated neutrophils and macrophages. Whereas

mTNF treatment resulted in a prolonged activation of macrophages, TNC-scTNF$_{R2}$-treated animals showed only a transient increase in the number of activated macrophages after eight hours (Figure 34B). Concluding, TNC-scTNF$_{R2}$ was well tolerated in animals and exhibited only a transient short-time activation of immune cells, but no observable systemic physiological consequences.

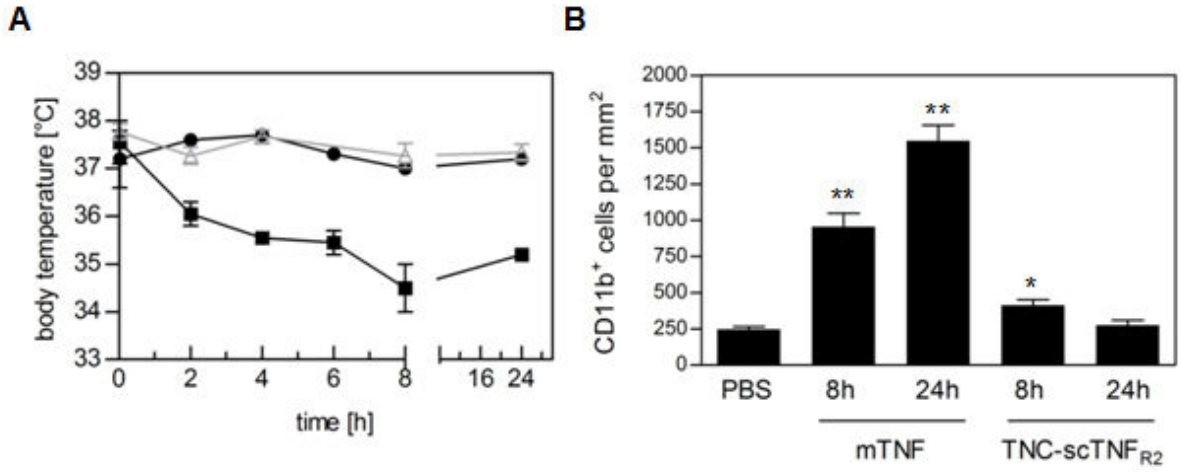

Figure 34: Systemic tolerance to TNC-scTNF$_{R2}$ treatment. mTNF (■; 20µg/mouse) or PBS (Δ) was injected (i.p.) into C57BL/6 mice and TNC-scTNF$_{R2}$ (●; 100µg/mouse) into huTNFR2-transgenic C57BL/6 mice (n = 3; each). (A) Body temperature, as an indicator for systemic effects of TNF, was measured over a period of 24 hours. (B) Spleens were removed and cryosections were stained for activated macrophages and neutrophils with CD11b-specific antibodies. The number of CD11b-postitve cells per mm^2 was determined. Six different sections with at least 500 cells were analyzed per sample. *p values less than 0.01 (** less than 0.0001) versus PBS treated controls were considered to be significant.

4. Discussion

4.1. Dynamics of TNFR2 signaling and turnover

In contrast to TNFR1, the expression of TNFR2 is more restricted to selected cell types and subjected to stimulus-dependent regulation, both at transcriptional and posttranscriptional levels. To study dynamics of TNFR2 signaling and turnover at the membrane, the mouse fibroblast cell line R2 MEF with constitutive, stable expression of human TNFR2 was generated. A di-leucine internalization motif was identified, which is responsible for the clathrin-dependent internalization of TNFR2. Furthermore, evidence is provided that internalization is dispensable for TNFR2 signaling, i.e. activation of NFκB. Rather, internalization of TNFR2 leads to lysosomal degradation and causes, together with spontaneous shedding of the extracellular domain, a depletion of functional TNFR2 at the plasma membrane thereby limiting the responsiveness towards TNFR2 signaling.

4.1.1. Modulation of NFκB activity by PKB/Akt signaling

R2 MEF display high level human TNFR2 expression on a mouse TNF receptor negative background, which is of relevance because of constitutive TNFR1 expression in basically all cell types and species cross-reactivity of human TNF with TNFR1 of mouse and many other species. The general advantage of this cell model is that cellular responses to TNF can be clearly assigned to huTNFR2, allowing a broad range of potential applications like analysis of TNFR2 signal complex formation, identification of receptor-associated proteins and analysis of TNFR2 signaling pathways at a molecular level. TNF-induced recruitment of TRAF2 into membrane TNFR2 complexes is readily detected by both biochemical and microscopic methods and provides a rational to apply proteomics for identification of the molecular components of the TNFR2 signaling complex and will be helpful to unravel the as yet unclear molecular linkage of TNFR2 activation to downstream pathways leading to PI3K-PKB/Akt activation.

In vivo, it was reported that PKB/Akt transiently associates with the IκK complex and together with NIK mediates the phosphorylation of IKKα at the specific residues threonine 23 (PKB/Akt) and serine 176 (NIK), leading to the degradation of IκBα and the nuclear translocation of NFκB in human embryonic kidney 293 cells (Ozes et al., 1999; Romashkova and Makarov, 1999).

I obtained similar results using the cell line R2 MEF. Inhibition of PI3K-PKB/Akt signaling resulted in the abolishment of IκBα-phosphorylation at position serine 32 and a significant reduced degradation of IκBα, suggesting that PKB/Akt is involved in controlling the degradation of IκBα. Nevertheless, degradation of IκBα was observed, indicating that

additional mechanisms contribute to IκBα degradation. In accordance with these observations, a decreased TNF-induced translocation of NFκB was noted after blocking PKB/Akt signaling.

However, arguments against the involvement of PKB/Akt and NIK in controlling phosphorylation of the IκK complex and nuclear accumulation of NFκB have been reported (Delhase et al., 2000). Furthermore, it was shown that NFκB activation but not PKB/Akt is required for dexamethasone-dependent protection against TNF cytotoxicity in L929 cells (Mendoza-Milla et al., 2005), indicating that NFκB can be activated independent from PKB/Akt. Additionally, PKB/Akt and NFκB contribute independently towards the resistance to TNF-mediated cytotoxicity in human glioma cell lines. The TNF-induced NFκB activation, analyzed through the key events degradation of IκBα, nuclear translocation of the NFκB p65 subunit and NFκB promoter activation was independent of the PI3K/Akt pathway (Sudheerkumar et al., 2008).

It has been elucidated that NFκB activity is controlled by a dual mechanism: the induction of nuclear translocation as well as the regulation of the transcriptional activity of NFκB. TNF stimulation not only can lead to the degradation of IκBα, it also induces the phosphorylation of NFκB subunit p65 and the subsequent stimulation of NFκB transactivation through pathways distinct from induced nuclear translocation (Bird et al., 1997; Wang and Baldwin, 1998). In addition to its role in the degradation of IκBα, activated PI3K or PKB/Akt have been shown to stimulate the transcription function of NFκB by phosphorylating the transactivation domain 1 of the p65 subunit thereby activating NFκB independent of nuclear translocation (Madrid et al., 2000; Sizemore et al., 1999).

At the moment, I cannot exclude that PKB/Akt additionally regulates NFκB phosphorylation in R2 MEF. But, further arguments are provided that involvement of PKB/Akt in the activation of NFκB is a stimulus and cell-specific event.

4.1.2. TNFR2 is degraded upon internalization

R2 MEF are particularly suited for microscopic analysis to investigate the fate of TNFR2 after ligand binding. Both shedding of the ectodomain (Solomon et al., 1999) and ligand-induced internalization of TNFR2 (Pennica et al., 1992) have been described. However, the relevance of receptor internalization for signaling as well as the fate and route of internalized receptors have not been studied so far.

The transmembrane metalloproteinase TACE/ADAM-17 is responsible for the proteolytic release of several cell-surface proteins, including TNF and TNFR2 (Reddy et al., 2000). Accordingly, it could be confirmed that shedding of the TNFR2 ectodomain in R2 MEF is dependent on MMP activity. Shedding of TNFR2 was ligand-independent and was reduced

after stimulation with TNF. Potentially, the formation of large TNF/TNFR2 complexes, evident from microscopic analysis of ligand-mediated receptor clustering at the cell surface could interfere with the access of TACE to the receptor cleavage site. At present, this possibility cannot be excluded, but a more evident explanation is internalization and lysosomal degradation of TNF/TNFR2 complexes.

Receptor internalization is a widely used mechanism to modulate signaling. Binding of hormones and growth factors to their cognate receptors typically trigger internalization, leading to transient receptor clearance from the surface, followed by either recycling to the membrane or lasting clearance through degradation in lysosomes (Bonifacino and Traub, 2003). However, en route to a late endosomal/lysosomal compartment, signaling may ensue and the relevance of endocytic vs. plasma membrane signaling of receptors is in part controversially discussed, depending on the ligand/receptor system studied. Recent studies show that receptor signal transduction is not primarily restricted to the cell surface (Schütze et al., 2008; von Zastrow and Sorkin, 2007). In early endosomes ligated receptor tyrosine kinases maintain their kinase activity and are still accessible for cytosolic signaling proteins, suggesting that intracellular signaling may continue from these sorting organelles (Baass et al., 1995). There is now strong evidence that specific signals can arise from the endosomal compartment, thereby supporting the signaling endosome hypothesis.

Among signaling receptors, trafficking of the epidermal growth factor (EGF) receptor is the best-characterized system. Depending on the localization of the receptor and its accessibility for downstream signaling partners, different signaling pathways are induced. Whereas signaling through the phospholipase C and PI3K pathway seems to be restricted to the cell surface (Haugh and Meyer, 2002), signaling through the Ras pathway occurs through both the cell surface and intracellular compartments (Haugh et al., 1999a; Haugh et al., 1999b). Furthermore, these data not only suggest that signaling can arise from endosomes, but also that receptor trafficking can modulate both the specificity and the duration of the signal transduction process (Wiley, 2003).

For the TNF/TNFR system, an active signaling function of endocytosed TNFR1 has been clearly shown, which is qualitatively different from cell surface receptor signaling because of a different molecular composition of plasma membrane vs. internalized TNFR1 signal complexes (Schneider-Brachert et al., 2004; Schütze et al., 1999). By contrast, the fate and the potential functional role of the TNF/TNFR2 complex after internalization was so far not known.

The results, presented in this study, show that the TNFR2 signaling complex including its ligand is internalized into endosomes. Endosomes comprise three different compartments, early endosomes, late endosomes and recycling endosomes (Mellman, 1996). They are distinguished by different markers, like EEA1 (early endosome antigen 1) for early

endosomes or Rab7 for late endosomes. The TNF/TNFR2 complex showed colocalization with early endosome marker EEA1 and late endosome marker Rab7. Rab7, which is controlling the aggregation and fusion of late endocytic structures/lysosomes, is essential for maintenance of the perinuclear lysosome compartment (Bucci et al., 2000). As indicated by the colocalization with Rab7, the TNFR2 signaling complex is transported to late endosomes and thus enters the lysosomal pathway, where it is degraded together with TNF and proximal components. Mechanistically, TNFR2 internalization follows the same pathway as described recently for other TNF receptor superfamily members, in particular CD95 (Algeciras-Schimnich and Peter, 2003) and TNFR1 (Schütze et al., 1999), which both use a clathrin-dependent pathway.

4.1.3. Internalization of TNFR2 is mediated by a di-leucin motif

Internalization of TNFR1 via clathrin-coated vesicles depends on a YXXØ motif (Schneider-Brachert et al., 2004). In contrast, in the present study, a di-leucine motif in the cytoplasmic domain of TNFR2 was identified that is required for internalization of the TNF/TNFR2 complex. In accordance with previous studies showing that di-leucine motifs mediate clathrin-dependent internalization (Bonifacino and Traub, 2003), mutation of the two leucines to alanine in the TNFR2 cytoplasmic domain (L319A, L320A) suppressed binding of TNFR2 to clathrin-coated pits. Consequently, ligand-induced internalization of the mutant receptor was inhibited.

At present, it cannot be excluded that additional mechanisms, such as caveolin-mediated internalization, are involved in the internalization of TNFR2. Caveolin-1 has been described to associate with TRAF2 to form a complex that is recruited to TNF receptors (Feng et al., 2001). In addition, TRAF2 is able to interact with the actin binding protein filamin (Leonardi et al., 2000). Thus, recruitment of TRAF2 might directly link TNFR2 to actin and other structures of the cytoskeleton, which are known to play an active role in endocytosis (Jeng and Welch, 2001). TRAF2 recruitment may therefore be a cofactor for TNFR2 internalization.

4.1.4. Internalization of TNFR2 is dispensable for TNFR2 signaling

Compared to R2 MEF, NFκB activation appeared to occur with the same kinetics and efficiency in LL/AA MEFs, demonstrating that the NFκB pathway can be activated independently of clathrin-dependent internalization. In contrast, as internalization is followed by fast degradation of the TNF/TNFR2 complex, it may primarily serve to attenuate cellular responsiveness to extracellular ligands.

The membrane bound form of TNF, but not soluble TNF is a strong activator of TNFR2. *In vitro*, the TNFR2-specific monoclonal antibody 80M2 mimics, in concert with soluble homotrimeric TNF, the stimulation by memTNF. Thus, 80M2 is able to hyperstimulate TNFR2

in the presence of the soluble ligand, although it is, on its own, neither agonistic nor antagonistic (Grell et al., 1995). The simultaneous binding and triggering of TNFR2 by antibody and soluble TNF may have an enhancing effect on the kinetics of internalization. *In vivo*, memTNF and TNFR2 may be expressed on the same cells, potentially allowing autotropic signaling, but more often are expressed on two different cells, thus interacting *in trans*. Therefore in this situation, to be of physiological relevance, internalization of the TNF/TNFR2 complex needs processing of memTNF.

To scrutinize the role of memTNF processing for internalization, CHO cells stably transfected with the $TNF_{\Delta[1\text{-}12]}$ mutant (Grell et al., 1995) were used for stimulation of R2 MEF. This mutant cannot be processed by TACE due to genetic deletion of the TACE cleavage site. Accordingly, in contrast to the stimulation with TNF in combination with 80M2, no signs of internalized TNF were observed. But, since binding of TNF to its receptor is a reversible process, TNFR2 could still be internalized after dissociation of the ligand/receptor complex.

Concluding, I assume that because of the missing protease cleavage site in $TNF_{\Delta[1\text{-}12]}$, this molecule is not processed and the internalization of TNF/TNFR2 complexes is blocked. As a consequence of the blocked internalization, signaling may ensue due to the formation of stable, persisting membrane-signaling complexes, as reported previously for TNF and CD95L (Gerspach et al., 2006; Henkler et al., 2005). Indeed, the data obtained here with engineered non-cleavable TNF-expressing cells, revealing strong NFκB activation in those R2 MEF that showed contacts with memTNF-expressing CHO cells, are in full accordance with superior signaling of memTNF.

Under physiological situations, TACE/ADAM17 expressed on TNF producing cells is able to cleave memTNF. As a consequence receptor bound TNF is released from the juxtaposed membrane and can be internalized as a complex with TNFR2 into endosomes of the target cells. Receptor internalization after stimulation with a membrane bound ligand has been observed for other members of the TNF receptor superfamily, too, e.g. CD40 (Yellin et al., 1994) and CD95 (Lee et al., 2006). Because both internalization-defective TNFR2 and TACE-processing-defective TNF efficiently induce NFκB translocation, I propose that internalization of TNFR2 is dispensable for activation of the NFκB pathway and primarily serves as a negative feedback to limit TNF responses via TNFR2.

The data show that TNFR2 is constitutively shed from the plasma membrane and undergoes ligand-induced internalization and lysosomal degradation. Because TNF signaling occurs at the plasma membrane, I conclude that both receptor shedding and internalization primarily serve to downregulate cellular responsiveness to TNF. TNFR2 is predominantly activated by memTNF. Therefore, termination of signaling requires either shedding of the TNFR2

ectodomain or the shedding of mTNF, followed by internalization of the TNF/TNFR2 complex.

4.2. Soluble TNF with membrane TNF mimetic activity

Signaling via TNFR2 has been implicated in protection and regeneration of tissues, such as pancreas, heart and brain (Faustman and Davis, 2010). Accordingly, TNF variants selectively activating TNFR2 could be a useful therapeutic regimen in a variety of diseases, including heart failure, autoimmune and neurodegenerative diseases.

The recently introduced scTNF-format, where three TNF modules are connected via peptide-linkers (Krippner-Heidenreich et al., 2008) was not sufficient to efficiently activate TNFR2 and therefore cannot be used to activate TNFR2 *in vivo*. Therefore in the present study, a nonameric TNF mutein was constructed by genetic fusion of the human TNC domain to the TNFR2-specifc (D143N/A145R; Loetscher et al., 1993) $scTNF_{R2}$, yielding in the molecule TNC-$scTNF_{R2}$. TNC-$scTNF_{R2}$, a humanized molecule, was optimized for eukaryotic production and fulfills the constructional requirements for the future use as a therapeutic. Using different cell lines, it was demonstrated that TNC-$scTNF_{R2}$ efficiently induced TNF/TNFR2 clustering and TNFR2 signaling pathways, such as recruitment of TRAF2, activation of PKB/Akt and nuclear translocation of NFκB without the need for exogenous cross-linking of TNF/TNFR2 complexes.

4.2.1. Genetic engineering of TNC-$scTNF_{R2}$

Soluble recombinant TNF is a strong mediator of inflammation, predominantly through TNFR1, which is efficiently activated by the membrane-bound as well as the soluble form of TNF in the picomolar range (Grell et al., 1995). Whereas TNFR2 binds sTNF as well as memTNF, it is only fully activated by the latter (Grell et al., 1995). Therefore, TNFR2-specific therapeutics need to comply with two basic requirements, mimicry of memTNF and receptor selectivity in order to avoid dose limiting severe inflammatory responses.

Different approaches have been exploited to generate soluble TNF ligands mimicking membrane-bound TNF, e.g. by increasing the avidity of TNF ligands through mutagenesis or by immobilizing them on a cell surface or the extracellular matrix. Similar to TNFR2, soluble trimeric human CD95 ligand (CD95L) binds its cognate receptor CD95, but fails to activate it and even acts as an antagonist of membrane-bound CD95L-induced activation of CD95 (Schneider et al., 1998). Antibody-mediated multimerization of a Flag-tagged variant of soluble CD95L with anti-Flag antibody M2 or genetic fusion of soluble CD95L trimers with an oligomerization domain, such as the collagen domain of ACRP30/adiponectin, resulted in a dramatic increase in the avidity and activated CD95 (Holler et al., 2003; Schneider et al., 1998).

A similar strategy was used to construct a TNFR2-specific agonist with memTNF-mimetic activity. Instead of antibody-mediated multimerization, the human TNC trimerization domain was fused to a TNFR2-specific single-chain variant of soluble TNF ($scTNF_{R2}$), leading to the assembly of $scTNF_{R2}$ trimers (TNC- $scTNF_{R2}$), which in previous studies were shown to exert memTNF-like activity (Rauert et al., 2010). The introduced double mutation D143N/A145R leads to a complete loss of binding to TNFR1 (Loetscher et al., 1993). Therefore, as demonstrated using apoptosis induction in the cell line MEF TNFR1-Fas, $scTNF_{R2}$ and TNC-$scTNF_{R2}$ did not bind and activate TNFR1. In contrast to $scTNF_{R2}$, TNC-$scTNF_{R2}$ was not dependent on additional cross-linking of TNFR2 via 80M2 to efficiently activate TNFR2 nor did 80M2 cross-linking further enhance TNC-$scTNF_{R2}$ signaling, indicating that the nonameric TNF mutein is able to simulate the activation via memTNF.

Both $scTNF_{R2}$ and TNC-$scTNF_{R2}$ could be expressed in stably transfected HEK293 cells and were purified in soluble form. The yields obtained for both TNF molecules were similar, indicating that the trimerization of $scTNF_{R2}$ via the TNC domain does not reduce the production efficiency. Using HPLC analysis to determine the molecular weight of both molecules, the size of the scTNF muteins appeared to be much smaller than expected from molecular weight calculations and demonstrated by SDS-PAGE analysis. The decreased size can be a result of the compact molecular structure of $scTNF_{R2}$, which in contrast to previous formats is connected by short GGGGS-linkers. Nevertheless the HPLC and SDS-PAGE data strongly suggest that for $scTNF_{R2}$ the majority of the molecules were present in monomeric form, whereas the TNC-$scTNF_{R2}$ monomers assembled into functional multimers, most likely trimers.

Different results were obtained for both molecules, when they were produced by a cooperating partner (Celonic, Jülich). Using the upscaled industrial production process both scTNF muteins aggregated, as evident by the formation of $scTNF_{R2}$ dimers and TNC-$scTNF_{R2}$ multimers (data not shown). The dimerization of $scTNF_{R2}$ can be easily explained by the exposed N-terminal cysteine, which under oxidizing conditions can build disulfide bridges, thereby linking two $scTNF_{R2}$ molecules. Also the TNC-$scTNF_{R2}$ multimerization can be a consequence of disulfide bridges. In the tissue, TNC exists as a large disulfide-bonded hexamer arranged in a six-armed structure called hexabrachion (Jones et al., 1989), which appears to consist of two trimers joined at their centers by short linker arms and a central knob (Erickson and Inglesias, 1984). Three heptad repeats are located within the N-terminal segment (Spring et al., 1989). Heptad repeats of seven amino acid residues are the hallmark of proteins with a potential for coiled-coil formation (Cohen and Parry, 1990). Therefore it is assumed, that the TNC hexabrachion assembly involves the formation of a trimer intermediate via a parallel three-stranded coiled coil, initiated by the sequence between alanine 114 and glutamine 139 (Kammerer et al., 1998). Three conserved cysteines 64, 111,

and 113 can covalently connect the trimer intermediates, but TNC hexamer formation seems not to be dependent on disulfide bonds (Kammerer et al., 1998). The TNC trimerization domain (aa 110-139) used for constructing TNC-scTNF$_{R2}$ includes two of the three conserved cysteines. These cysteines could link TNC-scTNF$_{R2}$ molecules via the formation of disulfide bonds, resulting in TNC-scTNF$_{R2}$ dimers or even hexamers. Since the TNC-scTNF$_{R2}$ aggregates were only observed in the production batches from Celonic, I assume that the aggregation of TNC-scTNF$_{R2}$ is a consequence of the industrial production process or of oxidizing storage conditions by Celonic.

4.2.2. TNC-scTNF$_{R2}$ induces clustering of TNFR2

Receptors of the TNF family are activated by ligand-mediated oligomerization (Wallach et al., 1991) and efficient signal initiation requires the formation of ligand/receptor complexes comprising more than a single (homotrimeric) ligand molecule and three receptors (Holler et al., 2003; Krippner-Heidenreich et al., 2002). As previously mentioned, cross-linking reagents, such as antibodies, which due to their multivalent nature lead to the formation of large receptor clusters (Grassme et al., 2001; Grassme et al., 2002), are commonly used to efficiently activate signal transduction of CD95, TNFR2 or CD40 (Grell et al., 1993; Pound et al., 1999; Schneider et al., 1998).

In previous studies, the initiation of cluster formation of TNFR2 was found to be dependent on exogenous cross-linking of the ligand-receptor complexes and correlated with the particular signaling strength (Krippner-Heidenreich et al., 2002). Using a concentration (10ng/ml), where scTNF$_{R2}$ as well as TNC-scTNF$_{R2}$ induced apoptosis in Kym-I cells, as measured by crystal violet staining 24 hours afterwards, it could be demonstrated that only TNC-scTNF$_{R2}$ induced cluster formation of TNF/TNFR2 complexes, which can be visualized using fluorescence microscopy, within 10 minutes. In contrast, no TNF/TNFR2 clusters were observed after stimulation with scTNF$_{R2}$. As expected, exogenous cross-linking via 80M2 led to the formation of TNF/TNFR2 clusters, which colocalized with scTNF$_{R2}$.

In addition, differences in the dynamics of intracellular signal induction between the two TNF variants were found. The formation of TNF/TNFR2 clusters is an essential component of signal induction via TNFR2. Accordingly, only TNC-scTNF$_{R2}$ efficiently induced nuclear translocation of NFκB p65 within 30 minutes, whereas stimulation with scTNF$_{R2}$ only resulted in a marginal translocation after 60 minutes. This weak signal seems to be strong enough to induce expression and secretion of TNF thereby activating TNFR1, which then secondarily activates the apoptotic signaling-cascade, resulting in cell death after 24 hours.

Concluding, I propose that TNC-scTNF$_{R2}$ can induce the formation of TNF/TNFR2 clusters, subsequently leading to the efficient induction of downstream signaling pathways. Therefore,

the soluble TNC-scTNF$_{R2}$ mutein mimics memTNF-like activation of TNFR2 and can be used to induce TNFR2 signaling *in vitro* and *in vivo*.

4.3. Functional activity of TNC-scTNF$_{R2}$

4.3.1. TNC-scTNF$_{R2}$ enhances IL-2-dependent T cell activation

TNF is widely known for its proinflammatory effects, but recent studies suggest that TNF also has an unexpected immunosuppressive function, e.g. TNF-deficient mice exhibit more severe inflammation in chronic inflammatory states (Cope et al., 1997; Zakharova and Ziegler, 2005; Zganiacz et al., 2004). These antithetic effects mediated by TNF could be a result of different signaling pathways initiated by its two receptors, TNFR1 and TNFR2. Whereas TNFR1 is constitutively expressed on all tissues, the expression of TNFR2 is tightly regulated and limited to specific cell types, such as cells of the immune system. In contrast to thymic $CD4^+CD25^-$ cells, human thymic $CD4^+CD25^+$ Tregs constitutively express high levels of TNFR2 (Annunziato et al., 2002) and the expression of TNFR2 defines a unique subtype of Tregs with highly potent suppressive activity (Chen et al., 2008).

The present study further indicates that the immunosuppressive function of TNF is connected to TNFR2 by showing that the activation of TNFR2 in cultures of human PBMCs by TNC-scTNF$_{R2}$ increased the number of $CD25^+FoxP3^+$ Tregs. The expansion of Tregs was dependent on the presence of IL-2, which is required for the sustained expression of FoxP3 and CD25 in natural Tregs and the enhancement of their suppressive function (Fontenot et al., 2005; Shevach et al., 2006). In addition IL-2 is crucial for the survival of *in vitro* cultured Tregs (Chen et al., 2004). Therefore IL-2 is an essential prerequisite for TNFR2-mediated enhancement of Treg differentiation *in vitro*. These observations are in line with other studies, demonstrating that TNF in combination with IL-2 activates and expands Tregs (Chen et al., 2007).

Further studies demonstrated that activation of TNFR2 resulted in the generation and expansion of a subpopulation of protective regulatory T cells that may suppress autoimmunity (Askenasy et al., 2008; Nagar et al., 2010; Ryu et al., 2001). Whereas TNFR2 seems not to be necessary to maintain Treg activity, recent results suggest that TNFR2 mediates the activation of Tregs (Chen et al., 2007) and plays a functional role in the expansion of Tregs (Chen et al., 2010). It is assumed that TNF exerts a dual role in immune regulation. Short-term effects of TNF enable $CD4^+CD25^-$ effector T cells to expand despite the presence of Tregs, whereas more prolonged exposure to TNF may favor expansion and activation of Tregs (Chen et al., 2007).

It was further shown here that TNC-scTNF$_{R2}$ in combination with IL-2 also induced the secretion of IFN-γ in human PBMC cultures. IFN-γ is mainly secreted by Th1 cells and is

responsible for activating cell-mediated immune responses. Overactive or dysregulated Th1 responses may cause organ-specific autoimmune diseases, including type I diabetes, multiple sclerosis and arthritis (Wood and Sawitzki, 2006).

Th1 type encephalitogenic T cells are the characteristic immunological feature of EAE (Liblau et al., 1995). Therefore, IFN-γ was believed to play an important role in the activation of encephalitogenic T cells and CNS inflammation. But, in the last years accumulating evidence suggested that IFN-γ can also exert immune regulatory and anti-inflammatory functions, e.g. by inducing Th2 responses, thereby triggering the secretion of cytokines that counter-regulate Th1 activity (Bocek et al., 2004). Thus, endogenous IFN-γ was shown to act as a protective factor preventing the onset of EAE and collagen induced arthritis (CIA), an experimental animal model for rheumatoid arthritis. Mice deficient for IFN-γ or the IFN-γ receptor (IFN-γR) are more susceptible to CIA (Kelchtermans et al., 2005) or EAE (Wang et al., 2006b) and *in vivo* inhibition of IFN-γ accelerates the clinical severity of EAE whereas administration of IFN-γ suppresses EAE (Furlan et al., 2001; Voorthuis et al., 1990; Willenborg et al., 1995).

The elevated disease susceptibility is associated with a functional impairment of $CD4^+CD25^+$ Tregs, showing that the protective effect of IFN-γ in preventing the disease is related to antigen-induced Tregs (Kelchtermans et al., 2005; Wang et al., 2006b). Both normal cell numbers and cell function of $CD4^+CD25^+$ are preserved in IFN-$\gamma R^{-/-}$-mice, suggesting that IFN-γ is not required for $CD4^+CD25^+$ T cell development. But IFN-γ is critically required for the conversion of conventional $CD4^+CD25^-$ T cells to $CD4^+CD25^+$ Tregs by increasing the expression of FoxP3 and enhancing the regulatory function (Chen and Liu, 2009; Wang et al., 2006b). IFN-γ thus is able to limit the immune response by promoting the generation of Tregs. Similar results were found in other Th1 autoimmune conditions, including experimental autoimmune uveitis (EAU) (Caspi et al., 1994; Jones et al., 1997), which implies a generalized role of IFN-γ in the regulation of autoimmune T cell responses. The increased secretion of IFN-γ after TNC-scTNF$_{R2}$ stimulation could be a cofactor for Treg development and therefore be necessary for the expansion of Tregs. However, at the moment it cannot be excluded that TNC-scTNF$_{R2}$ also mediates additional T cell-specific responses, such as Th1 activity. But systemic administration of TNC-scTNF$_{R2}$ showed only a mild transient inflammatory response without any further signs of systemic inflammation thereby indicating that the elevated secretion of IFN-γ is most likely not due to Th1 immunity.

4.3.2. TNFR2 signaling increases CNTF transcription levels in astrocytes

Astrocytes are a heterogeneous population of cells with many important and diverse functions, including neuronal survival and neurite formation, induction of the BBB,

detoxification and tissue homeostasis (Montgomery, 1994; Zlokovic, 2008). As an alternative to the animal-consuming experiments, necessary to prepare primary astrocytes, I established IMA1335, an immortal cell line with astrocyte-like character, from huTNFR2-transgenic TgE1335 Balb/c mice. IMA1335 expressed GFAP as well as the mouse TNF receptors and the human TNFR2. Both the mouse and the ectopically expressed huTNFR2 were functional, as demonstrated by the degradation of IκBα. Whereas stimulation with mTNF resulted in a strong NFκB response, the kinetic was different for TNC-scTNF$_{R2}$. Since TNFR2 can only be efficiently activated by memTNF, stimulation with soluble mouse TNF should predominantly activate mTNFR1, suggesting that mTNF mainly acted via mTNFR1, whereas TNC-scTNF$_{R2}$ specifically activated the huTNFR2. The cell line therefore was particularly suited to analyze receptor expression and regulation in astrocyte cultures.

Next to its pro-apoptotic effects, TNF can act as an anti-apoptotic signal and promotes cell survival and proliferation. Especially cancer cells tend to proliferate in response to TNF (Liu et al., 2000; Wu et al., 1993). Activation of huTNFR2 by TNC-scTNF$_{R2}$ in IMA1335 resulted in an increased proliferation rate, whereas induction of signaling by the endogenous mouse TNF receptors, most likely via mTNFR1, showed no proliferative effect.

Similar, the effects of TNF on proliferation of astrocytes are controversially discussed in the literature. Several groups demonstrated that TNF is a potent mitogen for primary astrocytes both under *in vitro* and *in vivo* conditions (Barna et al., 1990; Selmaj et al., 1991b), whereas other studies showed that TNF had no proliferative effect on primary astrocytes (Moretto et al., 1993). Another group demonstrated that the proliferative effect of TNF was dependent on the concentration of serum in the feeding medium, being mitogenic only under conditions of over 15% serum in the medium (Tejada-Berges and Yong, 1994).

Interestingly, serum concentration as well as cell density had an important impact on TNFR2 expression in the astrocyte cultures studied here. Increased serum concentrations or cell densities elevated the expression of huTNFR2. As expected by the *in vivo* distribution of TNF receptors in TgE1335 mice (Douni and Kollias, 1998) the transgenic huTNFR2 was expressed at higher levels than the endogenous mTNFR2. Nevertheless, increased serum concentrations or high cell densities still elevated the surface expression of huTNFR2. This regulation may be of particular relevance for efficient stimulation of the endogenous mouse TNF receptors, too, since the expression levels might be subjected to the specific growth conditions, such as serum concentrations.

Astrocyte proliferation can be a characteristic feature of reactive astrogliosis, a process were astrocytes become “reactive” in response to a CNS insult, such as injury, ischemia or neurodegenerative diseases (Hamby and Sofroniew, 2010; Sofroniew, 2005). After a CNS insult, microglia and other immune cells are recruited to the site of a lesion and secrete proinflammatory cytokines such as TNF or interleukins. The microglia recruitment is followed

by the appearance of astroglial reactivity (Giulian et al., 1989). These reactive astrocytes become larger, elongate their processes, increase their level of GFAP and upregulate their number of mitochondria, glycogen content and various enzyme levels (Norenberg, 1994). Reactive astrogliosis can promote harmful effects during injury or disease, e.g. through the release of reactive oxygen-species (ROS) or certain inflammatory cytokines and cytotoxins (Sofroniew, 2009; 2005; Swanson et al., 2004). A long-term outcome of the astrocytic reactivity can be the formation of a glial scar at the lesion site, which can inhibit axonal regeneration (Cafferty et al., 2008).

In contrast, more recent evidence suggests that astroglial reactivity can be an attempt by these cells to promote CNS recovery by regulating inflammation and repair, e.g. by producing and secreting neurotrophic factors around the site of CNS lesions (Liberto et al., 2004). Reactive astrogliosis can protect CNS cells and the tissue in multiple ways, e.g. via uptake of glutamate (Swanson et al., 2004), protection from oxidative stress via glutathione production (Swanson et al., 2004), neuroprotection via degradation of amyloid-β-peptides (Koistinaho et al., 2004) or facilitation of BBB repair (Bush et al., 1999). Dysfunctions of the processes underlying reactive astrogliosis and scar formation can contribute, or even be the primary cause of CNS disease mechanisms (Hamby and Sofroniew, 2010).

Using primary astrocytes from huTNFR2-transgenic animals I could demonstrate that stimulation with TNC-scTNF$_{R2}$ increased the transcription rate of the neurotrophic factor CNTF. Interestingly, astrocyte-derived CNTF switched mature retinal ganglion cells to a regenerative state following inflammatory stimulation (Müller et al., 2007). In addition, CNTF stimulated axon regeneration of retinal ganglion cells (Müller et al., 2009) and enhanced the formation of myelin (Stankoff et al., 2002). The TNFR2-induced release of CNTF by astrocytes therefore might be a key component of the TNFR2-dependent remyelination after the cuprizone-induced demyelination (Arnett et al., 2001).

4.3.3. TNFR2 signaling increases neuronal regeneration after cytotoxic insult

A variety of neurodegenerative diseases, including Alzheimer's disease (Richardson, 1993), Parkinson's disease (Olanow, 1993), amyotrophic lateral sclerosis (Olanow, 1993) and conditions such as ischemia and excitotoxicity (Smith et al., 1991) have been associated with oxidative damage or stress. Oxidative damage is thought to be mediated by excessive exposure of cells to ROS, such as free radicals (Richter and Kass, 1991). Evidence suggests that the neuronal death observed in neurodegenerative diseases may be the result of direct exposure to ROS (Olanow, 1992; Patten et al., 2010; Richter and Kass, 1991).

Oxidative stress can be simulated *in vitro* by brief exposure of cultured neurons to hydrogen peroxide, which results in the induction of cell death via the apoptotic cell suicide pathway (Whittemore et al., 1994; Whittemore et al., 1995).

LUHMES cells are conditionally-immortalized non-transformed human fetal cells that can be differentiated to acquire a neuron-like phenotype and were used as a model for neuronal cells. These neuronal cells were sensitive to hydrogen peroxide-induced cell death, as demonstrated by MTT and TUNEL assay.

In a previous study, Marchetti et al. (2004) demonstrated that TNFR2 signaling protected primary cortical neurons from excitotoxic cell death by activation of NFκB in a PKB/Akt-dependent manner. Similar, primary oligodendrocyte progenitor cells were protected from hydrogen peroxide-induced cell death by TNFR2 signaling (Olaf Maier, IZI, personal communication). In the experiments mentioned above, the cells were preconditioned by TNFR2 stimulation. In contrast, in the present work TNFR2 signaling was induced by TNC-scTNF$_{R2}$ subsequent to the toxic stimulus. Interestingly, simulating a therapeutic setting resulted in a dramatically increased survival, too. Nearly 80% of the cells were protected after 24 hours and already after one-hour treatment with TNC-scTNF$_{R2}$, the amount of TUNEL-positive cells was reduced from 13.5% without TNC-scTNF$_{R2}$ to 3.7% after treatment with TNC-scTNF$_{R2}$.

The amount of apoptotic cells measured by the TUNEL assay one hour after removal of hydrogen peroxide is likely underestimated, because at this point in time, a significantly decreased number of cells was observed, as indicated by the reduced number of β-III-tubulin-expressing cells and the number of cell nuclei. LUHMES cells seem to undergo morphological changes shortly after addition of hydrogen peroxide, leading to the rapid detachment of a certain amount of cells from the culture dish. These cells are washed away and thus could not be detected in the TUNEL analysis.

Several pathways induced by TNFR2 are known to mediate protective or regenerative responses. In particular, activation of NFκB p65 induces expression of anti-apoptotic and/or neurotrophic factor genes (Marchetti et al., 2004; Yabe et al., 2001) such as the cIAP proteins, which are involved in facilitating the downregulation of apoptosis sensitivity within neurons (Fotin-Mleczek et al., 2002; Wiese et al., 1999).

TNFR2 activation subsequent to a toxic exposure to hydrogen peroxide resulted in a fast protective response. This was evident from the reduction of TUNEL-positive cells one hour after removal of hydrogen peroxide. I therefore propose that these anti-apoptotic effects were probably not strictly dependent on *de novo* gene expression and protein synthesis induced by NFκB activation. One possible mechanism is the activation of PKB/Akt, which, as already mentioned exerts anti-apoptotic effects (Nicholson and Anderson, 2002) and is involved in mediating cell protection in neurodegenerative diseases (Gary and Mattson, 2001; Noshita et al., 2002; Yano et al., 2001). A critical function of PKB/Akt in neuronal survival has been proposed and several downstream targets aside from NFκB (Ozes et al., 1999; Romashkova

and Makarov, 1999) potentially interfere with apoptotic signals and thus could be involved in neuroprotection, too (Datta et al., 1999).

For example, several components of the apoptotic machinery share the PKB/Akt consensus phosphorylation sequence (RXRXXS/T), e.g. pro-death components such as Bad, caspase 9 and caspase 8 or pro-survival factors like Bcl-2, cIAP and X-IAP (Datta et al., 1999). PKB/Akt therefore can regulate apoptosis by either inhibiting cell death or promoting cell survival. In particular, Bad interacts with pro-survival proteins, such as Bcl-X_L (Yang et al., 1995) thereby inhibiting cell survival. Phosphorylation of either serine 112 or serine 136 induces the dissociation of Bad from Bcl-X_L. Released Bcl-X_L then can promote cell survival. Both phosphorylation sites lie within the PKB/Akt phosphorylation consensus sequence and PKB/Akt was found to phosphorylate Bad *in vitro* (Datta et al., 1997; del Peso et al., 1997) thereby blocking Bad-induced cell death in multiple cell types (Blume-Jensen et al., 1998; Datta et al., 1997; Wang et al., 1999).

In addition to activation of anti-apoptotic proteins, PKB/Akt can also directly block cell death after mitochondrial cytochrome C release, most likely by phosphorylating caspase 9 at serine 196 (Cardone et al., 1998) thereby inactivating the caspase. PKB/Akt therefore can interfere even at this rather late stage with the apoptotic pathway. The exact molecular mechanism by which TNFR2 promotes the fast anti-apoptotic response after hydrogen peroxide-induced cell death need to be further unraveled, but rapid simulation of PKB/Akt could play a major role.

4.4. Stability and systemic tolerance of TNC-scTNF$_{R2}$

Krippner-Heidenreich et al. reported that the covalent stabilization of the TNF trimers in the scTNF format resulted in an enormously enhanced half-life when incubated in culture media with or without serum (2008). Similar results were obtained for the scTNF subunits of TNC-scTNF$_{R2}$, which were stable at 37°C in serum for at least seven days. The TNC-scTNF$_{R2}$ trimers displayed enhanced *in vitro* stability, too. Although the bioactivity was slightly decreased after 72 hours, it was still significantly higher than the activity of scTNF$_{R2}$ stored in PBS at 4°C, indicating that most of the trimers are highly stable under these *in vitro* conditions.

In vivo, TNC-scTNF$_{R2}$ showed a strongly improved monophasic plasma half-life compared to scTNF$_{R2}$ (diphasic half-life), with an initial half-life of 21.59 ± 0.82 hours and a terminal half-life of 27.72 ± 9.04 hours. The area under the curve (AUC_{d0-7}) was increased 3.3-fold, demonstrating that trimerization of the scTNF$_{R2}$ improves the pharmacokinetic properties. This result was expected, because the increased molecular weight from approximately 56.8kDa to 170.4kDa affects e.g. renal clearance. Even 24 hours after injecting TNC-scTNF$_{R2}$, a biological effective concentration of 84.67 ± 10.84ng/ml was detected in the blood. Nevertheless, I can only speculate whether this TNC-scTNF$_{R2}$-concentration is

sufficient for effective signaling at the designated tissue. But monitoring the therapeutic effects of TNC-scTNF$_{R2}$ in animal models of specific diseases will indirectly answer that question. Summarizing, at physiological temperature, TNC-scTNF$_{R2}$ is stable in serum *in vitro* and stays in the blood stream for several days.

Interestingly, previous studies revealed different pharmacokinetics for scTNF, with a significantly higher clearance rate (Krippner-Heidenreich et al., 2008). These differences are most likely due to the different injection methods. Whereas Krippner-Heidenreich et al. injected the scTNF intravenous (i.v.), I injected the TNF variants in the peritoneum. An i.p. injection of TNF, in contrast to i.v. injection, results in a TNF-reservoir in the peritoneum, from which TNF is constantly exchanged into the blood-stream until the reservoir is empty. Therefore, using the i.p. injection, the overall TNF concentration will be significantly lower, but TNF will be retained in the circulation for a longer time.

Since sTNF is a strong mediator of inflammation, predominantly through TNFR1 (Mackay et al., 1993; Van Zee et al., 1994), in man systemic administration of soluble recombinant TNF at doses higher than 200µg/m^2 causes significant toxicity including fever, rigor, nausea, diarrhea and hypotension (Sidhu and Bollon, 1993).

In huTNFR2-transgenic mice, I could clearly demonstrate that TNC-scTNF$_{R2}$ is not nearly as toxic as wildtype mTNF with regard to its capacity to induce inflammation when administered systemically. Injection of mTNF led to a hypothermic reaction and a strong inflammatory response, as described in the literature (Bauss et al., 1987; Männel et al., 1987). In contrast, administration of TNC-scTNF$_{R2}$ only resulted in a mild transient inflammatory reaction, as shown by the low number of activated CD11b-positive macrophages in the spleen. Even at high doses (4mg/kg) TNC-scTNF$_{R2}$ was well tolerated.

Several years ago, Welborn et al. (1996) investigated the systemic tolerance of a monomeric TNFR2-selective mutant by intravenous infusion of the molecule at a dose of 1mg/kg into baboons. This mutein had no affinity for TNFR1 while binding to TNFR2 with about one tenth the affinity of wildtype TNF (Loetscher et al., 1993). The treatment resulted in an enhancement of thymocyte proliferation *in vitro* and *in vivo*, a febrile reaction and a small, transient inflammation produced by infiltration of mononuclear cells upon intradermal administration of the agonist (Welborn et al., 1996). The dose, used in the present study was four times higher and still no inflammation or severe systemic side-effects were observed.

Due to the enhanced stability, the elongated blood-circulation and the systemic tolerance, even at high doses, TNC-scTNF$_{R2}$ fulfills all requirements for the evaluation in animal disease models.

4.5. Outlook for the use of TNC-scTNF$_{R2}$ as a therapeutic

4.5.1. TNC-scTNF$_{R2}$ and the blood-brain barrier

All therapeutic regimens with direct effects on the CNS need to pass the BBB. TNF is known to cross the BBB by receptor-mediated endocytosis (Gutierrez et al., 1993; Pan and Kastin, 2002). Interestingly, the transport is upregulated under conditions that appear to concur with regeneration after CNS trauma, inflammation, autoimmune disorder or global ischemia (Pan and Kastin, 2001).

Both TNF receptors seem to be essential for the transport of TNF across the normal BBB (Pan and Kastin, 2002), but TNFR2 appears to have a greater role than TNFR1 (Osburg et al., 2002). Interestingly, I could show that the uptake of TNFR2 in the fibroblast cell line R2 MEF is followed by the lysosomal degradation of the TNFR2 signaling complex (Fischer et al., 2011). Thus it is important to distinguish between TNF-mediated receptor-internalization, which can result in the degradation of the TNF/TNFR2-complex, and receptor-mediated endocytosis followed by the transcytosis of TNF at the BBB, a process that has to be regulated by different mechanisms to avoid lysosomal degradation.

So far, it is unclear if a TNFR2-specific TNF mutein will be transported across the BBB. Nevertheless, since the BBB undergoes rapid changes in permeability in response to CNS insults, it is possible that TNC-scTNF$_{R2}$ can reach the CNS without being specifically transported over the BBB. Whether this alteration of the permeability is sufficient to reach therapeutically effective concentrations in the brain is presently uncertain. An unequivocal demonstration of BBB passage of a therapeutic and presence in brain parenchyma is experimentally demanding, but can be revealed indirectly through monitoring therapeutic effects of TNC-scTNF$_{R2}$ in animal models of CNS diseases.

4.5.2. TNC-scTNF$_{R2}$ and stroke

The current treatment for complete stroke has limited success in reversing neurodegeneration and restoring the premorbid function. Although it is established that stroke disrupts the BBB, it is less well known that the altered BBB in turn affects stroke progression and neuroregeneration (Pan and Kastin, 2007).

TNF is seen as an important mediator of stroke (Berti et al., 2002) and TNF expression correlates with stroke damage. Nevertheless, TNF is not only involved in the initiation and progression of stroke, it may at certain times also play a role in tissue regeneration and therefore be beneficial for stroke recovery (Sairanen et al., 2001). In addition, TNF participates in the development of tolerance to ischemia (Hallenbeck, 2002; Masada et al., 2001).

Ischemic and hypoxic tolerance or preconditioning is an adaptive mechanism in many organs and species whereby mild ischemia and hypoxia can induce neuroprotection against the more severe injury that occurs subsequently. Preconditioning is seen in a variety of pathophysiological conditions, including inflammation, transplantation, epilepsy and ischemia of many organs (Pan and Kastin, 2007). The preconditioning effects of mild ischemia and hypoxia can be reproduced by TNF pretreatment (Nawashiro et al., 1997b), indicating that TNF can be neuroprotective even though it also exerts deleterious effects (Ginis et al., 2000; Hallenbeck, 2002; Nawashiro et al., 1997a).

Interestingly, the level of TNF in the CSF of stroke patients correlates with anti-apoptotic Bcl-2 expression, indicating that TNF may interfere with detrimental apoptotic signals (Tarkowski et al., 1997). Both deleterious and regenerative roles have been proposed for TNF in the pathogenesis of cerebral ischemia (Dziewulska and Mossakowski, 2003; Meistrell et al., 1997). On the one hand, for example blockade of TNF signaling reduces the infarct volume after permanent middle cerebral artery occlusion (MCAO), an animal model of ischemic stroke (Nawashiro et al., 1997a), whereas otherwise pretreatment with TNF is neuroprotective against permanent MCAO (Nawashiro et al., 1997b).

The role of TNF and its cognate receptors in ischemia-reperfusion-induced retinal damage was analyzed in mice deficient for TNF, TNFR1 or TNFR2 by quantifying the neuronal cell loss after the insult. Whereas TNF deficiency did not affect overall cell loss, the absence of TNFR1 led to a strong reduction of neurodegeneration and genomic ablation of TNFR2 resulted in an enhancement of neurodegeneration, indicating that TNFR1 augmented neuronal cell death whereas TNFR2 promoted neuroprotection (Fontaine et al., 2002). Therefore it will be of interest to evaluate the effects of TNC-scTNF$_{R2}$ in mouse models of stroke, e.g. MCAO or retinal ischemia.

4.5.3. TNC-scTNF$_{R2}$ and heart failure

Next to stroke cardiac ischemia is the most common form of ischemia. Analogous to stroke, TNF plays an important role in the pathophysiology of heart failure (Feldman et al., 2000). The cytokine is released during myocardial ischemia from resident mast cells and macrophages (Gilles et al., 2003) and the circulating levels of TNF directly correlate with the functional capacity and survival in patients with heart failure (Torre-Amione et al., 1996).

Although the blocking of TNF signaling by anti-TNF antibodies is cardioprotective in experimental animal models of heart failure (Iversen et al., 2001; Kadokami et al., 2001; Moe et al., 2004), randomized trials of anti-TNF therapy of human heart failure failed to show beneficial effects and unexpectedly demonstrated a time- and dose-related increase in death and heart failure hospitalization (Anker and Coats, 2002; Mann, 2002). This failure may be due to opposing effects of the two TNF receptors on remodeling, hypertrophy, NFκB

activation, inflammation and apoptosis in heart failure. Whereas TNFR1 exacerbates these events, TNFR2 has an ameliorative effect (Hamid et al., 2009).

Additional data demonstrate that TNF worsens left ventricular remodeling via TNFR1 and improves it via TNFR2 after myocardial infarction (Monden et al., 2007; Ramani et al., 2004). In addition, prolonged stimulation of TNFR1 increases ischemia/reperfusion injury and worsens the outcome after myocardial ischemia, whereas TNFR2 activation counteracts such deleterious effects (Schulz, 2008). All together these results indicate that complete blocking of TNF was not protective in heart failure and even led to serious side-effects predominantly due to inactivation of TNFR2 signaling.

An important aspect in ischemia and many other physiological and pathological settings is angiogenesis, the process of new blood-vessel formation, which is involved in many physiological and pathological settings, e.g. ischemia, atherosclerosis or arthritis (Carmeliet and Jain, 2000; Walsh, 1999). Next to angiogenic factors, such as the vascular endothelial growth factor (VEGF), inflammatory responses, defined by the presence of infiltrated macrophages and proinflammatory cytokines, are essential for angiogenesis (Arras et al., 1998; Leibovich et al., 1987).

In particular, TNF has been shown to stimulate angiogenesis *in vitro*, *in vivo* and in disease settings (Pan et al., 2002) mainly via TNFR2 signaling (Zhang et al., 2003). Angiogenic agonists are under current investigations to revascularize ischemic tissue. Since TNFR2 signaling is involved in protection and regeneration of myocardial infarction and additionally can induce angiogenesis, TNC-scTNF$_{R2}$ could be a useful therapeutic in heart diseases.

4.5.4. TNC-scTNF$_{R2}$ and autoimmune diseases

Immune suppression is the major treatment of autoimmune diseases. The data that TNC-scTNF$_{R2}$ induced the expansion of CD25$^+$FoxP3$^+$ Tregs together with data from the literature (Chen et al., 2007; Chen et al., 2010) indicate that TNFR2 has immunosuppressive functions.

A well-studied example is type I diabetes, which is caused by the chronic destruction of insulin-producing beta cells in the pancreatic islets by auto-aggressive T lymphocytes. Its pathogenesis is related to increased CD4$^+$ and CD8$^+$ T cell cytotoxicity and a biased Th1 immune pathway (Moutschen et al., 1992). CD8$^+$ T cells can destroy beta-cells and also increase cytotoxicity of CD4$^+$ T cells (Wong et al., 2008). Recently it has been shown that the autoreactive CD8$^+$ T cells against insulin can be selectively destroyed by activation of TNFR2 (Ban et al., 2008), which results in the expansion of a subpopulation of protective Tregs that may suppress autoimmunity (Askenasy et al., 2008; Nagar et al., 2010; Ryu et al., 2001). In addition it has been shown that injections of Treg and NK T cells are protective in type I diabetes (Lehuen et al., 1998; Tarbell et al., 2007).

TNC-scTNF$_{R2}$ induced the expansion of CD25$^+$FoxP3$^+$ Tregs and due to the literature TNFR2 triggering potentially can induce apoptosis of the autoreactive CD8$^+$ T cells. Therefore TNC-scTNF$_{R2}$ holds promise as an efficient treatment for autoimmune diseases, such as type I diabetes.

4.5.5. TNC-scTNF$_{R2}$ and demyelinating diseases

The loss of myelinating oligodendrocytes and oligodendrocyte progenitor cells is a feature of many CNS injuries and diseases, e.g. Alzheimer's disease or Huntington's disease (Bartzokis et al., 2007; Roth et al., 2005) or as a consequence of traumatic injury to the adult spinal cord (Crowe et al., 1997; Emery et al., 1998).

Oligodendrocytes arise in the brain and spinal cord from a pool of progenitors, which proliferate and migrate. Upon reaching their destination, the progenitors begin to differentiate by increasing the number and complexity of processes and by changing the expression pattern of different proteins, e.g. platelet-derived growth factor is downregulated, whereas myelin protein expression is upregulated. At this stage, the differentiated oligodendrocytes begin to form membrane wraps around axons.

Since oligodendrocytes play an important role in protecting axons, demyelinated axons are particularly vulnerable. To ensure the best recovery from injury or disease, oligodendrocyte replacement is an important goal. Once oligodendrocytes are lost in the adult CNS, they are not replaced by surviving mature oligodendrocytes (Di Bello et al., 1999; Keirstead and Blakemore, 1997). However, after CNS development is completed, a part of the oligodendrocyte progenitors persist in the adult brain and spinal cord (Noble et al., 1992; Wolswijk and Noble, 1989). These cycling progenitors can migrate to sites of oligodendrocyte loss, divide and differentiate into mature myelinating oligodendrocytes, resulting in the remyelination of axons (Gensert and Goldman, 1997; McTigue and Tripathi, 2008). Thereby, the adult CNS retains the capacity to remyelinate by specific oligodendrocyte progenitors.

Demyelination is one of the hallmarks of multiple sclerosis and its animal model EAE. The cuprizone model is a well-established model for controlled de- and remyelination, independent of primary inflammation. Cuprizone is a neurotoxin, which leads to demyelination after oral administration. After discontinuing the toxin, oligodendrocytes progenitor cells migrate to the lesions and differentiate into mature oligodendrocytes, which remyelinate the axons again. Using the cuprizone model, Arnett et al. (2001) could demonstrate that the lack of TNF leads to a significant delay in remyelination. Analysis of TNFR1$^{-/-}$- or TNFR2$^{-/-}$-mice indicated that TNFR2, not TNFR1, is critical for oligodendrocyte regeneration. Neither the cell type, that directly responds to the TNFR2 stimulus, nor the underlying molecular mechanisms of oligodendrocyte regeneration are known yet.

However, in a different setting, oligodendrocyte genesis has been detected along the borders of ischemic lesions in the brain, where the new cells co-localized with astrocytes, microglia and macrophages (Komitova et al., 2006; Mabuchi et al., 2000; Mandai et al., 1997). The presence of astrocytes and macrophages seems to be essential for new oligodendrocyte formation (Franklin et al., 1993; 1991; Kotter et al., 2001; Talbott et al., 2005).

The myelin debris, a feature of demyelinated lesions, impairs the CNS remyelination by inhibiting oligodendrocyte precursor cell differentiation (Kotter et al., 2001). The phagocytic clearance by microglia/macrophages, following an injury is more than simply tidying up, but instead plays a fundamental role in facilitating the reorganization of neuronal circuits and triggers neuronal repair (Neumann et al., 2009).

Brain-infiltrating macrophages and microglia were found to express considerably higher levels of TNFR2 than any other cell type in the mouse brain after induction of ischemia (Lambertsen et al., 2007), indicating that TNF, through constitutive and induced expression of TNFR2 on macrophages/microglia, may control the functional state of these cell populations. Accordingly, TNFR2 stimulation in microglia regulated the expression of genes involved in immune processes, including molecules with anti-inflammatory and neuroprotective function like granulocyte colony-stimulating factor, adrenomedullin and IL-10, indicating that, through TNFR2, microglia may contribute to the counter-regulatory response activated in neuropathological conditions (Veroni et al., 2010).

Interestingly, in the EAE mouse model $TNFR1^{-/-}$-mice were completely resistant to the induction of the disease, whereas $TNFR2^{-/-}$-mice exhibited more severe EAE (Suvannavejh et al., 2000) indicating that TNFR2 exerts a protective role in EAE. Since signaling via TNFR2 promotes the expansion of Tregs and plays a neuroprotective role, TNC-scTNF$_{R2}$ could influence the course of EAE at different levels, e.g. suppression of immune reactions as well as regeneration of demyelinated EAE lesions.

Summarizing, the huTNFR2-specific agonist TNC-scTNF$_{R2}$ exerts memTNF-mimetic activity, is well tolerated *in vivo* and displays improved pharmacokinetic properties. In ongoing studies using animal models of neurodegenerative diseases, TNC-scTNF$_{R2}$ is evaluated for its therapeutic potential. All together there is overwhelming evidence that specific activation of TNFR2 is a promising strategy to treat a variety of diseases, including autoimmune diseases, such as type I diabetes, neurodegenerative diseases, such as stroke, or demyelinating diseases, such as multiple sclerosis.

Bibliography

Abbott, N. J., A. A. Patabendige, D. E. Dolman, S. R. Yusof and D. J. Begley (2010). "Structure and function of the blood-brain barrier." Neurobiol Dis **37**(1): 13-25.

Adelman, B., A. Sandrock and M. A. Panzara (2005). "Natalizumab and progressive multifocal leukoencephalopathy." N Engl J Med **353**(4): 432-433.

Aggarwal, B. B. (2003). "Signalling pathways of the TNF superfamily: a double-edged sword." Nat Rev Immunol **3**(9): 745-756.

Alessi, D. R. (2001). "Discovery of PDK1, one of the missing links in insulin signal transduction. Colworth Medal Lecture." Biochem Soc Trans **29**(Pt 2): 1-14.

Alexopoulou, L., K. Kranidioti, S. Xanthoulea, M. Denis, A. Kotanidou, E. Douni, P. J. Blackshear, D. L. Kontoyiannis and G. Kollias (2006). "Transmembrane TNF protects mutant mice against intracellular bacterial infections, chronic inflammation and autoimmunity." Eur J Immunol **36**(10): 2768-2780.

Algeciras-Schimnich, A. and M. E. Peter (2003). "Actin dependent CD95 internalization is specific for Type I cells." FEBS Lett **546**(2-3): 185-188.

Alzani, R., E. Cozzi, A. Corti, M. Temponi, D. Trizio, M. Gigli and V. Rizzo (1995). "Mechanism of suramin-induced deoligomerization of tumor necrosis factor alpha." Biochemistry **34**(19): 6344-6350.

Anderson, R. G. (1998). "The caveolae membrane system." Annu Rev Biochem **67**: 199-225.

Anker, S. D. and A. J. Coats (2002). "How to RECOVER from RENAISSANCE? The significance of the results of RECOVER, RENAISSANCE, RENEWAL and ATTACH." Int J Cardiol **86**(2-3): 123-130.

Annunziato, F., L. Cosmi, F. Liotta, E. Lazzeri, R. Manetti, V. Vanini, P. Romagnani, E. Maggi and S. Romagnani (2002). "Phenotype, localization, and mechanism of suppression of CD4(+)CD25(+) human thymocytes." J Exp Med **196**(3): 379-387.

Arnett, H. A., J. Mason, M. Marino, K. Suzuki, G. K. Matsushima and J. P. Ting (2001). "TNF alpha promotes proliferation of oligodendrocyte progenitors and remyelination." Nat Neurosci **4**(11): 1116-1122.

Arras, M., W. D. Ito, D. Scholz, B. Winkler, J. Schaper and W. Schaper (1998). "Monocyte activation in angiogenesis and collateral growth in the rabbit hindlimb." J Clin Invest **101**(1): 40-50.

Asano, M., M. Toda, N. Sakaguchi and S. Sakaguchi (1996). "Autoimmune disease as a consequence of developmental abnormality of a T cell subpopulation." J Exp Med **184**(2): 387-396.

Askenasy, N., A. Kaminitz and S. Yarkoni (2008). "Mechanisms of T regulatory cell function." Autoimmun Rev **7**(5): 370-375.

Baass, P. C., G. M. Di Guglielmo, F. Authier, B. I. Posner and J. J. Bergeron (1995). "Compartmentalized signal transduction by receptor tyrosine kinases." Trends Cell Biol **5**(12): 465-470.

Balosso, S., T. Ravizza, C. Perego, J. Peschon, I. L. Campbell, M. G. De Simoni and A. Vezzani (2005). "Tumor necrosis factor-alpha inhibits seizures in mice via p75 receptors." Ann Neurol **57**(6): 804-812.

Ban, L., J. Zhang, L. Wang, W. Kuhtreiber, D. Burger and D. L. Faustman (2008). "Selective death of autoreactive T cells in human diabetes by TNF or TNF receptor 2 agonism." Proc Natl Acad Sci U S A **105**(36): 13644-13649.

Banner, D. W., A. D'Arcy, W. Janes, R. Gentz, H. J. Schoenfeld, C. Broger, H. Loetscher and W. Lesslauer (1993). "Crystal structure of the soluble human 55 kd TNF receptor-human TNF beta complex: implications for TNF receptor activation." Cell **73**(3): 431-445.

Barna, B. P., M. L. Estes, B. S. Jacobs, S. Hudson and R. M. Ransohoff (1990). "Human astrocytes proliferate in response to tumor necrosis factor alpha." J Neuroimmunol **30**(2-3): 239-243.

Bartzokis, G., P. H. Lu, T. A. Tishler, S. M. Fong, B. Oluwadara, J. P. Finn, D. Huang, Y. Bordelon, J. Mintz and S. Perlman (2007). "Myelin breakdown and iron changes in Huntington's disease: pathogenesis and treatment implications." Neurochem Res **32**(10): 1655-1664.

Bauss, F., W. Droge and D. N. Mannel (1987). "Tumor necrosis factor mediates endotoxic effects in mice." Infect Immun **55**(7): 1622-1625.

Bennett, C. L., J. Christie, F. Ramsdell, M. E. Brunkow, P. J. Ferguson, L. Whitesell, T. E. Kelly, F. T. Saulsbury, P. F. Chance and H. D. Ochs (2001). "The immune dysregulation, polyendocrinopathy, enteropathy, X-linked syndrome (IPEX) is caused by mutations of FOXP3." Nat Genet **27**(1): 20-21.

Berti, R., A. J. Williams, J. R. Moffett, S. L. Hale, L. C. Velarde, P. J. Elliott, C. Yao, J. R. Dave and F. C. Tortella (2002). "Quantitative real-time RT-PCR analysis of inflammatory gene expression associated with ischemia-reperfusion brain injury." J Cereb Blood Flow Metab **22**(9): 1068-1079.

Bertrand, M. J., S. Milutinovic, K. M. Dickson, W. C. Ho, A. Boudreault, J. Durkin, J. W. Gillard, J. B. Jaquith, S. J. Morris and P. A. Barker (2008). "cIAP1 and cIAP2 facilitate cancer cell survival by functioning as E3 ligases that promote RIP1 ubiquitination." Mol Cell **30**(6): 689-700.

Bien, C. G., J. Bauer, T. L. Deckwerth, H. Wiendl, M. Deckert, O. D. Wiestler, J. Schramm, C. E. Elger and H. Lassmann (2002). "Destruction of neurons by cytotoxic T cells: a new pathogenic mechanism in Rasmussen's encephalitis." Ann Neurol **51**(3): 311-318.

Bird, T. A., K. Schooley, S. K. Dower, H. Hagen and G. D. Virca (1997). "Activation of nuclear transcription factor NF-kappaB by interleukin-1 is accompanied by casein kinase II-mediated phosphorylation of the p65 subunit." J Biol Chem **272**(51): 32606-32612.

Black, R. A., C. T. Rauch, C. J. Kozlosky, J. J. Peschon, J. L. Slack, M. F. Wolfson, B. J. Castner, K. L. Stocking, P. Reddy, S. Srinivasan, N. Nelson, N. Boiani, K. A. Schooley, M. Gerhart, R. Davis, J. N. Fitzner, R. S. Johnson, R. J. Paxton, C. J. March and D. P. Cerretti (1997). "A metalloproteinase disintegrin that releases tumour-necrosis factor-alpha from cells." Nature **385**(6618): 729-733.

Blasi, E., R. Barluzzi, V. Bocchini, R. Mazzolla and F. Bistoni (1990). "Immortalization of murine microglial cells by a v-raf/v-myc carrying retrovirus." J Neuroimmunol **27**(2-3): 229-237.

Blume-Jensen, P., R. Janknecht and T. Hunter (1998). "The kit receptor promotes cell survival via activation of PI 3-kinase and subsequent Akt-mediated phosphorylation of Bad on Ser136." Curr Biol **8**(13): 779-782.

Bocek, P., Jr., G. Foucras and W. E. Paul (2004). "Interferon gamma enhances both in vitro and in vivo priming of CD4+ T cells for IL-4 production." J Exp Med **199**(12): 1619-1630.

Boldin, M. P., T. M. Goncharov, Y. V. Goltsev and D. Wallach (1996). "Involvement of MACH, a novel MORT1/FADD-interacting protease, in Fas/APO-1- and TNF receptor-induced cell death." Cell **85**(6): 803-815.

Bonifacino, J. S. and L. M. Traub (2003). "Signals for sorting of transmembrane proteins to endosomes and lysosomes." Annu Rev Biochem **72**: 395-447.

Bonizzi, G., M. Bebien, D. C. Otero, K. E. Johnson-Vroom, Y. Cao, D. Vu, A. G. Jegga, B. J. Aronow, G. Ghosh, R. C. Rickert and M. Karin (2004). "Activation of IKKalpha target genes depends on recognition of specific kappaB binding sites by RelB:p52 dimers." EMBO J **23**(21): 4202-4210.

Booss, J., M. M. Esiri, W. W. Tourtellotte and D. Y. Mason (1983). "Immunohistological analysis of T lymphocyte subsets in the central nervous system in chronic progressive multiple sclerosis." J Neurol Sci **62**(1-3): 219-232.

Boschert, V., A. Krippner-Heidenreich, M. Branschadel, J. Tepperink, A. Aird and P. Scheurich (2010). "Single chain TNF derivatives with individually mutated receptor binding sites reveal differential stoichiometry of ligand receptor complex formation for TNFR1 and TNFR2." Cell Signal **22**(7): 1088-1096.

Boucher, L. M., L. E. Marengere, Y. Lu, S. Thukral and T. W. Mak (1997). "Binding sites of cytoplasmic effectors TRAF1, 2, and 3 on CD30 and other members of the TNF receptor superfamily." Biochem Biophys Res Commun **233**(3): 592-600.

Bryde, S., I. Grunwald, A. Hammer, A. Krippner-Heidenreich, T. Schiestel, H. Brunner, G. E. Tovar, K. Pfizenmaier and P. Scheurich (2005). "Tumor necrosis factor (TNF)-functionalized nanostructured particles for the stimulation of membrane TNF-specific cell responses." Bioconjug Chem **16**(6): 1459-1467.

Bucci, C., P. Thomsen, P. Nicoziani, J. McCarthy and B. van Deurs (2000). "Rab7: a key to lysosome biogenesis." Mol Biol Cell **11**(2): 467-480.

Bush, T. G., N. Puvanachandra, C. H. Horner, A. Polito, T. Ostenfeld, C. N. Svendsen, L. Mucke, M. H. Johnson and M. V. Sofroniew (1999). "Leukocyte infiltration, neuronal degeneration, and neurite outgrowth after ablation of scar-forming, reactive astrocytes in adult transgenic mice." Neuron **23**(2): 297-308.

Cafferty, W. B., A. W. McGee and S. M. Strittmatter (2008). "Axonal growth therapeutics: regeneration or sprouting or plasticity?" Trends Neurosci **31**(5): 215-220.

Cantley, L. C. (2002). "The phosphoinositide 3-kinase pathway." Science **296**(5573): 1655-1657.

Cardone, M. H., N. Roy, H. R. Stennicke, G. S. Salvesen, T. F. Franke, E. Stanbridge, S. Frisch and J. C. Reed (1998). "Regulation of cell death protease caspase-9 by phosphorylation." Science **282**(5392): 1318-1321.

Cardoso, F. L., D. Brites and M. A. Brito (2010). "Looking at the blood-brain barrier: molecular anatomy and possible investigation approaches." Brain Res Rev **64**(2): 328-363.

Carmeliet, P. and R. K. Jain (2000). "Angiogenesis in cancer and other diseases." Nature **407**(6801): 249-257.

Carson, M. J. (2002). "Microglia as liaisons between the immune and central nervous systems: functional implications for multiple sclerosis." Glia **40**(2): 218-231.

Carson, M. J., J. M. Doose, B. Melchior, C. D. Schmid and C. C. Ploix (2006). "CNS immune privilege: hiding in plain sight." Immunol Rev **213**: 48-65.

Caspi, R. R., C. C. Chan, B. G. Grubbs, P. B. Silver, B. Wiggert, C. F. Parsa, S. Bahmanyar, A. Billiau and H. Heremans (1994). "Endogenous systemic IFN-gamma has a protective role against ocular autoimmunity in mice." J Immunol **152**(2): 890-899.

Castro, C. N., A. E. Barcala Tabarrozi, M. A. Noguerol, A. C. Liberman, R. A. Dewey, E. Arzt, A. E. Morelli and M. J. Perone (2010). "Disease-modifying immunotherapy for the management of autoimmune diabetes." Neuroimmunomodulation **17**(3): 173-176.

Chan, F. K., H. J. Chun, L. Zheng, R. M. Siegel, K. L. Bui and M. J. Lenardo (2000). "A domain in TNF receptors that mediates ligand-independent receptor assembly and signaling." Science **288**(5475): 2351-2354.

Chatzidakis, I. and C. Mamalaki (2010). "T cells as sources and targets of TNF: implications for immunity and autoimmunity." Curr Dir Autoimmun **11**: 105-118.

Chen, J. and X. Liu (2009). "The role of interferon gamma in regulation of CD4+ T-cells and its clinical implications." Cell Immunol **254**(2): 85-90.

Chen, X., M. Baumel, D. N. Mannel, O. M. Howard and J. J. Oppenheim (2007). "Interaction of TNF with TNF receptor type 2 promotes expansion and function of mouse CD4+CD25+ T regulatory cells." J Immunol **179**(1): 154-161.

Chen, X., T. Murakami, J. J. Oppenheim and O. M. Howard (2004). "Differential response of murine CD4+CD25+ and CD4+CD25- T cells to dexamethasone-induced cell death." Eur J Immunol **34**(3): 859-869.

Chen, X., J. J. Subleski, R. Hamano, O. M. Howard, R. H. Wiltrout and J. J. Oppenheim (2010). "Co-expression of TNFR2 and CD25 identifies more of the functional CD4+FOXP3+ regulatory T cells in human peripheral blood." Eur J Immunol **40**(4): 1099-1106.

Chen, X., J. J. Subleski, H. Kopf, O. M. Howard, D. N. Mannel and J. J. Oppenheim (2008). "Cutting edge: expression of TNFR2 defines a maximally suppressive subset of mouse CD4+CD25+FoxP3+ T regulatory cells: applicability to tumor-infiltrating T regulatory cells." J Immunol **180**(10): 6467-6471.

Chiu, Y. H., M. Zhao and Z. J. Chen (2009). "Ubiquitin in NF-kappaB signaling." Chem Rev **109**(4): 1549-1560.

Cohen, C. and D. A. Parry (1990). "Alpha-helical coiled coils and bundles: how to design an alpha-helical protein." Proteins **7**(1): 1-15.

Conner, S. D. and S. L. Schmid (2003). "Regulated portals of entry into the cell." Nature **422**(6927): 37-44.

Cope, A. P., D. Aderka, M. Doherty, H. Engelmann, D. Gibbons, A. C. Jones, F. M. Brennan, R. N. Maini, D. Wallach and M. Feldmann (1992). "Increased levels of soluble tumor necrosis factor receptors in the sera and synovial fluid of patients with rheumatic diseases." Arthritis Rheum **35**(10): 1160-1169.

Cope, A. P., R. S. Liblau, X. D. Yang, M. Congia, C. Laudanna, R. D. Schreiber, L. Probert, G. Kollias and H. O. McDevitt (1997). "Chronic tumor necrosis factor alters T cell responses by attenuating T cell receptor signaling." J Exp Med **185**(9): 1573-1584.

Corti, A., G. Fassina, F. Marcucci, E. Barbanti and G. Cassani (1992). "Oligomeric tumour necrosis factor alpha slowly converts into inactive forms at bioactive levels." Biochem J **284 (Pt 3)**: 905-910.

Crowe, M. J., J. C. Bresnahan, S. L. Shuman, J. N. Masters and M. S. Beattie (1997). "Apoptosis and delayed degeneration after spinal cord injury in rats and monkeys." Nat Med **3**(1): 73-76.

Daginakatte, G. C., A. Gadzinski, R. J. Emnett, J. L. Stark, E. R. Gonzales, P. Yan, J. M. Lee, A. H. Cross and D. H. Gutmann (2008). "Expression profiling identifies a molecular signature of reactive astrocytes stimulated by cyclic AMP or proinflammatory cytokines." Exp Neurol **210**(1): 261-267.

Datta, S. R., A. Brunet and M. E. Greenberg (1999). "Cellular survival: a play in three Akts." Genes Dev **13**(22): 2905-2927.

Datta, S. R., H. Dudek, X. Tao, S. Masters, H. Fu, Y. Gotoh and M. E. Greenberg (1997). "Akt phosphorylation of BAD couples survival signals to the cell-intrinsic death machinery." Cell **91**(2): 231-241.

del Peso, L., M. Gonzalez-Garcia, C. Page, R. Herrera and G. Nunez (1997). "Interleukin-3-induced phosphorylation of BAD through the protein kinase Akt." Science **278**(5338): 687-689.

Delhase, M., N. Li and M. Karin (2000). "Kinase regulation in inflammatory response." Nature **406**(6794): 367-368.

Deng, L., C. Wang, E. Spencer, L. Yang, A. Braun, J. You, C. Slaughter, C. Pickart and Z. J. Chen (2000). "Activation of the IkappaB kinase complex by TRAF6 requires a dimeric ubiquitin-conjugating enzyme complex and a unique polyubiquitin chain." Cell **103**(2): 351-361.

Devin, A., A. Cook, Y. Lin, Y. Rodriguez, M. Kelliher and Z. Liu (2000). "The distinct roles of TRAF2 and RIP in IKK activation by TNF-R1: TRAF2 recruits IKK to TNF-R1 while RIP mediates IKK activation." Immunity **12**(4): 419-429.

Di Bello, I. C., M. R. Dawson, J. M. Levine and R. Reynolds (1999). "Generation of oligodendroglial progenitors in acute inflammatory demyelinating lesions of the rat brain stem is associated with demyelination rather than inflammation." J Neurocytol **28**(4-5): 365-381.

DiDonato, J. A., M. Hayakawa, D. M. Rothwarf, E. Zandi and M. Karin (1997). "A cytokine-responsive IkappaB kinase that activates the transcription factor NF-kappaB." Nature **388**(6642): 548-554.

Diez-Ruiz, A., G. P. Tilz, R. Zangerle, G. Baier-Bitterlich, H. Wachter and D. Fuchs (1995). "Soluble receptors for tumour necrosis factor in clinical laboratory diagnosis." Eur J Haematol **54**(1): 1-8.

Dolga, A. M., I. M. Nijholt, A. Ostroveanu, Q. Ten Bosch, P. G. Luiten and U. L. Eisel (2008). "Lovastatin induces neuroprotection through tumor necrosis factor receptor 2 signaling pathways." J Alzheimers Dis **13**(2): 111-122.

Douni, E. and G. Kollias (1998). "A critical role of the p75 tumor necrosis factor receptor (p75TNF-R) in organ inflammation independent of TNF, lymphotoxin alpha, or the p55TNF-R." J Exp Med **188**(7): 1343-1352.

Dziewulska, D. and M. J. Mossakowski (2003). "Cellular expression of tumor necrosis factor a and its receptors in human ischemic stroke." Clin Neuropathol **22**(1): 35-40.

Emery, E., P. Aldana, M. B. Bunge, W. Puckett, A. Srinivasan, R. W. Keane, J. Bethea and A. D. Levi (1998). "Apoptosis after traumatic human spinal cord injury." J Neurosurg **89**(6): 911-920.

Eramo, A., M. Sargiacomo, L. Ricci-Vitiani, M. Todaro, G. Stassi, C. G. Messina, I. Parolini, F. Lotti, G. Sette, C. Peschle and R. De Maria (2004). "CD95 death-inducing signaling complex formation and internalization occur in lipid rafts of type I and type II cells." Eur J Immunol **34**(7): 1930-1940.

Erickson, H. P. and J. L. Inglesias (1984). "A six-armed oligomer isolated from cell surface fibronectin preparations." Nature **311**(5983): 267-269.

Faustman, D. and M. Davis (2010). "TNF receptor 2 pathway: drug target for autoimmune diseases." Nat Rev Drug Discov **9**(6): 482-493.

Faustman, D., X. P. Li, H. Y. Lin, Y. E. Fu, G. Eisenbarth, J. Avruch and J. Guo (1991). "Linkage of faulty major histocompatibility complex class I to autoimmune diabetes." Science **254**(5039): 1756-1761.

Faustman, D. L. and M. Davis (2009). "The primacy of CD8 T lymphocytes in type 1 diabetes and implications for therapies." J Mol Med **87**(12): 1173-1178.

Feldman, A. M., A. Combes, D. Wagner, T. Kadakomi, T. Kubota, Y. Y. Li and C. McTiernan (2000). "The role of tumor necrosis factor in the pathophysiology of heart failure." J Am Coll Cardiol **35**(3): 537-544.

Feng, X., M. L. Gaeta, L. A. Madge, J. H. Yang, J. R. Bradley and J. S. Pober (2001). "Caveolin-1 associates with TRAF2 to form a complex that is recruited to tumor necrosis factor receptors." J Biol Chem **276**(11): 8341-8349.

Ferguson, B., M. K. Matyszak, M. M. Esiri and V. H. Perry (1997). "Axonal damage in acute multiple sclerosis lesions." Brain **120 (Pt 3)**: 393-399.

Ferrero-Miliani, L., O. H. Nielsen, P. S. Andersen and S. E. Girardin (2007). "Chronic inflammation: importance of NOD2 and NALP3 in interleukin-1beta generation." Clin Exp Immunol **147**(2): 227-235.

Fischer, R., O. Maier, M. Naumer, A. Krippner-Heidenreich, P. Scheurich and K. Pfizenmaier (2011). "Ligand-induced internalization of TNF receptor 2 mediated by a di-leucin motif is dispensable for activation of the NFkappaB pathway." Cell Signal **23**(1): 161-170.

Fontaine, V., S. Mohand-Said, N. Hanoteau, C. Fuchs, K. Pfizenmaier and U. Eisel (2002). "Neurodegenerative and neuroprotective effects of tumor Necrosis factor (TNF) in retinal ischemia: opposite roles of TNF receptor 1 and TNF receptor 2." J Neurosci **22**(7): RC216.

Fontenot, J. D., M. A. Gavin and A. Y. Rudensky (2003). "Foxp3 programs the development and function of CD4+CD25+ regulatory T cells." Nat Immunol **4**(4): 330-336.

Fontenot, J. D., J. P. Rasmussen, M. A. Gavin and A. Y. Rudensky (2005). "A function for interleukin 2 in Foxp3-expressing regulatory T cells." Nat Immunol **6**(11): 1142-1151.

Fotin-Mleczek, M., F. Henkler, D. Samel, M. Reichwein, A. Hausser, I. Parmryd, P. Scheurich, J. A. Schmid and H. Wajant (2002). "Apoptotic crosstalk of TNF receptors: TNF-R2-induces depletion of TRAF2 and IAP proteins and accelerates TNF-R1-dependent activation of caspase-8." J Cell Sci **115**(Pt 13): 2757-2770.

Fotin-Mleczek, M., S. Welte, O. Mader, F. Duchardt, R. Fischer, H. Hufnagel, P. Scheurich and R. Brock (2005). "Cationic cell-penetrating peptides interfere with TNF signalling by induction of TNF receptor internalization." J Cell Sci **118**(Pt 15): 3339-3351.

Fox, E. J. (2006). "Management of worsening multiple sclerosis with mitoxantrone: a review." Clin Ther **28**(4): 461-474.

Franklin, R. J., A. J. Crang and W. F. Blakemore (1991). "Transplanted type-1 astrocytes facilitate repair of demyelinating lesions by host oligodendrocytes in adult rat spinal cord." J Neurocytol **20**(5): 420-430.

Franklin, R. J., A. J. Crang and W. F. Blakemore (1993). "The role of astrocytes in the remyelination of glia-free areas of demyelination." Adv Neurol **59**: 125-133.

Furlan, R., E. Brambilla, F. Ruffini, P. L. Poliani, A. Bergami, P. C. Marconi, D. M. Franciotta, G. Penna, G. Comi, L. Adorini and G. Martino (2001). "Intrathecal delivery of IFN-gamma protects C57BL/6 mice from chronic-progressive experimental autoimmune encephalomyelitis by increasing apoptosis of central nervous system-infiltrating lymphocytes." J Immunol **167**(3): 1821-1829.

Gabay, C., N. Cakir, F. Moral, P. Roux-Lombard, O. Meyer, J. M. Dayer, T. Vischer, H. Yazici and P. A. Guerne (1997). "Circulating levels of tumor necrosis factor soluble receptors in systemic lupus erythematosus are significantly higher than in other rheumatic diseases and correlate with disease activity." J Rheumatol **24**(2): 303-308.

Gary, D. S. and M. P. Mattson (2001). "Integrin signaling via the PI3-kinase-Akt pathway increases neuronal resistance to glutamate-induced apoptosis." J Neurochem **76**(5): 1485-1496.

Gensert, J. M. and J. E. Goldman (1997). "Endogenous progenitors remyelinate demyelinated axons in the adult CNS." Neuron **19**(1): 197-203.

Gerspach, J., D. Muller, S. Munkel, O. Selchow, J. Nemeth, M. Noack, H. Petrul, A. Menrad, H. Wajant and K. Pfizenmaier (2006). "Restoration of membrane TNF-like activity by cell surface targeting and matrix metalloproteinase-mediated processing of a TNF prodrug." Cell Death Differ **13**(2): 273-284.

Ghosh, S. and M. S. Hayden (2008). "New regulators of NF-kappaB in inflammation." Nat Rev Immunol **8**(11): 837-848.

Gilles, S., S. Zahler, U. Welsch, C. P. Sommerhoff and B. F. Becker (2003). "Release of TNF-alpha during myocardial reperfusion depends on oxidative stress and is prevented by mast cell stabilizers." Cardiovasc Res **60**(3): 608-616.

Ginis, I., J. M. Hallenbeck, J. Liu, M. Spatz, R. Jaiswal and E. Shohami (2000). "Tumor necrosis factor and reactive oxygen species cooperative cytotoxicity is mediated via inhibition of NF-kappaB." Mol Med **6**(12): 1028-1041.

Giulian, D., J. Chen, J. E. Ingeman, J. K. George and M. Noponen (1989). "The role of mononuclear phagocytes in wound healing after traumatic injury to adult mammalian brain." J Neurosci **9**(12): 4416-4429.

Grassme, H., A. Jekle, A. Riehle, H. Schwarz, J. Berger, K. Sandhoff, R. Kolesnick and E. Gulbins (2001). "CD95 signaling via ceramide-rich membrane rafts." J Biol Chem **276**(23): 20589-20596.

Grassme, H., V. Jendrossek, J. Bock, A. Riehle and E. Gulbins (2002). "Ceramide-rich membrane rafts mediate CD40 clustering." J Immunol **168**(1): 298-307.

Grell, M., E. Douni, H. Wajant, M. Lohden, M. Clauss, B. Maxeiner, S. Georgopoulos, W. Lesslauer, G. Kollias, K. Pfizenmaier and P. Scheurich (1995). "The transmembrane form of tumor necrosis factor is the prime activating ligand of the 80 kDa tumor necrosis factor receptor." Cell **83**(5): 793-802.

Grell, M., P. Scheurich, A. Meager and K. Pfizenmaier (1993). "TR60 and TR80 tumor necrosis factor (TNF)-receptors can independently mediate cytolysis." Lymphokine Cytokine Res **12**(3): 143-148.

Grell, M., H. Wajant, G. Zimmermann and P. Scheurich (1998). "The type 1 receptor (CD120a) is the high-affinity receptor for soluble tumor necrosis factor." Proc Natl Acad Sci U S A **95**(2): 570-575.

Grell, M., G. Zimmermann, E. Gottfried, C. M. Chen, U. Grunwald, D. C. Huang, Y. H. Wu Lee, H. Durkop, H. Engelmann, P. Scheurich, H. Wajant and A. Strasser (1999). "Induction of cell death by tumour necrosis factor (TNF) receptor 2, CD40 and CD30: a role for TNF-R1 activation by endogenous membrane-anchored TNF." EMBO J **18**(11): 3034-3043.

Gross, A., J. Jockel, M. C. Wei and S. J. Korsmeyer (1998). "Enforced dimerization of BAX results in its translocation, mitochondrial dysfunction and apoptosis." EMBO J **17**(14): 3878-3885.

Gutierrez, E. G., W. A. Banks and A. J. Kastin (1993). "Murine tumor necrosis factor alpha is transported from blood to brain in the mouse." J Neuroimmunol **47**(2): 169-176.

Haas, T. L., C. H. Emmerich, B. Gerlach, A. C. Schmukle, S. M. Cordier, E. Rieser, R. Feltham, J. Vince, U. Warnken, T. Wenger, R. Koschny, D. Komander, J. Silke and H. Walczak (2009). "Recruitment of the linear ubiquitin chain assembly complex stabilizes the

TNF-R1 signaling complex and is required for TNF-mediated gene induction." Mol Cell **36**(5): 831-844.

Hallenbeck, J. M. (2002). "The many faces of tumor necrosis factor in stroke." Nat Med **8**(12): 1363-1368.

Hamby, M. E. and M. V. Sofroniew (2010). "Reactive astrocytes as therapeutic targets for CNS disorders." Neurotherapeutics **7**(4): 494-506.

Hamid, T., Y. Gu, R. V. Ortines, C. Bhattacharya, G. Wang, Y. T. Xuan and S. D. Prabhu (2009). "Divergent tumor necrosis factor receptor-related remodeling responses in heart failure: role of nuclear factor-kappaB and inflammatory activation." Circulation **119**(10): 1386-1397.

Hartung, H. P., R. Gonsette, N. Konig, H. Kwiecinski, A. Guseo, S. P. Morrissey, H. Krapf and T. Zwingers (2002). "Mitoxantrone in progressive multiple sclerosis: a placebo-controlled, double-blind, randomised, multicentre trial." Lancet **360**(9350): 2018-2025.

Haugh, J. M., A. C. Huang, H. S. Wiley, A. Wells and D. A. Lauffenburger (1999a). "Internalized epidermal growth factor receptors participate in the activation of p21(ras) in fibroblasts." J Biol Chem **274**(48): 34350-34360.

Haugh, J. M. and T. Meyer (2002). "Active EGF receptors have limited access to PtdIns(4,5)P(2) in endosomes: implications for phospholipase C and PI 3-kinase signaling." J Cell Sci **115**(Pt 2): 303-310.

Haugh, J. M., K. Schooler, A. Wells, H. S. Wiley and D. A. Lauffenburger (1999b). "Effect of epidermal growth factor receptor internalization on regulation of the phospholipase C-gamma1 signaling pathway." J Biol Chem **274**(13): 8958-8965.

Hayashi, T. and D. Faustman (1999). "NOD mice are defective in proteasome production and activation of NF-kappaB." Mol Cell Biol **19**(12): 8646-8659.

Heldmann, U., P. Thored, J. H. Claasen, A. Arvidsson, Z. Kokaia and O. Lindvall (2005). "TNF-alpha antibody infusion impairs survival of stroke-generated neuroblasts in adult rat brain." Exp Neurol **196**(1): 204-208.

Henkler, F., E. Behrle, K. M. Dennehy, A. Wicovsky, N. Peters, C. Warnke, K. Pfizenmaier and H. Wajant (2005). "The extracellular domains of FasL and Fas are sufficient for the formation of supramolecular FasL-Fas clusters of high stability." J Cell Biol **168**(7): 1087-1098.

Hieber, U. and M. E. Heim (1994). "Tumor necrosis factor for the treatment of malignancies." Oncology **51**(2): 142-153.

Hofman, F. M., D. R. Hinton, K. Johnson and J. E. Merrill (1989). "Tumor necrosis factor identified in multiple sclerosis brain." J Exp Med **170**(2): 607-612.

Holler, N., A. Tardivel, M. Kovacsovics-Bankowski, S. Hertig, O. Gaide, F. Martinon, A. Tinel, D. Deperthes, S. Calderara, T. Schulthess, J. Engel, P. Schneider and J. Tschopp (2003). "Two adjacent trimeric Fas ligands are required for Fas signaling and formation of a death-inducing signaling complex." Mol Cell Biol **23**(4): 1428-1440.

Hori, S., T. Nomura and S. Sakaguchi (2003). "Control of regulatory T cell development by the transcription factor Foxp3." Science **299**(5609): 1057-1061.

Hsu, H., J. Huang, H. B. Shu, V. Baichwal and D. V. Goeddel (1996a). "TNF-dependent recruitment of the protein kinase RIP to the TNF receptor-1 signaling complex." Immunity **4**(4): 387-396.

Hsu, H., H. B. Shu, M. G. Pan and D. V. Goeddel (1996b). "TRADD-TRAF2 and TRADD-FADD interactions define two distinct TNF receptor 1 signal transduction pathways." Cell **84**(2): 299-308.

Hsu, H., J. Xiong and D. V. Goeddel (1995). "The TNF receptor 1-associated protein TRADD signals cell death and NF-kappa B activation." Cell **81**(4): 495-504.

Huang, D., Y. Han, M. R. Rani, A. Glabinski, C. Trebst, T. Sorensen, M. Tani, J. Wang, P. Chien, S. O'Bryan, B. Bielecki, Z. L. Zhou, S. Majumder and R. M. Ransohoff (2000). "Chemokines and chemokine receptors in inflammation of the nervous system: manifold roles and exquisite regulation." Immunol Rev **177**: 52-67.

Itoh, M., T. Takahashi, N. Sakaguchi, Y. Kuniyasu, J. Shimizu, F. Otsuka and S. Sakaguchi (1999). "Thymus and autoimmunity: production of CD25+CD4+ naturally anergic and suppressive T cells as a key function of the thymus in maintaining immunologic self-tolerance." J Immunol **162**(9): 5317-5326.

Iversen, P. O., G. Nicolaysen and M. Sioud (2001). "DNA enzyme targeting TNF-alpha mRNA improves hemodynamic performance in rats with postinfarction heart failure." Am J Physiol Heart Circ Physiol **281**(5): H2211-2217.

Jansen, J., T. van der Poll, M. Levi, H. ten Cate, H. Gallati, J. W. ten Cate and S. J. van Deventer (1995). "Inhibition of the release of soluble tumor necrosis factor receptors in experimental endotoxemia by an anti-tumor necrosis factor-alpha antibody." J Clin Immunol **15**(1): 45-50.

Jeng, R. L. and M. D. Welch (2001). "Cytoskeleton: actin and endocytosis--no longer the weakest link." Curr Biol **11**(17): R691-694.

Jones, F. S., S. Hoffman, B. A. Cunningham and G. M. Edelman (1989). "A detailed structural model of cytotactin: protein homologies, alternative RNA splicing, and binding regions." Proc Natl Acad Sci U S A **86**(6): 1905-1909.

Jones, L. S., L. V. Rizzo, R. K. Agarwal, T. K. Tarrant, C. C. Chan, B. Wiggert and R. R. Caspi (1997). "IFN-gamma-deficient mice develop experimental autoimmune uveitis in the context of a deviant effector response." J Immunol **158**(12): 5997-6005.

Jones, T. R., Carpenter, A., Golland, P. (2005). "Voronoi-Based Segmentation of Cells on Image Manifolds." Proc. ICCV Workshop on Computer Vision for Biomedical Image Applications

Jupp, O. J., S. M. McFarlane, H. M. Anderson, A. F. Littlejohn, A. A. Mohamed, R. H. MacKay, P. Vandenabeele and D. J. MacEwan (2001). "Type II tumour necrosis factor-alpha receptor (TNFR2) activates c-Jun N-terminal kinase (JNK) but not mitogen-activated protein kinase (MAPK) or p38 MAPK pathways." Biochem J **359**(Pt 3): 525-535.

Kadokami, T., C. Frye, B. Lemster, C. L. Wagner, A. M. Feldman and C. F. McTiernan (2001). "Anti-tumor necrosis factor-alpha antibody limits heart failure in a transgenic model." Circulation **104**(10): 1094-1097.

Kammerer, R. A., T. Schulthess, R. Landwehr, A. Lustig, D. Fischer and J. Engel (1998). "Tenascin-C hexabrachion assembly is a sequential two-step process initiated by coiled-coil alpha-helices." J Biol Chem **273**(17): 10602-10608.

Kanayama, A., R. B. Seth, L. Sun, C. K. Ea, M. Hong, A. Shaito, Y. H. Chiu, L. Deng and Z. J. Chen (2004). "TAB2 and TAB3 activate the NF-kappaB pathway through binding to polyubiquitin chains." Mol Cell **15**(4): 535-548.

Keirstead, H. S. and W. F. Blakemore (1997). "Identification of post-mitotic oligodendrocytes incapable of remyelination within the demyelinated adult spinal cord." J Neuropathol Exp Neurol **56**(11): 1191-1201.

Kelchtermans, H., B. De Klerck, T. Mitera, M. Van Balen, D. Bullens, A. Billiau, G. Leclercq and P. Matthys (2005). "Defective CD4+CD25+ regulatory T cell functioning in collagen-induced arthritis: an important factor in pathogenesis, counter-regulated by endogenous IFN-gamma." Arthritis Res Ther **7**(2): R402-415.

Kent, W. J., C. W. Sugnet, T. S. Furey, K. M. Roskin, T. H. Pringle, A. M. Zahler and D. Haussler (2002). "The human genome browser at UCSC." Genome Res **12**(6): 996-1006.

Kim, E. Y., J. J. Priatel, S. J. Teh and H. S. Teh (2006). "TNF receptor type 2 (p75) functions as a costimulator for antigen-driven T cell responses in vivo." J Immunol **176**(2): 1026-1035.

Kim, E. Y. and H. S. Teh (2001). "TNF type 2 receptor (p75) lowers the threshold of T cell activation." J Immunol **167**(12): 6812-6820.

Kirisako, T., K. Kamei, S. Murata, M. Kato, H. Fukumoto, M. Kanie, S. Sano, F. Tokunaga, K. Tanaka and K. Iwai (2006). "A ubiquitin ligase complex assembles linear polyubiquitin chains." EMBO J **25**(20): 4877-4887.

Kirk, J., J. Plumb, M. Mirakhur and S. McQuaid (2003). "Tight junctional abnormality in multiple sclerosis white matter affects all calibres of vessel and is associated with blood-brain barrier leakage and active demyelination." J Pathol **201**(2): 319-327.

Kodama, S., M. Davis and D. L. Faustman (2005). "The therapeutic potential of tumor necrosis factor for autoimmune disease: a mechanistically based hypothesis." Cell Mol Life Sci **62**(16): 1850-1862.

Kodama, S., W. Kuhtreiber, S. Fujimura, E. A. Dale and D. L. Faustman (2003). "Islet regeneration during the reversal of autoimmune diabetes in NOD mice." Science **302**(5648): 1223-1227.

Koistinaho, M., S. Lin, X. Wu, M. Esterman, D. Koger, J. Hanson, R. Higgs, F. Liu, S. Malkani, K. R. Bales and S. M. Paul (2004). "Apolipoprotein E promotes astrocyte colocalization and degradation of deposited amyloid-beta peptides." Nat Med **10**(7): 719-726.

Komitova, M., E. Perfilieva, B. Mattsson, P. S. Eriksson and B. B. Johansson (2006). "Enriched environment after focal cortical ischemia enhances the generation of astroglia and NG2 positive polydendrocytes in adult rat neocortex." Exp Neurol **199**(1): 113-121.

Kontermann, R. E., S. Munkel, J. Neumeyer, D. Muller, M. Branschadel, P. Scheurich and K. Pfizenmaier (2008). "A humanized tumor necrosis factor receptor 1 (TNFR1)-specific antagonistic antibody for selective inhibition of tumor necrosis factor (TNF) action." J Immunother **31**(3): 225-234.

Kotter, M. R., A. Setzu, F. J. Sim, N. Van Rooijen and R. J. Franklin (2001). "Macrophage depletion impairs oligodendrocyte remyelination following lysolecithin-induced demyelination." Glia **35**(3): 204-212.

Kreuz, S., D. Siegmund, P. Scheurich and H. Wajant (2001). "NF-kappaB inducers upregulate cFLIP, a cycloheximide-sensitive inhibitor of death receptor signaling." Mol Cell Biol **21**(12): 3964-3973.

Kriegler, M., C. Perez, K. DeFay, I. Albert and S. D. Lu (1988). "A novel form of TNF/cachectin is a cell surface cytotoxic transmembrane protein: ramifications for the complex physiology of TNF." Cell **53**(1): 45-53.

Krippner-Heidenreich, A., I. Grunwald, G. Zimmermann, M. Kuhnle, J. Gerspach, T. Sterns, S. D. Shnyder, J. H. Gill, D. N. Mannel, K. Pfizenmaier and P. Scheurich (2008). "Single-chain TNF, a TNF derivative with enhanced stability and antitumoral activity." J Immunol **180**(12): 8176-8183.

Krippner-Heidenreich, A., F. Tubing, S. Bryde, S. Willi, G. Zimmermann and P. Scheurich (2002). "Control of receptor-induced signaling complex formation by the kinetics of ligand/receptor interaction." J Biol Chem **277**(46): 44155-44163.

Lambertsen, K. L., B. H. Clausen, C. Fenger, H. Wulf, T. Owens, F. Dagnaes-Hansen, M. Meldgaard and B. Finsen (2007). "Microglia and macrophages express tumor necrosis factor receptor p75 following middle cerebral artery occlusion in mice." Neuroscience **144**(3): 934-949.

Lantz, M., S. Malik, M. L. Slevin and I. Olsson (1990). "Infusion of tumor necrosis factor (TNF) causes an increase in circulating TNF-binding protein in humans." Cytokine **2**(6): 402-406.

Lassmann, H. (2007a). "Multiple sclerosis: is there neurodegeneration independent from inflammation?" J Neurol Sci **259**(1-2): 3-6.

Lassmann, H. (2007b). "New concepts on progressive multiple sclerosis." Curr Neurol Neurosci Rep **7**(3): 239-244.

Lawlor, M. A. and D. R. Alessi (2001). "PKB/Akt: a key mediator of cell proliferation, survival and insulin responses?" J Cell Sci **114**(Pt 16): 2903-2910.

Le Roy, C. and J. L. Wrana (2005). "Clathrin- and non-clathrin-mediated endocytic regulation of cell signalling." Nat Rev Mol Cell Biol **6**(2): 112-126.

Lee, K. H., C. Feig, V. Tchikov, R. Schickel, C. Hallas, S. Schutze, M. E. Peter and A. C. Chan (2006). "The role of receptor internalization in CD95 signaling." EMBO J **25**(5): 1009-1023.

Lehuen, A., O. Lantz, L. Beaudoin, V. Laloux, C. Carnaud, A. Bendelac, J. F. Bach and R. C. Monteiro (1998). "Overexpression of natural killer T cells protects Valpha14- Jalpha281 transgenic nonobese diabetic mice against diabetes." J Exp Med **188**(10): 1831-1839.

Leibovich, S. J., P. J. Polverini, H. M. Shepard, D. M. Wiseman, V. Shively and N. Nuseir (1987). "Macrophage-induced angiogenesis is mediated by tumour necrosis factor-alpha." Nature **329**(6140): 630-632.

Leonardi, A., H. Ellinger-Ziegelbauer, G. Franzoso, K. Brown and U. Siebenlist (2000). "Physical and functional interaction of filamin (actin-binding protein-280) and tumor necrosis factor receptor-associated factor 2." J Biol Chem **275**(1): 271-278.

Liberto, C. M., P. J. Albrecht, L. M. Herx, V. W. Yong and S. W. Levison (2004). "Pro-regenerative properties of cytokine-activated astrocytes." J Neurochem **89**(5): 1092-1100.

Liblau, R. S., S. M. Singer and H. O. McDevitt (1995). "Th1 and Th2 CD4+ T cells in the pathogenesis of organ-specific autoimmune diseases." Immunol Today **16**(1): 34-38.

Liu, R. Y., C. Fan, G. Liu, N. E. Olashaw and K. S. Zuckerman (2000). "Activation of p38 mitogen-activated protein kinase is required for tumor necrosis factor-alpha -supported proliferation of leukemia and lymphoma cell lines." J Biol Chem **275**(28): 21086-21093.

Lo, Y. C., S. C. Lin, C. C. Rospigliosi, D. B. Conze, C. J. Wu, J. D. Ashwell, D. Eliezer and H. Wu (2009). "Structural basis for recognition of diubiquitins by NEMO." Mol Cell **33**(5): 602-615.

Locksley, R. M., N. Killeen and M. J. Lenardo (2001). "The TNF and TNF receptor superfamilies: integrating mammalian biology." Cell **104**(4): 487-501.

Loetscher, H., D. Stueber, D. Banner, F. Mackay and W. Lesslauer (1993). "Human tumor necrosis factor alpha (TNF alpha) mutants with exclusive specificity for the 55-kDa or 75-kDa TNF receptors." J Biol Chem **268**(35): 26350-26357.

Lotharius, J., S. Barg, P. Wiekop, C. Lundberg, H. K. Raymon and P. Brundin (2002). "Effect of mutant alpha-synuclein on dopamine homeostasis in a new human mesencephalic cell line." J Biol Chem **277**(41): 38884-38894.

Lotharius, J., J. Falsig, J. van Beek, S. Payne, R. Dringen, P. Brundin and M. Leist (2005). "Progressive degeneration of human mesencephalic neuron-derived cells triggered by dopamine-dependent oxidative stress is dependent on the mixed-lineage kinase pathway." J Neurosci **25**(27): 6329-6342.

Mabuchi, T., K. Kitagawa, T. Ohtsuki, K. Kuwabara, Y. Yagita, T. Yanagihara, M. Hori and M. Matsumoto (2000). "Contribution of microglia/macrophages to expansion of infarction and response of oligodendrocytes after focal cerebral ischemia in rats." Stroke **31**(7): 1735-1743.

Mackay, F., H. Loetscher, D. Stueber, G. Gehr and W. Lesslauer (1993). "Tumor necrosis factor alpha (TNF-alpha)-induced cell adhesion to human endothelial cells is under dominant control of one TNF receptor type, TNF-R55." J Exp Med **177**(5): 1277-1286.

Madrid, L. V., C. Y. Wang, D. C. Guttridge, A. J. Schottelius, A. S. Baldwin, Jr. and M. W. Mayo (2000). "Akt suppresses apoptosis by stimulating the transactivation potential of the RelA/p65 subunit of NF-kappaB." Mol Cell Biol **20**(5): 1626-1638.

Maehama, T. and J. E. Dixon (1999). "PTEN: a tumour suppressor that functions as a phospholipid phosphatase." Trends Cell Biol **9**(4): 125-128.

Malek, T. R. and A. L. Bayer (2004). "Tolerance, not immunity, crucially depends on IL-2." Nat Rev Immunol **4**(9): 665-674.

Malinin, N. L., M. P. Boldin, A. V. Kovalenko and D. Wallach (1997). "MAP3K-related kinase involved in NF-kappaB induction by TNF, CD95 and IL-1." Nature **385**(6616): 540-544.

Mandai, K., M. Matsumoto, K. Kitagawa, K. Matsushita, T. Ohtsuki, T. Mabuchi, D. R. Colman, T. Kamada and T. Yanagihara (1997). "Ischemic damage and subsequent proliferation of oligodendrocytes in focal cerebral ischemia." Neuroscience **77**(3): 849-861.

Mann, D. L. (2002). "Inflammatory mediators and the failing heart: past, present, and the foreseeable future." Circ Res **91**(11): 988-998.

Männel, D. N., H. Northoff, F. Bauss and W. Falk (1987). "Tumor necrosis factor: a cytokine involved in toxic effects of endotoxin." Rev Infect Dis **9 Suppl 5**: S602-606.

Marchetti, L., M. Klein, K. Schlett, K. Pfizenmaier and U. L. Eisel (2004). "Tumor necrosis factor (TNF)-mediated neuroprotection against glutamate-induced excitotoxicity is enhanced by N-methyl-D-aspartate receptor activation. Essential role of a TNF receptor 2-mediated phosphatidylinositol 3-kinase-dependent NF-kappa B pathway." J Biol Chem **279**(31): 32869-32881.

Masada, T., Y. Hua, G. Xi, S. R. Ennis and R. F. Keep (2001). "Attenuation of ischemic brain edema and cerebrovascular injury after ischemic preconditioning in the rat." J Cereb Blood Flow Metab **21**(1): 22-33.

McCoy, M. K. and M. G. Tansey (2008). "TNF signaling inhibition in the CNS: implications for normal brain function and neurodegenerative disease." J Neuroinflammation **5**: 45.

McTigue, D. M. and R. B. Tripathi (2008). "The life, death, and replacement of oligodendrocytes in the adult CNS." J Neurochem **107**(1): 1-19.

Medzhitov, R. (2007). "Recognition of microorganisms and activation of the immune response." Nature **449**(7164): 819-826.

Meistrell, M. E., 3rd, G. I. Botchkina, H. Wang, E. Di Santo, K. M. Cockroft, O. Bloom, J. M. Vishnubhakat, P. Ghezzi and K. J. Tracey (1997). "Tumor necrosis factor is a brain damaging cytokine in cerebral ischemia." Shock **8**(5): 341-348.

Mellman, I. (1996). "Membranes and sorting." Curr Opin Cell Biol **8**(4): 497-498.

Mendoza-Milla, C., C. Machuca Rodriguez, E. Cordova Alarcon, A. Estrada Bernal, E. M. Toledo-Cuevas, E. Martinez Martinez and A. Zentella Dehesa (2005). "NF-kappaB activation but not PI3K/Akt is required for dexamethasone dependent protection against TNF-alpha cytotoxicity in L929 cells." FEBS Lett **579**(18): 3947-3952.

Mercurio, F., H. Zhu, B. W. Murray, A. Shevchenko, B. L. Bennett, J. Li, D. B. Young, M. Barbosa, M. Mann, A. Manning and A. Rao (1997). "IKK-1 and IKK-2: cytokine-activated IkappaB kinases essential for NF-kappaB activation." Science **278**(5339): 860-866.

Messerschmidt, S. K., A. Kolbe, D. Muller, M. Knoll, J. Pleiss and R. E. Kontermann (2008). "Novel single-chain Fv' formats for the generation of immunoliposomes by site-directed coupling." Bioconjug Chem **19**(1): 362-369.

Messerschmidt, S. K., A. Musyanovych, M. Altvater, P. Scheurich, K. Pfizenmaier, K. Landfester and R. E. Kontermann (2009). "Targeted lipid-coated nanoparticles: delivery of tumor necrosis factor-functionalized particles to tumor cells." J Control Release **137**(1): 69-77.

Micheau, O. and J. Tschopp (2003). "Induction of TNF receptor I-mediated apoptosis via two sequential signaling complexes." Cell **114**(2): 181-190.

Moe, G. W., J. Marin-Garcia, A. Konig, M. Goldenthal, X. Lu and Q. Feng (2004). "In vivo TNF-alpha inhibition ameliorates cardiac mitochondrial dysfunction, oxidative stress, and apoptosis in experimental heart failure." Am J Physiol Heart Circ Physiol **287**(4): H1813-1820.

Monden, Y., T. Kubota, T. Inoue, T. Tsutsumi, S. Kawano, T. Ide, H. Tsutsui and K. Sunagawa (2007). "Tumor necrosis factor-alpha is toxic via receptor 1 and protective via receptor 2 in a murine model of myocardial infarction." Am J Physiol Heart Circ Physiol **293**(1): H743-753.

Montgomery, D. L. (1994). "Astrocytes: form, functions, and roles in disease." Vet Pathol **31**(2): 145-167.

Moretto, G., A. Yoo and S. U. Kim (1993). "Human astrocytes and cytokines: tumor necrosis factor alpha and interferon gamma do not promote astrocytic proliferation." Neurosci Lett **151**(1): 17-20.

Moss, M. L., L. Sklair-Tavron and R. Nudelman (2008). "Drug insight: tumor necrosis factor-converting enzyme as a pharmaceutical target for rheumatoid arthritis." Nat Clin Pract Rheumatol **4**(6): 300-309.

Moutschen, M. P., A. J. Scheen and P. J. Lefebvre (1992). "Impaired immune responses in diabetes mellitus: analysis of the factors and mechanisms involved. Relevance to the increased susceptibility of diabetic patients to specific infections." Diabete Metab **18**(3): 187-201.

Müller, A., T. G. Hauk and D. Fischer (2007). "Astrocyte-derived CNTF switches mature RGCs to a regenerative state following inflammatory stimulation." Brain **130**(Pt 12): 3308-3320.

Müller, A., T. G. Hauk, M. Leibinger, R. Marienfeld and D. Fischer (2009). "Exogenous CNTF stimulates axon regeneration of retinal ganglion cells partially via endogenous CNTF." Mol Cell Neurosci **41**(2): 233-246.

Nagar, M., J. Jacob-Hirsch, H. Vernitsky, Y. Berkun, S. Ben-Horin, N. Amariglio, I. Bank, Y. Kloog, G. Rechavi and I. Goldstein (2010). "TNF activates a NF-kappaB-regulated cellular program in human CD45RA- regulatory T cells that modulates their suppressive function." J Immunol **184**(7): 3570-3581.

Naismith, J. H., T. Q. Devine, T. Kohno and S. R. Sprang (1996). "Structures of the extracellular domain of the type I tumor necrosis factor receptor." Structure **4**(11): 1251-1262.

Nait-Oumesmar, B., L. Decker, F. Lachapelle, V. Avellana-Adalid, C. Bachelin and A. B. Van Evercooren (1999). "Progenitor cells of the adult mouse subventricular zone proliferate, migrate and differentiate into oligodendrocytes after demyelination." Eur J Neurosci **11**(12): 4357-4366.

Nawashiro, H., D. Martin and J. M. Hallenbeck (1997a). "Inhibition of tumor necrosis factor and amelioration of brain infarction in mice." J Cereb Blood Flow Metab **17**(2): 229-232.

Nawashiro, H., K. Tasaki, C. A. Ruetzler and J. M. Hallenbeck (1997b). "TNF-alpha pretreatment induces protective effects against focal cerebral ischemia in mice." J Cereb Blood Flow Metab **17**(5): 483-490.

Neuhaus, O., J. J. Archelos and H. P. Hartung (2003). "Immunomodulation in multiple sclerosis: from immunosuppression to neuroprotection." Trends Pharmacol Sci **24**(3): 131-138.

Neumann, H., M. R. Kotter and R. J. Franklin (2009). "Debris clearance by microglia: an essential link between degeneration and regeneration." Brain **132**(Pt 2): 288-295.

Newton, R. C., K. A. Solomon, M. B. Covington, C. P. Decicco, P. J. Haley, S. M. Friedman and K. Vaddi (2001). "Biology of TACE inhibition." Ann Rheum Dis **60 Suppl 3**: iii25-32.

Nicholson, K. M. and N. G. Anderson (2002). "The protein kinase B/Akt signalling pathway in human malignancy." Cell Signal **14**(5): 381-395.

Noble, M., D. Wren and G. Wolswijk (1992). "The O-2A(adult) progenitor cell: a glial stem cell of the adult central nervous system." Semin Cell Biol **3**(6): 413-422.

Norenberg, M. D. (1994). "Astrocyte responses to CNS injury." J Neuropathol Exp Neurol **53**(3): 213-220.

Noshita, N., A. Lewen, T. Sugawara and P. H. Chan (2002). "Akt phosphorylation and neuronal survival after traumatic brain injury in mice." Neurobiol Dis **9**(3): 294-304.

Olanow, C. W. (1992). "An introduction to the free radical hypothesis in Parkinson's disease." Ann Neurol **32 Suppl**: S2-9.

Olanow, C. W. (1993). "A radical hypothesis for neurodegeneration." Trends Neurosci **16**(11): 439-444.

Osburg, B., C. Peiser, D. Domling, L. Schomburg, Y. T. Ko, K. Voigt and U. Bickel (2002). "Effect of endotoxin on expression of TNF receptors and transport of TNF-alpha at the blood-brain barrier of the rat." Am J Physiol Endocrinol Metab **283**(5): E899-908.

Ozes, O. N., L. D. Mayo, J. A. Gustin, S. R. Pfeffer, L. M. Pfeffer and D. B. Donner (1999). "NF-kappaB activation by tumour necrosis factor requires the Akt serine-threonine kinase." Nature **401**(6748): 82-85.

Pan, S., P. An, R. Zhang, X. He, G. Yin and W. Min (2002). "Etk/Bmx as a tumor necrosis factor receptor type 2-specific kinase: role in endothelial cell migration and angiogenesis." Mol Cell Biol **22**(21): 7512-7523.

Pan, W. and A. J. Kastin (2001). "Upregulation of the transport system for TNFalpha at the blood-brain barrier." Arch Physiol Biochem **109**(4): 350-353.

Pan, W. and A. J. Kastin (2002). "TNFalpha transport across the blood-brain barrier is abolished in receptor knockout mice." Exp Neurol **174**(2): 193-200.

Pan, W. and A. J. Kastin (2007). "Tumor necrosis factor and stroke: role of the blood-brain barrier." Prog Neurobiol **83**(6): 363-374.

Patten, D. A., M. Germain, M. A. Kelly and R. S. Slack (2010). "Reactive oxygen species: stuck in the middle of neurodegeneration." J Alzheimers Dis **20 Suppl 2**: S357-367.

Pennica, D., V. T. Lam, N. K. Mize, R. F. Weber, M. Lewis, B. M. Fendly, M. T. Lipari and D. V. Goeddel (1992). "Biochemical properties of the 75-kDa tumor necrosis factor receptor. Characterization of ligand binding, internalization, and receptor phosphorylation." J Biol Chem **267**(29): 21172-21178.

Perez, C., I. Albert, K. DeFay, N. Zachariades, L. Gooding and M. Kriegler (1990). "A nonsecretable cell surface mutant of tumor necrosis factor (TNF) kills by cell-to-cell contact." Cell **63**(2): 251-258.

Peter, M. E., R. C. Budd, J. Desbarats, S. M. Hedrick, A. O. Hueber, M. K. Newell, L. B. Owen, R. M. Pope, J. Tschopp, H. Wajant, D. Wallach, R. H. Wiltrout, M. Zornig and D. H. Lynch (2007). "The CD95 receptor: apoptosis revisited." Cell **129**(3): 447-450.

Pfizenmaier, K. and D. E. Szymkowski (2011). "Workshop Summary: Introduction to Rational Design of New Means for Therapeutic Modulation of Function of the TNF Family." Adv Exp Med Biol **691**: 487-491.

Polazzi, E. and A. Contestabile (2002). "Reciprocal interactions between microglia and neurons: from survival to neuropathology." Rev Neurosci **13**(3): 221-242.

Polman, C. H., P. W. O'Connor, E. Havrdova, M. Hutchinson, L. Kappos, D. H. Miller, J. T. Phillips, F. D. Lublin, G. Giovannoni, A. Wajgt, M. Toal, F. Lynn, M. A. Panzara and A. W. Sandrock (2006). "A randomized, placebo-controlled trial of natalizumab for relapsing multiple sclerosis." N Engl J Med **354**(9): 899-910.

Porteu, F. and C. Nathan (1990). "Shedding of tumor necrosis factor receptors by activated human neutrophils." J Exp Med **172**(2): 599-607.

Pound, J. D., A. Challa, M. J. Holder, R. J. Armitage, S. K. Dower, W. C. Fanslow, H. Kikutani, S. Paulie, C. D. Gregory and J. Gordon (1999). "Minimal cross-linking and epitope requirements for CD40-dependent suppression of apoptosis contrast with those for promotion of the cell cycle and homotypic adhesions in human B cells." Int Immunol **11**(1): 11-20.

Prineas, J. W., E. E. Kwon, P. Z. Goldenberg, A. A. Ilyas, R. H. Quarles, J. A. Benjamins and T. J. Sprinkle (1989). "Multiple sclerosis. Oligodendrocyte proliferation and differentiation in fresh lesions." Lab Invest **61**(5): 489-503.

Probert, L., K. Akassoglou, M. Pasparakis, G. Kontogeorgos and G. Kollias (1995). "Spontaneous inflammatory demyelinating disease in transgenic mice showing central nervous system-specific expression of tumor necrosis factor alpha." Proc Natl Acad Sci U S A **92**(24): 11294-11298.

Rahighi, S., F. Ikeda, M. Kawasaki, M. Akutsu, N. Suzuki, R. Kato, T. Kensche, T. Uejima, S. Bloor, D. Komander, F. Randow, S. Wakatsuki and I. Dikic (2009). "Specific recognition of linear ubiquitin chains by NEMO is important for NF-kappaB activation." Cell **136**(6): 1098-1109.

Ramakrishnan, P., W. Wang and D. Wallach (2004). "Receptor-specific signaling for both the alternative and the canonical NF-kappaB activation pathways by NF-kappaB-inducing kinase." Immunity **21**(4): 477-489.

Ramani, R., M. Mathier, P. Wang, G. Gibson, S. Togel, J. Dawson, A. Bauer, S. Alber, S. C. Watkins, C. F. McTiernan and A. M. Feldman (2004). "Inhibition of tumor necrosis factor receptor-1-mediated pathways has beneficial effects in a murine model of postischemic remodeling." Am J Physiol Heart Circ Physiol **287**(3): H1369-1377.

Rao, P., K. C. Hsu and M. V. Chao (1995). "Upregulation of NF-kappa B-dependent gene expression mediated by the p75 tumor necrosis factor receptor." J Interferon Cytokine Res **15**(2): 171-177.

Rauert, H., A. Wicovsky, N. Muller, D. Siegmund, V. Spindler, J. Waschke, C. Kneitz and H. Wajant (2010). "Membrane tumor necrosis factor (TNF) induces p100 processing via TNF receptor-2 (TNFR2)." J Biol Chem **285**(10): 7394-7404.

Reddy, P., J. L. Slack, R. Davis, D. P. Cerretti, C. J. Kozlosky, R. A. Blanton, D. Shows, J. J. Peschon and R. A. Black (2000). "Functional analysis of the domain structure of tumor necrosis factor-alpha converting enzyme." J Biol Chem **275**(19): 14608-14614.

Regnier, C. H., H. Y. Song, X. Gao, D. V. Goeddel, Z. Cao and M. Rothe (1997). "Identification and characterization of an IkappaB kinase." Cell **90**(2): 373-383.

Richardson, J. S. (1993). "Free radicals in the genesis of Alzheimer's disease." Ann N Y Acad Sci **695**: 73-76.

Richter, C. and G. E. Kass (1991). "Oxidative stress in mitochondria: its relationship to cellular Ca2+ homeostasis, cell death, proliferation, and differentiation." Chem Biol Interact **77**(1): 1-23.

Romashkova, J. A. and S. S. Makarov (1999). "NF-kappaB is a target of AKT in anti-apoptotic PDGF signalling." Nature **401**(6748): 86-90.

Roth, A. D., G. Ramirez, R. Alarcon and R. Von Bernhardi (2005). "Oligodendrocytes damage in Alzheimer's disease: beta amyloid toxicity and inflammation." Biol Res **38**(4): 381-387.

Rothberg, K. G., J. E. Heuser, W. C. Donzell, Y. S. Ying, J. R. Glenney and R. G. Anderson (1992). "Caveolin, a protein component of caveolae membrane coats." Cell **68**(4): 673-682.

Rothe, M., M. G. Pan, W. J. Henzel, T. M. Ayres and D. V. Goeddel (1995). "The TNFR2-TRAF signaling complex contains two novel proteins related to baculoviral inhibitor of apoptosis proteins." Cell **83**(7): 1243-1252.

Rothe, M., S. C. Wong, W. J. Henzel and D. V. Goeddel (1994). "A novel family of putative signal transducers associated with the cytoplasmic domain of the 75 kDa tumor necrosis factor receptor." Cell **78**(4): 681-692.

Rothwarf, D. M., E. Zandi, G. Natoli and M. Karin (1998). "IKK-gamma is an essential regulatory subunit of the IkappaB kinase complex." Nature **395**(6699): 297-300.

Rozen, S. and H. Skaletsky (2000). "Primer3 on the WWW for general users and for biologist programmers." Methods Mol Biol **132**: 365-386.

Ryu, S., S. Kodama, K. Ryu, D. A. Schoenfeld and D. L. Faustman (2001). "Reversal of established autoimmune diabetes by restoration of endogenous beta cell function." J Clin Invest **108**(1): 63-72.

Sairanen, T., O. Carpen, M. L. Karjalainen-Lindsberg, A. Paetau, U. Turpeinen, M. Kaste and P. J. Lindsberg (2001). "Evolution of cerebral tumor necrosis factor-alpha production during human ischemic stroke." Stroke **32**(8): 1750-1758.

Sakaguchi, S. (2000). "Regulatory T cells: key controllers of immunologic self-tolerance." Cell **101**(5): 455-458.

Sakaguchi, S., N. Sakaguchi, M. Asano, M. Itoh and M. Toda (1995). "Immunologic self-tolerance maintained by activated T cells expressing IL-2 receptor alpha-chains (CD25). Breakdown of a single mechanism of self-tolerance causes various autoimmune diseases." J Immunol **155**(3): 1151-1164.

Sakaguchi, S., T. Takahashi and Y. Nishizuka (1982). "Study on cellular events in postthymectomy autoimmune oophoritis in mice. I. Requirement of Lyt-1 effector cells for oocytes damage after adoptive transfer." J Exp Med **156**(6): 1565-1576.

Sakaguchi, S., K. Wing and M. Miyara (2007). "Regulatory T cells - a brief history and perspective." Eur J Immunol **37 Suppl 1**: S116-123.

Sakaguchi, S., T. Yamaguchi, T. Nomura and M. Ono (2008). "Regulatory T cells and immune tolerance." Cell **133**(5): 775-787.

Sarbassov, D. D., D. A. Guertin, S. M. Ali and D. M. Sabatini (2005). "Phosphorylation and regulation of Akt/PKB by the rictor-mTOR complex." Science **307**(5712): 1098-1101.

Satoh, J., H. Seino, T. Abo, S. Tanaka, S. Shintani, S. Ohta, K. Tamura, T. Sawai, T. Nobunaga, T. Oteki and et al. (1989). "Recombinant human tumor necrosis factor alpha suppresses autoimmune diabetes in nonobese diabetic mice." J Clin Invest **84**(4): 1345-1348.

Schatz, D. G., M. A. Oettinger and M. S. Schlissel (1992). "V(D)J recombination: molecular biology and regulation." Annu Rev Immunol **10**: 359-383.

Schildknecht, S., D. Poltl, D. M. Nagel, F. Matt, D. Scholz, J. Lotharius, N. Schmieg, A. Salvo-Vargas and M. Leist (2009). "Requirement of a dopaminergic neuronal phenotype for toxicity of low concentrations of 1-methyl-4-phenylpyridinium to human cells." Toxicol Appl Pharmacol **241**(1): 23-35.

Schneider, P., N. Holler, J. L. Bodmer, M. Hahne, K. Frei, A. Fontana and J. Tschopp (1998). "Conversion of membrane-bound Fas(CD95) ligand to its soluble form is associated with downregulation of its proapoptotic activity and loss of liver toxicity." J Exp Med **187**(8): 1205-1213.

Schneider-Brachert, W., V. Tchikov, J. Neumeyer, M. Jakob, S. Winoto-Morbach, J. Held-Feindt, M. Heinrich, O. Merkel, M. Ehrenschwender, D. Adam, R. Mentlein, D. Kabelitz and S. Schutze (2004). "Compartmentalization of TNF receptor 1 signaling: internalized TNF receptosomes as death signaling vesicles." Immunity **21**(3): 415-428.

Schulz, R. (2008). "TNFalpha in myocardial ischemia/reperfusion: damage vs. protection." J Mol Cell Cardiol **45**(6): 712-714.

Schulze-Osthoff, K., D. Ferrari, M. Los, S. Wesselborg and M. E. Peter (1998). "Apoptosis signaling by death receptors." Eur J Biochem **254**(3): 439-459.

Schütze, S., T. Machleidt, D. Adam, R. Schwandner, K. Wiegmann, M. L. Kruse, M. Heinrich, M. Wickel and M. Kronke (1999). "Inhibition of receptor internalization by monodansylcadaverine selectively blocks p55 tumor necrosis factor receptor death domain signaling." J Biol Chem **274**(15): 10203-10212.

Schütze, S., V. Tchikov and W. Schneider-Brachert (2008). "Regulation of TNFR1 and CD95 signalling by receptor compartmentalization." Nat Rev Mol Cell Biol **9**(8): 655-662.

Schwartz, R. H. (2003). "T cell anergy." Annu Rev Immunol **21**: 305-334.

Seckinger, P., S. Isaaz and J. M. Dayer (1988). "A human inhibitor of tumor necrosis factor alpha." J Exp Med **167**(4): 1511-1516.

Seckinger, P., S. Isaaz and J. M. Dayer (1989). "Purification and biologic characterization of a specific tumor necrosis factor alpha inhibitor." J Biol Chem **264**(20): 11966-11973.

Sekiguchi, M., Y. Shiroko, T. Suzuki, M. Imada, M. Miyahara and G. Fujii (1985). "Characterization of a human rhabdomyosarcoma cell strain in tissue culture." Biomed Pharmacother **39**(7): 372-380.

Selmaj, K., W. Papierz, A. Glabinski and T. Kohno (1995). "Prevention of chronic relapsing experimental autoimmune encephalomyelitis by soluble tumor necrosis factor receptor I." J Neuroimmunol **56**(2): 135-141.

Selmaj, K., C. S. Raine and A. H. Cross (1991a). "Anti-tumor necrosis factor therapy abrogates autoimmune demyelination." Ann Neurol **30**(5): 694-700.

Selmaj, K., C. S. Raine, M. Farooq, W. T. Norton and C. F. Brosnan (1991b). "Cytokine cytotoxicity against oligodendrocytes. Apoptosis induced by lymphotoxin." J Immunol **147**(5): 1522-1529.

Selmaj, K., B. Shafit-Zagardo, D. A. Aquino, M. Farooq, C. S. Raine, W. T. Norton and C. F. Brosnan (1991c). "Tumor necrosis factor-induced proliferation of astrocytes from mature brain is associated with down-regulation of glial fibrillary acidic protein mRNA." J Neurochem **57**(3): 823-830.

Selmaj, K. W. and C. S. Raine (1995). "Experimental autoimmune encephalomyelitis: immunotherapy with anti-tumor necrosis factor antibodies and soluble tumor necrosis factor receptors." Neurology **45**(6 Suppl 6): S44-49.

Sharief, M. K. and R. Hentges (1991). "Association between tumor necrosis factor-alpha and disease progression in patients with multiple sclerosis." N Engl J Med **325**(7): 467-472.

Shevach, E. M., R. A. DiPaolo, J. Andersson, D. M. Zhao, G. L. Stephens and A. M. Thornton (2006). "The lifestyle of naturally occurring CD4+ CD25+ Foxp3+ regulatory T cells." Immunol Rev **212**: 60-73.

Shibata, H., Y. Yoshioka, A. Ohkawa, Y. Abe, T. Nomura, Y. Mukai, S. Nakagawa, M. Taniai, T. Ohta, T. Mayumi, H. Kamada, S. Tsunoda and Y. Tsutsumi (2008a). "The therapeutic effect of TNFR1-selective antagonistic mutant TNF-alpha in murine hepatitis models." Cytokine **44**(2): 229-233.

Shibata, H., Y. Yoshioka, A. Ohkawa, K. Minowa, Y. Mukai, Y. Abe, M. Taniai, T. Nomura, H. Kayamuro, H. Nabeshi, T. Sugita, S. Imai, K. Nagano, T. Yoshikawa, T. Fujita, S. Nakagawa, A. Yamamoto, T. Ohta, T. Hayakawa, T. Mayumi, P. Vandenabeele, B. B. Aggarwal, T. Nakamura, Y. Yamagata, S. Tsunoda, H. Kamada and Y. Tsutsumi (2008b). "Creation and X-ray structure analysis of the tumor necrosis factor receptor-1-selective mutant of a tumor necrosis factor-alpha antagonist." J Biol Chem **283**(2): 998-1007.

Shu, H. B., M. Takeuchi and D. V. Goeddel (1996). "The tumor necrosis factor receptor 2 signal transducers TRAF2 and c-IAP1 are components of the tumor necrosis factor receptor 1 signaling complex." Proc Natl Acad Sci U S A **93**(24): 13973-13978.

Sicotte, N. L. and R. R. Voskuhl (2001). "Onset of multiple sclerosis associated with anti-TNF therapy." Neurology **57**(10): 1885-1888.

Sidhu, R. S. and A. P. Bollon (1993). "Tumor necrosis factor activities and cancer therapy--a perspective." Pharmacol Ther **57**(1): 79-128.

Sizemore, N., S. Leung and G. R. Stark (1999). "Activation of phosphatidylinositol 3-kinase in response to interleukin-1 leads to phosphorylation and activation of the NF-kappaB p65/RelA subunit." Mol Cell Biol **19**(7): 4798-4805.

Smith, C. D., J. M. Carney, P. E. Starke-Reed, C. N. Oliver, E. R. Stadtman, R. A. Floyd and W. R. Markesbery (1991). "Excess brain protein oxidation and enzyme dysfunction in normal aging and in Alzheimer disease." Proc Natl Acad Sci U S A **88**(23): 10540-10543.

Smith, R. A. and C. Baglioni (1987). "The active form of tumor necrosis factor is a trimer." J Biol Chem **262**(15): 6951-6954.

Sofroniew, M. V. (2005). "Reactive astrocytes in neural repair and protection." Neuroscientist **11**(5): 400-407.

Sofroniew, M. V. (2009). "Molecular dissection of reactive astrogliosis and glial scar formation." Trends Neurosci **32**(12): 638-647.

Solomon, K. A., N. Pesti, G. Wu and R. C. Newton (1999). "Cutting edge: a dominant negative form of TNF-alpha converting enzyme inhibits proTNF and TNFRII secretion." J Immunol **163**(8): 4105-4108.

Spring, J., K. Beck and R. Chiquet-Ehrismann (1989). "Two contrary functions of tenascin: dissection of the active sites by recombinant tenascin fragments." Cell **59**(2): 325-334.

Stankoff, B., M. S. Aigrot, F. Noel, A. Wattilliaux, B. Zalc and C. Lubetzki (2002). "Ciliary neurotrophic factor (CNTF) enhances myelin formation: a novel role for CNTF and CNTF-related molecules." J Neurosci **22**(21): 9221-9227.

Steed, P. M., M. G. Tansey, J. Zalevsky, E. A. Zhukovsky, J. R. Desjarlais, D. E. Szymkowski, C. Abbott, D. Carmichael, C. Chan, L. Cherry, P. Cheung, A. J. Chirino, H. H. Chung, S. K. Doberstein, A. Eivazi, A. V. Filikov, S. X. Gao, R. S. Hubert, M. Hwang, L. Hyun, S. Kashi, A. Kim, E. Kim, J. Kung, S. P. Martinez, U. S. Muchhal, D. H. Nguyen, C. O'Brien, D. O'Keefe, K. Singer, O. Vafa, J. Vielmetter, S. C. Yoder and B. I. Dahiyat (2003).

"Inactivation of TNF signaling by rationally designed dominant-negative TNF variants." Science **301**(5641): 1895-1898.

Stoll, G., S. Jander and M. Schroeter (2002). "Detrimental and beneficial effects of injury-induced inflammation and cytokine expression in the nervous system." Adv Exp Med Biol **513**: 87-113.

Sudheerkumar, P., A. Shiras, G. Das, J. C. Jagtap, V. Prasad and P. Shastry (2008). "Independent activation of Akt and NF-kappaB pathways and their role in resistance to TNF-alpha mediated cytotoxicity in gliomas." Mol Carcinog **47**(2): 126-136.

Suvannavejh, G. C., H. O. Lee, J. Padilla, M. C. Dal Canto, T. A. Barrett and S. D. Miller (2000). "Divergent roles for p55 and p75 tumor necrosis factor receptors in the pathogenesis of MOG(35-55)-induced experimental autoimmune encephalomyelitis." Cell Immunol **205**(1): 24-33.

Swanson, R. A., W. Ying and T. M. Kauppinen (2004). "Astrocyte influences on ischemic neuronal death." Curr Mol Med **4**(2): 193-205.

Talbott, J. F., D. N. Loy, Y. Liu, M. S. Qiu, M. B. Bunge, M. S. Rao and S. R. Whittemore (2005). "Endogenous Nkx2.2+/Olig2+ oligodendrocyte precursor cells fail to remyelinate the demyelinated adult rat spinal cord in the absence of astrocytes." Exp Neurol **192**(1): 11-24.

Tarbell, K. V., L. Petit, X. Zuo, P. Toy, X. Luo, A. Mqadmi, H. Yang, M. Suthanthiran, S. Mojsov and R. M. Steinman (2007). "Dendritic cell-expanded, islet-specific CD4+ CD25+ CD62L+ regulatory T cells restore normoglycemia in diabetic NOD mice." J Exp Med **204**(1): 191-201.

Tarkowski, E., L. Rosengren, C. Blomstrand, C. Wikkelso, C. Jensen, S. Ekholm and A. Tarkowski (1997). "Intrathecal release of pro- and anti-inflammatory cytokines during stroke." Clin Exp Immunol **110**(3): 492-499.

Tartaglia, L. A., T. M. Ayres, G. H. Wong and D. V. Goeddel (1993a). "A novel domain within the 55 kd TNF receptor signals cell death." Cell **74**(5): 845-853.

Tartaglia, L. A., D. V. Goeddel, C. Reynolds, I. S. Figari, R. F. Weber, B. M. Fendly and M. A. Palladino, Jr. (1993b). "Stimulation of human T-cell proliferation by specific activation of the 75-kDa tumor necrosis factor receptor." J Immunol **151**(9): 4637-4641.

Tartaglia, L. A., R. F. Weber, I. S. Figari, C. Reynolds, M. A. Palladino, Jr. and D. V. Goeddel (1991). "The two different receptors for tumor necrosis factor mediate distinct cellular responses." Proc Natl Acad Sci U S A **88**(20): 9292-9296.

Tejada-Berges, T. and V. W. Yong (1994). "The astrocyte mitogen, tumor necrosis factor-alpha, inhibits the proliferative effect of more potent adult human astrocyte mitogens, gamma-interferon and activated T-lymphocyte supernatants." Brain Res **653**(1-2): 297-304.

Testa, J. R. and P. N. Tsichlis (2005). "AKT signaling in normal and malignant cells." Oncogene **24**(50): 7391-7393.

Theiss, A. L., J. G. Simmons, C. Jobin and P. K. Lund (2005). "Tumor necrosis factor (TNF) alpha increases collagen accumulation and proliferation in intestinal myofibroblasts via TNF receptor 2." J Biol Chem **280**(43): 36099-36109.

The Lenercept Study Group (1999). "TNF neutralization in MS: results of a randomized, placebo-controlled multicenter study. The Lenercept Multiple Sclerosis Study Group and The University of British Columbia MS/MRI Analysis Group." Neurology **53**(3): 457-465.

Tokunaga, F., S. Sakata, Y. Saeki, Y. Satomi, T. Kirisako, K. Kamei, T. Nakagawa, M. Kato, S. Murata, S. Yamaoka, M. Yamamoto, S. Akira, T. Takao, K. Tanaka and K. Iwai (2009). "Involvement of linear polyubiquitylation of NEMO in NF-kappaB activation." Nat Cell Biol **11**(2): 123-132.

Torre-Amione, G., S. Kapadia, C. Benedict, H. Oral, J. B. Young and D. L. Mann (1996). "Proinflammatory cytokine levels in patients with depressed left ventricular ejection fraction: a report from the Studies of Left Ventricular Dysfunction (SOLVD)." J Am Coll Cardiol **27**(5): 1201-1206.

Van Zee, K. J., S. A. Stackpole, W. J. Montegut, M. A. Rogy, S. E. Calvano, K. C. Hsu, M. Chao, C. L. Meschter, H. Loetscher, D. Stuber and et al. (1994). "A human tumor necrosis factor (TNF) alpha mutant that binds exclusively to the p55 TNF receptor produces toxicity in the baboon." J Exp Med **179**(4): 1185-1191.

Varfolomeev, E., T. Goncharov, A. V. Fedorova, J. N. Dynek, K. Zobel, K. Deshayes, W. J. Fairbrother and D. Vucic (2008). "c-IAP1 and c-IAP2 are critical mediators of tumor necrosis factor alpha (TNFalpha)-induced NF-kappaB activation." J Biol Chem **283**(36): 24295-24299.

Vercammen, D., P. Vandenabeele, W. Declercq, M. Van de Craen, J. Grooten and W. Fiers (1995). "Cytotoxicity in L929 murine fibrosarcoma cells after triggering of transfected human p75 tumour necrosis factor (TNF) receptor is mediated by endogenous murine TNF." Cytokine **7**(5): 463-470.

Veroni, C., L. Gabriele, I. Canini, L. Castiello, E. Coccia, M. E. Remoli, S. Columba-Cabezas, E. Arico, F. Aloisi and C. Agresti (2010). "Activation of TNF receptor 2 in microglia promotes induction of anti-inflammatory pathways." Mol Cell Neurosci **45**(3): 234-244.

von Zastrow, M. and A. Sorkin (2007). "Signaling on the endocytic pathway." Curr Opin Cell Biol **19**(4): 436-445.

Voorthuis, J. A., B. M. Uitdehaag, C. J. De Groot, P. H. Goede, P. H. van der Meide and C. D. Dijkstra (1990). "Suppression of experimental allergic encephalomyelitis by intraventricular administration of interferon-gamma in Lewis rats." Clin Exp Immunol **81**(2): 183-188.

Wajant, H., K. Pfizenmaier and P. Scheurich (2003). "Tumor necrosis factor signaling." Cell Death Differ **10**(1): 45-65.

Wallach, D., H. Engelmann, Y. Nophar, D. Aderka, O. Kemper, V. Hornik, H. Holtmann and C. Brakebusch (1991). "Soluble and cell surface receptors for tumor necrosis factor." Agents Actions Suppl **35**: 51-57.

Walsh, D. A. (1999). "Angiogenesis and arthritis." Rheumatology (Oxford) **38**(2): 103-112.

Wang, C. Y., M. W. Mayo, R. G. Korneluk, D. V. Goeddel and A. S. Baldwin, Jr. (1998). "NF-kappaB antiapoptosis: induction of TRAF1 and TRAF2 and c-IAP1 and c-IAP2 to suppress caspase-8 activation." Science **281**(5383): 1680-1683.

Wang, D. and A. S. Baldwin, Jr. (1998). "Activation of nuclear factor-kappaB-dependent transcription by tumor necrosis factor-alpha is mediated through phosphorylation of RelA/p65 on serine 529." J Biol Chem **273**(45): 29411-29416.

Wang, H. G., N. Pathan, I. M. Ethell, S. Krajewski, Y. Yamaguchi, F. Shibasaki, F. McKeon, T. Bobo, T. F. Franke and J. C. Reed (1999). "Ca2+-induced apoptosis through calcineurin dephosphorylation of BAD." Science **284**(5412): 339-343.

Wang, X., G. Z. Feuerstein, L. Xu, H. Wang, W. A. Schumacher, M. L. Ogletree, R. Taub, J. J. Duan, C. P. Decicco and R. Q. Liu (2004). "Inhibition of tumor necrosis factor-alpha-converting enzyme by a selective antagonist protects brain from focal ischemic injury in rats." Mol Pharmacol **65**(4): 890-896.

Wang, Y., R. Singh, J. H. Lefkowitch, R. M. Rigoli and M. J. Czaja (2006a). "Tumor necrosis factor-induced toxic liver injury results from JNK2-dependent activation of caspase-8 and the mitochondrial death pathway." J Biol Chem **281**(22): 15258-15267.

Wang, Z., J. Hong, W. Sun, G. Xu, N. Li, X. Chen, A. Liu, L. Xu, B. Sun and J. Z. Zhang (2006b). "Role of IFN-gamma in induction of Foxp3 and conversion of CD4+ CD25- T cells to CD4+ Tregs." J Clin Invest **116**(9): 2434-2441.

Welborn, M. B., 3rd, K. Van Zee, P. D. Edwards, J. H. Pruitt, A. Kaibara, J. N. Vauthey, M. Rogy, W. L. Castleman, S. F. Lowry, J. S. Kenney, D. Stuber, U. Ettlin, B. Wipf, H. Loetscher, E. M. Copeland, 3rd, W. Lesslauer and L. L. Moldawer (1996). "A human tumor necrosis factor p75 receptor agonist stimulates in vitro T cell proliferation but does not produce inflammation or shock in the baboon." J Exp Med **184**(1): 165-171.

Whittemore, E. R., D. T. Loo and C. W. Cotman (1994). "Exposure to hydrogen peroxide induces cell death via apoptosis in cultured rat cortical neurons." Neuroreport **5**(12): 1485-1488.

Whittemore, E. R., D. T. Loo, J. A. Watt and C. W. Cotman (1995). "A detailed analysis of hydrogen peroxide-induced cell death in primary neuronal culture." Neuroscience **67**(4): 921-932.

Wiese, S., M. R. Digby, J. M. Gunnersen, R. Gotz, G. Pei, B. Holtmann, J. Lowenthal and M. Sendtner (1999). "The anti-apoptotic protein ITA is essential for NGF-mediated survival of embryonic chick neurons." Nat Neurosci **2**(11): 978-983.

Wiley, H. S. (2003). "Trafficking of the ErbB receptors and its influence on signaling." Exp Cell Res **284**(1): 78-88.

Willenborg, D. O., S. A. Fordham, W. B. Cowden and I. A. Ramshaw (1995). "Cytokines and murine autoimmune encephalomyelitis: inhibition or enhancement of disease with antibodies to select cytokines, or by delivery of exogenous cytokines using a recombinant vaccinia virus system." Scand J Immunol **41**(1): 31-41.

Wolswijk, G. and M. Noble (1989). "Identification of an adult-specific glial progenitor cell." Development **105**(2): 387-400.

Wong, F. S., L. K. Siew and L. Wen (2008). "CD8+ T-cells and their interaction with other cells in damage to islet beta-cells." Biochem Soc Trans **36**(Pt 3): 316-320.

Wong, W. W., I. E. Gentle, U. Nachbur, H. Anderton, D. L. Vaux and J. Silke (2010). "RIPK1 is not essential for TNFR1-induced activation of NF-kappaB." Cell Death Differ **17**(3): 482-487.

Wood, K. J. and B. Sawitzki (2006). "Interferon gamma: a crucial role in the function of induced regulatory T cells in vivo." Trends Immunol **27**(4): 183-187.

Woronicz, J. D., X. Gao, Z. Cao, M. Rothe and D. V. Goeddel (1997). "IkappaB kinase-beta: NF-kappaB activation and complex formation with IkappaB kinase-alpha and NIK." Science **278**(5339): 866-869.

Wu, S., C. M. Boyer, R. S. Whitaker, A. Berchuck, J. R. Wiener, J. B. Weinberg and R. C. Bast, Jr. (1993). "Tumor necrosis factor alpha as an autocrine and paracrine growth factor for ovarian cancer: monokine induction of tumor cell proliferation and tumor necrosis factor alpha expression." Cancer Res **53**(8): 1939-1944.

Wyzgol, A., N. Muller, A. Fick, S. Munkel, G. U. Grigoleit, K. Pfizenmaier and H. Wajant (2009). "Trimer stabilization, oligomerization, and antibody-mediated cell surface immobilization improve the activity of soluble trimers of CD27L, CD40L, 41BBL, and glucocorticoid-induced TNF receptor ligand." J Immunol **183**(3): 1851-1861.

Yabe, T., D. Wilson and J. P. Schwartz (2001). "NFkappaB activation is required for the neuroprotective effects of pigment epithelium-derived factor (PEDF) on cerebellar granule neurons." J Biol Chem **276**(46): 43313-43319.

Yamamoto, M., T. Okamoto, K. Takeda, S. Sato, H. Sanjo, S. Uematsu, T. Saitoh, N. Yamamoto, H. Sakurai, K. J. Ishii, S. Yamaoka, T. Kawai, Y. Matsuura, O. Takeuchi and S.

Akira (2006). "Key function for the Ubc13 E2 ubiquitin-conjugating enzyme in immune receptor signaling." Nat Immunol **7**(9): 962-970.

Yang, E., J. Zha, J. Jockel, L. H. Boise, C. B. Thompson and S. J. Korsmeyer (1995). "Bad, a heterodimeric partner for Bcl-XL and Bcl-2, displaces Bax and promotes cell death." Cell **80**(2): 285-291.

Yano, S., M. Morioka, K. Fukunaga, T. Kawano, T. Hara, Y. Kai, J. Hamada, E. Miyamoto and Y. Ushio (2001). "Activation of Akt/protein kinase B contributes to induction of ischemic tolerance in the CA1 subfield of gerbil hippocampus." J Cereb Blood Flow Metab **21**(4): 351-360.

Yellin, M. J., K. Sippel, G. Inghirami, L. R. Covey, J. J. Lee, J. Sinning, E. A. Clark, L. Chess and S. Lederman (1994). "CD40 molecules induce down-modulation and endocytosis of T cell surface T cell-B cell activating molecule/CD40-L. Potential role in regulating helper effector function." J Immunol **152**(2): 598-608.

Zakharova, M. and H. K. Ziegler (2005). "Paradoxical anti-inflammatory actions of TNF-alpha: inhibition of IL-12 and IL-23 via TNF receptor 1 in macrophages and dendritic cells." J Immunol **175**(8): 5024-5033.

Zalevsky, J., T. Secher, S. A. Ezhevsky, L. Janot, P. M. Steed, C. O'Brien, A. Eivazi, J. Kung, D. H. Nguyen, S. K. Doberstein, F. Erard, B. Ryffel and D. E. Szymkowski (2007). "Dominant-negative inhibitors of soluble TNF attenuate experimental arthritis without suppressing innate immunity to infection." J Immunol **179**(3): 1872-1883.

Zganiacz, A., M. Santosuosso, J. Wang, T. Yang, L. Chen, M. Anzulovic, S. Alexander, B. Gicquel, Y. Wan, J. Bramson, M. Inman and Z. Xing (2004). "TNF-alpha is a critical negative regulator of type 1 immune activation during intracellular bacterial infection." J Clin Invest **113**(3): 401-413.

Zhang, R., Y. Xu, N. Ekman, Z. Wu, J. Wu, K. Alitalo and W. Min (2003). "Etk/Bmx transactivates vascular endothelial growth factor 2 and recruits phosphatidylinositol 3-kinase to mediate the tumor necrosis factor-induced angiogenic pathway." J Biol Chem **278**(51): 51267-51276.

Zhao, Y., S. Li, E. E. Childs, D. K. Kuharsky and X. M. Yin (2001). "Activation of pro-death Bcl-2 family proteins and mitochondria apoptosis pathway in tumor necrosis factor-alpha-induced liver injury." J Biol Chem **276**(29): 27432-27440.

Zlokovic, B. V. (2008). "The blood-brain barrier in health and chronic neurodegenerative disorders." Neuron **57**(2): 178-201.

Supplementary Data

Plasmid Maps

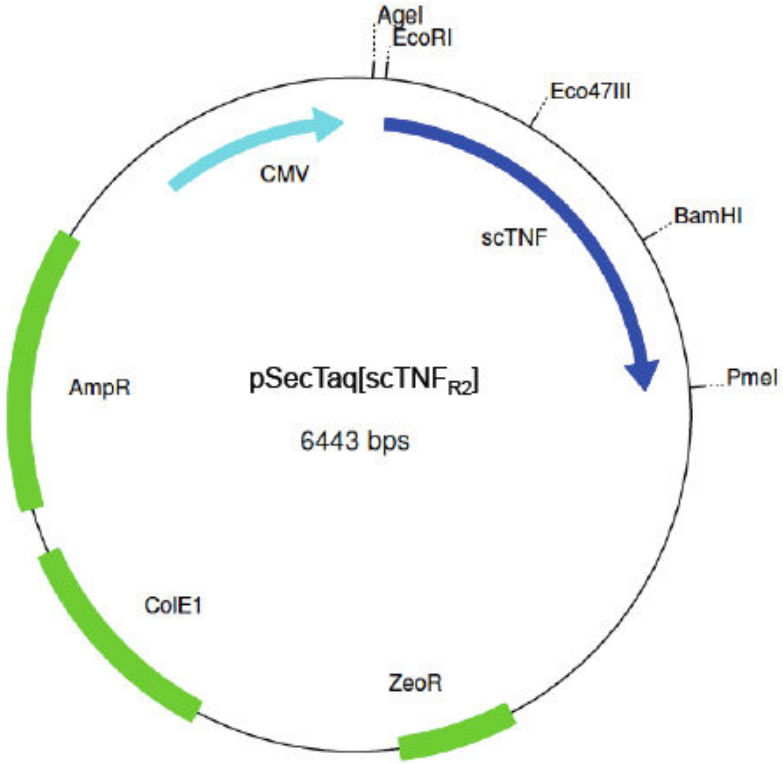

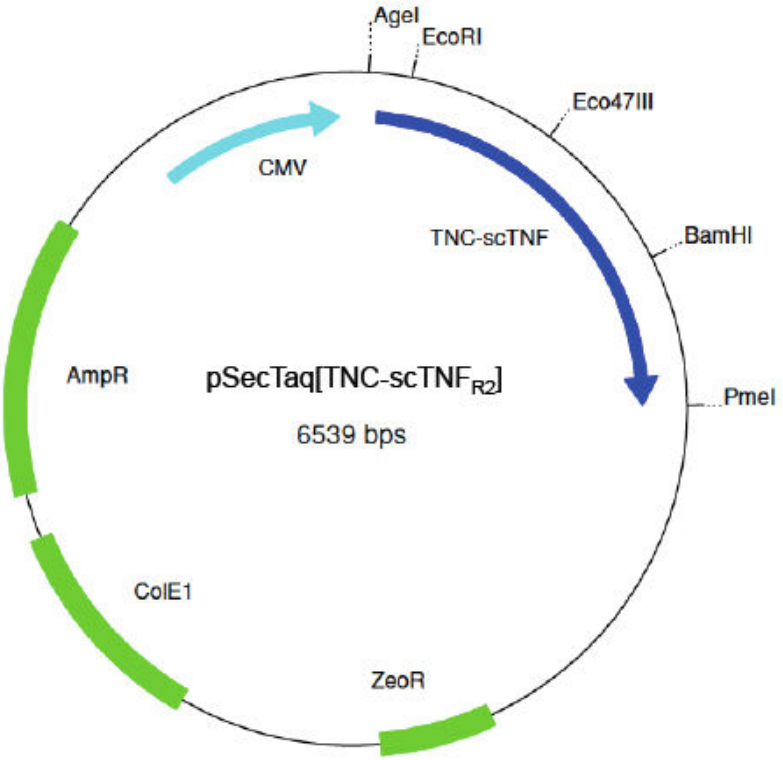

DNA sequences

scTNF$_{R2}$

```
      >.....................................TNF-module 3.....................................>
        v  e  l   r  d  n   q  l  v  v   p  s  e   g  l  y   l  i  y  s   q  v  l   f  k  g   q  g  c  p

1261  tccactcatg tgctgctgac tcacactatc tctcggattg ctgtgtccta ccagactaaa gtgaatctgc tgtctgctat taagtctcct
      aggtgagtac acgacgactg agtgtgatag agagcctaac gacacaggat ggtctgattt cacttagacg acagacgata attcagagga
      >.....................................TNF-module 3.....................................>
        s  t  h   v  l  l   t  h  t  i   s  r  i   a  v  s   y  q  t  k   v  n  l   l  s  a   i  k  s  p

1351  tgccagcgcg agactccaga gggggctgaa gccaagccct ggtatgagcc aatctatctg ggaggggtgt tccagctgga aaaggggat
      acggtcgcgc tctgaggtct cccccgactt cggttcggga ccatactcgg ttagatagac cctccccaca aggtcgacct tttccccta
      >.....................................TNF-module 3.....................................>
        c  q  r   e  t  p   e  g  a  e   a  k  p   w  y  e   p  i  y  l   g  g  v   f  q  l   e  k  g  d

1441  cgcctgagcg ccgaaatcaa tagaccagac tatctgaact ttcgcgagtc tggacaggtg tactttggaa tcattgctct gtgatgagtt
      gcggactcgc ggctttagtt atctggtctg atagacttga aagcgctcag acctgtccac atgaaacctt agtaacgaga cactactcaa
      >.....................................TNF-module 3.....................................>>
        r  l  s   a  e  i   n  r  p  d   y  l  n   f  r  e   s  g  q  v   y  f  g   i  i  a   l  -  -

     PmeI
   ----+---
1531  taaacccgct gatcagcctc gactgtgcct tctagttgcc agccatctgt tgtttgcccc tcccccgtgc cttccttgac cctggaaggt
      atttgggcga ctagtcggag ctgacacgga agatcaacgg tcggtagaca acaaacgggg agggggcacg gaaggaactg ggaccttcca
```

TNC-scTNF$_{R2}$

```
                                                                          AgeI
                                                                         -+----
  1   atggagacag acacactcct gctatgggta ctgctgctct gggttccagg ttccaccggt atgcaccacc accatcacca cggtggtggt
      tacctctgtc tgtgtgagga cgatacccat gacgacgaga cccaaggtcc aaggtggcca tacgtggtgg tggtagtggt gccaccacca
                              Igk leader
                                                                                >>....his-tag.....>>
                                                                                  h  h   h  h  h   h

 91   agcgcttgtg gttgtgctgc tgctcctgat gttaaagaac ttctttctcg tcttgaagaa cttgaaaatc ttgtttcttc tcttcgtgaa
      tcgcgaacac caacacgacg acgaggacta caatttcttg aagaaagagc agaacttctt gaacttttag aacaaagaag agaagcactt
      >>.....................................tenascin C.....................................>
        s  a  c   g  c  a   a  a  p  d   v  k  e   l  l  s   r  l  e  e   l  e  n   l  v  s   s  l  r  e

                EcoRI
               -+----
181   caaggcggcg gaattcccgc cagcagccgg acccctagcg ataagcccgt ggcccacgtg gtggccaatc ctcaggccga gggccagctg
      gttccgccgc cttaagggcg gtcgtcggcc tggggatcgc tattcgggca ccgggtgcac caccggttag gagtccggct cccggtcgac
                 linker
      >>> tenascin C
        q
                           >>.............................TNF-module 1.............................>
                             s  s  r   t  p  s   d  k  p   v  a  h  v   v  a  n   p  q  a   e  g  q  l

271   cagtggctga acagacgggc caacgccctg ctggccaacg gcgtggagct gcgggacaac cagctggtcg tgcccagcga gggcctgtac
      gtcaccgact tgtctgcccg gttgcgggac gaccggttgc cgcacctcga cgccctgttg gtcgaccagc acgggtcgct cccggacatg
      >.....................................TNF-module 1.....................................>
        q  w  l   n  r  r   a  n  a  l   l  a  n   g  v  e   l  r  d  n   q  l  v   v  p  s   e  g  l  y

361   ctgatctaca gccaggtgct gttcaagggc cagggctgcc cttctaccca cgtgctgctg acccacacca tcagccggat cgccgtgagc
      gactagatgt cggtccacga caagttcccg gtcccgacgg gaagatgggt gcacgacgac tgggtgtggt agtcggccta gcggcactcg
      >.....................................TNF-module 1.....................................>
        l  i  y   s  q  v   l  f  k  g   q  g  c   p  s  t   h  v  l  l   t  h  t   i  s  r   i  a  v  s

451   taccagacca aagtgaacct gctgtccgcc atcaagagcc cctgccagag agagacacct gagggcgccg aggccaagcc ttggtacgag
      atggtctggt ttcacttgga cgacaggcgg tagttctcgg ggacggtctc tctctgtgga ctcccgcggc tccggttcgg aaccatgctc
      >.....................................TNF-module 1.....................................>
        y  q  t   k  v  n   l  l  s  a   i  k  s   p  c  q   r  e  t  p   e  g  a   e  a  k   p  w  y  e

541   cccatctacc tgggcggcgt gttccagctg gaaaagggcg accggctgtc cgccgagatc aaccggcccg actacctgaa cttccgggag
      gggtagatgg acccgccgca caaggtcgac cttttcccgc tggccgacag gcggctctag ttggccgggc tgatggactt gaaggccctc
      >.....................................TNF-module 1.....................................>
        p  i  y   l  g  g   v  f  q  l   e  k  g   d  r  l   s  a  e  i   n  r  p   d  y  l   n  f  r  e

                              Eco47III
                              ---+---
631   agcggccagg tgtacttcgg catcatagcg ctgggcggag ggggcagcag cagcagaacc ccctccgaca agcctgtggc tcatgtggtg
      tcgccggtcc acatgaagcc gtagtatcgc gacccgcctc ccccgtcgtc gtcgtcttgg gggaggctgt tcggacaccg agtacaccac
                                       GGGGS linker
      >..........TNF-module 1.........>>
        s  g  q   v  y  f   g  i  i  a   l
                                                  >>.............TNF-module 2.............>
                                                    s  s  r   t  p  s   d  k  p   v  a  h   v  v

721   gctaaccccc aggctgaagg acagctgcag tggctgaatc ggagagctaa tgctctgctg gctaatgggg tggaactgag agataatcag
      cgattggggg tccgacttcc tgtcgacgtc accgacttag cctctcgatt acgagacgac cgattacccc accttgactc tctattagtc
      >.....................................TNF-module 2.....................................>
        a  n  p   q  a  e   g  q  l  q   w  l  n   r  r  a   n  a  l  l   a  n  g   v  e  l   r  d  n  q

811   ctggtcgtgc cttctgaggg gctgtatctg atctattctc aggtgctgtt taaaggacag gggtgtccca gcacacatgt gctgctgaca
```

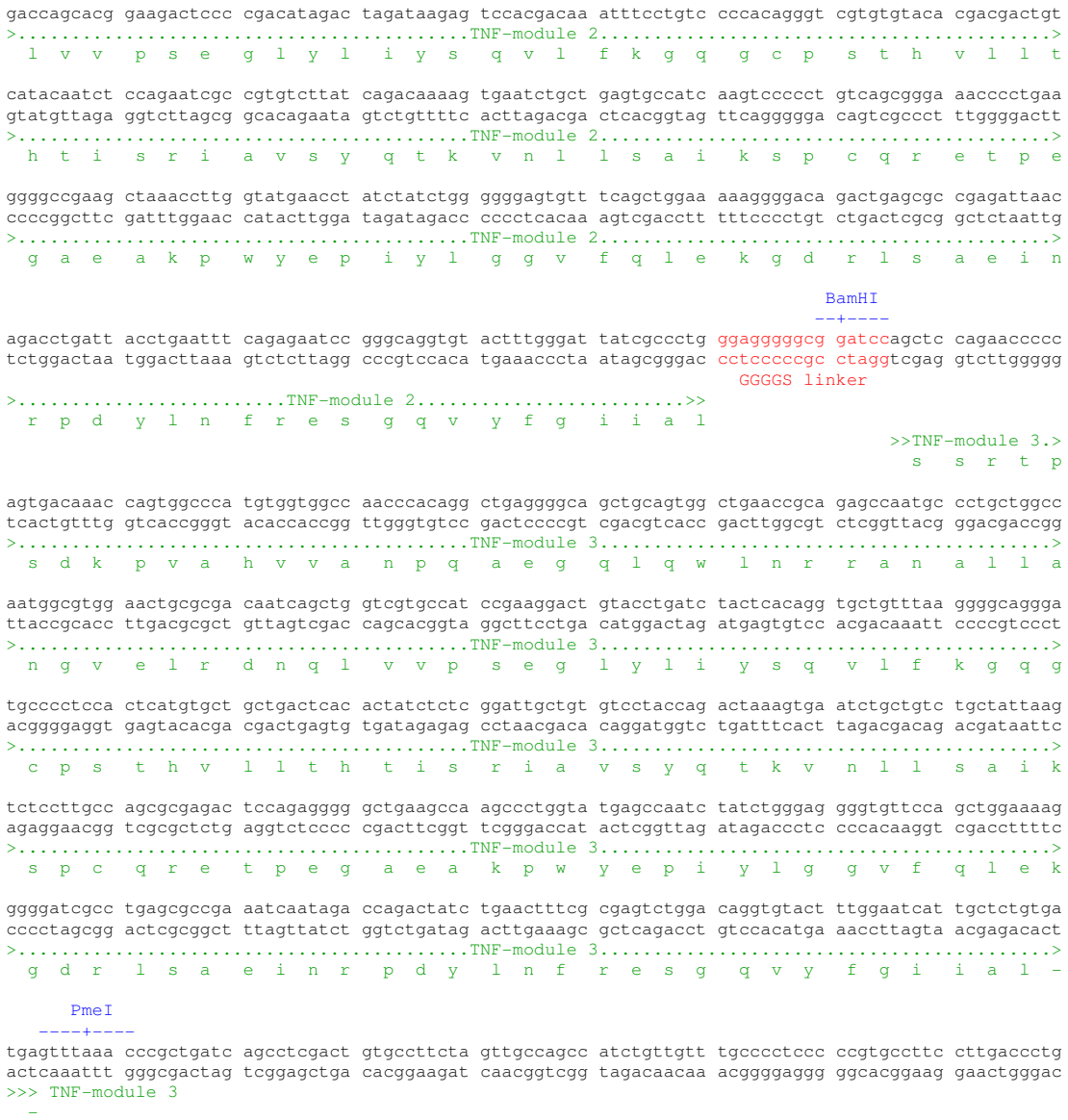

Protein sequences

Wildtype huTNFR2

```
        10          20          30          40          50          60
MAPVAVWAAL AVGLELWAAA HALPAQVAFT PYAPEPGSTC RLREYYDQTA QMCCSKCSPG
        70          80          90         100         110         120
QHAKVFCTKT SDTVCDSCED STYTQLWNWV PECLSCGSRC SSDQVETQAC TREQNRICTC
       130         140         150         160         170         180
RPGWYCALSK QEGCRLCAPL RKCRPGFGVA RPGTETSDVV CKPCAPGTFS NTTSSTDICR
       190         200         210         220         230         240
PHQICNVVAI PGNASMDAVC TSTSPTRSMA PGAVHLPQPV STRSQHTQPT PEPSTAPSTS
       250         260         270         280         290         300
FLLPMGPSPP AEGSTGDFAL PVGLIVGVTA LGLLIIGVVN CVIMTQVKKK PLCLQREAKV
       310         320         330         340         350         360
```

```
PHLPADKARG TQGPEQQHLL ITAPSSSSSS LESSASALDR RAPTRNQPQA PGVEASGAGE
       370        380        390        400        410        420
ARASTGSSDS SPGGHGTQVN VTCIVNVCSS SDHSSQCSSQ ASSTMGDTDS SPSESPKDEQ
       430        440        450        460
VPFSKEECAF RSQLETPETL LGSTEEKPLP LGVPDAGMKP S
```

Internalization motif EQQHLL is marked in bold letters.

Acknowledgements

First, I want to thank Prof. Dr. Klaus Pfizenmaier for giving me the opportunity to perform this interesting research project under his excellent supervision and for all the helpful advice and suggestions during the experimental and theoretical part and all concerns of this study.

I want to especially thank Prof. Dr. Peter Scheurich for his very helpful support, for sorting several cell lines with the FACSDiVa and for always having an open door, whenever I had questions.
Moreover, I want to thank Prof. Dr. Roland Kontermann for his helpful advice and the interesting conversations, which promoted my research project.

I would especially like to thank Dr. Olaf Maier for his technical and theoretical support, for fruitful discussions and the ongoing encouragement. Special thanks go to all the members of the laboratory: Dr. Jens Neumeyer, Michaela Strotbek, Kristian Kiilerich, Tini Lorey, Anita Friese, Bernat Elvira, and Sandra Böker for helpful discussions and the excellent working atmosphere. Special thanks go to Sandra Böker for supporting me with analyzing the IMA1335 cells.
Furthermore, I want to thank Dr. Felix Neugart for the technical and theoretical support with the microscopes and for quantifying the microscopy data. Special thanks go to Prof. Dr. Harald Wajant for providing the Flag-TNC-TNF prototype, Dr. Martin Siegemund for his kind support with the HPLC, Dr. Dafne Müller for providing the PBMCs, Dr. Jeanette Gerspach for assistance with the animal experiments, Dr. Kornelia Ellwanger for providing the plasmid psV3neo, Dr. Monilola Olayioye and Jessica Tepperink for providing several antibodies and reagents and Margarete Witkowski for her help at the microscope. In addition, I want to thank the team from the animal facility, Aniela Kraiczy, Ludmila Guseva and Eric Konrath.
I would like to thank Prof. Dr. Marcel Leist and Dr. Stefan Schildknecht from the University of Konstanz for providing the LUHMES cells and for helpful conversations.

Finally, I wish to thank Nadine for her love and attendance on my way towards the PhD.
Last but not least, I want to particularly thank my parents, Horst und Ursula, for all their indefatigable support during my whole studies! Thank you for always listening to all my concerns and for investing so much time in reading and correcting this thesis!

The project was funded by a grant from EC FP6, Project NeuroproMiSe, contract # LSHM-CT-2005-018637.

Curriculum vitae

PERSÖNLICHE DATEN

Roman Fischer
geb. am 01. Oktober 1981 in Nürnberg

SCHULAUSBILDUNG

09/1988 – 08/1992	Grundschule Altenfurt, Nürnberg
09/1992 – 06/2001	Martin-Behaim-Gymnasium, Nürnberg Abschluss: Allgemeine Hochschulreife

ZIVILER ERSATZDIENST

07/2001 – 04/2002	Mobiler Sozialer Hilfsdienst, Arbeiter-Samariter-Bund, Nürnberg

STUDIUM

10/2002 – 05/2007	**Friedrich-Alexander Universität Erlangen-Nürnberg** Studium der Biologie, mit dem Hauptfach Genetik/Humangenetik und den Nebenfächern Entwicklungsbiologie, Biochemie und Biotechnik Abschluss: Diplom (Dipl. Biologe)
08/2006 – 05/2007	**Universitätsklinikum Erlangen, Institut für Humangenetik** Diplomarbeit: *„Genomweite Kopplungsanalyse zur Kartierung eines Krankheitslokus für Paroxysmale Kinesiogene Choreoathetose und Suche nach Kandidatengenen“* (Supervisor: Prof. Dr. André Reis)

PROMOTION

Seit 05/2007	**Universität Stuttgart, Institut für Zellbiologie und Immunologie** *„A soluble TNF receptor 2 agonist as a new therapeutic approach to treat autoimmune and demyelinating diseases“ (*Supervisor: Prof. Dr. Klaus Pfizenmaier)
03/2010	**Open University Milton Keynes, Department of Life Sciences** Research Visit (Supervisor: Dr. Ignacio Romero)

PUBLIKATIONEN

Fischer, R., O. Maier, M. Naumer, A. Krippner-Heidenreich, P. Scheurich and K. Pfizenmaier (2011). "Ligand-induced internalization of TNF receptor 2 mediated by a di-leucin motif is dispensable for activation of the NFkappaB pathway." Cell Signal **23**(1): 161-170.

Stuttgart, im Februar 2011